Advances and Technical Standards in Neurosurgery
Editor in Chief: Johannes Schramm

Advances and Technical Standards in Neurosurgery

Volume 43

Springer

Advances and Technical Standards in Neurosurgery

Volume 43

For further volumes
http://www.springer.com/series/578

Sponsored by the
European Association of Neurosurgical Societies

Johannes Schramm
Editor-in-chief

Advances and Technical Standards in Neurosurgery

Volume 43

Springer

Editor-in-chief
Johannes Schramm
Medical Faculty
University of Bonn
Bonn
Germany

ISSN 0095-4829 ISSN 1869-9189 (electronic)
Advances and Technical Standards in Neurosurgery
ISBN 978-3-319-21358-3 ISBN 978-3-319-21359-0 (eBook)
DOI 10.1007/978-3-319-21359-0

Library of Congress Control Number: 2015954243

Springer Cham Heidelberg New York Dordrecht London

Printed on acid-free paper

Springer International Publishing AG Switzerland is part of Springer Science+Business Media (www.springer.com)

Contents

Part I
Advances

Hearing Outcomes After Stereotactic Radiosurgery for Vestibular Schwannomas

Mechanism of Hearing Loss and How to Preserve Hearing

Jung Ho Han, Dong Gyu Kim, Hyun-Tai Chung, Sun Ha Paek, and Hee-Won Jung

Contents

J.H. Han, MD
Department of Neurosurgery, Seoul National University College of Medicine, Seoul, Korea

Department of Neurosurgery, Seoul National University Bundang Hospital, Gyeonggi-do, Korea

D.G. Kim, MD, PhD (✉) • H.-T. Chung, PhD • S.H. Paek, MD, PhD • H.-W. Jung, MD, PhD
Department of Neurosurgery, Seoul National University College of Medicine, Seoul, Korea

Department of Neurosurgery, Seoul National University Hospital, Seoul, Korea
e-mail: gknife@plaza.snu.ac.kr

J. Schramm (ed.), *Advances and Technical Standards in Neurosurgery*,
Advances and Technical Standards in Neurosurgery, Vol. 43,
DOI 10.1007/978-3-319-21359-0_1

Abstract The use of stereotactic radiosurgery (SRS) expanded to include the treatment of vestibular schwannomas (VSs) in 1969; since then, efforts to increase tumour control and to reduce cranial neuropathy have continued. Using the currently recommended marginal dose of 12–13 Gy, long-term reported outcomes after SRS include not only excellent tumour control rates of 92–100 % but also outstanding functional preservation of the trigeminal and facial nerves, with values of 92–100 % and 94–100 %, respectively. Nonetheless, hearing preservation remains in the range of 32–81 %. Previous studies have suggested possible prognostic factors of hearing preservation such as the Gardner-Robertson grade, radiation dose to the cochlea, transient volume expansion (TVE) after SRS, length of irradiated cochlear nerve, marginal dose to the tumour, and age. However, we still do not clearly understand why patients lose their hearing after SRS for VS.

Relevant to these considerations, one study recently reported that the auditory brainstem response (ABR) wave V latency and waves I and V interval (IL_I–V) correlated well with intracanalicular pressure values and even with hearing level. The demonstration that ABR values, especially wave V latency and IL_I–V, correlate well with intracanalicular pressure suggests that patients with previously elevated intracanalicular pressure might have an increased chance of hearing loss on development of TVE, which has been recognised as a common phenomenon after SRS or stereotactic radiotherapy (SRT) for intracranial schwannomas.

In our experience, the ABR IL_I–V increased during the first 12 months after SRS for VSs in patients who lost their serviceable hearing. The effect of increased ABR IL_I–V on hearing outcome also became significant over time, especially at 12 months after SRS, and was more prominent in patients with poor initial pure-tone average (PTA) and/or ABR values. We hypothesise that patients with considerable intracanalicular pressure at the time of SRS are prone to lose their serviceable hearing due to the added intracanalicular pressure induced by TVE, which usually occurs within the first 12 months after SRS for VSs. Using these findings, we suggested a classification system for the prediction of hearing outcomes after SRS for VSs. This classification system could be useful in the proper selection of management modalities for hearing preservation, especially in patients with only hearing ear schwannoma or neurofibromatosis type 2.

Advances in diagnostic tools, treatment modalities, and optimisation of radiosurgical dose have improved clinical outcomes, including tumour control and cranial neuropathies, in patients with VSs. However, the preservation of hearing function still falls short of our expectation. A prediction model for hearing preservation after each treatment modality will guide the proper selection of treatment modalities and permit the appropriate timing of active treatment, which will lead to the preservation of hearing function in patients with VSs.

Keywords Stereotactic radiosurgery • Vestibular schwannoma • Hearing preservation • Intracanalicular pressure • Transient volume expansion • Auditory brainstem response

Introduction

It was Harvey Cushing who, recognising the dire problems of haemorrhage during vestibular schwannoma (VS) surgery, compared the cerebellopontine angle with the corner fence at the Battle of Gettysburg and suggested that it might well be called the 'bloody angle' [93]. In his monograph 'Tumors of the Nervus Acusticus and the Syndrome of the Cerebellopontine Angle', published in 1917, he demonstrated how he was able to reduce the perioperative mortality associated with this surgery from 72 %–84 % to 35 % and then to 10 % by employing the technique of intracapsular debulking [93]. Cushing's results were a dramatic improvement on those of all of his predecessors. Nevertheless, his method of subtotal removal by intracapsular debulking inevitably resulted in a high recurrence rate, and his great rival of the time, Walter Dandy, soon espoused the philosophy of total tumour removal through a unilateral suboccipital approach [24].

Despite these advances in VS surgery by two great surgeons, most of the neurosurgeons at that time were reluctant to recommend surgery until the tumours became very large. This approach, of course, resulted in a self-perpetuating cycle of poor clinical outcome. The operative results were indeed extremely poor when the tumours become large. Perioperative mortality was 20 % in a series of 130 cases, all of which had rather large tumours at the time of surgery [88]. In one series of partial removals, 60 % of the patients died of tumour recurrence within 4 years [34]. In Northfield's 1970 series, the average tumour size was 3–4 cm at the time of surgery, and the perioperative death rate was as high as 16 % [83]. He recommended total extirpation of the tumours without procrastination at the first attempt after review of his early experience of partial removal and secondary extirpation. However, the facial and auditory nerves incorporated into the tumour capsule were usually ignored, and the contiguity of the lower cranial nerves, which could consequently be damaged, rendered patients prone to disturbances of swallowing and to respiratory infections [83]. Preservation of the facial nerve was a matter of concern in only a few cases with small tumours, but auditory function was not of interest. Hearing preservation surgery for VSs has only recently become a popular concept on the strength of modern neurosurgical and neurophysiological advances. However, the functional hearing preservation rates are approximately 50–70 %, even if small VSs are in the safe hands of the experts [98, 115].

In these circumstances, the use of stereotactic radiosurgery (SRS) has expanded to include the management of tumours in the 'bloody angle' using a bloodless treatment method [64, 93]. Since the first operation performed in 1951 by Lars Leksell [63], SRS, which originated from his idea of replacing the needle electrode with narrow beams of radiant energy, has been an effective alternative to conventional surgery in the management of inoperable intracranial tumours [39]. In his 1971 article [64], Leksell wrote, 'the lower marginal tumour dose and a rapid dose fall-off using the 50 % isodose line would make serious injury to the neighbouring structures unlikely'. Since the publication of his report, efforts to chase two hares in the management of VSs, namely, to increase the tumour control rate and reduce the risk

of cranial nerve injury, including hearing preservation, have continued. The results were in part as Leksell expected, however. Even with a lower tumour marginal dose of 12–13 Gy, numerous reports of long-term outcomes after SRS show not only excellent progression-free survival of 92–100 % but also outstanding preservation of the trigeminal and facial nerves in 92–100 % and 94–100 % of cases, respectively [18, 22, 45, 50, 59].

The efficacy of SRS, especially in relatively small tumours, created interest in hearing function. Nonetheless, hearing preservation still falls short of our expectations. The range of hearing preservation after SRS with long-term follow-up has been reported as 32–81 % [18, 22, 33, 45, 49, 57, 81]. Furthermore, the exact mechanisms of hearing loss after SRS for VSs are not yet understood. Thus, we will review the possible factors associated with hearing deterioration or preservation after SRS for patients with VSs and will suggest the hypothetical causes of hearing loss in patients with VSs after SRS based on our experience. We will also discuss possible methods to preserve hearing in patients with VSs after SRS.

Natural History of Vestibular Schwannomas and Hearing Outcomes

According to a population-based cohort study, the number of diagnosed VSs gradually increased from 7.8 to 23 VSs per one million population per year over approximately 30 years since 1976; since then, the incidence has gradually decreased to 19 VSs per one million individuals [103]. After several decades during which the incidence of diagnosed tumours increased due to easy access to neuroimaging and heightened symptom awareness among the general population, a peak seems to have been reached [103]. This levelling may reflect an approximation of the true incidence of VSs in the general population [103].

Microsurgery or SRS for VSs has been in use for decades with reasonably convincing evidence of efficacy albeit in the absence of randomised trials comparing these treatments with other treatment modalities, particularly the ‘wait-and-see’ strategy. One argument against the conservative management of VSs is the risk of progressive hearing deterioration over time, which cannot be reversed by any treatment [104]. Advocates of hearing preservation microsurgery insist that if patients with small VSs and good hearing are not operated upon, their hearing could deteriorate and they might lose the opportunity to have their hearing preserved by microsurgery [104]. However, long gone are the days when the diagnosis of VS was followed by indiscriminate surgery on the assumption that the presence of the tumour represented a risk to life and function [11]. The initial enthusiasm for SRS or hearing preservation microsurgery for VSs and the assertions for efficacy without toxicity have been replaced by a more sophisticated approach that combines a better understanding of the natural history of untreated VSs with clear recognition of what the treatment can achieve.

Tumour size at diagnosis has decreased from a mean extrameatal diameter of approximately 30 mm in the mid-1970s to a mean diameter of 10 mm over the last several decades. The level of auditory function has also been improved from a mean pure-tone average (PTA) of 70 dB and a mean speech discrimination (SD) of 30 %–48 dB and 60 %, respectively [103]. The improved hearing at diagnosis is even more evident when considering patients with 100 % SD at diagnosis. In 1976, 3 % of the patients had modified word recognition scoring class 0 compared with 21 % in 2008 [103]. Auditory function has become a matter of concern, and various methods for hearing preservation have been developed and advanced in the management of patients with VSs.

Most vestibular schwannoma ears have deteriorated hearing compared with the normal side; one study reported at least a 10-dB PTA difference in over 90 % of patients and at least 10 %-SD difference in 74 % of patients [104]. Of note, patients with even minor loss of SD at diagnosis (1–10 %) are more prone to lose good hearing over the observation period than those with normal hearing function. The actual good hearing preservation rates of patients with even a minimal loss were 72 %, 60 %, and 38 % after 1, 5, and 10 years, respectively, of the wait-and-see strategy [103]. In patients with modified word recognition who scored class 0 hearing at diagnosis (SD = 100 %), 3 % had lost class 1 hearing at the first year of observation, and 12 % and 31 % had lost class 1 hearing after 5 and 10 years of observation, respectively [103]. Therefore, patients in whom the process of hearing deterioration in VS ears has already begun at the time of diagnosis are prone to lose their hearing during the period of observation [5, 37, 105].

In this context, the outcome of proactive treatment in patients with minimal hearing deficits at diagnosis should be compared with that of the wait-and-see strategy, especially in terms of whether proactive treatment can preserve good hearing or prolong the duration of good hearing in vestibular schwannoma ears. A recent meta-analysis showed better hearing preservation in patients treated with SRS compared with conservative management. However, that study did not provide evidence strong enough to permit clear conclusions, especially in the case of patients with small VSs [75], and further studies are mandatory in the near future. Reported hearing outcomes after the wait-and-see strategy for VSs are summarised in Table 1.

Prognostic Factors Related to Hearing Outcome After Stereotactic Radiosurgery

Despite the many suggested possible prognostic factors related to hearing preservation, such as radiation dose to the cochlea and its structures, the occurrence of transient volume expansion (TVE) after SRS, the length of the irradiated cochlear nerve, marginal dose to the tumour itself, and age, it is not precisely known why patients often lose their hearing after SRS for VSs. This uncertainty regarding the exact mechanism of hearing loss after SRS may be one of the principal causes of

Table 1 Hearing outcomes in published series after the wait-and-see strategy for vestibular schwannomas

References	Number of patients	Mean age (years)	Mean follow-up duration (range)	Classification of hearing	Serviceable hearing at diagnosis	Hearing outcome	Tumour growth and hearing deterioration
Stangerup et al. [104]	636	57.9	3.9 years (0.3–11.4)	AAO-HNS[a]	49 %	49 % (serviceable hearing preservation rate)	Related
Malhotra et al. [73]	202	59.8	2.48 years (0.1–16)	Mean PTA[b] only	–	20 % (deterioration of the initial hearing)	Related
Grayeli et al. [36]	105	59	33 months (6–11)	AAO-HNS	41 %	23 % (serviceable hearing at the last visit)	Related
Hajioff et al. [38]	72	Median 61	Median 121 months (89–271)	Mean PTA only	–	Mean added change of 35.6 dB from baseline	Related
Bakkouri et al. [8]	386 (Follow-up in 325)	58	Range only in months (12–108)	AAO-HNS	51 %	Deterioration 14.7 % at 1 year 14.3 % at 3 year 14.9 % at 5 year (Not cumulative data)	Partly related
Ferri et al. [27]	123	61	4.8 years (Not suggested)	AAO-HNS	46 %	73 % (serviceable hearing preservation rate)	Not related

[a]The American Academy of Otolaryngology-Head and Neck Surgery
[b]The pure-tone average

unsatisfactory hearing preservation. In the following section, the possible factors affecting hearing outcome are reviewed, and we suggest several hypothetical causes of hearing loss after SRS for patients with VSs based on our experience.

Tumour Control and Dose Prescription

Tumour control is the initial goal of SRS for VSs, and the efficacy of SRS in tumour control has been proven over several decades even in the absence of randomised controlled studies [43, 76]. After achieving good tumour control, cranial nerve preservation, especially hearing preservation, became an important issue. The relationship between tumour control and hearing preservation only received minor attention because of the very high rates of tumour control achieved using contemporary techniques and dose guidelines for SRS. However, failure of tumour control after SRS directly results in hearing deterioration. In fact, all patients who experienced tumour recurrence during the follow-up period after SRS or stereotactic radiotherapy lost their initial useful hearing with tumour progression [23]. In most series of the natural history of VSs, tumour growth is also associated with an increased risk of hearing deterioration [36, 38, 73, 106]. However, hearing deterioration can occur in the absence of tumour growth when the wait-and-see strategy is followed [94, 104]. Failure of tumour control after SRS may lead directly to ipsilateral hearing loss; however, tumour control does not guarantee preservation of the patient's initial or useful hearing.

In the first report by Leksell [64], the tumour control rate of SRS for VS was reported to be approximately 80 % using tumour marginal doses of 18–20 Gy at a 50 % isodose line, and approximately 20 % of patients developed cranial neuropathies. Thereafter, the dose prescribed to the tumour margin gradually decreased to 12–13 Gy in an effort to avoid cranial neuropathies; now, with the aid of modern technology, tumour control rates have improved significantly to 92–100 % [18, 45, 50].

By decreasing the tumour marginal dose to 12–13 Gy, hearing outcomes have improved, but not to the same extent as other cranial neuropathies [18, 22, 33, 45, 49, 57, 81]. Preservation of trigeminal and facial nerve function has improved to 92–100 % and 94–100 % of cases, respectively [18, 22, 45, 50, 59]. However, improvement in hearing outcome after SRS with long-term follow-up still falls short of expectations; the range of post-radiosurgery hearing preservation has been reported as 32–81 % [18, 22, 33, 45, 49, 57, 81].

In 2007, a useful hearing preservation rate of 74–77 % using a tumour marginal dose of 12–13 Gy was reported [18]. However, the authors of that study excluded patients who were followed up for less than 3 years. If these patients had been included in the analysis, the reported hearing preservation rate might be lower considering that most patients experience hearing deterioration within 2 or 3 years after SRS for VSs, as described by the same group [52]. Another study by the same group showed a useful hearing preservation rate of 71.4 %; however, the median follow-up duration was only 20 months [52]. Therefore, useful hearing preservation rates after

long-term follow-up of more than 5 years are estimated to be approximately 50 % or less [14, 22, 57], and rates differ according to follow-up duration and tumour parameters. The fact that hearing outcomes have not considerably improved, even with excellent tumour control rates, suggests that there may be underlying pathophysiological mechanisms of hearing deterioration after SRS for VSs that differ from those in conservatively managed cases.

Radiation to the Temporal Bone Structures

Among the temporal bone structures that are known to be related to hearing function, the cochlea is at the centre of the dispute over hearing preservation after SRS for VSs. The first attempt to link cochlear dose with hearing preservation outcomes after SRS for VSs was made by our Seoul National University Hospital (SNUH) Gamma Knife group in 2005; however, we could not find any statistically significant correlation [67, 86]. The first report to demonstrate a significant relationship between hearing preservation and cochlear dose was published in 2007 [77]. Thereafter, many studies reported similar findings. The cochlear threshold dose most likely lies somewhere in the range of 4–5.33 Gy (Table 2) [9, 44, 52].

Several issues should be considered when interpreting these results. First, cochlear threshold doses were evaluated in different parts of the cochlea or using different methods in various studies. For example, dose was evaluated either at a point within the cochlea or for the whole cochlea and as either the maximum dose or the mean dose to the cochlea [9, 52, 77, 109]; these differences in methodology have led to some debate concerning the results [59, 69].

Second, a relationship between cochlear dose and hearing preservation has not been demonstrated in cases involving other intracranial benign tumours near the internal auditory canal (IAC), even when these tumours were treated with the same radiosurgical protocol [12, 58]. We recently determined that the useful hearing preservation rate after SRS for meningiomas near or extending into the IAC (para-IAC meningiomas) was as high as 97.6 % (41 of 42 patients preserved their useful hearing) during the median follow-up duration of 48 months, even with a considerable radiation dose to the ipsilateral cochlea (the average values of maximal and mean cochlear dose were 6.3 ± 0.4 Gy [range, 3.1–13.1] and 4.6 ± 0.2 Gy [range, 2.2–9.6], respectively) [58]. Actually, one patient with para-IAC meningioma that was treated with maximal and mean cochlear doses of 6.9 Gy and 5.5 Gy, respectively, experienced an improvement in hearing from 30 dB of PTA and 80 % of SD to 26 dB of PTA and 90 % of SD at 12 months after radiosurgery (Fig. 1) [58]. In another patient treated with maximal and mean cochlear doses of 11.5 Gy and 7.5 Gy, respectively, the initial useful hearing was preserved at 72 months after SRS for para-IAC meningioma [58]. A similar finding was presented by an American group in patients with glomus jugulare tumours treated with SRS. Only one of eight patients with clinically serviceable hearing before SRS experienced hearing deterioration after SRS during the mean follow-up duration of 26 months, and three of the four patients who received a mean cochlear dose greater than 8 Gy suffered no hearing deterioration [12].

Table 2 The cochlear threshold dose and hearing outcomes after stereotactic radiosurgery for vestibular schwannomas

References	Number of patients	Mean age (years)	Mean follow-up duration (range)	Point of the cochlea Where radiation dose was evaluated	Measured value of the cochlear dose[b]	The cochlear threshold dose (Gy)	Multivariate analysis	Cochlear threshold dose and hearing deterioration
Massager et al. [77]	82	Median 57 (19–89)	Median 2 years (1–4)	Whole cochlea	Mean	Preserved: median 3.70 Deteriorated: median 5.33	Not done	Related
Timmer et al. [109]	69	51 (17–73)	14.2 months (3–56)	Whole cochlea	Maximum	Suggested as the range in the whole group	Not done	Related
Kano et al. [52]	77	Median 52 (22–82)	Median 20 months (6–40)	Modiolus	–	4.2	Done	Related (not significant in the whole group, but significant only in patients <60 years old)
Baschnagel et al. [9]	40	Median 59 (26–80)	Median 34.5 months (6.1–57.8)	Whole cochlea	Mean	3 (and 3 Gy-cochlear volume)	Done	Related (but, statistically not significant; [$p>0.05$])
SNUH series, Han et al. [41][a]	119	48 (21–71)	55.2 months (12.3–158)	Whole cochlea	Mean and maximum		Done	Not related

[a]*SNUH* Seoul National University Hospital

[b]The mean value is the average radiation dose irradiated to the whole cochlea; the maximum value is the highest radiation dose irradiated to the whole cochlea, irrespective of the cochlear specific part

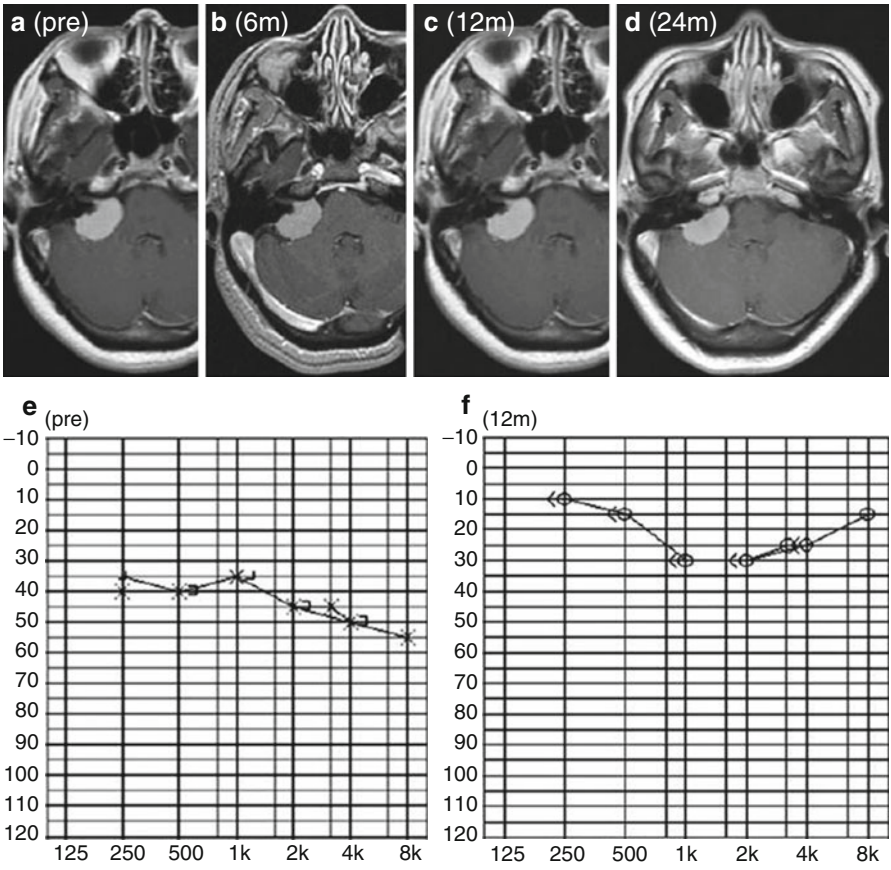

Fig. 1 A magnetic resonance imaging of a 47-year-old patient with a meningioma extending into the right internal auditory canal. The tumour volume was 5.6 cm^3, and the pure-tone audiometry (PTA) threshold and speech discrimination scores (SDS) were 40 dB and 12 %, respectively, corresponding to Gardner-Robertson (G-R) class 3 (**a** and **e**). Gamma Knife radiosurgery was performed. The maximal and mean cochlear radiation doses were 6.9 and 5.5 Gy, respectively. Six months later, the tumour volume was stable (**b**), and hearing function had improved to 30 dB of PTA and 80 % of SDS. Twelve months after radiosurgery, the tumour volume was 5.2 cm^3, and the PTA threshold and SDS were 26 dB and 90 %, respectively (**c** and **f**). Twenty-four months after radiosurgery, the tumour had continued to shrink to 4.4 cm^3 (**d**) (Adapted from Kim et al. [58])

Third, the radiation sensitivity of the cochlea was determined in a study that proved the efficacy and safety of intensity-modulated radiotherapy for paediatric patients with medulloblastoma [48]. The threshold cochlear dose in standard fractionated radiotherapy was approximately 35 Gy, which represents approximately 8 Gy of an equivalent radiosurgery dose. This indicates that the recently suggested guideline for the lowest threshold of 4 Gy may be too low [9, 44, 52, 109]. Therefore, the association between the cochlear dose and hearing outcomes after SRS for VSs most likely reflects the dose-volume relationship between the radiosurgical dose and the intracanalicular tumour volume [28, 78].

Transient Volume Expansion, Intracanalicular Pressure, and Auditory Brainstem Response

Hearing outcomes after SRS for VSs differ from those after SRS for other tumours near the IAC, as mentioned above [12, 41, 58]. The cochlear threshold dose has no effect or a minimal effect on hearing outcomes after SRS for tumours near the IAC except VSs. The features of response after SRS for VSs could differ from those after SRS for other tumours near the IAC. One such response could be a transient volume increase, i.e. TVE, which has been recognised as a common phenomenon after SRS and after stereotactic radiotherapy (SRT) for intracranial schwannomas [3, 59, 89]. TVE has also been reported, but not as frequently as in schwannomas, after radiotherapy for other intracranial benign tumours [16, 62]. Infiltration by foamy macrophages, myxoid degeneration, and/or necrosis has been suggested as the underlying histopathological causes of TVE after SRS for VSs [51]. TVE has been reported to occur in 14–74 % of patients 6–16 months after SRS or SRT for VSs [3, 46, 53, 74, 80, 91]. The wide range of its incidence could be caused by differences in the definition of TVE [59], the fractionation scheme of radiation therapy [111], and the method and timing of follow-up tumour measurements in various studies [59, 113, 114].

TVE has been regarded as a remarkable feature of VSs after SRS because it often causes neurological aggravation [40, 91]. In addition, TVE has been considered one of the principal factors that is significantly related to hearing deterioration after SRS for VSs [3, 59, 80], because the period of serviceable hearing loss after SRS often overlaps with that of the development of TVE after SRS for VSs [22, 52, 56]. TVE usually reaches its peak at 6 months after SRS and regresses 12–24 months after surgery. It is also known that most cases of post-SRS auditory neuropathy occur within 24 months, with a median onset of 6 months after SRS (Fig. 2). This finding suggests a possible relationship between post-radiosurgery hearing deterioration and TVE.

The mechanism of hearing deterioration caused by TVE might be increased intracanalicular pressure resulting in compression of the intracanalicular path of the cochlear nerve, vascular compromise of the auditory apparatus, or accumulation of intralabyrinthine protein by obstruction of the cochlear pore [5, 61]. However, the association between TVE and hearing outcomes after SRS for VSs has been controversial [59, 80, 112, 120], possibly due to differences in the definition of TVE. To exclude measurement error in the assessment of TVE, the increased volume should exceed the initial volume by at least 13–15 % for area-based manual volume measurements, especially in small-volume tumours [113, 114]. In one study in which TVE was defined as ≥10 % increase in volume, TVE was not related to hearing outcomes [112]. However, in another study in which TVE was defined as ≥30 % increase in volume, TVE was significantly associated with hearing deterioration after SRS for VSs [120]. TVE could therefore be correlated with hearing deterioration after SRS for small VSs, given a sufficient threshold of ≥20 %.

Nonetheless, to directly prove a relationship between TVE and hearing outcomes after SRS for VSs, several issues should be resolved. The first is whether pressure in the IAC can affect auditory function in the initial state before any treatment for VSs.

The second is whether a change in pressure in the IAC actually occurs after SRS for VSs, especially during the period of TVE. The last issue is whether the increased intracanalicular pressure is correlated with hearing deterioration after SRS for VSs.

During the period of the Second World War, several tests of auditory function, including Fowler's alternate loudness balance test, Carhart's test for tone decay, Bekesy audiometry, the short increment sensitivity index, and speech audiometry, were introduced, thus enabling the differentiation of neural and sensory deafness [93]. Currently, the most accurate auditory function test is the auditory brainstem response (ABR), with a quoted sensitivity of 98 %. It is certainly true that abnormalities of the ABR are found in almost all proven cases of vestibular schwannoma [93].

The mechanism by which the ABR is altered in the presence of VSs has been suggested to be compression of the auditory nerve in the internal auditory canal. Such compression has been shown to occur in an experimental animal model [17, 37] and was also recently demonstrated in humans. The intracanalicular pressure was significantly associated with the size of the tumour, which is confined only in the IAC [6, 61], and the intracanalicular pressure correlated well with the ABR values, especially wave V latency and the wave I and V interval. Overall, tumour growth has no significant relationship to changes in ABR latency during conservative management [95]. Changes in intracanalicular pressure caused by changes in tumour features such as TVE, especially in the IAC, could be indirectly identified using the ABR test after SRS for VSs.

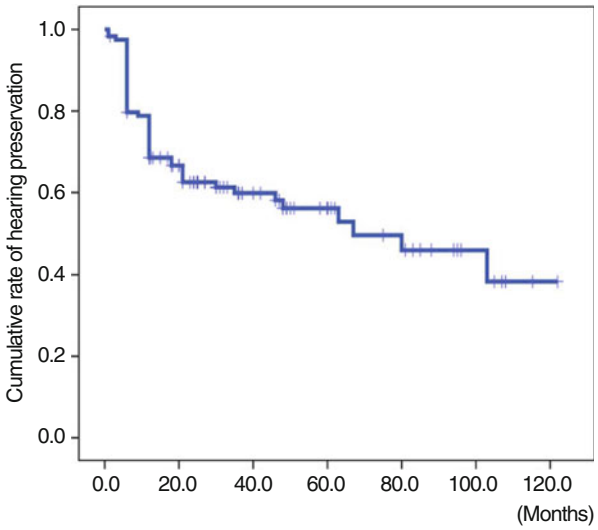

Fig. 2 This is a Kaplan-Meier plot of survival with serviceable hearing in patients with vestibular schwannoma. Until the last clinical follow-up, in total, 51 patients (42.9 %) lost their serviceable hearing. The median survival with serviceable hearing was 67 months after stereotactic radiosurgery (SRS). The actuarial rates of hearing preservation were 79.7 %, 68.5 %, 62.5 %, 59.9 %, and 56.2 % at 6 months, 12 months, 24 months, 36 months, and 60 months, respectively, after SRS. The patients usually lose their serviceable hearing within 24 months after stereotactic radiosurgery for vestibular schwannomas (Adapted from Han et al. [41])

Intracanalicular Pressure and Hearing Function

To test whether pressure in the IAC can affect auditory function, the initial state before any treatment for VSs should be evaluated. In one study [61], the intracanalicular pressure was directly measured by insertion of a microsensor into the IAC before any tumour manipulation during VS surgery via a retromastoid suboccipital approach. And then, the authors evaluated a possible relation between the intracanalicular pressure and the preoperative and intraoperative baseline ABR values.

The range of intracanalicular pressure in VS ears was 0–45 mmHg with a mean value of 15.4 mmHg, and 63 % of VS ears had intracanalicular pressure greater than or equal to 10 mmHg. These results indicate that most patients had a significant pressure difference between the IAC and the cerebellopontine angle cistern.

Patients with class A hearing as defined by the American Academy of Otolaryngology-Head and Neck Surgery [1] (AAO-HNS) (PTA < 30 dB, SD > 70 %) tend to have lower intracanalicular pressure than patients who have AAO-HNS class B hearing (PTA 30–50 dB, SD ≥ 50 %), although this difference did not reach statistical significance [61]. However, the intracanalicular pressure of patients with class A hearing was significantly lower than that of patients with AAO-HNS class C and D hearing (PTA > 50 dB, SD < 50 %) (Fig. 3) [61].

As expected, the ABR wave V latency and wave I and V interval (IL_I–V) also correlated well with intracanalicular pressure values (Fig. 4) [61]. This finding suggests that intracanalicular pressure can be indirectly estimated as a function of the ABR value in VS patients with testable hearing and especially in those with serviceable hearing.

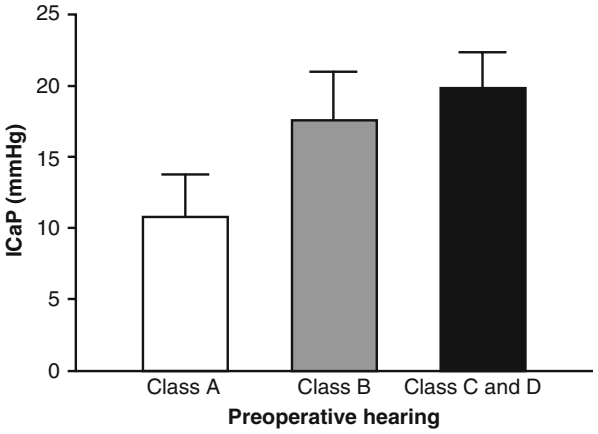

Fig. 3 Bar graph demonstrating the correlation of preoperative auditory function and intracanalicular pressure in 33 patients with intact hearing. Preoperative hearing was classified based on American Academy of Otolaryngology-Head and Neck Surgery criteria. Patients with Class A hearing had lower intracanalicular pressures. Although the difference between Class A and Class B groups was not statistically significant ($p = 0.16$), 12 patients with Class A hearing had significantly lower intracanalicular pressures compared with 12 patients in the combined Class C and D group ($p = 0.03$). Bars represent the standard error of the mean (Adapted from Lapsiwala et al. [61])

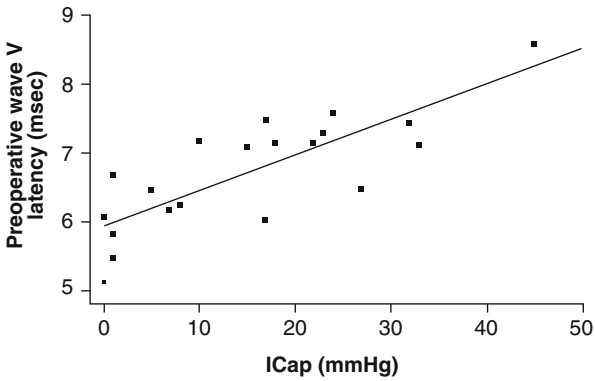

Fig. 4 Graph demonstrating the correlation of intracanalicular pressure (*ICaP*) measurements and the preoperative absolute latency of wave V in 20 patients with VS ($p=0.0001$, $r=0.75$) (Adapted from Lapsiwala et al. [61])

Pre-radiosurgery Auditory Brainstem Response and Hearing Outcome

Recently, we summarised our experience in the management of patients with VSs who were treated with SRS in our institute between 1997 and 2011. Our studies are divided into two parts. The first is based on data obtained between 1997 and 2009 and addresses whether pressure in the IAC affects auditory function in the initial state before any treatment for VSs has been performed. The second assesses data collected between 1997 and 2011 and addresses whether a change in pressure in the IAC after SRS for VSs actually occurs, especially during the period of TVE.

Among 728 VS patients treated with SRS in our institute between 1997 and 2009, 119 (16.3 %) patients with unilateral sporadic VSs who had serviceable hearing underwent SRS as primary treatment and were given a pre-radiosurgery ABR test [41]. When ABR testing showed no response regardless of the level of hearing, the maximum values of the baseline ABR tests obtained in our cohort were coded for the ABR IL_I–V value. The median tumour marginal dose was 12 Gy, and the mean tumour volume was 1.95 cm^3. The mean follow-up duration was 55 months. The actual rates of serviceable hearing preservation were 68.5 %, 62.5 %, 59.9 %, and 56.2 % at 12, 24, 36, and 60 months after SRS, respectively [41].

According to a report by Lapsiwala et al. [61], pre-radiosurgery ABR IL_I–V values did not differ between Gardner-Robertson (G-R) class 1 and class 2 [32]; they were 4.79 ± 0.62 mS and 4.82 ± 0.60 mS, respectively ($p=0.743$) (SNUH series, unpublished data). However, the initial ABR IL_I–V values of the 'post-radiosurgery serviceable hearing preservation group' were significantly different from those of the 'post-radiosurgery serviceable hearing loss group' (4.67 ± 0.49 and 4.97 ± 0.71, respectively [$p=0.007$]) (SNUH series, unpublished data). The results of multivariate analysis of prognostic factors of serviceable hearing preservation indicated that the initial PTA score and the ABR IL_I–V value remain significant and independent factors (HR, 1.072 [95 % CI, 1.046–1.098; $p<0.001$] and 1.534 [95 % CI, 1.008–2.336; $p=0.046$], respectively) [41].

The above findings suggest that the intracanalicular pressure in some regions of schwannoma ears with a serviceable hearing level on the PTA exam is already

increased. This increased intracanalicular pressure at the time of SRS could play a role in the development of hearing deterioration after SRS for VSs by adding additional pressure to the intracanalicular pressure caused by TVE. Thus, it may be possible to predict hearing outcomes after SRS for VSs according to the presence of increased intracanalicular pressure, indirectly determined by the ABR value, at the time of SRS.

Post-radiosurgery Auditory Brainstem Response Changes and Hearing Outcome

We continued the analysis of the data to determine whether a change in the intracanalicular pressure after SRS for VSs actually occurs during the period of TVE. Changes in intracanalicular pressure were measured by follow-up ABR tests after SRS. Of 936 patients treated with SRS for VSs between 1997 and 2011, 141 (15.1 %) with unilateral sporadic VSs who had serviceable hearing underwent SRS as a primary treatment and were also given pre-radiosurgery and one or more follow-up ABR tests between 1997 and 2011 (SNUH unpublished data). For patients in whom ABR testing produced no response regardless of the level of hearing, the ABR IL_I–V values were coded in the same manner as mentioned previously. The mean tumour marginal dose was 12.1 Gy, and the mean tumour volume was 1.94 cm^3. The mean follow-up duration was 57.6 months. The mean initial PTA of the patients was 25.6 dB. The analyses were performed using the follow-up data obtained within the first 12 months after SRS because TVE usually occurs within 12 months after SRS and because tumour volume increases with TVE, usually reaching a peak at 6 months after SRS and regressing during the 12–24 month period thereafter.

At 6 months post-radiosurgery, 33 (23.7 %, excluding 2 missing data points) patients lost their serviceable hearing (the ‘6-month hearing loss group’). G-R class 1 or class 2 was regarded as serviceable hearing. The mean value of the initial PTA in this group was higher than that of the patients whose serviceable hearing was preserved at 6 months post-radiosurgery (the ‘6-month hearing preservation group’) (34.73 dB vs. 22.59 dB, $p<0.001$). The mean values of PTA decreased over time; they were 56.61 dB and 58.22 dB at 6 and 12 months after SRS, respectively, in the ‘6-month hearing loss group’. The mean of the initial ABR IL_I–V values in the ‘6-month hearing loss group’ was also higher than that in the ‘6-month hearing preservation group’ (4.9242 mS vs. 4.7883 mS, $p=0.291$); however, the difference did not reach statistical significance. Interestingly, the mean ABR IL_I–V value in the ‘6-month hearing loss group’ increased over time, while that of the ‘6-month hearing preservation group’ increased at 6 months and then decreased to close to the initial level at 12 months after SRS. The difference in the mean ABR IL_I–V values of the two groups reached statistical significance at 12 months (5.2875 mS vs. 4.9427 mS at 6 months, $p=0.060$; 5.2905 mS vs. 4.7032 mS at 12 months, $p=0.001$). A representative case is illustrated in Table 3 and Fig. 5.

Table 3 The changes of post-radiosurgery auditory brainstem response and hearing outcomes

	Post-radiosurgery 6 months				Post-radiosurgery 12 months			
	Number of patients Whose data were available (Serviceable/unserviceable)	Serviceable hearing group	Unserviceable hearing group	*p* value	Number of patients Whose data were available (Serviceable/unserviceable)	Serviceable hearing group	Unserviceable hearing group	*p* value
Pre-GK PTA[a]	106/33	22.59	34.73	<0.001	81/41	21.56	34.17	<0.001
6 M PTA	101/33	26.65	56.61	<0.001	76/39	25.95	51.03	<0.001
12 M PTA	88/27	30.36	58.22	<0.001	78/39	26.00	59.90	<0.001
Pre-GK ABR IL_I–V[b]	106/33	4.7883	4.9242	0.291	81/41	4.7095	5.0300	0.008
6 M ABR IL_I–V	75/24	4.9427	5.2875	0.060	50/30	4.9146	5.2413	0.065
12 M ABR IL_I–V	74/20	4.7032	5.2905	0.001	68/28	4.6344	5.3425	<0.001

[a]The pure-tone average

[b]The interlatency of waves I and V on the auditory brainstem response

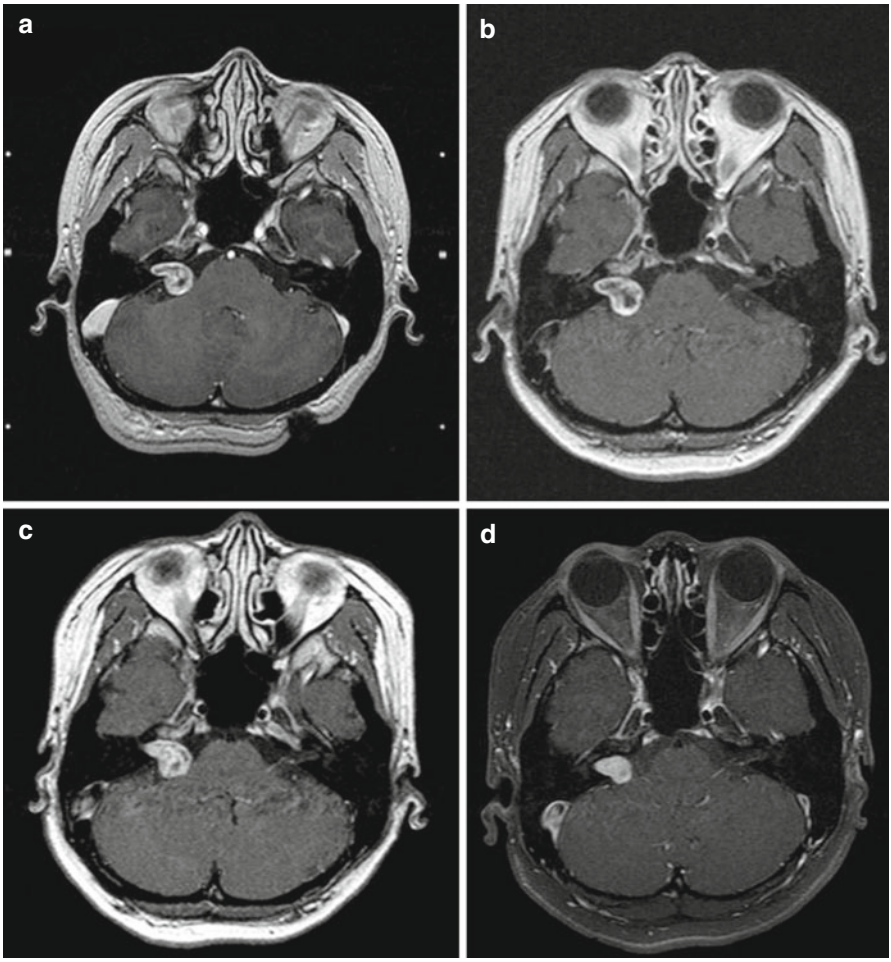

Fig. 5 Gamma Knife radiosurgery was performed using a tumour marginal dose of 12 Gy at 50 % isodose line for a 30-year-old woman with a vestibular schwannoma in the right side. The tumour volume of was 1.3 cm^3, and the pure-tone audiometry (PTA) threshold and speech discrimination scores (SDS) were 36 dB and 80 %, respectively, corresponding to Gardner-Robertson (G-R) class 2 (**a**). The interlatency of waves I and V on the auditory brainstem response (ABR IL_I–V) was 4.87 mS before stereotactic radiosurgery (**e**). Six months later, the tumour volume increased to 1.8 cm^3 (**b**) and the ABR IL_I–V also increased to 5.08 mS (**f**). However, her hearing function was slightly improved to G-R class 1. Twelve months after radiosurgery, the tumour volume decreased to 1.6 cm^3 (**c**) and interestingly the ABR IL_I–V also decreased to 4.79 mS (**g**). The hearing function was stable in the improved state as G-R class 1 at post-radiosurgery 12 months. And then the tumour volume gradually decreased until 24 months after radiosurgery to 0.9 cm^3 (**d**)

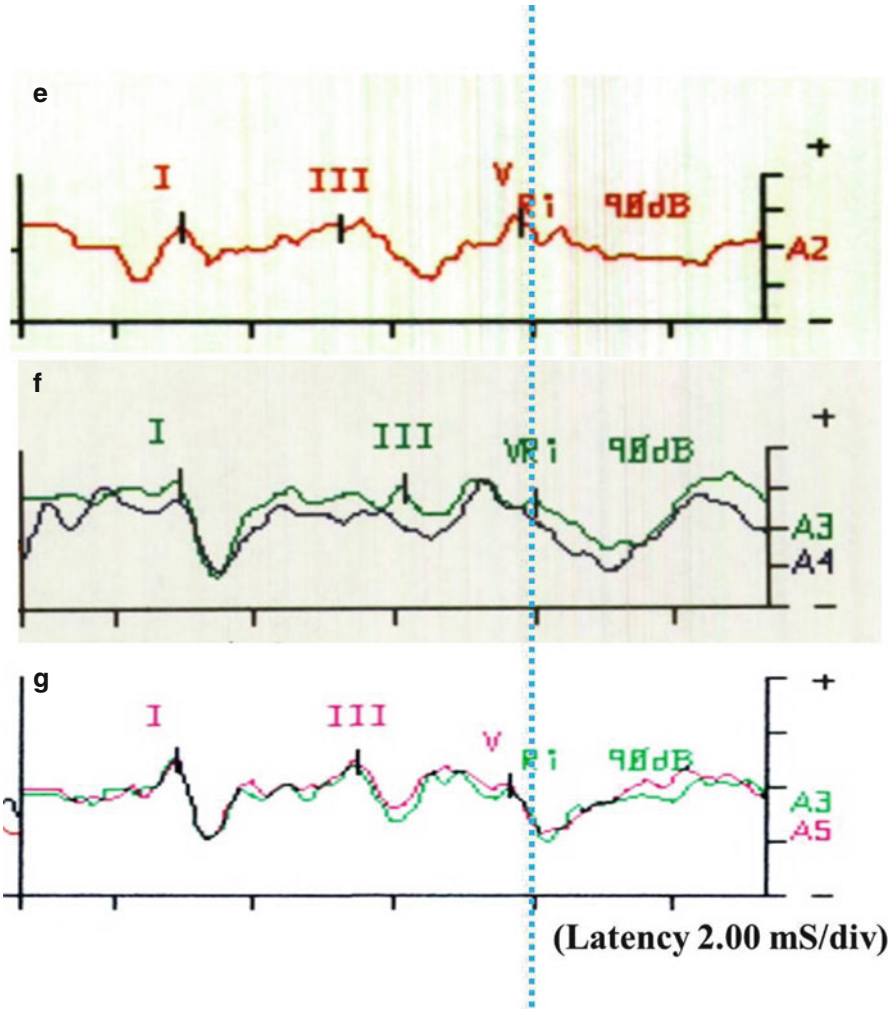

Fig. 5 (continued)

At 12 months after SRS, 41 (33.6 %, excluding 19 missing data points) patients reached an unserviceable hearing state. Changes in the ABR IL_I–V values of these patients over time showed similar patterns to those found at 6 months. The mean of the initial ABR IL_I–V values in the '12-month hearing loss group' was significantly higher than in the '12-month hearing preservation group' (5.0300 mS vs. 4.7095 mS, $p=0.008$). Similar to the trend observed at 6 months, the mean of the ABR IL_I–V values in the '12-month hearing loss group' increased over time; however, that of the '12-month hearing preservation group' increased at 6 months and then decreased below the initial level at 12 months after SRS (5.2413 mS vs. 4.9146 mS at 6 months, $p=0.065$; 5.3425 mS vs. 4.6344 mS at 12 months, $p<0.001$). The results are summarised in Table 4.

Table 4 The values of the auditory brainstem response of the illustrated case

	The wave I latency (mS)	The wave III latency (mS)	The wave V latency (mS)	The ABR IL_I–V (mS)[b]	Pure-tone average (dB)	Speech discrimination score (%)	Gardner-Robertson class
Before SRS[a]	1.49	3.74	6.36	4.87	30	80	2
Post-SRS 6 months	1.41	4.61	6.49	5.08	26	96	1
Post-SRS 12 months	1.37	3.95	6.15	4.79	26	98	1

[a]Stereotactic radiosurgery
[b]The interlatency of waves I and V on the auditory brainstem response

Prognostic factors of hearing outcomes were analysed separately according to the patients' hearing status at 6 months and at 12 months to determine the most significant time-dependent factors within the first 12 months after SRS. In the repeated analyses, $p<0.01$ was regarded as significant. Based on the results of multivariate analysis of the 6-month data, only the initial PTA value was a significant and independent factor for hearing loss (OR = 1.130; 95 % CI, 1.068–1.195; $p<0.001$) (SNUH unpublished data). Changes in ABR IL_I–V between the initial and 6-month values also tended to increase the risk of hearing deterioration (OR = 2.038; 95 % CI, 0.952–4.361; $p=0.067$); however, this association did not reach statistical significance. The results from the multivariate analysis of 12-month data, the initial PTA (OR = 1.114; 95 % CI, 1.057–1.174; $p<0.001$), the initial ABR IL_I–V value (OR = 8.799; 95 % CI, 2.678–28.91; $p<0.001$), and the change of ABR IL_I–V between the initial value and the 12-month value (OR = 3.784; 95 % CI, 1.532–9.347; $p=0.004$) were all significant and independent factors associated with hearing outcome. The cochlear dose and overall tumour volume did not reach statistical significance in the above two analyses.

In summary, ABR IL_I–V increased during the first 12 months after SRS for VSs in patients who lost their serviceable hearing. Its effect on hearing outcome also became significant over time, especially at 12 months after SRS, and was more prominent in patients with poor initial PTA and/or ABR values. We hypothesise that patients with considerable intracanalicular pressure at the time of SRS are prone to lose their serviceable hearing due to the added intracanalicular pressure resulting from TVE, which usually occurs within the first 12 months after SRS for VSs.

Seoul National University Hospital (SNUH) Classification for Prediction of Hearing Preservation After Stereotactic Radiosurgery for Vestibular Schwannomas

Based on our findings that initial intracanalicular pressure and added pressure during the period of TVE are two principal factors associated with the possible mechanism of hearing loss in patients treated with SRS for VSs, we suggested a

Table 5 Risk group splits based on the results of classification and regression trees

Risk group		Number of patients	Patients with hearing preservation	% of hearing preservation
Group A	PTA ≤ 20[a]	48	43	89.6
Group B	IL I–V < 5.225 mS and 21 ≤ PTA ≤ 30[b]	25	16	64.0
Group C	IL I–V < 5.225 mS and 31 ≤ PTA ≤ 50	31	8	25.8
Group D	IL I–V ≥ 5.225 mS and 21 ≤ PTA ≤ 50	15	1	6.7

Adapted from Han et al. [41]
[a]The pure-tone average
[b]The interlatency of waves I and V on the auditory brainstem response

classification system for the prediction of hearing preservation after SRS for VSs [36].

The most commonly used hearing level classification systems are the G-R classification and the AAO-HNS guidelines [1, 32], which are based on PTA values and SD score. However, these two classification systems are deficient in the ability to predict the exact rates of hearing preservation among patients treated with SRS for VSs. In fact, 10.9–39.2 % of patients with hearing levels of G-R class 1 lose their hearing after such treatment. Conversely, hearing can be preserved in approximately 50 % of patients who have a hearing level of G-R class 2 after SRS for VSs [52, 55, 108]. These findings cannot be explained only by the patients' initial hearing levels, which has, however, interestingly been regarded as the most important factor related to hearing outcome after SRS for VSs. In addition, we could not predict which patients with G-R class 1 hearing will lose their hearing or which patients with G-R class 2 hearing can preserve their serviceable hearing after SRS. This suggests that the underlying pathophysiology of hearing deterioration after SRS for VSs may depend on factors other than or in addition to those that determine baseline auditory function [41, 49, 52, 55].

In these circumstances, we determined another prognostic factor, the initial intracanalicular pressure measured as the initial ABR IL_I–V. Based on the two prognostic factors, the initial hearing level and ABR IL_I–V, we could propose a new classification model to predict hearing outcomes after SRS for VSs using classification and regression tree analysis [41].

Three nodes were identified, the first by an initial PTA score of 20 dB, the second by an initial ABR IL_I–V value of 5.225 mS, and the last by an initial PTA score of 30 dB. On the basis of the terminal nodes, we categorised the patients into four groups (Table 5) [41]. The ratios of patients with serviceable hearing at distant follow-up were 89.6 %, 64 %, 25.8 %, and 6.7 % for groups A–D, respectively. These results suggest that VS ears of patients with minimally deteriorated hearing before SRS have adequate space in the IAC for TVE and that the presence of this space can minimise increases in intracanalicular pressure. However, VS ears with

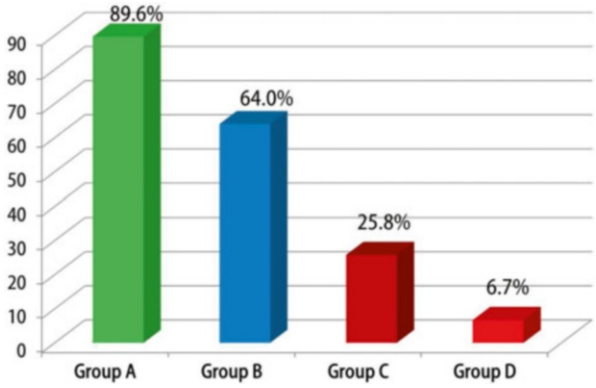

Fig. 6 The chart illustrates the rates of serviceable hearing preservation in the SNUH classification four groups based on a classification and regression tree analysis of the groups (Adapted from Han et al. [41])

considerable initial pressure before SRS, regardless of the hearing level, may not tolerate the increased pressure caused by TVE and may eventually lose their function.

This classification system could be useful in the proper selection of management modalities, especially in patients with only hearing ear schwannoma or neurofibromatosis type 2, because the predictive value is superior to those of previous classification systems. However, further studies should be performed to validate this classification system in a large population (Fig. 6).

How to Preserve and Aid Hearing After Stereotactic Radiosurgery

The improved hearing level at diagnosis of VSs due to the advancement and easy accessibility of neuroimaging makes preservation of auditory function a matter of concern in the management of patients with VSs. Prediction of hearing preservation in each individual with VSs becomes very important. Especially in cases of neurofibromatosis type 2, hearing preservation is one of the important goals of treatment. Therefore, we should be well aware of the rescue therapies for VS ears that have begun to lose their auditory function.

It is truly a blessing that the incidence of patients with poor hearing levels in the contralateral ear compared with the VS ear is not high; its incidence is approximately 1 % among patients with unilateral sporadic VSs [104], and neurofibromatosis type 2 is not common [85]. Unilateral hearing deterioration has been considered unlikely to contribute to a severe reduction in the quality of life of ordinary people with VSs [23, 35, 47]. However, based on our experience in the management of patients with VSs, most patients with unilateral hearing loss suffer from difficulties in sound localisation and verbal communication under reverberation and background noise due to loss of the benefits of binaural hearing [65, 116]. Therefore, serviceable hearing preservation should be attempted in the management of patients with VSs.

Patient Selection

Proactive treatment of small VSs in patients with good hearing should be considered carefully because of the possibility of deterioration of serviceable hearing in the early period after treatment [103]. From this point of view, the wait-and-see strategy seems to be rational, but its outcome is often not desirable. Because most patients have some degree of hearing deterioration at the diagnosis of VSs, tumour growth during the observation period may directly result in hearing loss [103, 118]. Moreover, data from studies addressing various management approaches, including the wait-and-see strategy, hearing preservation microsurgery, and even SRS for VSs, show that the better the hearing at diagnosis, the greater the chance of hearing preservation [10, 99, 104].

Two important decisions that affect hearing preservation in patients with VSs are the duration for which the wait-and-see strategy is continued and assessment of which patients are good candidates for proactive treatment. Tumour growth has typically been the endpoint of the wait-and-see strategy [8, 118]; however, it is not an ideal endpoint in terms of hearing preservation due to the deterioration of hearing that may occur regardless of tumour growth [104]. Tumour growth should be an indicator of active treatment only in patients whose hearing is already lost at diagnosis.

Less than 20 % of patients with VSs belong to AAO-HNS class 1 (PTA less than 30 dB and SD score more than 70 %), and more than 90 % of such patients already show deteriorated hearing of more than 10-dB PTA difference compared with the normal side [103]. This indicates that most VSs patients are classified as SNUH groups B–D. The tendency to hearing deterioration in VSs patients with minimal hearing loss at diagnosis is a very critical point because the chance of hearing preservation decreases from approximately 90 % to 26 %–64 % once the PTA score increases to over 20 dB, i.e. SNUH classification B–D, at the time of SRS [41]. A hearing level of PTA 20 dB may be used as an indicator of proactive treatment and as a clinical guideline to determine whether to actively treat after the wait-and-see period.

Another possible indicator of hearing outcome is the ABR value before SRS. Hearing outcome is generally very poor in patients treated with SRS for VSs who have ABR IL_I–V values over the threshold of 5.225 mS [41]. This value seems to be a threshold for proactive treatment because proactive treatment in patients with ABR IL_I–V values over 5.225 mS could shorten the duration of serviceable hearing rather than preserve hearing.

In patients with small to large VSs with serviceable hearing, hearing preservation rates after hearing preservation microsurgery range widely (2–93 %) in recent studies depending on a number of parameters, including surgical approach, pretreatment hearing level, tumour size, and nerve of origin [54]. One of the most important points of hearing preservation microsurgery is the need to shorten the learning curve of an individual neurosurgeon or neuro-otologist [99]. Hearing preservation microsurgery is not easy in some cases, especially with gross total resection, because the cranial nerves are often intermingled with the tumour capsule or with the tumour itself [82, 99].

SRS might be a superior tool for hearing preservation considering the shorter learning curve of the modality and the lower chance of damage to the cranial nerves

compared to hearing preservation microsurgery. In addition, a recent meta-analysis supports the superiority of SRS in hearing preservation in patients with VSs [76]. Each physician responsible for patients with VSs should apply the most suitable treatment before patients lose their good hearing of 20 dB or less. For patients who already have a hearing level of ≥21 dB, i.e. SNUH class B – D, multimodal or stepwise approaches should be integrated to preserve their serviceable hearing.

Radiosurgical Planning

With respect to radiosurgical planning for VSs, several issues should be considered including tumour marginal dose, distortion of magnetic resonance imaging, and the use of fractionation. The recommended dose to the tumour margin has been decreased to 12–13 Gy to help avoid cranial neuropathies and produce improved tumour control rates [18, 45, 50]. However, one should keep in mind that use of a decreased radiation dose coupled with the possible distortion of magnetic resonance images could cause some VSs to receive less than the optimal dose [92], leading to a failure of tumour control and to hearing loss. The importance of the accuracy and conformity of the prescribed dose is also shown by the fact that tumour control rates have improved with advances in the neuroimaging techniques used in radiosurgical planning, even with a decrease in the tumour marginal dose to approximately half of the dose initially used by Leksell [64]. To avoid the effect of distortion of magnetic resonance imaging on accuracy and conformity, it might be essential to use fused images of magnetic resonance images obtained at high imaging resolution and computed tomography, which has minimal imaging distortion, in radiosurgical planning [60].

Schwannomas are late-responding tissues with low proliferative indices and a low α/β ratio for the application of the linear quadratic formula [30, 66]. From a radiobiological point of view, better tumour control may be achieved with a single high dose of radiation than with multiple smaller doses [67], and normal brain sparing also favours single-fraction treatment for lesions with a low α/β ratio [72]. However, high-dose irradiation using a single fraction may result in a higher incidence of TVE, which may lead to poor hearing outcomes compared with SRT performed using multiple fractionations [111]. Therefore, fractionation techniques for VSs may yield equivalent or improved hearing preservation rates by reducing the chance of TVE [23, 29]. However, no comparative studies of hypo-fractionated SRS using 2–5 fractions vs. low-dose single-fraction SRS have been performed.

How to Manage Transient Volume Expansion and Tumour Growth

TVE is a common phenomenon after SRS for VSs [3, 59, 89]; it is caused by tumour cell necrosis or apoptosis and vascular damage [107]. Loss of central enhancement on magnetic resonance imaging has been regarded as a representative neuroimaging

feature of TVE and as a reliable indicator of tumour control [20, 70]. However, this is not always the case [111]. It is important to differentiate TVE from real tumour growth. The apparent diffusion coefficient values may be useful in differentiating TVE from tumour growth; however, their use is limited in VSs in the IAC [19].

As mentioned above, TVE may result in increased intracanalicular pressure and compression of the cochlear nerve, which can ultimately result in hearing deterioration, especially in patients in whom the IAC of the schwannoma ear does not have adequate space to buffer the increased intracanalicular pressure, i.e. SNUH class D patients. Currently, there are no proven rescue management approaches for VS patients showing hearing deterioration after SRS. Nonetheless, several possible methods to preserve or aid hearing in such patients are reviewed and discussed.

Corticosteroids

Although the specific action of steroids on the auditory apparatus is uncertain, their use has been based on their ability to decrease inflammatory reactions and neural oedema [4, 96, 117]. Thus, steroids might reduce compression of the acoustic apparatus and vascular structures by TVE after SRS for VSs [4, 56, 78, 96]. Notably, Sakamoto et al. [96] reported that hearing recovery occurred in all 8 patients who had experienced a hearing loss within 1 year after SRT for VSs. These patients were treated with a mean 30-mg daily dose of prednisone for approximately 2 weeks, and the degree of hearing recovery was approximately 10 dB.

However, our data reflect a somewhat different finding. Based on our experience, the administration of corticosteroids merely alleviates the deterioration in hearing compared with the historical control group [56]; in our study, the mean PTA score of the treated patients was significantly lower than that of the control group at distant follow-up. The difference in the mean PTA was approximately 12 dB; nonetheless, no benefit was gained in terms of serviceable hearing preservation. These conflicting results might be caused by differences in the initial PTA scores and in the patients' ages in the Hokkaido University series and our series; mean values for these parameters were 24 dB vs. 30 dB and 39 years vs. 49 years, respectively.

Two possibly more important points relevant to the different findings of these two studies are the method and timing of detection of hearing deterioration after SRS. The Hokkaido University group did not use corticosteroids in patients who already had practically useless hearing levels; in these patients, very low hearing levels were regularly found at every 3-month-interval follow-up evaluation. In contrast, we advised patients to immediately visit our clinic when they experienced a decrease in hearing level, and corticosteroids were given to all patients regardless of their hearing levels. The range of the PTA scores at visiting our clinic was wide, from 32 to 60 dB. The administration of corticosteroids might play a role in hearing preservation if it is performed for the appropriate patients (those with relatively good hearing) at the appropriate time, when hearing deterioration just begins. Recently developed smartphone-based ear-level pure-tone hearing test applications will make future studies more reliable and efficient [42].

According to our data on post-radiosurgery ABR changes, the mean of the ABR IL_I–V values in the post-radiosurgery 12-month unserviceable hearing group increased over time; however, that of the post-radiosurgery 12-month serviceable hearing group increased at 6 months and then decreased below the initial level at 12 months after SRS (5.2413 mS vs. 4.9146 mS at 6 months, $p = 0.065$; 5.3425 mS vs. 4.6344 mS at 12 months, $p < 0.001$). A similar finding was obtained in the analysis of the post-radiosurgery 6-month unserviceable and serviceable groups. This suggests that there might be a threshold of intracanalicular pressure as measured by the ABR value over which the hearing level cannot be restored; based on our data, this threshold could be near an ABR IL_I–V value of 5.000–5.225 mS.

Another point is whether a short-term (usually 2 weeks) use of corticosteroids can render the auditory apparatus able to tolerate a nearly 1-year period of standing pressure caused by TVE [4, 78, 96]. The dose of corticosteroids also should be evaluated and further compared with the doses used in patients with idiopathic sudden hearing loss [7, 117].

Decompression of the IAC

In terms of rescue therapy for hearing preservation after TVE, decompression of the IAC is another possible option. Slattery et al. [102] reported successful clinical outcomes of middle fossa decompression for hearing preservation in patients with only hearing ear schwannomas, including more than 90 % of neurofibromatosis type 2 patients. The use of this procedure preserved the hearing level in patients who had exhibited significant declines in hearing for a mean duration of approximately 2 years before being considered for middle fossa decompression. In addition, decompression can delay the need for further treatments that could result in the loss of hearing for over 40 months [31, 102]. Additionally, it is of great significance that most of the patients maintained serviceable hearing, though clinically insignificant loss of hearing developed, seemingly caused by surgical injury to the auditory apparatus.

Of note, patients who failed to preserve their preoperative hearing class apparently had poor hearing levels (≥50 dB) compared with a mean PTA of 40 dB in other patients [102]. A close reading of our SNUH classification reveals that the difference in hearing preservation rates between class B and C is large [41], which suggests a probable threshold PTA score between 30 and 50 dB. ABR values could provide additional information on decisions regarding the timing of intervention.

The effect of decompression of the IAC, which leaves the tumour itself, eventually abates in approximately 2 years because pathologies related to hearing loss, as well as tumour growth, progress over time after surgery [95, 106]. TVE has been known to persist for 1 or 2 years after its development [3, 46, 53, 74, 80, 91]. Therefore, the effect of decompression of the IAC for increased pressure due to TVE after SRS might be sufficient to produce a semipermanent effect.

In cases that show no response to corticosteroids for hearing deterioration due to TVE, decompression of the IAC could be considered. The middle fossa approach is safe and offers a better quality of postoperative hearing after resection of VSs than

other approaches [84]; however, selection of the approach primarily depends on individual anatomical considerations and the surgeons' experience.

Chemotherapy

In patients whose tumour size increases not due to TVE but by recurrence, there are not many management options for hearing preservation. Decompression of the IAC with or without internal debulking of growing tumours is one, and systemic chemotherapy might be another. Recently, the expression of vascular endothelial growth factor (VEGF) in schwannoma cells has been demonstrated especially in neurofibromatosis type 2 cases, and morphometric analysis has revealed a greater microvascular density, a larger vessel diameter, and a larger perimeter in schwannomas than in normal nerves [90]. Anti-VEGF therapy normalises the vasculature of schwannomas and successfully controls the growth of these tumours in an animal model, most likely by re-establishing a natural balance between VEGF and semaphorin 3 signalling [119]. In humans, anti-VEGF therapy reduced the volume of growing VSs in nine of ten neurofibromatosis type 2 patients, improved hearing function in four patients, and stabilised it in two of seven patients [25, 90].

Patients with a hearing response who were on anti-VEGF therapy showed progressive improvement in word recognition; this improvement usually began approximately 8 weeks after the initiation of chemotherapy and continued to improve for as long as 16 months [90]. The improved hearing was robust for 11–16 months with a median duration of treatment of 12 months (range, 3–19). The mechanism of improvement seems to be reduction in intraneural oedema as well as tumour shrinkage. Of 9 tumours that shrank after anti-VEGF treatment, six had an imaging response. Interestingly, a strong correlation was observed between the mean apparent diffusion coefficient at baseline within tumours and the per cent decrease in tumour volume at 3 months, which could provide a potential neuroimaging marker for volumetric response to anti-VEGF therapy [90]. However, VEGF-mediated angiogenesis in schwannomas is not yet fully understood, and drawbacks to this therapy are that it is limited in neurofibromatosis type 2 patients and lengthy and expensive until now.

Hearing Aids

In patients whose hearing deterioration continues over a possible threshold of the ABR IL_I–V, the use of corticosteroids, decompression of the IAC, and anti-VEGF therapy may rescue their hearing. Notwithstanding these rescue efforts, serviceable hearing may be lost eventually. In these situations, hearing aids could be helpful in improving the quality of daily life. There are several types of hearing aids that can be considered for patients with hearing loss after treatment for VSs, including a bone-anchored hearing aid (BAHA), cochlear implants, and auditory brainstem implants.

BAHA, a new type of bone conduction hearing device, has now become widely accepted for patients with conductive or mixed hearing loss as an alternative to a conventional air-conduction hearing aid [26]. Although directional hearing remains a problem for BAHA patients with unilateral hearing loss, its application has become popular [26, 65].

To place a cochlear implant, VS patients should undergo microsurgery with preservation of the cochlear nerve. However, neurofibromatosis-related schwannomas usually invade and grow within the cochlear nerve [68], and sporadic schwannomas may present the same situation as they grow. Identification of the surgical plane between the tumour and the cochlear nerve is demanding [97, 99, 100]; moreover, cochlear nerve function is not always preserved in spite of anatomical preservation of the nerve [79]. Nonetheless, the results of cochlear implantation in VS patients are promising [13, 15]. Approximately 70 % of patients achieve open-set speech discrimination, many scoring at the ceiling of audiometric testing [13]. This implies that a moderate injury that can cause hearing loss may still allow electrical transmission of the stimulus. Such transmission can be evaluated by electrical promontory stimulation [13, 15]. It is also interesting that cochlear implantation after SRS or SRT showed good results in a select group of patients with VSs [71, 110].

Lack of bilateral auditory function should be considered an indication for auditory brainstem implantation. Especially in neurofibromatosis type 2 patients, auditory brainstem implantation directly after tumour removal is a safe procedure and offers the best means of hearing rehabilitation if the cochlear nerve is not preserved [21, 101]. However, the results in neurofibromatosis type 2 cases in the literature are poor compared with the results of cochlear implantation [2, 15, 21, 87, 101, 110]. If a cochlear implant is possible, it is preferable compared to auditory brainstem implantation. The majority of indicated patients have benefitted from auditory brainstem implantation during daily life, particularly in combination with lip reading [101].

Conclusion

Advances in diagnostic tools and treatment modalities and the optimisation of radiosurgical dose have improved clinical outcomes, including tumour control and cranial neuropathies, in patients with VSs. However, preservation of hearing function still falls short of our expectations. A prediction model for the hearing preservation potential of each treatment modality will guide the proper selection of treatment modalities and the appropriate timing of active treatment, which will lead to improved hearing function in patients with VSs. In particular, patients with pre-radiosurgery good hearing levels and favourable initial values of the ABR test may have excellent hearing outcomes after SRS for VSs.

Notwithstanding these findings, most neurosurgeons and neurologists are still reluctant to recommend treatment until hearing deteriorates or is lost. This approach,

of course, could result in a self-perpetuating cycle of poor clinical hearing outcome. Most studies, including natural history data, hearing preservation microsurgery data, and hearing outcome data after SRS, have shown that early management of VSs in patients with good hearing level can result in good hearing outcomes.

References

1. Committee on Hearing and Equilibrium guidelines for the evaluation of hearing preservation in acoustic neuroma (vestibular schwannoma). American Academy of Otolaryngology-Head and Neck Surgery Foundation, INC (1995) Otolaryngol Head Neck Surg 113:179–180
2. Amoodi HA, Makki FM, Cavanagh J, Maessen H, Bance M (2012) Cochlear implant rehabilitation for patients with vestibular schwannoma: report of two cases. Cochlear Implants Int 13:124–127
3. Aoyama H, Onodera S, Takeichi N, Onimaru R, Terasaka S, Sawamura Y, Shirato H (2013) Symptomatic outcomes in relation to tumor expansion after fractionated stereotactic radiation therapy for vestibular schwannomas: single-institutional long-term experience. Int J Radiat Oncol Biol Phys 85:329–334
4. Aronzon A, Ruckenstein MJ, Bigelow DC (2003) The efficacy of corticosteroids in restoring hearing in patients undergoing conservative management of acoustic neuromas. Otol Neurotol 24:465–468
5. Asthagiri AR, Vasquez RA, Butman JA, Wu T, Morgan K, Brewer CC, King K, Zalewski C, Kim HJ, Lonser RR (2012) Mechanisms of hearing loss in neurofibromatosis type 2. PLoS One 7, e46132
6. Badie B, Pyle GM, Nguyen PH, Hadar EJ (2001) Elevation of internal auditory canal pressure by vestibular schwannomas. Otol Neurotol 22:696–700
7. Bae SC, Noh HI, Jun BC, Jeon EJ, Seo JH, Park SY, Kim JK, Lee DH, Oh JH, Park SN, Yeo SW (2013) Efficacy of intratympanic steroid therapy for idiopathic sudden sensorineural hearing loss: comparison with systemic steroid therapy and combined therapy. Acta Otolaryngol 133:428–433
8. Bakkouri WE, Kania RE, Guichard JP, Lot G, Herman P, Huy PT (2009) Conservative management of 386 cases of unilateral vestibular schwannoma: tumor growth and consequences for treatment. J Neurosurg 110:662–669
9. Baschnagel AM, Chen PY, Bojrab D, Pieper D, Kartush J, Didyuk O, Naumann IC, Maitz A, Grills IS (2013) Hearing preservation in patients with vestibular schwannoma treated with Gamma Knife surgery. J Neurosurg 118:571–578
10. Brackmann DE, Owens RM, Friedman RA, Hitselberger WE, De la Cruz A, House JW, Nelson RA, Luxford WM, Slattery WH 3rd, Fayad JN (2000) Prognostic factors for hearing preservation in vestibular schwannoma surgery. Am J Otol 21:417–424
11. Brada M (2013) Radiotherapy for benign brain tumours coming of age; example of vestibular schwannoma. Radiother Oncol 106:157–160
12. Bradley Lega JS, Michael Ruckinstein, Douglas Bigelow, Jay Dorsey, Michele Alonso-Basanta, John YK Lee (2012) Cochlear radiation dose does not predict hearing loss after gamma knife for glomus jugulare tumors. The 16th International Leksell Gamma Knife Society meeting Sydney
13. Carlson ML, Breen JT, Driscoll CL, Link MJ, Neff BA, Gifford RH, Beatty CW (2012) Cochlear implantation in patients with neurofibromatosis type 2: variables affecting auditory performance. Otol Neurotol 33:853–862
14. Carlson ML, Jacob JT, Pollock BE, Neff BA, Tombers NM, Driscoll CL, Link MJ (2013) Long-term hearing outcomes following stereotactic radiosurgery for vestibular schwannoma: patterns of hearing loss and variables influencing audiometric decline. J Neurosurg 118:579–587

15. Celis-Aguilar E, Lassaletta L, Gavilan J (2012) Cochlear implantation in patients with neurofibromatosis type 2 and patients with vestibular schwannoma in the only hearing ear. Int J Otolaryngol 2012:157497
16. Chen CH, Shen CC, Sun MH, Ho WL, Huang CF, Kwan PC (2007) Histopathology of radiation necrosis with severe peritumoral edema after gamma knife radiosurgery for parasagittal meningioma. A report of two cases. Stereotact Funct Neurosurg 85:292–295
17. Chinn J, Miller J (1975) Animal model acoustic neuroma. Arch Otolaryngol 101:222–226
18. Chopra R, Kondziolka D, Niranjan A, Lunsford LD, Flickinger JC (2007) Long-term follow-up of acoustic schwannoma radiosurgery with marginal tumor doses of 12 to 13 Gy. Int J Radiat Oncol Biol Phys 68:845–851
19. Chuang CC, Chang CS, Tyan YS, Chuang KS, Tu HT, Huang CF (2012) Use of apparent diffusion coefficients in evaluating the response of vestibular schwannomas to Gamma Knife surgery. J Neurosurg 117(Suppl):63–68
20. Chung WY, Liu KD, Shiau CY, Wu HM, Wang LW, Guo WY, Ho DM, Pan DH (2005) Gamma knife surgery for vestibular schwannoma: 10-year experience of 195 cases. J Neurosurg 102(Suppl):87–96
21. Colletti L, Shannon R, Colletti V (2012) Auditory brainstem implants for neurofibromatosis type 2. Curr Opin Otolaryngol Head Neck Surg 20:353–357
22. Combs SE, Thilmann C, Debus J, Schulz-Ertner D (2006) Long-term outcome of stereotactic radiosurgery (SRS) in patients with acoustic neuromas. Int J Radiat Oncol Biol Phys 64:1341–1347
23. Combs SE, Welzel T, Kessel K, Habermehl D, Rieken S, Schramm O, Debus J (2013) Hearing preservation after radiotherapy for vestibular schwannomas is comparable to hearing deterioration in healthy adults and is accompanied by local tumor control and a highly preserved quality of life (QOL) as patients' self-reported outcome. Radiother Oncol 106: 175–180
24. Dandy WE (1925) An operation for the total removal of cerebellopontine (acoustic) tumors. Surg Gynecol Obstet 41:129–148
25. Eminowicz GK, Raman R, Conibear J, Plowman PN (2012) Bevacizumab treatment for vestibular schwannomas in neurofibromatosis type two: report of two cases, including responses after prior gamma knife and vascular endothelial growth factor inhibition therapy. J Laryngol Otol 126:79–82
26. Faber HT, de Wolf MJ, Cremers CW, Snik AF, Hol MK (2013) Benefit of Baha in the elderly with single-sided deafness. Eur Arch Otorhinolaryngol 270:1285–1291
27. Ferri GG, Modugno GC, Pirodda A, Fioravanti A, Calbucci F, Ceroni AR (2008) Conservative management of vestibular schwannomas: an effective strategy. Laryngoscope 118: 951–957
28. Flickinger JC (2001) Cranial nerves. In: Shrieve DC (ed) Human radiation injury. Lippincott Williams & Wilkins, a Wolters Kluwer business, Philadelphia
29. Fong BM, Pezeshkian P, Nagasawa DT, De Salles A, Gopen Q, Yang I (2012) Hearing preservation after LINAC radiosurgery and LINAC radiotherapy for vestibular schwannoma. J Clin Neurosci 19:1065–1070
30. Fowler JF (1989) The linear-quadratic formula and progress in fractionated radiotherapy. Br J Radiol 62:679–694
31. Gadre AK, Kwartler JA, Brackmann DE, House WF, Hitselberger WE (1990) Middle fossa decompression of the internal auditory canal in acoustic neuroma surgery: a therapeutic alternative. Laryngoscope 100:948–952
32. Gardner G, Robertson JH (1988) Hearing preservation in unilateral acoustic neuroma surgery. Ann Otol Rhinol Laryngol 97:55–66
33. Gerosa M, Mesiano N, Longhi M, De Simone A, Foroni R, Verlicchi A, Zanotti B, Nicolato A (2010) Gamma Knife surgery in vestibular schwannomas: impact on the anterior and posterior labyrinth. J Neurosurg 113(Suppl):128–135
34. Givre A, Olivecrona H (1949) Surgical experiences with acoustic tumors. J Neurosurg 6:396–407

35. Godefroy WP, Kaptein AA, Vogel JJ, van der Mey AG (2009) Conservative treatment of vestibular schwannoma: a follow-up study on clinical and quality-of-life outcome. Otol Neurotol 30:968–974
36. Grayeli AB, Kalamarides M, Ferrary E, Bouccara D, Elgharem H, Rey A, Sterkers O (2005) Conservative management versus surgery for small vestibular schwannomas. Acta Otolaryngol 125:1063–1068
37. Greiman MC, Lusk RP (1991) Pressure-induced modifications of the acoustic nerve. Part II: Auditory brain stem responses. Am J Otolaryngol 12:12–19
38. Hajioff D, Raut VV, Walsh RM, Bath AP, Bance ML, Guha A, Tator CH, Rutka JA (2008) Conservative management of vestibular schwannomas: third review of a 10-year prospective study. Clin Otolaryngol 33:255–259
39. Han JH, Kim DG, Chung HT, Paek SH, Kim YH, Kim CY, Kim JW, Kim YH, Jeong SS (2009) Long-term outcome of gamma knife radiosurgery for treatment of typical trigeminal neuralgia. Int J Radiat Oncol Biol Phys 75:822–827
40. Han JH, Kim DG, Chung HT, Paek SH, Park CK, Kim CY, Hwang SS, Park JH, Kim YH, Kim JW, Kim YH, Song SW, Kim IK, Jung HW (2012) The risk factors of symptomatic communicating hydrocephalus after stereotactic radiosurgery for unilateral vestibular schwannoma: the implication of brain atrophy. Int J Radiat Oncol Biol Phys 84:937–942
41. Han JH, Kim DG, Chung HT, Paek SH, Park CK, Kim CY, Kim YH, Kim JW, Kim YH, Song SW, Kim IK, Jung HW (2012) Hearing preservation in patients with unilateral vestibular schwannoma who undergo stereotactic radiosurgery: reinterpretation of the auditory brainstem response. Cancer 118:5441–5447
42. Handzel O, Ben-Ari O, Damian D, Priel MM, Cohen J, Himmelfarb M (2013) Smartphone-based hearing test as an aid in the initial evaluation of unilateral sudden sensorineural hearing loss. Audiol Neurootol 18:201–207
43. Hasegawa T, Kida Y, Kato T, Iizuka H, Kuramitsu S, Yamamoto T (2013) Long-term safety and efficacy of stereotactic radiosurgery for vestibular schwannomas: evaluation of 440 patients more than 10 years after treatment with Gamma Knife surgery. J Neurosurg 118: 557–565
44. Hasegawa T, Kida Y, Kato T, Iizuka H, Yamamoto T (2011) Factors associated with hearing preservation after Gamma Knife surgery for vestibular schwannomas in patients who retain serviceable hearing. J Neurosurg 115:1078–1086
45. Hasegawa T, Kida Y, Kobayashi T, Yoshimoto M, Mori Y, Yoshida J (2005) Long-term outcomes in patients with vestibular schwannomas treated using gamma knife surgery: 10-year follow up. J Neurosurg 102:10–16
46. Hasegawa T, Kida Y, Yoshimoto M, Koike J, Goto K (2006) Evaluation of tumor expansion after stereotactic radiosurgery in patients harboring vestibular schwannomas. Neurosurgery 58:1119–1128; discussion 1119–1128
47. Hietanen A, Era P, Sorri M, Heikkinen E (2004) Changes in hearing in 80-year-old people: a 10-year follow-up study. Int J Audiol 43:126–135
48. Huang E, Strother DR, Davis QG, Chiu JK, Lu HH, Carpenter LS, Mai WY, Chintagumpala MM, South M, Grant WH, Butler EB, Woo SY (2002) Intensity-modulated radiation therapy for pediatric medulloblastoma: early report on the reduction of ototoxicity. Int J Radiat Oncol Biol Phys 52:599–605
49. Iwai Y, Yamanaka K, Kubo T, Aiba T (2008) Gamma knife radiosurgery for intracanalicular acoustic neuromas. J Clin Neurosci 15:993–997
50. Iwai Y, Yamanaka K, Shiotani M, Uyama T (2003) Radiosurgery for acoustic neuromas: results of low-dose treatment. Neurosurgery 53:282–287; discussion 287–288
51. Iwai Y, Yamanaka K, Yamagata K, Yasui T (2007) Surgery after radiosurgery for acoustic neuromas: surgical strategy and histological findings. Neurosurgery 60:ONS75–ONS82; discussion ONS82
52. Kano H, Kondziolka D, Khan A, Flickinger JC, Lunsford LD (2009) Predictors of hearing preservation after stereotactic radiosurgery for acoustic neuroma. J Neurosurg 111:863–873

53. Kapoor S, Batra S, Carson K, Shuck J, Kharkar S, Gandhi R, Jackson J, Wemmer J, Terezakis S, Shokek O, Kleinberg L, Rigamonti D (2011) Long-term outcomes of vestibular schwannomas treated with fractionated stereotactic radiotherapy: an institutional experience. Int J Radiat Oncol Biol Phys 81:647–653
54. Kari E, Friedman RA (2012) Hearing preservation: microsurgery. Curr Opin Otolaryngol Head Neck Surg 20:358–366
55. Kim CH, Chung KW, Kong DS, Nam DH, Park K, Kim JH, Hong SH, Cho YS, Chung WH, Lee JI (2010) Prognostic factors of hearing preservation after gamma knife radiosurgery for vestibular schwannoma. J Clin Neurosci 17:214–218
56. Kim JW, Kim DG, Paek SH, Chung HT, Kim YH, Han JH, Park CK, Jung HW (2011) Efficacy of corticosteroids in hearing preservation after radiosurgery for vestibular schwannoma: a prospective study. Stereotact Funct Neurosurg 89:25–33
57. Kim KM, Park CK, Chung HT, Paek SH, Jung HW, Kim DG (2007) Long-term outcomes of gamma knife stereotactic radiosurgery of vestibular schwannomas. J Korean Neurosurg Soc 42:286–292
58. Kim YH, Kim DG, Han JH, Chung HT, Kim IK, Song SW, Park JH, Kim JW, Kim YH, Park CK, Kim CY, Paek SH, Jung HW (2012) Radiosurgery for para-IAC meningiomas: the effect of radiation dose to the cochlea on hearing outcome. Int J Radiat Oncol Biol Phys 84:675–680
59. Kim YH, Kim DG, Han JH, Chung HT, Kim IK, Song SW, Park JH, Kim JW, Kim YH, Park CK, Kim CY, Paek SH, Jung HW (2013) Hearing outcomes after stereotactic radiosurgery for unilateral intracanalicular vestibular schwannomas: implication of transient volume expansion. Int J Radiat Oncol Biol Phys 85:61–67
60. Landi A, Marina R, DeGrandi C, Crespi A, Montanari G, Sganzerla EP, Gaini SM (2001) Accuracy of stereotactic localisation with magnetic resonance compared to CT scan: experimental findings. Acta Neurochir (Wien) 143:593–601
61. Lapsiwala SB, Pyle GM, Kaemmerle AW, Sasse FJ, Badie B (2002) Correlation between auditory function and internal auditory canal pressure in patients with vestibular schwannomas. J Neurosurg 96:872–876
62. Lee SR, Yang KA, Kim SK, Kim SH (2012) Radiation-induced intratumoral necrosis and peritumoral edema after gamma knife radiosurgery for intracranial meningiomas. J Korean Neurosurg Soc 52:98–102
63. Leksell L (1951) The stereotaxic method and radiosurgery of the brain. Acta Chir Scand 102:316–319
64. Leksell L (1971) A note on the treatment of acoustic tumours. Acta Chir Scand 137: 763–765
65. Lin LM, Bowditch S, Anderson MJ, May B, Cox KM, Niparko JK (2006) Amplification in the rehabilitation of unilateral deafness: speech in noise and directional hearing effects with bone-anchored hearing and contralateral routing of signal amplification. Otol Neurotol 27:172–182
66. Linskey ME (2000) Stereotactic radiosurgery versus stereotactic radiotherapy for patients with vestibular schwannoma: a Leksell Gamma Knife Society 2000 debate. J Neurosurg 93(Suppl 3):90–95
67. Linskey ME (2008) Hearing preservation in vestibular schwannoma stereotactic radiosurgery: what really matters? J Neurosurg 109(Suppl):129–136
68. Linthicum FH Jr, Brackmann DE (1980) Bilateral acoustic tumors. A diagnostic and surgical challenge. Arch Otolaryngol 106:729–733
69. Litre F, Rousseaux P, Jovenin N, Bazin A, Peruzzi P, Wdowczyk D, Colin P (2013) Fractionated stereotactic radiotherapy for acoustic neuromas: a prospective monocenter study of about 158 cases. Radiother Oncol 106:169–174
70. Lunsford LD, Kondziolka D, Maitz A, Flickinger JC (1998) Black holes, white dwarfs and supernovas: imaging after radiosurgery. Stereotact Funct Neurosurg 70(Suppl 1): 2–10

71. Lustig LR, Yeagle J, Driscoll CL, Blevins N, Francis H, Niparko JK (2006) Cochlear implantation in patients with neurofibromatosis type 2 and bilateral vestibular schwannoma. Otol Neurotol 27:512–518
72. Ma L, Sahgal A, Descovich M, Cho YB, Chuang C, Huang K, Laperriere NJ, Shrieve DC, Larson DA (2010) Equivalence in dose fall-off for isocentric and nonisocentric intracranial treatment modalities and its impact on dose fractionation schemes. Int J Radiat Oncol Biol Phys 76:943–948
73. Malhotra PS, Sharma P, Fishman MA, Grumbine FL, Tholey R, Dam VQ, Dasgupta A, Pequignot E, Willcox TO (2009) Clinical, radiographic, and audiometric predictors in conservative management of vestibular schwannoma. Otol Neurotol 30:507–514
74. Mandl ES, Meijer OW, Slotman BJ, Vandertop WP, Peerdeman SM (2010) Stereotactic radiation therapy for large vestibular schwannomas. Radiother Oncol 95:94–98
75. Maniakas A, Saliba I (2012) Conservative management versus stereotactic radiation for vestibular schwannomas: a meta-analysis of patients with more than 5 years' follow-up. Otol Neurotol 33:230–238
76. Maniakas A, Saliba I (2012) Microsurgery versus stereotactic radiation for small vestibular schwannomas: a meta-analysis of patients with more than 5 years' follow-up. Otol Neurotol 33:1611–1620
77. Massager N, Nissim O, Delbrouck C, Delpierre I, Devriendt D, Desmedt F, Wikler D, Brotchi J, Levivier M (2007) Irradiation of cochlear structures during vestibular schwannoma radiosurgery and associated hearing outcome. J Neurosurg 107:733–739
78. Massager N, Nissim O, Delbrouck C, Devriendt D, David P, Desmedt F, Wikler D, Hassid S, Brotchi J, Levivier M (2006) Role of intracanalicular volumetric and dosimetric parameters on hearing preservation after vestibular schwannoma radiosurgery. Int J Radiat Oncol Biol Phys 64:1331–1340
79. Merkus P, Lella FD, Trapani GD, Pasanisi E, Beltrame MA, Zanetti D, Negri M, Sanna M (2014) Indications and contraindications of auditory brainstem implants: systematic review and illustrative cases. Eur Arch Otorhinolaryngol 271:3–13
80. Nagano O, Higuchi Y, Serizawa T, Ono J, Matsuda S, Yamakami I, Saeki N (2008) Transient expansion of vestibular schwannoma following stereotactic radiosurgery. J Neurosurg 109: 811–816
81. Niranjan A, Mathieu D, Flickinger JC, Kondziolka D, Lunsford LD (2008) Hearing preservation after intracanalicular vestibular schwannoma radiosurgery. Neurosurgery 63:1054–1062; discussion 1062–1053
82. Nonaka Y, Fukushima T, Watanabe K, Friedman AH, Sampson JH, McElveen JT Jr, Cunningham CD 3rd, Zomorodi AR (2013) Contemporary surgical management of vestibular schwannomas: analysis of complications and lessons learned over the past decade. Neurosurgery 72:ons103–ons115; discussion ons115
83. Northfield DW (1970) Surgical treatment of acoustic neurinoma. The conventional approach. Proc R Soc Med 63:769–775
84. Noudel R, Gomis P, Duntze J, Marnet D, Bazin A, Roche PH (2009) Hearing preservation and facial nerve function after microsurgery for intracanalicular vestibular schwannomas: comparison of middle fossa and retrosigmoid approaches. Acta Neurochir (Wien) 151: 935–944; discussion 944–935
85. Odat HA, Piccirillo E, Sequino G, Taibah A, Sanna M (2011) Management strategy of vestibular schwannoma in neurofibromatosis type 2. Otol Neurotol 32:1163–1170
86. Paek SH, Chung HT, Jeong SS, Park CK, Kim CY, Kim JE, Kim DG, Jung HW (2005) Hearing preservation after gamma knife stereotactic radiosurgery of vestibular schwannoma. Cancer 104:580–590
87. Pai I, Dhar V, Kelleher C, Nunn T, Connor S, Jiang D, O'Connor AF (2013) Cochlear implantation in patients with vestibular schwannoma: a single United Kingdom center experience. Laryngoscope 123:2019–2023
88. Pennybacker JB, Cairns H (1950) Results in 130 cases of acoustic neurinoma. J Neurol Neurosurg Psychiatry 13:272–277

89. Phi JH, Paek SH, Chung HT, Jeong SS, Park CK, Jung HW, Kim DG (2007) Gamma Knife surgery and trigeminal schwannoma: is it possible to preserve cranial nerve function? J Neurosurg 107:727–732
90. Plotkin SR, Stemmer-Rachamimov AO, Barker FG 2nd, Halpin C, Padera TP, Tyrrell A, Sorensen AG, Jain RK, di Tomaso E (2009) Hearing improvement after bevacizumab in patients with neurofibromatosis type 2. N Engl J Med 361:358–367
91. Pollock BE (2006) Management of vestibular schwannomas that enlarge after stereotactic radiosurgery: treatment recommendations based on a 15 year experience. Neurosurgery 58:241–248; discussion 241–248
92. Pollock BE, Link MJ, Foote RL (2009) Failure rate of contemporary low-dose radiosurgical technique for vestibular schwannoma. J Neurosurg 111:840–844
93. Ramsden RT (1995) The bloody angle: 100 years of acoustic neuroma surgery. J R Soc Med 88:464–468
94. Raut VV, Walsh RM, Bath AP, Bance ML, Guha A, Tator CH, Rutka JA (2004) Conservative management of vestibular schwannomas – second review of a prospective longitudinal study. Clin Otolaryngol Allied Sci 29:505–514
95. Rosenberg SI (2000) Natural history of acoustic neuromas. Laryngoscope 110:497–508
96. Sakamoto T, Shirato H, Takeichi N, Aoyama H, Kagei K, Nishioka T, Fukuda S (2001) Medication for hearing loss after fractionated stereotactic radiotherapy (SRT) for vestibular schwannoma. Int J Radiat Oncol Biol Phys 50:1295–1298
97. Samii M (1995) Hearing preservation in bilateral acoustic neurinomas. Br J Neurosurg 9:413–424
98. Samii M, Gerganov V, Samii A (2008) Hearing preservation after complete microsurgical removal in vestibular schwannomas. Prog Neurol Surg 21:136–141
99. Samii M, Matthies C (1997) Management of 1000 vestibular schwannomas (acoustic neuromas): hearing function in 1000 tumor resections. Neurosurgery 40:248–260; discussion 260–242
100. Samii M, Matthies C, Tatagiba M (1997) Management of vestibular schwannomas (acoustic neuromas): auditory and facial nerve function after resection of 120 vestibular schwannomas in patients with neurofibromatosis 2. Neurosurgery 40:696–705; discussion 705–696
101. Sanna M, Di Lella F, Guida M, Merkus P (2012) Auditory brainstem implants in NF2 patients: results and review of the literature. Otol Neurotol 33:154–164
102. Slattery WH, Hoa M, Bonne N, Friedman RA, Schwartz MS, Fisher LM, Brackmann DE (2011) Middle fossa decompression for hearing preservation: a review of institutional results and indications. Otol Neurotol 32:1017–1024
103. Stangerup SE, Caye-Thomasen P (2012) Epidemiology and natural history of vestibular schwannomas. Otolaryngol Clin North Am 45(257–268):vii
104. Stangerup SE, Caye-Thomasen P, Tos M, Thomsen J (2008) Change in hearing during 'wait and scan' management of patients with vestibular schwannoma. J Laryngol Otol 122: 673–681
105. Sughrue ME, Kaur R, Kane AJ, Rutkowski MJ, Yang I, Pitts LH, Tihan T, Parsa AT (2011) Intratumoral hemorrhage and fibrosis in vestibular schwannoma: a possible mechanism for hearing loss. J Neurosurg 114:386–393
106. Sughrue ME, Yang I, Aranda D, Lobo K, Pitts LH, Cheung SW, Parsa AT (2010) The natural history of untreated sporadic vestibular schwannomas: a comprehensive review of hearing outcomes. J Neurosurg 112:163–167
107. Szeifert GT, Figarella-Branger D, Roche PH, Regis J (2004) Histopathological observations on vestibular schwannomas after Gamma Knife radiosurgery: the Marseille experience. Neurochirurgie 50:327–337
108. Thomas C, Di Maio S, Ma R, Vollans E, Chu C, Math M, Clark B, Lee R, McKenzie M, Martin M, Toyota B (2007) Hearing preservation following fractionated stereotactic radiotherapy for vestibular schwannomas: prognostic implications of cochlear dose. J Neurosurg 107:917–926

109. Timmer FC, Hanssens PE, van Haren AE, Mulder JJ, Cremers CW, Beynon AJ, van Overbeeke JJ, Graamans K (2009) Gamma knife radiosurgery for vestibular schwannomas: results of hearing preservation in relation to the cochlear radiation dose. Laryngoscope 119:1076–1081
110. Trotter MI, Briggs RJ (2010) Cochlear implantation in neurofibromatosis type 2 after radiation therapy. Otol Neurotol 31:216–219
111. van de Langenberg R, Dohmen AJ, de Bondt BJ, Nelemans PJ, Baumert BG, Stokroos RJ (2012) Volume changes after stereotactic LINAC radiotherapy in vestibular schwannoma: control rate and growth patterns. Int J Radiat Oncol Biol Phys 84:343–349
112. van Eck AT, Horstmann GA (2005) Increased preservation of functional hearing after gamma knife surgery for vestibular schwannoma. J Neurosurg 102(Suppl):204–206
113. Varughese JK, Wentzel-Larsen T, Vassbotn F, Moen G, Lund-Johansen M (2010) Analysis of vestibular schwannoma size in multiple dimensions: a comparative cohort study of different measurement techniques. Clin Otolaryngol 35:97–103
114. Vokurka EA, Herwadkar A, Thacker NA, Ramsden RT, Jackson A (2002) Using Bayesian tissue classification to improve the accuracy of vestibular schwannoma volume and growth measurement. AJNR Am J Neuroradiol 23:459–467
115. Wanibuchi M, Fukushima T, Friedman AH, Watanabe K, Akiyama Y, Mikami T, Iihoshi S, Murakami T, Sugino T, Mikuni N (2014) Hearing preservation surgery for vestibular schwannomas via the retrosigmoid transmeatal approach: surgical tips. Neurosurg Rev 37:431–444
116. Wazen JJ, Spitzer JB, Ghossaini SN, Fayad JN, Niparko JK, Cox K, Brackmann DE, Soli SD (2003) Transcranial contralateral cochlear stimulation in unilateral deafness. Otolaryngol Head Neck Surg 129:248–254
117. Wei BP, Stathopoulos D, O'Leary S (2013) Steroids for idiopathic sudden sensorineural hearing loss. Cochrane Database Syst Rev 7:CD003998
118. Whitehouse K, Foroughi M, Shone G, Hatfield R (2010) Vestibular schwannomas – when should conservative management be reconsidered? Br J Neurosurg 24:185–190
119. Wong HK, Lahdenranta J, Kamoun WS, Chan AW, McClatchey AI, Plotkin SR, Jain RK, di Tomaso E (2010) Anti-vascular endothelial growth factor therapies as a novel therapeutic approach to treating neurofibromatosis-related tumors. Cancer Res 70:3483–3493
120. Wowra B, Muacevic A, Jess-Hempen A, Hempel JM, Muller-Schunk S, Tonn JC (2005) Outpatient gamma knife surgery for vestibular schwannoma: definition of the therapeutic profile based on a 10-year experience. J Neurosurg 102(Suppl):114–118

Merits and Limits of Tractography Techniques for the Uninitiated

Christopher Nimsky, Miriam Bauer, and Barbara Carl

Contents

C. Nimsky (✉) • M. Bauer • B. Carl
Department of Neurosurgery, University Marburg,
Baldingerstrasse, Marburg 35033, Germany
e-mail: nimsky@med.uni-marburg.de

J. Schramm (ed.), *Advances and Technical Standards in Neurosurgery,*
Advances and Technical Standards in Neurosurgery, Vol. 43,
DOI 10.1007/978-3-319-21359-0_2

Abstract The implementation of fiber tracking or tractography modules in commercial navigation systems resulted in a broad availability of visualization possibilities for major white matter tracts in the neurosurgical community. Unfortunately the implemented algorithms and tracking approaches do not represent the state of the art of tractography strategies and may lead to false tracking results. The application of advanced tractography techniques for neurosurgical procedures poses even additional challenges that relate to effects of the individual anatomy that might be altered by edema and tumor, to stereotactic inaccuracies due to image distortion, as well as to registration inaccuracies and brain shift.

Keywords Diffusion modeling • Diffusion-weighted magnetic resonance imaging • Fiber tracking • Functional navigation • Major white matter tracts • Tractography

Introduction

Diffusion-weighted magnetic resonance imaging (DW-MRI) is a noninvasive imaging technique providing information about the microstructure of the brain in vivo. It is based on measuring the direction-dependent diffusion of water molecules, i.e., it depicts differences in tissue anisotropy. Diffusion is anisotropic, i.e., orientation-dependent, in areas with a strong aligned microstructure, like major white matter tracts.

DW-MRI has been increasingly used in imaging neuroscience over the last decade. An early form of this technique, diffusion tensor imaging (DTI) was rapidly implemented by major MRI scanner companies as a scanner selling point. Due to the ease of use of such implementations, and the plausibility of some of their results, DTI was leapt on by imaging neuroscientists who saw it as a powerful and unique new tool for exploring the structural connectivity of the human brain. However, DTI is a rather approximate technique, and its results have frequently been given implausible interpretations that have escaped proper critique and have appeared misleadingly in journals of high reputation [31].

Despite the wealth of publications, performing clinical research using DW-MRI is absolutely not straightforward. There is a plethora of available processing and analysis methods for DW-MRI, including multiple software platforms, data models, algorithms, and philosophies. Complicating the picture further, changes in the most commonly measured quantities are not specific to particular brain pathology. It is clear we can measure statistically significant brain changes with DW-MRI, but what do they mean? Today, the chief pitfall in applying DW-MRI to clinical research may well be the challenge of understanding and interpreting its meaning [53].

Tractography is the name given to any computational method that attempts to reconstruct white matter fiber tracts or “trace brain connections” based on DW-MRI

data. Accurately estimating the course of the brain's connections from DW-MRI is a difficult technical problem; therefore many methods for performing tractography have been developed [29, 53].

Most neurosurgical publications applying tractography techniques to real-world surgical procedures are dealing with DTI-based tractography approaches, despite that the DTI-based approach has several methodological limitations and pitfalls that may explain the failure of tractography in a clinical setting. Visualization of major white matter tracts has become routine in many neurosurgical centers due to the broad availability of free tractography software packages and integration of tractography algorithms in commercial navigation systems [14, 47, 51]. There are various reports on the beneficial effects of tractography techniques in several different neurosurgical procedures ranging from glioma surgery, surgery for vascular lesions, epilepsy surgery, and deep brain stimulation procedures [57]. However, there are also several reports and comments that emphasize that these techniques should not be used in the surgical environment uncritically [20, 21].

It is beyond this review to give a comprehensive overview on DW-MRI and tractography methods; it is rather the aim to show some examples for potential pitfalls of tractography techniques and to nevertheless provide some advice and how these techniques can be applied in a neurosurgical setting as well as to encourage to apply advanced DW-MRI and tractography methods.

DTI-Based Tractography

In 1994 the tensor model was introduced to describe the diffusion properties of water in white matter [6]. With DTI it was possible to noninvasively measure the organization and integrity of white matter fibers by quantifying the movement of water molecules inside the tissue. The tensor model was the simplest and probably most elegant way to characterize the diffusion, requiring only six parameters to be estimated. Understandably, the tensor model oversimplifies the underlying neuroanatomy. Thus it is important to interpret results derived from the tensor model with care [63].

Visualization

For visualization of these tensors, glyphs, generally defined as small visual representations of multivariate information, in the shape of ellipsoids were used. Isotropic diffusion can be represented as a sphere, whereas anisotropic diffusion is expressed as an ellipsoid, with the water molecules moving along the long axis of a fiber bundle and less movement perpendicularly. The ellipsoid can capture directionality and magnitude of all three eigenvectors. Tensors of rank two would be sufficient to describe the directionality of a voxel if the contents were all aligned in the

individual voxel. However, mapping a single tensor at each voxel is not sufficient to describe more complex fiber configurations and is in fact misleading [42].

Tractography

Soon after the introduction of the tensor model describing the diffusion behavior, tractography algorithms were proposed to reconstruct 3-D trajectories of major white matter tracts. The basic aim of tractography is to compute paths through the directional information that is visualized using glyphs [7, 17, 32, 44].

Tractography is probably the most clinically appealing and understandable technique for representing major white matter tracts in the neurosurgical context. Various tracking algorithms which compare local tensor field orientations measured by DTI from voxel to voxel have been developed, allowing a noninvasive tracing of large fiber tract bundles in the human brain.

DTI gained a wide clinical application in brain tumors, spinal cord diseases, epilepsy, diffuse axonal injury, multiple sclerosis, Alzheimer disease, and ischemic stroke; for an overview, see [38]. DTI tractography was established in the clinical routine in neurosurgery in the last decade. This was facilitated due to multiple free software packages, as well as the integration of tractography modules in the major commercial navigation software systems, so that DTI-based tractography has gained a broad application in neurosurgery [23]. DTI tractography provides information about the course, the displacement, or interruption of white matter tracts around a tumor, and a widening of fiber bundles due to edema or tumor infiltration can be detected.

Deterministic/Probabilistic Tractography

There are several principally different approaches to reconstruct major white matter tracts. Most tractography algorithms in common use rely on line propagation techniques to delineate white matter pathways. This general class of methods is also often referred to as deterministic streamline fiber tractography. These rely on the identification of a suitable position from which to initiate the algorithm (the seed point), the propagation of the track along the estimated fiber orientation, and the termination of the track when appropriate termination criteria are met.

Noise in the DW-MRI measurements will inevitably introduce uncertainty in the estimated fiber orientations, which may in turn introduce errors in the delineated pathway. These errors can lead to completely different connections being identified, as a small error at one point in the track can cause the algorithm to enter and follow a different white matter pathway. Unfortunately, deterministic tractography algorithms only provide a single estimate of the path of white matter fibers from each supplied seed point, without any indication of the confidence interval that can be placed around this estimate. Probabilistic tractography algorithms attempt to

address this limitation by providing their results in the form of a probability distribution, rather than a single "best fit" estimate. It should be emphasized that probabilistic methods are not more "accurate" than their deterministic counterparts, as they rely on the same underlying model. Many probabilistic tractography methods are based on deterministic techniques and hence suffer from the same limitations. As with deterministic approaches, manual guidance such as region of interest (ROI)-based editing may be needed to ensure the validity of the probabilistic results. The main benefit of probabilistic approaches, however, is that they can provide an estimate of the "precision" with which a tract pathway has been reconstructed. It is also critical to emphasize that the probability values produced by these algorithms are in no way related to the "connectivity" (e.g., number of axons) of the corresponding white matter pathways; they merely reflect the confidence that the particular connection of interest exists [63].

Compared to deterministic approaches in which the estimated fiber orientation (e.g., direction of maximum diffusivity for the tensor model) is assumed to represent the best estimate to propagate streamlines, probabilistic methods generate multiple solutions to reflect also the variability or "uncertainty" of the estimated fiber orientation. These methods, therefore, provide additional information on the reproducibility of each tractography reconstruction by mapping the intrinsic uncertainty of individual diffusion data sets. The magnetic resonance noise, partial volume effects, and inaccuracy of the chosen diffusion model mainly drive the uncertainty quantified by probabilistic tractography. Therefore, the probability of individual maps should not be considered as a direct measure of the anatomical probability of the tract. Indeed, in some cases trajectories based on artifacts can have high probability similar to true anatomical pathways. Ultimately, in datasets without noise, both deterministic and probabilistic approaches based on the same diffusion model would generate identical tractography maps [18].

A common misconception in the clinical setting is that the problems experienced using DTI-based tractography methods can be addressed by the application of more complex fiber tracking algorithms to fiber orientations estimated using the tensor model. The direct comparison of tensor-based data analyzed using a deterministic algorithm versus a probabilistic algorithm emphasizes that, while there remain some advantages to using probabilistic algorithms, the application of such an algorithm cannot compensate for fundamental limitations of the fiber orientation estimates obtained using the tensor model. The probabilistic tractography remains limited by the poor-quality fiber orientation information provided by the diffusion tensor model and does not alone provide an acceptable clinical solution [22].

Initial Neurosurgical Application

Bringing tractography techniques to neurosurgical applications the primary attempt was the visualization of the pyramidal tract, since the pyramidal tract represents the largest tract system, that should be traceable most easily and that should be most

robust against tracking errors. DTI tractography was increasingly used in the resection of both high- and low-grade gliomas [1, 19]. More complex situations include the visualization of the optic radiation and the complex language tract system [12].

Challenges in Tractography

To highlight the aspects of challenges of tractography strategies that apply also for the clinical setting, some aspects of the reconstruction of the pyramidal tract are detailed as most practitioners feel that it is the easiest traceable structure. The placement of seed regions becomes crucial for reconstruction of complex tract systems, even for the most prominent tract system, the pyramidal tract. This is of importance as emphasized by Kamali et al.: Many DTI studies seed the ROIs for tractography of the corticospinal tract at the pons and higher levels including the midbrain, internal capsule, or motor cortex. These studies mix the corticospinal and corticopontocerebellar tracts specifically the frontopontocerebellar tract which runs side by side with the corticospinal tract and inserts into the motor cortex. By adding a ROI below the level of the pons, for example, at the pontomedullary junction or medulla, the corticopontocerebellar pathways will be excluded as they have already crossed to the contralateral cerebellum at the level of the pons. In vivo depiction of three-dimensional anatomy of the major white matter tracts by fiber tracking is becoming more commonly used in preoperative and intraoperative planning of lesions located close to these eloquent brain structures to avoid postoperative deficits. It is very important to realize that even small misplacement of the ROI for the tracking algorithm may result in significantly different reconstructed fiber tracts. Better understanding of technical limitations and accurate placement of ROIs to distinguish the complex anatomical relationships between fiber tracts are essential to avoid confusing the neighboring fiber bundles with variant physiologic significance [33].

The challenges facing DTI tractography of the corticobulbar tract have been the crossing fibers at the white matter of the superior corona radiata at the centrum semiovale just lateral to the lateral ventricles. At the centrum semiovale, there is a heavy load of fiber bundles directed in the anterior–posterior orientation such as the superior longitudinal fasciculus intersecting with the vertically oriented ascending and descending fiber bundles. These crossing fibers result in intra-voxel orientation heterogeneity, which lowers the sensitivity and specificity of both probabilistic and deterministic tractography algorithms. Complex fiber architecture within the voxel may result in abrupt abortion of the tractography algorithm (false-negative result) or creation of incorrect fiber bundles as a result of switching to adjacent fiber tracts (false-positive result) due to the crossing and kissing fiber phenomenon. This phenomenon has been a major obstacle for tractography of the corticobulbar tracts in DTI studies using the single-tensor model. Since the corticobulbar tract projects to the lateral aspect of the motor cortex, the neurons have to bend laterally at the centrum semiovale; hence crossing fibers become the major issue for fiber tracking of the corticobulbar tract. The same issue has been a major obstacle in the way of study

of the lateral projections of the corticospinal tract corresponding to the somatotopic distribution of the motor cortex related to the arms and face using single-tensor tractography model [33].

Further Limitations

Despite of its fundamental limitations, DTI-based tractography is still the most widely applied tractography method in neurosurgical settings to delineate major white matter tracts. Correct identification of areas of fiber crossings is not possible by standard DTI because of its inability to resolve more than a single axon direction within each imaging voxel. Techniques, that can resolve multiple axon directions within a single voxel, try to solve the problem of white matter fiber crossings, as well as the problem to reconstruct the correct white matter insertions into the cortex.

The limitations of DTI tractography explain to some extent the heterogeneous and quite controversial evaluation of DTI tractography as a useful clinical tool for neurosurgeons ranging from positive statements like: "The concept of visualizing white matter tract anatomic relationships to guide surgical resection and clinical management certainly offers the potential of a paradigm shift in surgical practice. Just as neuronavigation has become the standard of practice across neurosurgery for discrete anatomic localization, the functional interplay of a given pathology and the eloquent cortical and subcortical structures, as revealed through multimodality imaging technologies, can only serve to improve the safety and efficacy of neurosurgical practice" [9] to very skeptical, even warning statements: "In summary, there is a double risk of DTI, (1) to not select a patient for surgery while the tumor was actually operable, or (2) to stop the resection prematurely, with a lower impact on the natural history of the disease. Last but not least, the risk for young neurosurgeons who use DTI regularly in the operating theater is becoming dependent on neuroimaging. The danger is for them to not learn optimally the functional anatomy of the brain by combining anatomic dissection, intraoperative electrical mapping, and models of cognitive neuroscience and thus to not be able to operate in the central nervous system without any intrasurgical neuroimaging, on the sole basis of their own mental imaging validated by online feedback provided by electrophysiology" [20].

Tractography in the Operating Room

Independent of the basic diffusion modeling and tractography method applied, there are additional challenges due to the specific neurosurgical setting compared to a pure neuroscientific approach that might have its sole focus in identifying and analyzing connectivity patterns.

Special problems in patients compared to healthy volunteers relate to the disease that might directly or indirectly affect the results of tractography. In patients, the time for imaging, i.e., the raw data acquisition, is restricted compared to volunteers, since patients might not be able to lie in a scanner for a longer time, without the risk of movement artifacts. In lesional cases the lesion itself, e.g., a tumor, and edema surrounding the lesion impede imaging and tractography. If the tractography results are to be integrated in a stereotactic/navigational setup, then the spatial accuracy of the raw data becomes a major concern.

The pyramidal tract as the most prominent white matter structure was the first target for intraoperative visualization and integration in modern navigation systems. This led to an extension of the concept of functional navigation [50], which was initially based on integrating functional data from functional magnetic resonance imaging (fMRI) or magnetoencephalography (MEG) for delineation of eloquent cortical brain areas. With the help of DTI tractography, also eloquent subcortical structures could be visualized in the surgical field.

Intraoperative Visualization

So what are the special needs of the neurosurgeon? For the visualization in the operating room and especially in the surgical field applying heads-up technology of modern navigation microscopes, most approaches provided by basic neuroscience did not satisfy the needs for neurosurgical use. Tensor glyphs visualizing DW-MRI data, as well as advanced renderings of anatomical tracts with graph-based representations of functional connectivity data visualizing the human connectome [42], all illustrate different aspects of major white matter tracts and connectivity; however these may not be suitable or the ideal solution for the representation in the clinical routine or even directly in the surgical field.

There is the risk of an information overflow when applying the heads-up display technology in operating microscopes distracting the neurosurgeon from the task of removing a tumor if a plethora of colored streamlines is superimposed on the surgical field. A flexible and user-driven intraoperative visualization is mandatory. For example, the interactive visualization of fiber tracts in the close proximity of a lesion allows an intuitive handling of the tractography data in the surgical context [25].

For clinical intraoperative use, the actual border of a major white matter tract is of main interest. A line or tube representation like the visualization in standard tractography lacks the ability to provide a border, so the user has to interpret the visualization as a model for the whole tract. The generation of hulls is a possibility to overcome this drawback. A surface wrapping a particular subset of previously computed streamlines represents a certain fiber tract bundle [47]. This results in an intuitive visualization of the tract system of interest as a 3-D object. The combination with volume rendering of anatomical MRI data provides a good spatial orientation. Alternatively to a wrapping approach of the streamlines from tractography,

volume-growing techniques are also a possibility to generate 3-D objects representing major white tracts.

Spatial Accuracy

When tractography results are incorporated into a 3-D navigational setting, image distortion is an important factor influencing the spatial accuracy, independent of the tractography method and quality. Echo planar imaging (EPI) distortions are caused by magnetic susceptibility differences and concomitant fields and result in displaced tractography results. These distortions mainly manifest themselves as displacements along the phase encoding direction. The correction of EPI distortion using an image-based registration approach showed a significant improvement in tract consistency and accuracy [27, 43]. Propeller EPI is an alternative approach for distortion correction demonstrated in a Q-ball imaging study [15].

All challenges relating to navigation accuracy like registration errors and intraoperative events like brain shift [26, 45, 46] further diminish the spatial accuracy and apply also to tractography integrated in navigational settings [47–49, 51].

Image distortion, registration inaccuracies among different imaging modalities, patient registration inaccuracies, and inaccuracies due to positional shift, and brain shift, have to be taken into account, when intraoperative electrophysiological mapping methods are directly compared in a spatial fashion to tractography – this is independent to all the problems and challenges of DW-MRI, modeling the diffusion behavior and tractography itself.

Validation

To select an appropriate approach to delineate major white matter tracts for neurosurgical needs, the validation of tractography results would be a crucial factor. Tractography relies on complex mathematical models that provide anatomical information indirectly, which cannot be validated easily. In humans, up to now, tractography has mainly been validated by a qualitative comparison with data obtained from dissection. No quantitative comparison was possible because MRI and dissection data are obtained in different reference spaces and because fiber tracts are progressively destroyed by dissection. A recent paper proposes a method of fiber tract dissection in an ex vivo reference space [69], which might be able to overcome this shortcoming. There is no gold standard to which human tractography can be compared. Our knowledge of human neuroanatomy comes primarily from postmortem investigation using techniques such as the Klingler dissection technique and from invasive tracer injection studies in non-human primates. Particularly for white matter pathways involved in language, there could be significant interspecies variation that impacts how easily tracer studies translate to humans. Hence,

validation of diffusion MRI consists of scanning animals in which we have a de facto ground truth connectivity profile from other means or scanning phantoms in which the connectivity is known [11].

Up to now in the clinical setting, there was only the possibility of indirect clinical validation by evaluating the postoperative motor or language function, visual field deficits correlation, etc. That is, the clinician analyzes whether the patients have a better neurological outcome and then concludes that the applied method seems to be beneficial. The major question is whether the tractography results actually reflect reality. First attempts correlating the DTI tractography findings to intraoperative electrophysiological measurements showed quite some discrepancies [34] which were probably mainly attributable to a distinct shifting of major white matter tracts during a neurosurgical procedure, which could be demonstrated by comparing pre- and intraoperative fiber tracking, acquired by high-field MRI applied during surgery [39, 49].

Maximal safety may require combining electrophysiological brain mapping with functional navigation that integrates fMRI/MEG data and DTI-based tractography acquired before or during surgery. Like intraoperative electrophysiological mapping can identify cortical eloquent brain areas, subcortical electrical stimulation helps to identify major white matter tracts intraoperatively. Recent studies emphasize that functional navigation and subcortical stimulation are complementary methods that may facilitate the preservation of pyramidal tracts [8, 54, 59].

The intraoperative visualization of the course of the pyramidal tract by microscope-based navigation during the resection of supratentorial gliomas has resulted in reduced neurological deficits, which may serve as a proof of concept per se. This is also supported by studies comparing pre- and postoperative reconstructions of major white matter structures in the brain stem well correlating to clinical deficits. Visual field deficits in temporal lobe surgery for pharmacoresistant epilepsy provide an ideal model to analyze the clinical validity of changes in tractography by correlating the extent of visual field defects with the changes in pre- and intraoperative DTI tractography-based reconstruction of the optic radiation. The significant correlation between postoperative visual field deficits and the extent of alterations of the optic radiation also proved that reconstruction of major white matter tracts can be reliably used in a clinical setting [13, 56, 68].

All these data clearly support the concept of functional neuronavigation, i.e., adding functional information to 3-D anatomical datasets to reduce postoperative morbidity when operating lesions close to eloquent brain structures. Of course the intraoperative knowledge of the exact position of the pyramidal tract does not prevent neurological deficits per se; intraoperative events such as the necessity to coagulate small vessels close to the pyramidal tract may result in an injury of the pyramidal tract leading to neurological deficits. The distance of how close a reconstructed major white matter tract can be approached is not yet clearly defined. Analyzing DTI tractography-based navigation data in regard to the distance between tumor and pyramidal tract revealed that a distance of 5 mm seems to be a critical

distance, which should be taken into account as safety margin [52]. This corresponds well to an identical critical distance of about 5 mm when approaching functionally eloquent cortical brain areas delineated by fMRI or MEG data.

Additional hulls around the reconstructed 3-D objects representing major white matter tracts are a possibility to visualize these safety margins. These encompassing hulls ideally would vary in thickness respective to the quality and reliability of the reconstructed fiber bundle. In case of noisy unreliable data, a thick hull would be added, while in highly reliable data, the hull would be thinner. The technical, as well as clinical, definition of the extent of these safety margins has still to be established.

Multimodal Navigation

The integration of tractography data into a navigation environment offers the possibility to correlate tractography findings in a multimodal setup, e.g., correlations with MR spectroscopy, and PET become possible. Besides preservation of neurological deficits, tractography-based navigation also allows to directly correlate histological findings with diffusion imaging parameters. Thus tumor invasion of major white matter tracts can be detected and quantified [60, 61].

Tumor Effects

Further important aspects influencing the quality of the reconstructed systems, especially when tractography is applied in the vicinities of a tumor, are the disruption of the fibers by tumor invasion and a widening of the fibers by the effects of edema surrounding a tumor. The standard diffusion modeling and tractography algorithms do not account enough for the effects of the edema and the tumor itself impedes the correct tracking so that either existing fibers are not visualized at all or even an erroneous tracking may result. An approach with generalized q-sampling imaging (GQI) seems to provide better results for visualization of tracts in edema than DTI-based tractography [70].

The special challenges for the neurosurgical application of tractography relate to the problem that different tract systems have different degrees of complexity, so that different reconstruction strategies might be necessary. The biggest and potentially most robust tract system in respect to visualization is the pyramidal tract. It might be sufficient to use a more simple approach to delineate the pyramidal tract than the complex language tract systems. However, the algorithms easily available for the neurosurgeons, due to the integration into the commercial navigation systems, might not be suitable for reconstruction of complex systems, despite the fact that they might produce trustworthy results for a large and more robust system.

Function and Tractography

It is important that the neurosurgeon is aware of the fact that the ability to reconstruct a tract system prior to surgery not automatically implies that the system the tract belongs to has normal function. On the other hand, alterations of reconstructed tract systems in pre-/postoperative comparison might well correspond to neurological deficits due to surgery. A conceptual issue is that DTI tractography should not be considered as a tool of functional mapping, but only as a tool allowing an indirect study of fiber anatomy [20]. Intraoperative monitoring with direct cortical stimulation and subcortical stimulation enables preserving essential tissue during surgery, while preoperative functional imaging including fMRI and DTI tractography allows to assess the surgical risk [55].

Combining the various methods from functional navigation, integrating fMRI and tractography information, in parallel to intraoperative electrophysiological measurements increases the safety for the patient. The different methods are not rivaling against each other but should be used in a complementary fashion.

In contrast to tractography in cohorts of healthy volunteers like it is applied in basic neuroscience, single-subject tractography like it is used and needed for surgical planning and guidance falls in the category of exploring unknown connectivity, because an individual variation even of known pathways, as well as a variation with disease, has to be expected. This is especially important when dealing with complex tract systems, e.g., like the language tracts [11].

Advanced Tractography Techniques

Diffusion-weighted imaging is inherently a noise-sensitive and artifact-prone MRI technique. To obtain a reliable representation of major white matter tracts, the following three steps are required in the process of DW-MRI tractography: the acquisition of appropriate diffusion-weighted image data; the correct estimations of fiber orientations, i.e., choosing the appropriate model; and finally the appropriate tracking algorithm.

Limitations of the DTI Approach

The DTI approach to model the complex anatomical diffusion information has some distinct limitations. It is far beyond the possibility of this chapter to provide a comprehensive overview on all different advanced techniques that are available and published. The review “Diffusion tensor imaging and beyond” by Tournier et al. [63] is recommended for further reading: Although attractive in its simplicity, the diffusion tensor model has been shown to be inadequate in the many

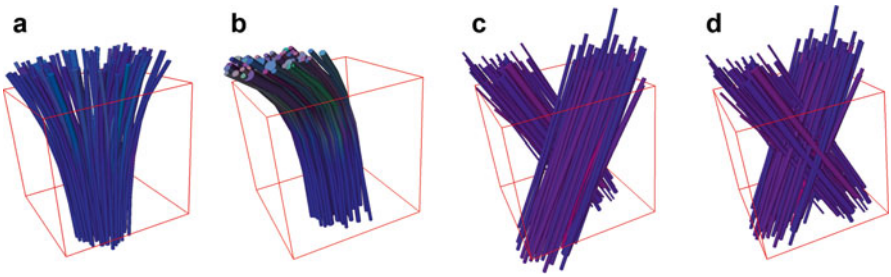

Fig. 1 Fiber orientations that cannot be resolved correctly by the DTI approach such as fanning (**a**), bending (**b**), kissing (**c**), and crossing (**d**) fibers; the *red cube* represents the measured voxel that incorporates a huge amount of fibers that might have one of these problematic configurations

regions of the brain that contain so-called "crossing fibers," whereby two or more differently oriented fiber bundles are colocated within the same voxel. The term "crossing fibers" is itself somewhat misleading, as it includes any situation where multiple fiber orientations contribute to the signal measured for the same imaging voxel. Therefore, this also applies to configurations that may not initially have been thought of as "crossing fibers," e.g., fiber bundles that "brush" past each other within the same imaging voxel, or even curving or "fanning" fibers (Fig. 1). Crossing fibers are endemic to DW-MRI, due to its coarse resolution (2–3 mm) compared with the white matter structures of interest; even the pyramidal tracts are only 3 mm thick in subcortical regions. Indeed, recent studies have shown that a significant proportion of the white matter contains crossing fibers with the most recent estimating that multiple fiber orientations can be detected in over 90 % of white matter voxels. Crossing fibers are even more problematic for tensor-based tractography methods: if one corrupt orientation estimate is encountered, the tracking algorithm may venture off course into an adjacent white matter structure, leading to both false-positive and false-negative connections. Moreover, the problem is far greater than might initially be expected: any given white matter tract of interest will traverse a large number of voxels, any of which might contain crossing fibers. It can readily be appreciated that the proportion of tracts traversing at least one affected voxel must be much greater than the proportion of affected voxels. If as much as 90 % of white matter voxels are affected, it is unlikely that any tracts will remain unaffected throughout their entire course.

A recent literature research by Abhinav et al. [3] identified 1838 papers dealing with fiber tracking or tractography among them the majority on DTI-based tractography approaches. Among the 735 papers applying tractography techniques beyond DTI, 84 papers with clinical applications were identified; among these 57 % applied a ball and stick (B&S) model and 15 % diffusion spectrum imaging (DSI), followed by 11 % for constrained spherical deconvolution (CSD) techniques. Sixty-four percent of the studies used probabilistic, and 36 % deterministic fiber tracking.

Advanced Diffusion Models

Among the advanced diffusion models replacing the DTI model as basis for tractography are sophisticated approaches including multitensor models, high angular resolution diffusion imaging (HARDI), hybrid diffusion imaging (HYDI), diffusion spectrum imaging (DSI), Q-ball imaging (QBI), Q-space imaging (QSI), the constraint spherical deconvolution model (CSD), and persistent angular structure MRI (PAS-MRI) [4, 5, 28, 37, 63–67]. These methods have gained increasing popularity, replacing the traditional tensor model for tractography. For instance, DSI and QBI use probability density functions instead of single tensors, which can describe the diffusion process in many different directions at each voxel. This however comes with the limitation of requiring longer acquisition times as it needs more encoding directions [58].

The major improvement for both probabilistic and deterministic tractography approaches is the introduction of these advanced diffusion models for the estimation of multiple fiber orientations. These models may be grouped in (overview taken from: [18]):

1. Multiparametric methods (e.g., multitensor or "ball and stick" (B&S) models) are model-dependent approaches in which the diffusion data are fitted with a chosen model that assumes a discrete number of fiber orientations (e.g., two or more).
2. Nonparametric, model-independent methods such as DSI, QBI, or diffusion orientation transform have been developed to better characterize the water molecular displacement by using a spherical function or the diffusion orientation distribution function (dODF). The multilobe shape of the dODF provides information on the number of fiber orientations, their orientation, and the weight of each fiber component.
3. Methods that try to take advantage of both approaches by extracting directly the underlying fiber orientation (i.e., fiber ODF) using a specific diffusion model for white matter fibers. The latter approaches are usually described as spherical deconvolution methods and they generally show higher angular resolution (i.e., the ability to resolve crossing fibers at smaller angles) compared with methods based on dODFs. Spherical deconvolution methods are becoming the methods of choice in an increasing number of studies, as they require acquisition protocols that are close to clinical DTI protocols (e.g., low number of diffusion gradient directions and b-values that are accessible in most clinical scanners).

Advanced Tractography Algorithms

In parallel to all these advanced diffusion models, there are advanced tractography algorithms taking into account that with the new diffusion models describing multiple fiber directions in a single voxel, there is the increased risk of false-positive

reconstructions. However, most of the current tractography algorithms are still based on the same tracking strategies originally introduced by the first tractography approaches. These strategies apply rules to avoid, for example, unrealistic fiber bending (i.e., angular thresholds) or tracking outside white matter regions (i.e., anisotropy thresholds) and are effective in reducing some of the reconstructions based on artifacts. Different approaches have been recently proposed to guide the propagation of the tractography algorithm across regions with multiple fiber orientations and try to discriminate between crossing, kissing, and bending configurations. Some of these approaches use "directional consistency" or similarity between fiber orientations across neighboring voxels; others use tract-specific properties or microstructural characteristics (e.g., axonal diameter) to propagate and differentiate tracts [18].

Global tractography is an alternative method in which the entire tract is generated simultaneously without a direct propagation of streamlines. By piecing together smaller tracts, the entire pathway is globally fitted to a chosen model that maximizes the consistency of the whole tract with the corresponding diffusion data. Because of small local errors, the final pathway can be formed by different anatomical tracts; for this reason anatomical constraints (or priors) are applied to distinguish between true tracts and artifacts.

In a recent paper giving an overview on global tracking techniques, Mangin et al. emphasize: "In the early days of MR diffusion-based tractography, the potential impact of the technique was so uplifting that the neuroscience community was comfortably blind to the "ill-posed" nature of the problem: the step-by-step reconstruction of a fiber bundle trajectory cannot afford any serious mistake in the evaluation of the local fiber orientations. This major risk was difficult to deal with because it does not exist in the well-known invasive techniques used with animals: a marker injected in a neuron is trapped inside the axon except when it can be transmitted into another neuron via synaptic connections. Hence invasive methods are not at risk of losing a bundle during tracking. Unfortunately, apart from the large bundles of deep white matter where axons are parallel, the evaluation of local fiber orientations in diffusion data is difficult. Indeed the myriad axons passing through a given MRI voxel usually have different orientations. Numerous ambiguities arise when one gets close to grey matter because of crossing, kissing and more exotic configurations. Considering the over-simplistic tensor models used at the beginning of the field, it is easy to understand why the first tractograms were full of spurious forks leading to barely exploitable connectivity maps" [41].

There are various technical attempts to approach the limitations of tractography; an agreed standard, or ideal solution, is not yet defined. It will be important to compare the different approaches especially in respect to their reliability and also clinical applicability.

So for the clinician, it is more or less impossible at the moment to find the right algorithm. Up to now, there is no definite solution. It seems to be obvious that advanced white matter imaging techniques have advantages over the simplified DTI-based tractography approach also in a clinical setting [2, 3, 10, 22, 35, 36, 70]. Figures 2 and 3 illustrate some typical advantages of advanced tractography techniques.

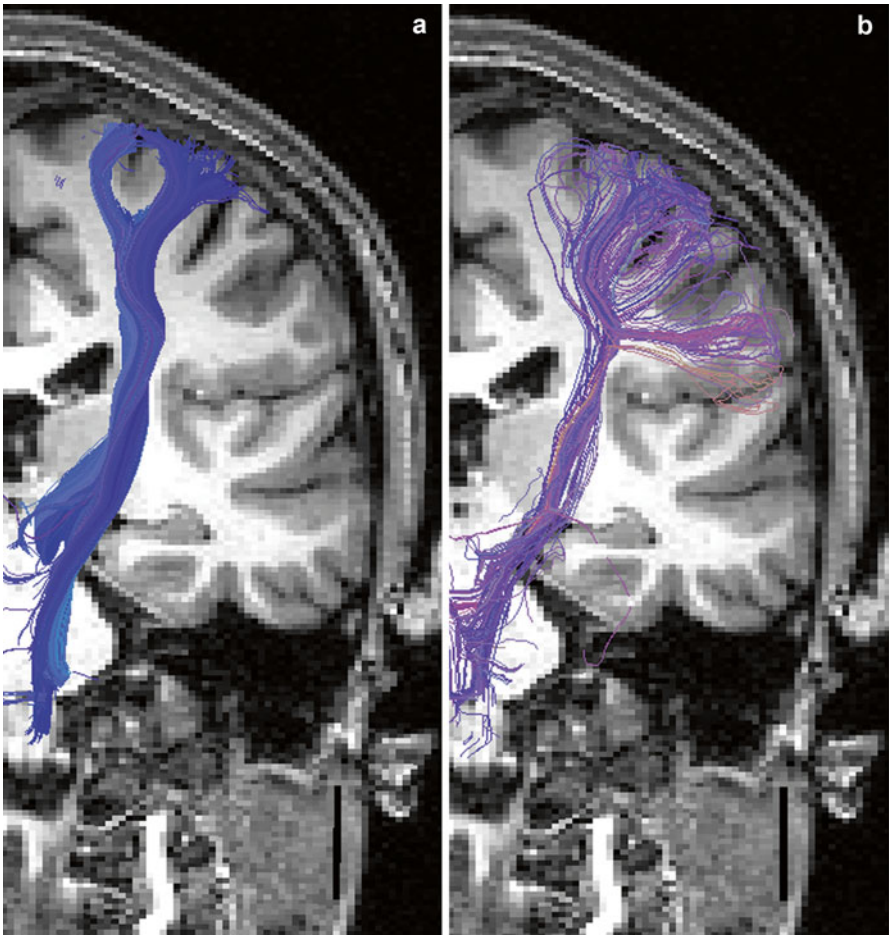

Fig. 2 The DTI tractography reconstruction of the pyramidal tract (**a**) misses a lot of fibers that are part of the pyramidal tract connecting to the lateral aspects of the precentral gyrus; this is much better represented by advanced tractography techniques (**b**, multidirectional tractography with an HARDI/ODF approach based on spherical ridgelets)

The most widely used clinical tractography method (i.e., DTI-based tractography) results in systematically unreliable and clinically misleading information. Higher-order tractography models, using the same diffusion-weighted data clearly demonstrate fiber tracts more accurately, providing improved estimates of safety margins that may be useful in neurosurgical procedures. We therefore need to move beyond the diffusion tensor framework [22]. However, even highly sophisticated recently published methods like multi-tissue constrained spherical deconvolution approaches for the improved analysis of multi-shell diffusion MRI data might be compromised by the mass effect of brain pathologies, like a tumor or edema [30].

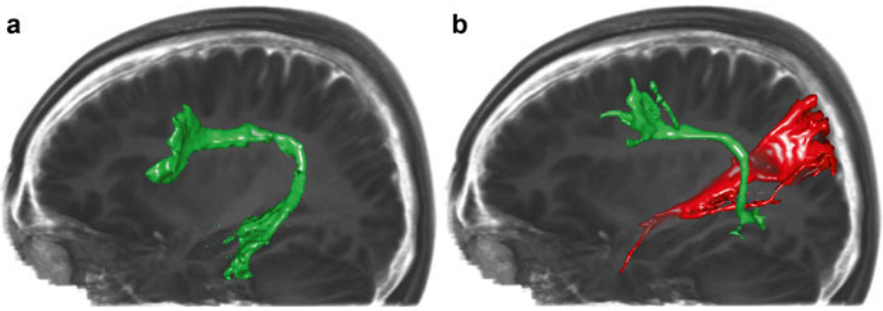

Fig. 3 DTI tractography of the arcuate fasciculus (**a**) often shows a false continuation that can be resolved correctly applying advanced tractography techniques (**b**), where the middle longitudinal fasciculus (*red*) is separated from the arcuate fasciculus (*green*) (tractography results rendered as 3-D objects: (**a**) DTI and (**b**) multidirectional HARDI/ODF approach based on spherical ridgelets)

A comparison of several clinically available tractography programs [23] demonstrated significant anatomical differences among nine different tractography programs (NeuroQLab (modified tensor deflection [TEND] algorithm), Sörensen DTI task card (modified streamline tracking technique algorithm), Siemens DTI module (modified fourth-order Runge-Kutta algorithm), six different software packages from Trackvis (interpolated streamline algorithm, modified FACT (fiber assignment continuous tracking) algorithm, second-order Runge-Kutta algorithm, Q-ball [FACT algorithm], tensorline algorithm, Q-ball [second-order Runge-Kutta algorithm]), DTI Query (modified streamline tracking technique algorithm), Medinria (modified TEND algorithm), Brainvoyager (modified TEND algorithm), DTI Studio modified FACT algorithm, and the BrainLab DTI module based on the modified Runge-Kutta algorithm). As a main pitfall of clinical tractography, the fact is identified that results can easily be manipulated by "cleaning up" the image with exclusion regions of interest. The final image shows fibers only where the user wants them to be shown, potentially hiding relevant tracts; this can present a serious problem when planning a surgical procedure where displaced fibers could unintentionally be hidden.

The Medical Image Computing and Computer Assisted Intervention Society (MICCAI) performs so-called MICCAI challenges where different research groups compare their tractography approaches in relation to identical data (for details, see the website dti-challenge.org). A quantitative evaluation of ten different algorithms applying a diffusion phantom demonstrated, as expected, that single-tensor-based methods performed worse than others in crossing regions for the obvious reason that a single tensor is unable to correctly characterize the two-fiber compartment specific of those regions. However, the single DTI model is still able to correctly characterize numerous fiber bundles. Notably, the DTI model with only few degrees of freedom is by essence less sensitive to noise than more complex models, which often makes it the unique alternative in clinical applications. Second, in case of good-quality datasets, the best option seems to use a fiber orientation distribution

function in conjunction with a streamline tractography algorithm where the next direction of propagation is directly inferred from the fiber orientation distribution (FOD) maxima. Indeed, with reasonable SNR (signal to noise ratio) datasets, FODs seem successful in modeling the fiber directions within a voxel and can be trusted. Finally, for datasets of medium and low quality as it is often encountered in real situations, several options are possible but all of them are using a spatial prior to make the model estimation more robust to noise. Conversely, without spatial prior, not any diffusion model was shown to correctly estimate the different fiber contributions within a voxel and consequently should be used with extreme caution [24].

Practical Guidelines and Proposal for the Future

Despite all complex possibilities and sophisticated developments in basic research, how can an individual neurosurgeon try to use "simple" tractography tools for the benefit of the patients? Most important seem to be: (1) to stay critical to the results provided by a software tool, (2) to compare the results of several tools, and (3) to have a good knowledge of anatomy, to be able to judge whether tractography results may be possible at all. Furthermore it is advisable not to rely exclusively on tractography to guide surgery, as well as, to combine several methods, like additional integration of functional MRI for identification of eloquent brain areas and like applying intraoperative electrophysiological methods, since tractography provides information on structure but not actual reliable information about function.

Guidelines toward a clinical application of tractography proposed by Chung et al. [16] are: always control the original image quality, choose the algorithm you understand, perform reproducibility tests on healthy subjects, and bear limitations in mind, when applying it to clinical practice.

Qualitative data from tractography-based studies with DTI or advanced white matter imaging techniques should be interpreted with a sound knowledge of the perilesional or loco-regional anatomy. In the setting of mass lesions, this problem is accentuated further as an abnormal trajectory of a fiber may be either technical in origin or be real. Good neuroanatomical knowledge therefore may help with an accurate interpretation of the data. In order to reduce the subjectivity of the interpretation of qualitative data, particularly in the setting of mass lesions, the use of a combined qualitative and quantitative approach may be helpful [2, 3].

The combined use of DW-MRI and cortical and subcortical stimulations could offer better information and a higher predictive value in preserving motor functions. For the validation and improvement of fiber tracking algorithms for neurosurgical planning, the use of electrophysiological data and functional image guidance can be very useful, especially under difficult pathological conditions. Using the most appropriate diffusion model combined with an adequate choice of tractography algorithm will increase the clinical relevance of the use of DW-MRI in neurosurgical planning. This reliability can be further improved by the combination with intraoperative mapping, which should be assessed systematically [10, 40].

Tractography for connectivity analysis in neuroscience has the problems of finding the exact termination of connections, detecting collaterals, tracking the very dense network of horizontal intracortical connections, discriminating between afferents and efferents, detecting synapses, etc. [29], which may be of lower relevance when applying tractography in neurosurgery, where these methods are mainly used to delineate a tract system close to a lesion, to decide on the extent of a resection or choosing a low-risk approach.

Future improvements in the accuracy of diffusion tractography will require innovations in MRI hardware, sequence design, data acquisition strategies, diffusion modeling, and tractography algorithms. Although such advances will lead to incremental improvements in the overall accuracy, they may not overcome the inherent ambiguities in inferring long-range axonal connectivity based on local diffusion displacement profiles. One suggestion, therefore, is to select the tractography method, or combination of methods, most appropriate for a specific objective. For example, if the objective is to reduce the possibility of identifying spurious pathways, a tractography method with better specificity, such as DTI, QBI, or B&S probabilistic tractography (using a conservative threshold), should be used. Alternatively, if it were the objective to reduce the likelihood of missing salient pathways, a tractography technique with relatively high sensitivity, such as CSD and B&S probabilistic tractography (using a liberal visualization threshold), would be more appropriate. For example, to avoid inadvertent transection of critical fibers of passage, as in the case of surgery for brain tumors, a tractography technique with low specificity but high sensitivity would be appropriate [62].

It is important to keep in mind that DW-MRI tractography alone is unlikely to provide an anatomically accurate map of the brain connectome. It is crucial to complement tractography results with a combination of histological or neurophysiological methods to map structural connectivity accurately [62].

The neurosurgical community has to find a consensus for adequate tractography strategies for different clinical situations and demands. It should be evident whether a rough estimation of the course of a well-defined tract system, which might be adequately described by a simple DTI-based tractography approach accompanied with some additional safety hulls, is sufficient for an intraoperative situation or whether the neurosurgeon has the demand to apply more reliable techniques; then advanced, sophisticated diffusion modeling and tractography approaches beyond the DTI approach have to be used.

Commercial navigation systems have to be open for the integration of research platforms, so that these sophisticated tractography approaches can be used in the clinical routine, and these techniques should also be implemented in the commercial systems directly.

A practical solution in the clinical setting includes besides using good clinical judgment the parallel application of different tractography approaches in complicated cases and comparing the results of these in each individual case. The clinician has to learn the pros and cons of the available software tools in the clinical setting like any surgical technique. Looking at the raw data should not be forgotten, using

a cookbook strategy with an identical evaluation sequence to minimize errors is essential, and the additional use of complementary techniques like intraoperative mapping and monitoring to gain additional safety is recommended.

Conclusion

DW-MRI provides a unique way of probing tissue microstructure in vivo and non-invasively and is by far the most promising tool for studying white matter and its organization in living humans. It is, however, a difficult technique to apply correctly due to its unique imaging artifacts, the often very intricate interactions between microstructure and signal, the sophistication of the reconstruction algorithms used, and the shear complexity of white matter itself [63].

There is a distinct delay of application of modern methods to reconstruct white matter tracts in neurosurgical procedures compared to the state of the art of basic neurosciences. Progress was made in recent years in all three major steps for the reconstruction of white matter tracts: raw data acquisition, modeling the diffusion behavior, and tractography approaches. Each of these steps influences the others and is not independent. Despite of all these developments, still most neurosurgeons use the DTI tractography method, because it is easily available, e.g., as software package part of commercial navigation systems. It is mandatory that either these commercial systems become more open to facilitate integration of better solutions that exist outside the operating room or the technical advantages are directly implemented into these commercial systems, so that they are available for the whole neurosurgical community.

References

1. Abdullah KG, Lubelski D, Nucifora PG, Brem S (2013) Use of diffusion tensor imaging in glioma resection. Neurosurg Focus 34, E1
2. Abhinav K, Pathak S, Richardson RM, Engh J, Gardner P, Yeh FC, Friedlander RM, Fernandez-Miranda JC (2014) Application of high-definition fiber tractography in the management of supratentorial cavernous malformations: a combined qualitative and quantitative approach. Neurosurgery 74:668–680; discussion 680–681
3. Abhinav K, Yeh FC, Pathak S, Suski V, Lacomis D, Friedlander RM, Fernandez-Miranda JC (2014) Advanced diffusion MRI fiber tracking in neurosurgical and neurodegenerative disorders and neuroanatomical studies: a review. Biochim Biophys Acta 1842:2286–2297
4. Alexander AL, Wu YC, Venkat PC (2006) Hybrid diffusion imaging (HYDI). Conf Proc IEEE Eng Med Biol Soc 1:2245–2248
5. Assemlal HE, Tschumperle D, Brun L, Siddiqi K (2011) Recent advances in diffusion MRI modeling: angular and radial reconstruction. Med Image Anal 15:369–396
6. Basser PJ, Mattiello J, LeBihan D (1994) Estimation of the effective self-diffusion tensor from the NMR spin echo. J Magn Reson B 103:247–254
7. Basser PJ, Pajevic S, Pierpaoli C, Duda J, Aldroubi A (2000) In vivo fiber tractography using DT-MRI data. Magn Reson Med 44:625–632

8. Berman JI, Berger MS, Chung SW, Nagarajan SS, Henry RG (2007) Accuracy of diffusion tensor magnetic resonance imaging tractography assessed using intraoperative subcortical stimulation mapping and magnetic source imaging. J Neurosurg 107:488–494
9. Bi WL, Chiocca EA (2014) From localization to pathways: the continuing evolution of diffusion tensor imaging. World Neurosurg 82:e47–e48
10. Bucci M, Mandelli ML, Berman JI, Amirbekian B, Nguyen C, Berger MS, Henry RG (2013) Quantifying diffusion MRI tractography of the corticospinal tract in brain tumors with deterministic and probabilistic methods. Neuroimage Clin 3:361–368
11. Campbell JS, Pike GB (2014) Potential and limitations of diffusion MRI tractography for the study of language. Brain Lang 131:65–73
12. Chang EF, Raygor KP, Berger MS (2015) Contemporary model of language organization: an overview for neurosurgeons. J Neurosurg 122:250–261
13. Chen X, Weigel D, Ganslandt O, Buchfelder M, Nimsky C (2009) Prediction of visual field deficits by diffusion tensor imaging in temporal lobe epilepsy surgery. Neuroimage 45: 286–297
14. Cho JM, Kim EH, Kim J, Lee SK, Kim SH, Lee KS, Chang JH (2014) Clinical use of diffusion tensor image-merged functional neuronavigation for brain tumor surgeries: review of preoperative, intraoperative, and postoperative data for 123 cases. Yonsei Med J 55:1303–1309
15. Chou MC, Huang TY, Chung HW, Hsieh TJ, Chang HC, Chen CY (2013) Q-ball imaging with PROPELLER EPI acquisition. NMR Biomed 26:1723–1732
16. Chung HW, Chou MC, Chen CY (2011) Principles and limitations of computational algorithms in clinical diffusion tensor MR tractography. AJNR Am J Neuroradiol 32:3–13
17. Conturo TE, Lori NF, Cull TS, Akbudak E, Snyder AZ, Shimony JS, McKinstry RC, Burton H, Raichle ME (1999) Tracking neuronal fiber pathways in the living human brain. Proc Natl Acad Sci U S A 96:10422–10427
18. Dell'Acqua F, Catani M (2012) Structural human brain networks: hot topics in diffusion tractography. Curr Opin Neurol 25:375–383
19. Dimou S, Battisti RA, Hermens DF, Lagopoulos J (2013) A systematic review of functional magnetic resonance imaging and diffusion tensor imaging modalities used in presurgical planning of brain tumour resection. Neurosurg Rev 36:205–214; discussion 214
20. Duffau H (2014) The dangers of magnetic resonance imaging diffusion tensor tractography in brain surgery. World Neurosurg 81:56–58
21. Duffau H (2014) Diffusion tensor imaging is a research and educational tool, but not yet a clinical tool. World Neurosurg 82:e43–e45
22. Farquharson S, Tournier JD, Calamante F, Fabinyi G, Schneider-Kolsky M, Jackson GD, Connelly A (2013) White matter fiber tractography: why we need to move beyond DTI. J Neurosurg 118:1367–1377
23. Feigl GC, Hiergeist W, Fellner C, Schebesch KM, Doenitz C, Finkenzeller T, Brawanski A, Schlaier J (2014) Magnetic resonance imaging diffusion tensor tractography: evaluation of anatomic accuracy of different fiber tracking software packages. World Neurosurg 81:144–150
24. Fillard P, Descoteaux M, Goh A, Gouttard S, Jeurissen B, Malcolm J, Ramirez-Manzanares A, Reisert M, Sakaie K, Tensaouti F, Yo T, Mangin JF, Poupon C (2011) Quantitative evaluation of 10 tractography algorithms on a realistic diffusion MR phantom. Neuroimage 56:220–234
25. Golby AJ, Kindlmann G, Norton I, Yarmarkovich A, Pieper S, Kikinis R (2011) Interactive diffusion tensor tractography visualization for neurosurgical planning. Neurosurgery 68:496–505
26. Hastreiter P, Rezk-Salama C, Soza G, Bauer M, Greiner G, Fahlbusch R, Ganslandt O, Nimsky C (2004) Strategies for brain shift evaluation. Med Image Anal 8:447–464
27. Irfanoglu MO, Walker L, Sarlls J, Marenco S, Pierpaoli C (2012) Effects of image distortions originating from susceptibility variations and concomitant fields on diffusion MRI tractography results. Neuroimage 61:275–288
28. Jansons KM, Alexander DC (2003) Persistent Angular Structure: new insights from diffusion MRI data. Dummy version. Inf Process Med Imaging 18:672–683
29. Jbabdi S, Johansen-Berg H (2011) Tractography: where do we go from here? Brain Connect 1: 169–183

30. Jeurissen B, Tournier JD, Dhollander T, Connelly A, Sijbers J (2014) Multi-tissue constrained spherical deconvolution for improved analysis of multi-shell diffusion MRI data. Neuroimage 103:411–426
31. Jones DK, Knosche TR, Turner R (2013) White matter integrity, fiber count, and other fallacies: the do's and don'ts of diffusion MRI. Neuroimage 73:239–254
32. Jones DK, Simmons A, Williams SC, Horsfield MA (1999) Non-invasive assessment of axonal fiber connectivity in the human brain via diffusion tensor MRI. Magn Reson Med 42:37–41
33. Kamali A, Hasan KM (2014) The importance of using a proper technique and accurate seeding of regions-of-interest in diffusion tensor tractography. J Neurol Sci 339:235–236
34. Kinoshita M, Yamada K, Hashimoto N, Kato A, Izumoto S, Baba T, Maruno M, Nishimura T, Yoshimine T (2005) Fiber-tracking does not accurately estimate size of fiber bundle in pathological condition: initial neurosurgical experience using neuronavigation and subcortical white matter stimulation. Neuroimage 25:424–429
35. Kuhnt D, Bauer MH, Egger J, Richter M, Kapur T, Sommer J, Merhof D, Nimsky C (2013) Fiber tractography based on diffusion tensor imaging compared with high-angular-resolution diffusion imaging with compressed sensing: initial experience. Neurosurgery 72(Suppl 1): 165–175
36. Kuhnt D, Bauer MH, Sommer J, Merhof D, Nimsky C (2013) Optic radiation fiber tractography in glioma patients based on high angular resolution diffusion imaging with compressed sensing compared with diffusion tensor imaging – initial experience. PLoS One 8, e70973
37. Landman BA, Bogovic JA, Wan H, El Zahraa ElShahaby F, Bazin PL, Prince JL (2012) Resolution of crossing fibers with constrained compressed sensing using diffusion tensor MRI. Neuroimage 59:2175–2186
38. Lerner A, Mogensen MA, Kim PE, Shiroishi MS, Hwang DH, Law M (2014) Clinical applications of diffusion tensor imaging. World Neurosurg 82:96–109
39. Maesawa S, Fujii M, Nakahara N, Watanabe T, Wakabayashi T, Yoshida J (2010) Intraoperative tractography and motor evoked potential (MEP) monitoring in surgery for gliomas around the corticospinal tract. World Neurosurg 74:153–161
40. Mandelli ML, Berger MS, Bucci M, Berman JI, Amirbekian B, Henry RG (2014) Quantifying accuracy and precision of diffusion MR tractography of the corticospinal tract in brain tumors. J Neurosurg 121:349–358
41. Mangin JF, Fillard P, Cointepas Y, Le Bihan D, Frouin V, Poupon C (2013) Toward global tractography. Neuroimage 80:290–296
42. Margulies DS, Bottger J, Watanabe A, Gorgolewski KJ (2013) Visualizing the human connectome. Neuroimage 80:445–461
43. Merhof D, Soza G, Stadlbauer A, Greiner G, Nimsky C (2007) Correction of susceptibility artifacts in diffusion tensor data using non-linear registration. Med Image Anal 11:588–603
44. Mori S, Crain BJ, Chacko VP, van Zijl PC (1999) Three-dimensional tracking of axonal projections in the brain by magnetic resonance imaging. Ann Neurol 45:265–269
45. Nabavi A, Black PM, Gering DT, Westin CF, Mehta V, Pergolizzi RS Jr, Ferrant M, Warfield SK, Hata N, Schwartz RB, Wells WM 3rd, Kikinis R, Jolesz FA (2001) Serial intraoperative magnetic resonance imaging of brain shift. Neurosurgery 48:787–797; discussion 797–798
46. Nimsky C, Ganslandt O, Cerny S, Hastreiter P, Greiner G, Fahlbusch R (2000) Quantification of, visualization of, and compensation for brain shift using intraoperative magnetic resonance imaging. Neurosurgery 47:1070–1079; discussion 1079–1080
47. Nimsky C, Ganslandt O, Fahlbusch R (2006) Implementation of fiber tract navigation. Neurosurgery 58:ONS-292–ONS-303; discussion ONS-303–4
48. Nimsky C, Ganslandt O, Hastreiter P, Wang R, Benner T, Sorensen AG, Fahlbusch R (2005) Intraoperative diffusion-tensor MR imaging: shifting of white matter tracts during neurosurgical procedures–initial experience. Radiology 234:218–225
49. Nimsky C, Ganslandt O, Hastreiter P, Wang R, Benner T, Sorensen AG, Fahlbusch R (2005) Preoperative and intraoperative diffusion tensor imaging-based fiber tracking in glioma surgery. Neurosurgery 56:130–137; discussion 138

50. Nimsky C, Ganslandt O, Kober H, Moller M, Ulmer S, Tomandl B, Fahlbusch R (1999) Integration of functional magnetic resonance imaging supported by magnetoencephalography in functional neuronavigation. Neurosurgery 44:1249–1255; discussion 1255–1256
51. Nimsky C, Ganslandt O, Merhof D, Sorensen AG, Fahlbusch R (2006) Intraoperative visualization of the pyramidal tract by diffusion-tensor-imaging-based fiber tracking. Neuroimage 30:1219–1229
52. Nimsky C, Ganslandt O, Weigel D, Keller B, Stadbauer A, Akutsu H, Hammen T, Buchfelder M (2008) Intraoperative tractography and neuronavigation of the pyramidal tract. Jpn J Neurosurg 17:21–26
53. O'Donnell LJ, Pasternak O (2015) Does diffusion MRI tell us anything about the white matter? An overview of methods and pitfalls. Schizophr Res 161:133–141
54. Ohue S, Kohno S, Inoue A, Yamashita D, Harada H, Kumon Y, Kikuchi K, Miki H, Ohnishi T (2012) Accuracy of diffusion tensor magnetic resonance imaging-based tractography for surgery of gliomas near the pyramidal tract: a significant correlation between subcortical electrical stimulation and postoperative tractography. Neurosurgery 70:283–293; discussion 294
55. Ottenhausen M, Krieg SM, Meyer B, Ringel F (2015) Functional preoperative and intraoperative mapping and monitoring: increasing safety and efficacy in glioma surgery. Neurosurg Focus 38, E3
56. Piper RJ, Yoong MM, Kandasamy J, Chin RF (2014) Application of diffusion tensor imaging and tractography of the optic radiation in anterior temporal lobe resection for epilepsy: a systematic review. Clin Neurol Neurosurg 124:59–65
57. Potgieser AR, Wagemakers M, van Hulzen AL, de Jong BM, Hoving EW, Groen RJ (2014) The role of diffusion tensor imaging in brain tumor surgery: a review of the literature. Clin Neurol Neurosurg 124:51–58
58. Soares JM, Marques P, Alves V, Sousa N (2013) A hitchhiker's guide to diffusion tensor imaging. Front Neurosci 7:31
59. Spena G, Panciani PP, Fontanella MM (2015) Resection of supratentorial gliomas: the need to merge microsurgical technical cornerstones with modern functional mapping concepts. An overview. Neurosurg Rev 38:59–70
60. Stadlbauer A, Hammen T, Buchfelder M, Bachmair J, Dorfler A, Nimsky C, Ganslandt O (2012) Differences in metabolism of fiber tract alterations in gliomas: a combined fiber density mapping and magnetic resonance spectroscopic imaging study. Neurosurgery 71:454–463
61. Stadlbauer A, Hammen T, Grummich P, Buchfelder M, Kuwert T, Dorfler A, Nimsky C, Ganslandt O (2011) Classification of peritumoral fiber tract alterations in gliomas using metabolic and structural neuroimaging. J Nucl Med 52:1227–1234
62. Thomas C, Ye FQ, Irfanoglu MO, Modi P, Saleem KS, Leopold DA, Pierpaoli C (2014) Anatomical accuracy of brain connections derived from diffusion MRI tractography is inherently limited. Proc Natl Acad Sci U S A 111:16574–16579
63. Tournier JD, Mori S, Leemans A (2011) Diffusion tensor imaging and beyond. Magn Reson Med 65:1532–1556
64. Tuch DS (2004) Q-ball imaging. Magn Reson Med 52:1358–1372
65. Tuch DS, Reese TG, Wiegell MR, Makris N, Belliveau JW, Wedeen VJ (2002) High angular resolution diffusion imaging reveals intravoxel white matter fiber heterogeneity. Magn Reson Med 48:577–582
66. Vos SB, Jones DK, Jeurissen B, Viergever MA, Leemans A (2012) The influence of complex white matter architecture on the mean diffusivity in diffusion tensor MRI of the human brain. Neuroimage 59:2208–2216
67. Wedeen VJ, Wang RP, Schmahmann JD, Benner T, Tseng WY, Dai G, Pandya DN, Hagmann P, D'Arceuil H, de Crespigny AJ (2008) Diffusion spectrum magnetic resonance imaging (DSI) tractography of crossing fibers. Neuroimage 41:1267–1277
68. Winston GP, Daga P, White MJ, Micallef C, Miserocchi A, Mancini L, Modat M, Stretton J, Sidhu MK, Symms MR, Lythgoe DJ, Thornton J, Yousry TA, Ourselin S, Duncan JS, McEvoy AW (2014) Preventing visual field deficits from neurosurgery. Neurology 83:604–611

69. Zemmoura I, Serres B, Andersson F, Barantin L, Tauber C, Filipiak I, Cottier JP, Venturini G, Destrieux C (2014) FIBRASCAN: a novel method for 3D white matter tract reconstruction in MR space from cadaveric dissection. Neuroimage 103:106–118
70. Zhang H, Wang Y, Lu T, Qiu B, Tang Y, Ou S, Tie X, Sun C, Xu K, Wang Y (2013) Differences between generalized q-sampling imaging and diffusion tensor imaging in the preoperative visualization of the nerve fiber tracts within peritumoral edema in brain. Neurosurgery 73:1044–1053; discussion 1053

5-Aminolevulinic Acid–Protoporphyrin IX Fluorescence-Guided Surgery of High-Grade Gliomas: A Systematic Review

Jacques Guyotat, Johan Pallud, Xavier Armoiry, Vladislav Pavlov, and Philippe Metellus

Contents

J. Guyotat, MD, PhD (✉)
Department of Neurosurgery, Neurological Hospital, Lyon, France
e-mail: jacques.guyotat@chu-lyon.fr

J. Pallud, MD, PhD
Department of Neurosurgery, Sainte Anne Hospital, Paris, France

Paris Descartes University, Paris, France
e-mail: johanpallud@hotmail.com

X. Armoiry, PharmD, PhD
Délégation à la recherche clinique et à l'innovation, cellule innovation Hospices Civils de, Lyon, France
e-mail: xavier.armoiry@chu-lyon.fr

V. Pavlov, MD
Department of Neurosurgery, Neurological Hospital, Lyon, France
e-mail: vladislav.pavlov@neurochirurgie.fr

P. Metellus, MD, PhD
Department of Neurosurgery, Timone Hospital, Marseille, France

University Aix Marseille, Marseille, France
e-mail: philippe.metellus@ap-hm.fr

J. Schramm (ed.), *Advances and Technical Standards in Neurosurgery,*
Advances and Technical Standards in Neurosurgery, Vol. 43,
DOI 10.1007/978-3-319-21359-0_3

Abstract The current first-line treatment of malignant gliomas consists in surgical resection (if possible) as large as possible. The existing tools don't permit to identify the limits of tumor infiltration, which goes beyond the zone of contrast enhancement on MRI. The fluorescence-guided malignant gliomas surgery was started 15 years ago and had become a standard of care in many countries. The technique is based on fluorescent molecule revelation using the filters, positioned within the surgical microscope. The fluorophore, protoporphyrin IX (PpIX), is converted in tumoral cells from 5-aminolevulinic acid (5-ALA), given orally before surgery. Many studies have shown that the ratio of gross total resections was higher if the fluorescence technique was used. The fluorescence signal intensity is correlated to the cell density and the PpIX concentration. The current method has a very high specificity but still lower sensibility, particularly regarding the zones with poor tumoral infiltration. This book reviews the principles of the technique and the results (extent of resection and survival).

Keywords High-grade glioma • 5-Aminolevulinic acid • Surgery • Fluorescence • Review

Introduction

Standard treatment strategies for glioblastoma (GBM) include microsurgical resection followed by concomitant chemo- and radiotherapy [95]. Despite these multiple therapies, the prognosis is poor, with a median survival duration of 12–14 months [90, 96]. Most current efforts are based on biological knowledge of the tumor and developmental advances in chemotherapy protocols, leading to significant improvement in both patient's life expectancy and quality of life in selected populations [32, 76, 114]. Surgery remains the first line of treatment for GBM whenever possible [51]. After establishing the histological diagnosis, reduction of tumor volume will ease compression of the surrounding normal brain tissue and increase the therapeutic

efficacy of adjuvant therapies while also improving quality of life [90, 95, 115]. Patients with the most favorable combination of prognostic factors and who are receiving combined radio-/chemotherapy after total macroscopic resection have 2- and 5-year survival rates of around 55 and 30 %, respectively [52, 96].

However, survival benefit in relation to the extent of GBM resection remains a critical question in neuro-oncology with no class I evidence from prospective trials [24, 65, 92, 93]. An inability to achieve total microscopic resection due to the infiltrative nature of these gliomas may explain the controversy [57]. Furthermore, most studies concluding that surgery is not a significant outcome factor proved to have been inadequately powered and failed to assess the extent of resection using postoperative imaging [16, 62]. Recent reviews have examined every major clinical report in the last two decades covering the role of the extent of resection (EOR) in GBM outcomes, and the overwhelming majority of large series have shown greater survival benefit with greater EOR [28, 36, 44, 74, 78]. In 2008, surgeons produced the guidelines for the management of newly diagnosed GBM and recommended maximum safe resection based on class II evidence [60]. Unfortunately, reported rates of gross total resection (GTR) of GBM over the past decade have remained comparatively low, ranging from 13 to 60 % [39, 119].

Currently, the major challenge to the neurosurgeon is complete resection, as assessed by enhanced magnetic resonance imaging (MRI) of the tumor [78]. Numerous surgical methods have been developed to facilitate optimal resection and to guide the surgeon during resection, including intraoperative neuronavigation, intraoperative ultrasonography, and intraoperative MRI [29, 80, 104, 118, 119]. However, each of these technologies is well known by neurosurgeons to have limitations (e.g., brain shift, technical expertise, and cost) [29, 80, 104, 118, 119].

History of Fluorescence Use in Surgery

Fluorescence imaging of brain tumor tissue during resection dates back to 1948, when Moore reported using fluorescein to image 46 patients with brain tumors [54]. However, until the past decade, fluorescence use in neurosurgery has remained a matter of personal choice, discussed only in published case reports [26, 56, 70, 84]. Since then, much of the real-time intraoperative work has been done by neurosurgeons in Germany and Japan using not only fluorescein but also, in particular, 5-aminolevulinic acid (5-ALA)-induced protoporphyrin IX (PpIX) fluorescence [1, 5, 10, 47, 61].

Marking tumors with 5-ALA is conceptually different from earlier fluorescence investigations, as the molecule in itself is not fluorescent but is metabolized into fluorescent PpIX by a number of malignant tumors [10]. Currently, 5-ALA-induced PpIX-guided surgery is considered effective and much simpler and less expensive to use than other types of surgical devices for patients with malignant glioma [67, 122]. Approved for intracranial use in Europe, Australia, Canada, and Japan,

5-ALA in the USA has not yet received the approval of the US Food and Drug Administration (FDA) [9, 17]. This means that any clinical investigation in that country has been performed under an Investigational New Drug (IND) exemption [72].

This book focuses on the use of 5-ALA-induced fluorescence and its current role in the surgical resection of GBM.

Theoretical Concepts (Fig. 1)

Biosynthesis and Regulation of PpIX

ALA, a molecule naturally found in all living mammalian cells, is a prodrug converted to PpIX via the heme synthesis pathway [50]. ALA is made in the mitochondria by the enzyme ALA synthase from succinyl-CoA and glycine from the Krebs cycle. ALA is then transported to the cytoplasm, where it undergoes enzymatic modifications through intermediate porphyrins (porphobilinogen, uroporphyrinogen III, coproporphyrinogen III) before being transported back to the mitochondria by adenine nucleotide transporters. Coproporphyrinogen III is converted by coproporphyrinogen oxidase to protoporphyrinogen IX which, in turn, undergoes oxidation by protoporphyrinogen IX oxidase, thereby creating the final heme precursor, the fluorescent molecule PpIX [10, 69]. In physiological terms,

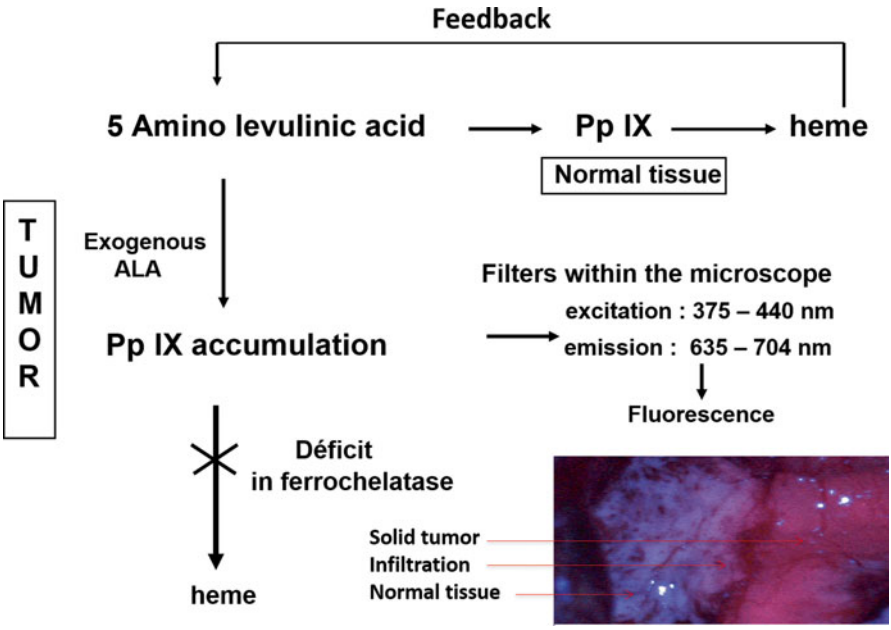

Fig. 1 Physiological principles of 5-ALA fluorescence functioning

ferrochelatase catalyzes iron incorporation into PpIX to produce the non-fluorescent heme molecule, which is then transformed into hemoglobin [100].

Transformation of ALA in the heme molecule is inhibited by feedback driven by high concentrations of heme that directly reduce the activity of ALA synthetase. However, this control can be bypassed by exogenous ALA, which enters the cytosol and results in increased levels of pathway intermediates, especially the fluorescent PpIX molecule [14, 49]. These elevated levels of PpIX persist for a limited amount of time, as ferrochelatase cannot immediately convert it to heme [55]. The capacity to synthesize heme is present in all normal tissues but is highly variable across different organs [38]. Systemic exogenous ALA administration induces strong PpIX fluorescence in epithelial and glandular structures, including the epidermis, mucosa, conjunctiva, endometrium, urothelium, liver, kidney, gallbladder, and mammary glands [40]. On the other hand, extremely limited fluorescence can be seen in tissues of mesodermal origin, such as muscle, connective tissue, and bone [35, 111]. In normal brain tissue, PpIX accumulation is almost impossible to detect except in limited amounts in the choroid plexus, ventricular ependyma, pia mater, and some areas of the white matter [30, 85, 87].

The principles and theoretical concepts of 5-ALA fluorescence are illustrated in Fig. 1.

Mechanisms of PpIX Accumulation in Tumor Tissue

Cancerous tissue produces higher levels of PpIX than does normal, thus allowing the molecule to be used for intraoperative guidance [40]. The amount, however, varies according to cancer cell type and the local cellular milieu, with the skin, bladder, uterine, gastrointestinal, bronchial, and ear–nose–throat (ENT) tumors having higher levels of PpIX [25, 41, 46, 68]. Brain tumors, especially high-grade gliomas, also manifest strong PpIX fluorescence after ALA ingestion with ratios of 20:1 to 50:1 compared with normal brain tissue [108, 109, 116].

Nevertheless, the capacity of neoplastic cells to selectively synthesize and produce high levels of fluorescent PpIX after exogenous ALA administration is as yet not fully understood [15]. In contrast to other molecules such as fluorescein and Photofrin (porfimer sodium), which are primarily synthesized in the liver and reach the brain via the blood circulation before penetrating the edematous tumor, PpIX synthesis takes place within the tumor cell, which explains its specificity and good tolerability compared with other agents. Several studies have confirmed these data [84]. Topical and local applications of 5-ALA to a number of malignant tissues have also resulted in local accumulation of fluorescent porphyrins while clearly circumventing the liver [14, 38]. Tests in vitro with different malignant cell lines, notably C6 glioma cells, have proven them capable of synthesizing significant amounts of porphyrins when 5-ALA was added to the media [48, 81]. In addition, after 5-ALA ingestion, porphyrin was found to be almost completely sequestered in erythrocytes

whereas its plasma concentration was low [85–87, 112]. The role of the blood–brain barrier is still a topic of debate [15, 58]. In terms of physiological status, the blood–brain barrier has very low permeability to radiolabeled ALA due to poor lipid solubility [15, 101] Also, carrier-mediated ALA transport from the blood to the brain has not been demonstrated [15]. On the other hand, there is a saturable mechanism of transport at the blood–cerebrospinal fluid (CSF) barrier at the choroid plexus to limit the brain effects of changes in plasma ALA concentrations [59].

For malignant gliomas, most studies have suggested that the main mechanism of PpIX accumulation may be due to higher 5-ALA uptakes essentially through passive diffusion into tumor tissue because of a disrupted blood–brain barrier [15]. Recently, positive correlations between PpIX and gadolinium (Gd) concentrations in tumor tissue and PpIX concentration and microvascular density have been found, suggesting a significant but limited association between blood–brain barrier breakdown and 5-ALA-induced PpIX fluorescence [110].

Other studies have demonstrated that a disrupted blood–brain barrier is not the only mechanism and that a specificity for malignant cells may be involved. Indeed, neoangiogenesis, overexpression of membrane transporters in malignant glioma tissue, and altered enzyme activity in the heme biosynthesis pathway might also play important roles. For instance, ferrochelatase, which converts PpIX to heme, has reduced activity in cancer cells, resulting in the accumulation of PpIX [11]. Inhibition of this reaction by the addition of iron chelators such as 1,2-diethyl-3-hydroxypyridin-4-one hydrochloride (CP94), 1,2-dimethyl-3-hydroxy-4-pyridone (L1), and desferrioxamine leads to increased ALA-mediated PpIX accumulation [6, 106]. Nevertheless, iron chelation may be a viable method of increasing PpIX production without having to modify the administered ALA dose to avoid potential side effects [7]. Also, some studies have identified ALA dehydratase and coproporphyrinogen oxidase as rate-limiting enzymes [99]. The cellular and extracellular environment can also affect cell function and the formation of PpIX. Both neoplastic and nonneoplastic cells have significantly reduced intracellular PpIX concentrations after incubation in serum-containing media compared with serum-free media [48, 81]. PpIX accumulation is also increased by hypoglycemia, hyperthermia, and acidosis, whereas hypoxia can mildly decrease PpIX accumulation [23, 53, 120, 121]. Thus, increased proliferation, neovascularization, and cell density play a role in why PpIX accumulates more in high-grade vs. low-grade gliomas even when low PpIX concentrations are detected by spectrophotometry in the latter tumors [13, 53, 107–109].

Optics of Fluorescence

The mechanisms behind fluorescence are well known. Electromagnetic radiation excites the electrons in atoms and molecules from their ground state (S0) to a greater energy state (S1). Fluorescence happens when electrons relax from their S1 state to an S0 state on emitting photons of light. Light in an excited state has a shorter wavelength (higher frequency and higher energy), whereas the emitted fluorescent

radiation has a longer wavelength (lower frequency and lower energy). The PpIX molecule is excited by blue light at wavelengths of 375–440 nm and emits red light in the visible spectrum at 635 nm, with a smaller peak at 704 nm [85–87]. To visualize fluorescence, a combination of excitation and emission filters is positioned within the surgical microscope: a shortpass filter in the excitation light path filters out the proper PpIX excitation wavelength, which is shorter than the fluorescence emission wavelength, and a longpass filter in the observer light path blocks out any excited light at wavelengths <440 nm and only allows red porphyrin fluorescence to pass.

The excitation and emission spectrum profiles have a small amount of overlap. This means that a small fraction of excited light is also remitted from the tissue to give the normal brain a blue color in contrast to the bright red porphyrin fluorescence of glioma. The degree of filter overlap is crucial for neurosurgical applications. If the remitted light is too strong, then the porphyrin fluorescence is no longer discernible and the sensitivity of detection is impaired. Conversely, if the remitted light is too weak, a faint autofluorescence in the red spectrum becomes visible and may be mistaken for porphyrin fluorescence. The operation becomes difficult due to a lack of tissue detail, and specificity may be reduced as a consequence of unnecessary resection [85–87, 102].

To visualize fluorescence on a video monitoring system for documentation purposes, specially modified video cameras optimalized for red porphyrin fluorescence detection are necessary [85–87]. This means that when the neurosurgeon switches to fluorescence mode, the gain in the red channel is automatically increased relative to the other channels (blue and green) to increase red sensitivity. During surgery, however, it is advisable to rely on impressions obtained directly from the human eye, which has a greater capacity for perceiving differences in fluorescence intensity and distinguishing fluorescing from non-fluorescent tissues [85–88].

Neurosurgical operating fluorescent microscopes designed for PpIX fluorescence-guided resection are commercially available and include models from Carl Zeiss (Göttingen, Germany), Leica (Wetzlar, Germany), and Möller-Wedel (Wedel, Germany).

Practical Aspects

Fluorescence-Guided Surgery

Fluorescence-guided surgery (FGS) using 5-ALA is a procedure that has been undergoing full development in many countries over the past decade. However, although the learning curve has become smaller, it is still essential for neurosurgeons to have a complete understanding of its technical performance. For this reason, a training course offered by Medac Pharma (Wedel, Germany), which has also made the 5-ALA molecule commercially available, is recommended for surgeons before doing the operation for the first time [18].

5-ALA Administration

The 5-ALA compound is sold as a white powder in a glass vial (1.5 g/vial) [88, 102]. ALA is administered orally after dissolving it in 50 mL of drinking water. The mildly sour-tasting solution is well tolerated by patients. Dissolving it in fruit juice makes it more acidic, which can modify its passage through the stomach and so is not to be recommended [102]. Clinical studies have demonstrated that the optimal dose is 20 mg/kg body weight for producing adequate PpIX fluorescence levels allowing visualization of the extent of the tumor core with minimal side effects [18].

One prospective double-blind randomized study tested lower doses of 5-ALA (0.2 and 2 mg/kg); the resulting levels of fluorescence were weaker, and the sensitivity of the method was considered unsatisfactory [85–87]. On the other hand, when higher doses of 5-ALA (40, 50 and 60 mg/kg) were used for tumors other than GBM, systemic side effects (hypotension, nausea, vomiting) were reported [37, 68, 112, 113]. In an animal model of glioma, doses of 100 mg induced significant non-specific fluorescence in edematous brain tissue [85–87] Thus, 5-ALA dosages >20 mg/kg can decrease fluorescence specificity with a risk of resecting non-tumor tissue while inducing neurological deficits [85–87].

The best time schedule for ALA administration has been also studied [85–87, 112, 113]. The timing needs to take into account two facts: First, complete intestinal ALA absorption takes about an hour and is then followed by ALA conversion to fluorescent PpIX within tumor cells, and second, ALA uptake should not be <3 h prior to the induction of anesthesia before beginning the operation (although it may be up to 5 h earlier). Maximum tumor fluorescence is reached at approximately 6 h after 5-ALA administration and may even be observed 12–16 h later before disappearing after 20 h [85–87].

Stummer has reported the importance of giving dexamethasone as pretreatment (3–4 mg/kg for 48 h) [88, 102]. This corticosteroid influences ALA uptake by reducing PpIX efflux and peritumor fluorescence by tightening up the blood–brain barrier. Also, pretreatment with steroids allows the identification of patients at risk of postoperative neurological deficit after fluorescence-guided resection. If there is no resolution of a preoperative deficit after dexamethasone treatment, the patient should not be operated on with fluorescence, as it indicates that the deficit is secondary to functional tumor infiltration and not due to edema [90].

5-ALA FGS Procedure

FGS using 5-ALA does not differ greatly from conventional microneurosurgical operations. Anesthesia induction, patient positioning, draping, and craniotomy are all performed in the usual way. In addition, conventional imaging guidance is often helpful for planning the craniotomy and locating tumors that are situated beneath the cortical surface.

Fluorescence appears to be especially useful for defining the corticectomy boundaries at the beginning of resection and for assessing of completeness of tumor removal near the end of the operation [88, 90, 102].

If the tumor is small, superficial, and away from a functional area, the surgeon may choose to begin the procedure with a blue excitation light. On occasions, even when the cortical surface appears normal under white light, switching to a blue excitation light may reveal cortical and subcortical tumor extensions, thereby providing an invaluable guide for the initial corticotomy [88, 102]. In this case, tumor resection is more efficient if the surgeon begins at the periphery between the fluorescent and non-fluorescent tissues while debulking the tumor centripetally. If the tumor is large and/or near an eloquent area, the surgeon might prefer to remove any easily distinguishable necrotic and solid tumor tissue predominantly under white light. However, to remove infiltrating residual tumor that is not distinguishable under white light, fluorescence-guided resection is essential.

The surgeon progresses from the tumor core to the periphery while switching between white-light and blue-light illumination until all signs of fluorescence are gone [102]. Unlike other imaging methods, the surgeon never has to move his eyes from the microscope, as switching between white light and blue light is done by the touch of a finger on the microscope. Also, the neurosurgeon can see tumor tissue "online" during the resection that is not otherwise visible to the naked eye [13, 102].

During the resection procedure, the surgeon usually seeks to identify four zones: first, necrotic tissue that is non-fluorescent; second, a solid tumor, which gives a strong red fluorescence (Fig. 2b, c) (both of which are generally easily distinguishable under white light); third, infiltrating tumor, which gives a more or less distinctive pink fluorescence that is visualized only under blue light (Fig. 3b, c); and, fourth, normal tissue that is non-fluorescent (Fig. 4b, c) [85–88, 94]. Red fluorescence corresponds to contrast-enhanced MRI (Fig. 2a–c), whereas pink fluorescence and non-fluorescence are the equivalent of non-contrast-enhanced MRI (Figs. 3a–c and 4a–c) [3, 94, 98].

With more working surgical experience, longer periods of the operation can be performed under the blue excitation light alone, although white-light illumination may still be necessary for discerning anatomical structures such as blood vessels, although these can be identified on fluorescence by their blue-green color under blue light [102]. Near the end of the procedure, as conventional imaging guidance is too imprecise because of brain shift to assess quality of resection, the value of FGS becomes particularly evident through its ability to highlight any residual tumor tissue. This means that it is essential that the surgeon inspects, under a direct blue light, the entire tumor cavity for any residual pink fluorescence [102].

Pitfalls

There are certain errors that might explain incomplete tumor resection and/or normal brain tissue resection leading to neurological deficits that the surgeon should be aware of. The following are such pitfalls according to their different causes.

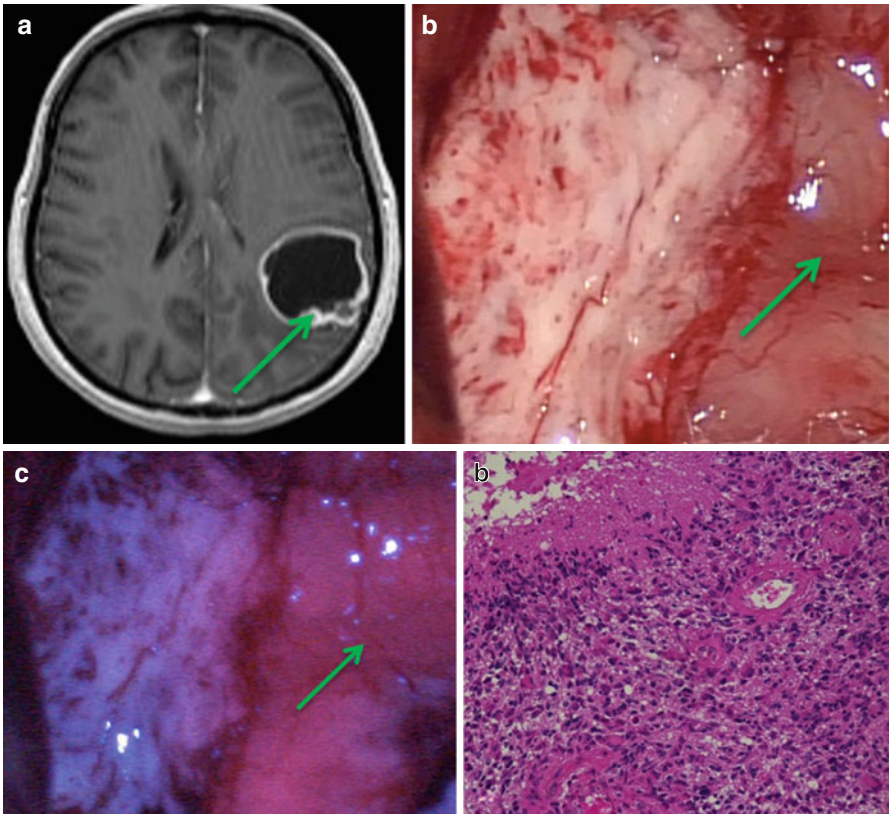

Fig. 2 Illustration of different areas during 5-ALA fluorescence-guided glioblastoma resection. T1-weighted MRI with gadolinium contrast enhancement – white-light illumination – blue-light illumination – corresponding histopathology. T1-weighted MRI with gadolinium contrast enhancement. (**a**) Ringlike *contrast enhancement* (*green arrows*); (**b**) *white-light* appearance: grayish solid tumor which is easy distinguishable; (**c**) *blue-light* appearance: strong fluorescence; (**d**) histological slice. Red fluorescence always indicates a solid tumor with high cell density, atypia, mitosis, and vascular proliferation. Fluorescence has a specificity of 1, sensitivity of 0.85–1, and an NPV of 0.79 and PPV of 1 [33, 107–109]

Due to Light-Related Principles

It is essential to understand that only exposed tissues can be excited and visualized. Blue-violet light has a penetration power of only about 0.5 mm from the tissue surface. This means that blood, non-fluorescent necrotic tissue, and normal thin brain tissue can all obstruct the fluorescence signal. Any persistent oozing should be sucked away to make a bloodless cavity [102]. The fluorescence signal is also subject to PpIX photobleaching, chemical degradation of fluorophores as a result of exposure to light [85–87]. This phenomenon is influenced by stronger light intensities, longer exposures, lower fluorophore concentrations, and the photochemical

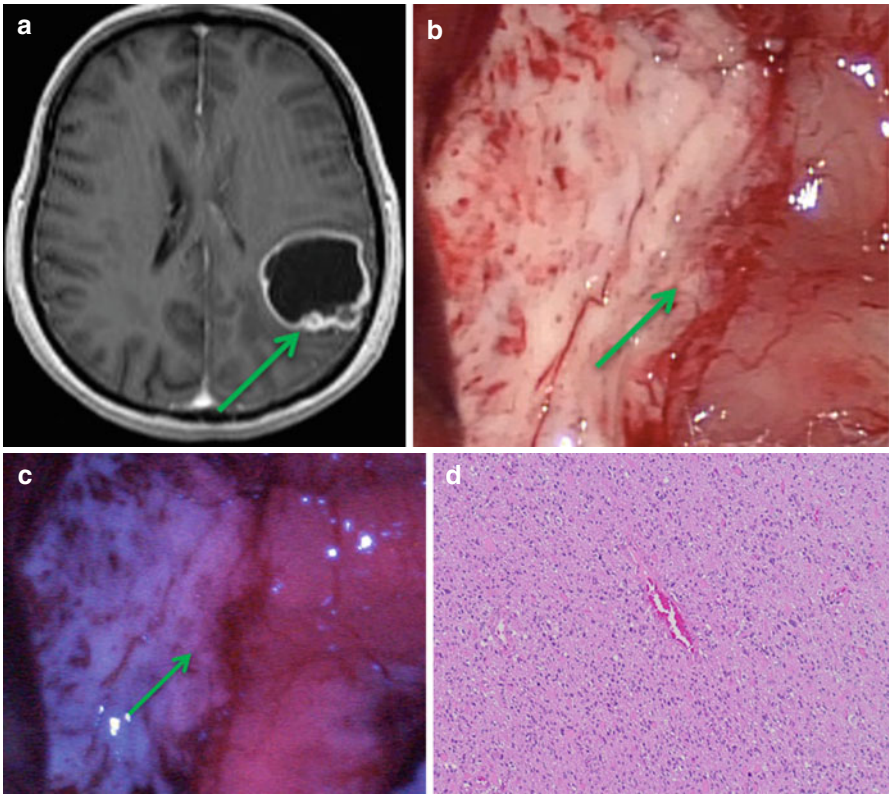

Fig. 3 Illustration of different areas during 5-ALA fluorescence-guided glioblastoma resection. T1-weighted MRI with gadolinium contrast enhancement – white-light illumination – blue-light illumination – corresponding histopathology. T1-weighted MRI with gadolinium contrast enhancement. (**a**) Tumor *periphery of the contrast enhancement limits* (*green arrows*); (**b**) *white-light* appearance: normal tissue aspect; (**c**) *blue-light* appearance: pink fluorescence; (**d**) histological slice. Macroscopically normal tissue shows weak fluorescence signal, corresponding to tumor infiltration zone. Note a less cell density. Only 6.6 % of the pink areas sampled show criteria for a diagnosis of GBM. Taken out of context, most of these samples could be diagnosed as low-grade glioma. Vague fluorescence has 0.85–0.92 specificity, 0.66–0.85 sensitivity, and a PPV of 0.97 [33, 107–109]

stability of the fluorophore itself. The rate of photobleaching has been analyzed by spectroscopy, which found that visible PpIX fluorescence decays to 36 % in 25 min with blue-violet light and in 87 min with white light [85–87]. However, photobleaching may be considerably slower than anticipated depending on light intensity. In fact, appreciable bleaching happens not in minutes, but after more than an hour of continuous white-light illumination, a condition that would normally never arise during surgery for malignant gliomas [89, 102]. During surgery, only a small part of the resection cavity is exposed to the microscope's light, and other parts are often covered by coagulated blood and cotton pads, and the fluorescence can be refreshed by the suctioning and removal of any blood, necrotic tissue, and superficial cell

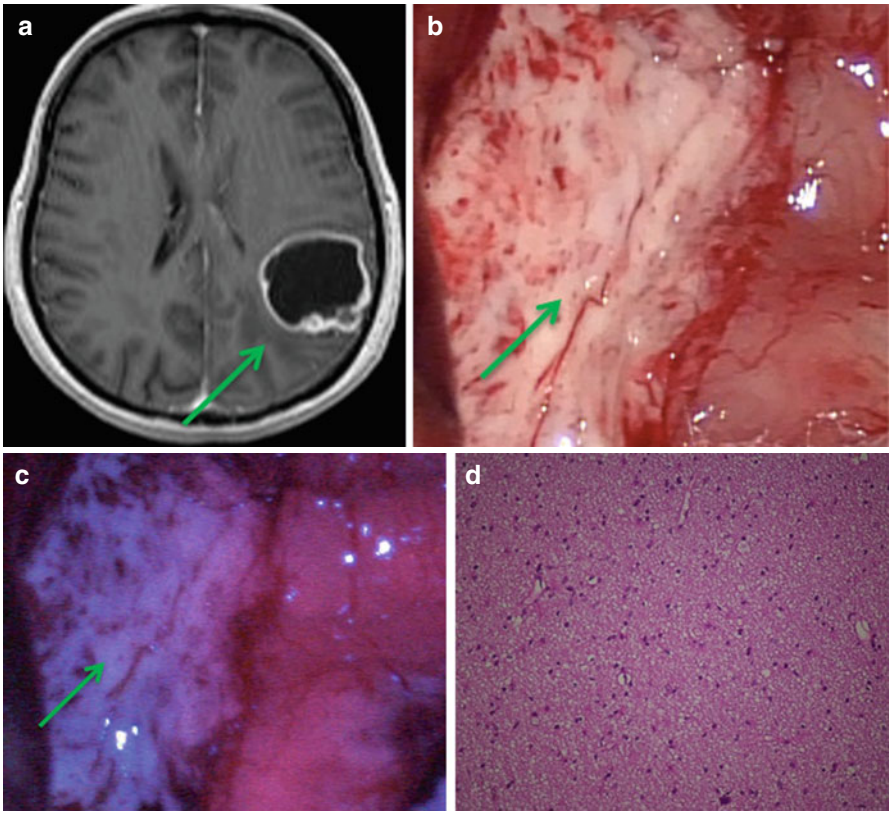

Fig. 4 Illustration of different areas during 5-ALA fluorescence-guided glioblastoma resection. T1-weighted MRI with gadolinium contrast enhancement – white-light illumination – blue-light illumination – corresponding histopathology. T1-weighted MRI with gadolinium contrast enhancement. (**a**) Tumor periphery *outside the contrast enhancement* (*green arrows*); (**b**) *white-light* appearance: normal tissue aspect; (**c**) *blue-light* appearance: no fluorescence; (**d**) histological slice. Non-fluorescent tissue immediately adjacent to the fluorescent border indicates normal tissue or slightly increased cellular density with isolated atypia. The mitotic index is always very low in non-fluorescent tissue, although dividing cells and atypia can be found in 33 % of samples, even those that appear normal. Of the non-fluorescent samples, 67 % are diagnosed as negative for tumor [33, 107–109]

layers. Also, at the end of the procedure, it is important to rub the resection cavity margins with cotton pads to remove any superficial cell layers. When fluorescence can no longer be seen, the resection may be considered complete [102].

Due to Tumor Characteristics

The problem of overhanging margins is not unusual in deep subcortical and cystic tumors. During the course of tumor resection, surgeons tend to undercut the cortex, leaving residual tumor hidden under the margins that remains unvisualized by the

blue excitation light and outside of the surgeon's direct field of vision. This "shadow cone" phenomenon should be borne in mind during the operation. Likewise, cyst opening can lead to the collapse of parts of the tumor that, in some cases, may go unnoticed [102].

Other Causes

Other technical details should not be ignored when attempting to achieve maximum surgical efficiency. The microscope should be positioned in a way to let the illumination light be perpendicular to the resection surface. The light source should be close to the cavity, as the intensity of light excitation diminishes over distance. The system should automatically switch to full intensity to have the highest possible level of blue excitation light. Ambient operating-room lighting should be lowered, with the operating light directed away from the resection cavity to reduce the risk of interference to fluorescence signals, which can cause normal brain tissue to falsely appear red [102].

Side Effects and Precautions

Due to the PpIX Molecule

Side effects and severe adverse events have been studied in several papers [13, 31, 63, 90, 91, 112, 113]. 5-ALA is a well-tolerated molecule so long as preventative measures and contraindications are applied and respected. This means that between the time of 5-ALA administration and positioning the patient for surgery, any ambient lighting should be reduced. More importantly, the direct exposure of patients to sunlight or to strong room lighting should be avoided for up to 24 h after 5-ALA administration [102]. ALA should not be given to patients with either inherited or acquired porphyria, severe renal, or hepatic insufficiency or during pregnancy. Coadministration with other potentially phototoxic agents (tetracycline, sulfonamide, hypericin extracts) should also be avoided for 24 h because of possible interactions; indeed, methotrexate, quinolones, and motexafin have increased, while phenytoin has decreased, PpIX levels in vitro [10, 17]. Nevertheless, the clinical effects of these molecules on PpIX have yet to be determined.

In practice, the reported side effects include nausea, vomiting, and raised transaminase levels with no accompanying clinical symptoms 7–14 days after surgery. The most common side effect is sunlight-induced erythema for 24 h, while severe adverse effects are very rarely seen [90]. Only a single case of mucosal edema has been reported thus far [31]. The risk of normal brain photosensitization has also been raised, but this is only theoretical for two reasons. First, PpIX levels in normal brain tissue are very low. Second, the currently used fluorescence microscopy equipment cannot create high-enough energy levels to cause phototoxic damage in the normal brain [85–87].

Due to the Surgical Procedure

Maximizing the extent of tumor resection using FGS may increase the risk of neurological deficits. Stummer reported a neurological impairment rate of 17.1 % with ALA after analyzing the risks of the technique based on measuring neurological function using the US National Institutes of Health Stroke Scale (NIHSS) and the Karnofsky Performance Status (KPS) score. Differences were noted only 48 h after surgery: 26 % of patients in the ALA group had fallen by one to three levels on their NIHSS score compared with 14.5 % in the white-light (WL) group. This deterioration was not sufficient to be detected by the KPS and was not significant at 7 days, 6 weeks, and 6 months after surgery [90]. In fact, patients operated on without 5-ALA had a higher risk of developing neurological deficits within the next 6 months [90]. Other studies of FGS have reported complication rates ranging from 2 to 9 %, which is consistent with the most recent series of surgery without 5-ALA [8, 29, 43].

The risk of neurological deterioration was also higher in patients with preexisting neurological deficits unresponsive to steroids; it is likely that these deficits were more related to tumor infiltration than to surrounding edema [92, 93].

It is also important to remember that FGS offers no functional information. For this reason, preoperative neuroradiological examinations, including classical MR imaging as well as functional MRI (fMRI) and diffusion tensor imaging (DTI) sequences, to visualize functional areas and fiber tracts are essential. Moreover, surgery needs to be combined with intraoperative monitoring for cortical and subcortical stimulation [12, 21, 64, 98]. When using such a multimodal approach, the morbidity rate is very low. Feigl performed 25 procedures in 18 patients with primary malignant brain tumors in eloquent areas using 5-ALA with intraoperative monitoring. In 24 % of all cases, the resection was stopped even though fluorescent tumor cells could still be seen intraoperatively because a functional area or cortical tract had been identified. The reported morbidity rate was 12 % [21]. Pastor operated on 34 patients harboring malignant glioma near eloquent cortical areas and the semioval center using different combinations of neurophysiological techniques. A week after surgery, only one patient worsened and, after 3 months, none of the patients had deteriorated [64]. Schucht reported on 53 patients eligible for complete resection of an enhancing tumor, 19 (36 %) of which were located in presumed eloquent brain areas. The combined rate of motor, speech, and visual deficits was 7.5 % for the complete-resection patients and 12 % for patients with tumors located in functional brain areas [98]. In Della Puppa's study, 31 patients with high-grade gliomas in eloquent areas who underwent surgery assisted by FGS and intraoperative monitoring were prospectively enrolled. At the 7-day assessment, 64 % of patients presented with neurological impairment, but after 3 months, the severe morbidity rate was 3 % [12].

Results

Several clinical studies have examined the value of intraoperative 5-ALA guidance for high-grade gliomas in terms of sensitivity/specificity, extent of tumor resection, and rate of survival [3, 13, 33, 71, 88, 94, 107–109, 117]. Recently, a systematic

review and meta-analysis of prospective studies was performed (Medline, Embase, and the Cochrane Library electronic database). Ten studies out of 473 reports screened were included in the qualitative analysis [122].

Sensitivity and Specificity of 5-ALA FGS

Correlation Between Visible Intraoperative Fluorescence and Histology

FGS diagnostic accuracy was investigated by correlating the surgical biopsy histology of tumor tissue excised from different sites (necrotic tissue, tumor core, and tumor margins) with the degree of fluorescence [13, 63, 71, 88, 107–109]. Histopathological characteristics according to the World Health Organization (WHO) criteria for glial tumors were assessed, and MIB-1 antibody labeling (anti-Ki-67) was used to evaluate tumor cell proliferation [107–109]. The degree of fluorescence was classified as high for strong fluorescence (bright red), low for vague fluorescence (shades of pink), and nil for no fluorescence (blue). This permitted evaluation of the specificity (probability of not observing intraoperative fluorescence when no tumor cells are present in tissue), sensitivity (probability of observing intraoperative fluorescence when tumor cells are present in tissue), positive predictive value (PPV; probability that tissue with observable intraoperative PpIX fluorescence is a true positive for the presence of tumor cells), negative predictive value (NPV; probability that tissue with no observable intraoperative PpIX fluorescence is a true negative for the presence of tumor cells), true and false positives, and true and false negatives with the technique.

The most accurate measure was thought to be the PPV as an indicator of whether fluorescence correctly shows tumor [94]. For high-grade glioma, 5-ALA had a sensitivity of 0.75–0.91 with an overall sensitivity of 0.87 and a specificity of 0.71–0.96 with an overall specificity of 0.89 [63, 71, 107–109]. The PPV ranged from 0.85 to 1, and the NPV was from 0.26 to 0.97 [13, 63, 71, 88, 107–109]. In contrast, under white light, the surgeon's ability to distinguish high-grade glioma appears to be much less accurate, with a sensitivity of 0.66 and specificity of 0.68 [33].

The results indicate that variation of PpIX fluorescence intensity within the tumor correlates statistically with histological grade, degree of tumor infiltration, and a high proliferation index using Ki-67 antigen as the biomarker [13, 63, 71, 88, 107–109]. Red fluorescence always indicates a solid tumor with high cell density, atypia, mitosis, and vascular proliferation, and strong fluorescence has a specificity of 1, sensitivity of 0.85–1, and an NPV of 0.79 and PPV of 1 (Fig. 2b–d) [33, 107–109]. Vague fluorescence areas show a wide range of cell density but always considerably less than the tumor core. Some parts may be highly cellular while other parts can be difficult to diagnose as pathological. Necrosis is not found in samples of low fluorescence, and vascular proliferation is less marked. Only 6.6 % of the pink areas sampled show criteria for a diagnosis of GBM. The Ki-67 index in pink areas is clearly less than in the center, although in some cases, the proliferative fraction may be high, up to 20–30 % in some samples [33]. Taken out of context, most of these samples could be diagnosed as low-grade astrocytoma [33]. Vague

fluorescence has 0.85–0.92 specificity, 0.66–0.85 sensitivity, and a PPV of 0.97 (Fig. 3b–d) [13, 71, 107–109].

Non-fluorescent tissue immediately adjacent to the fluorescent border indicates normal tissue or slightly increased cellular density with isolated atypia [107–109]. The mitotic index is always very low in non-fluorescent tissue, although dividing cells and atypia can be found in 33 % of samples, even those that appear normal. Of the non-fluorescent samples, 67 % are diagnosed as negative for tumor (Fig. 4b–d) [13, 33]. This agrees with previous reports of isolated cells located some distance from the tumor center. The absence of any PpIX fluorescence can be considered moderately accurate for identifying normal brain tissue, as Stummer has demonstrated that tissue with <20 % tumor cells can still fluoresce [88]. There is a significant correlation between samples with red-to-pink fluorescence and samples with pink-to-blue fluorescence and the mitotic index: Ki-67 labeling is 23.9 % (95 % CI, 15.2–32.7) in central areas, 6.4 % (95 % CI, 3.7–9.1) in pink areas, and 1.7 % (95 % CI, 0.9–2.5) in blue areas [33, 107, 109].

Nevertheless, cases of false positives are also described in the literature, albeit rarely, as rates vary from 0.4 to 11 % [13, 63, 88]. Perinecrotic areas during radiotherapy, peritumor edema, inflammatory cells, and reactive astrocytes can be labeled as fluorescent positive, especially in recurrent glioma after adjuvant treatment [31, 63, 105].

To increase FGS sensitivity, different approaches have been proposed. The most interesting is quantitative ex vivo measurement of PpIX concentration (C_{PpIX}) from biopsies of human gliomas [71, 72]. However, interpretation of fluorescence levels is subjective, which significantly decreases the correlation between true levels of fluorophores and visualized fluorescence. A significant trend has been noted between C_{PpIX} and subjective fluorescence levels observed intraoperatively. A statistically significant correlation can also be found between C_{PpIX} from human glioma biopsies and the proliferation index as well as between C_{PpIX} and the total number of abnormal cells [71]. These results indicate the utility of C_{PpIX} for differentiating between varying degrees of tissue malignancy at the microscopic level comparable to the "gold standard" Ki-67 proliferation index [71]. Around 40 % of tumor-positive biopsies that are not visibly fluorescent under the operating microscope have C_{PpIX} levels >0.1 mg/mL, indicating the presence of significant PpIX accumulation below the detection threshold of the current fluorescent imaging techniques [72, 107–109].

In another study, the diagnostic accuracy of FGS alone and in combination with conventional neuronavigation-guided surgery was investigated [13, 63]. Fluorescent and non-fluorescent specimens were collected from inside and outside of tumor boundaries, as delineated by neuronavigation, and their correlations with histopathological results were then assessed. The sensitivity and specificity of 5-ALA alone were 91.1 and 89.4 %, respectively, while the sensitivity and specificity of the imaging-guided system alone were 57.8 and 57.4 %, respectively. Combining the two procedures improved the sensitivity of 5-ALA from 91 to 96 %. On the other hand, specificity was reduced from 89 to 63 % if the tissue showing positive features with at least one technique (5-ALA or neuronavigation) was considered pathological [63].

Extent of Tumor Resection

Improving tumor resection quality is the main objective of surgery, but given their invasive nature, tumor borders are generally unclear and often indistinguishable from the surrounding normal tissue. Over the past decade, many studies have suggested that complete resection of an enhancing tumor, classically known as "gross total resection" (GTR), is associated with overall survival improvement, starting with an extent of resection (EOR) of 78 % of tumor volume up to 100 % EOR [78]. Thus, the major challenge for the neurosurgeon is complete resection of an enhancing tumor even when it has been shown that the contrast-enhanced parts of the tumor on MRI correspond mostly to a solid tumor, with the infiltrative parts of the tumor going beyond the borders of contrast enhancement. Other techniques, such as amino-acid positron emission tomography (FET-PET), can detect larger tumor spread but are rarely used in clinical practice [66].

Intraoperative Assessment: Series Results

For years, the intraoperative assessment of the EOR has relied on the surgeon's report, which gave considerable importance to the volume of resection [2]. Complete resection using conventional white-light microsurgical techniques confirmed by postoperative MRI was only achieved in 23–68 % of all GBM resections [2, 24, 28, 36, 44, 62, 77, 74, 96]. Thus, advances in intraoperative techniques such as intraoperative ultrasound, neuronavigation, and intraoperative MRI (iMRI) were developed to maximize tumor resection and minimize surgical morbidity in cases of high-grade glioma [29, 104, 118, 119].

However, all these techniques have limitations. Ultrasonography can overestimate the amount of tumor tissue during resection and cannot detect tumor remnants in the surgical cavity [75]. Frameless neuronavigation is widely used in brain tumor surgery, and some studies have claimed significant impacts of 33–76 % with GTR, although these reports were all retrospective analyses, whereas only one prospective randomized study found that the EOR was not enhanced by the use of a frameless stereotactic system [118, 119]. However, it is now well recognized that the effectiveness of neuronavigation is limited by the brain shift phenomenon [82]. In addition, intraoperative neuronavigation may not be able to completely visualize the full extent of diffuse infiltrative glial tumor like in Gd-enhanced MRI. However, despite these limitations, neuronavigation has currently emerged as the standard of care.

IMRI is a morphological technique that has only recently been evaluated [42]. It compensates for any potential errors due to brain shift by updating the information provided by neuronavigation with intraoperative imaging data. This permits evaluation of the extent of resection in real time, thereby enabling additional cytoreduction during the same procedure in around 40 % of operations [29, 42, 45]. In one randomized controlled trial, more patients in the iMRI group (96 %) had complete tumor resection confirmed by early postoperative MRI than in the control group

(68 %), and the difference was significant [80]. This suggests that iMRI can increase the extent of glioma surgery without additional morbidity. Nevertheless, other limitations should be mentioned. The precise identification of tumor margins using Gd enhancement is of limited precision. IMRI also represents a so-called "offline" method, as its use necessitates pausing surgery to evaluate the results. The cost is also a severely limiting factor, restricting its use only to specialized neurosurgical centers and not as a standard neurosurgical tool.

These limitations may explain why an increasing number of neurosurgical units use 5-ALA as a standard tool instead. So far, numerous studies have proved the value of 5-ALA FGS in increasing GBM resection. The earliest and most interesting trials were reported by Stummer and the ALA-Glioma Study Group. In 2000, Stummer reported on 52 patients with confirmed GBM who underwent FGS and showed that no contrast-enhanced tumor on postoperative MRI was found in 63 % of the patients [88]. In 2006, the same team described a randomized, controlled, multicenter phase III trial comparing 5-ALA-induced FGS with conventional white-light surgery for malignant gliomas in 270 randomly enrolled patients from 17 centers. Complete resection of contrast-enhanced tumor was achieved in 90 (65 %) of the 139 patients in the 5-ALA group and in 47 (36 %) of the 131 patients in the white-light group ($p < 0.0001$). Stummer subsequently reported that the percentage of patients without residual tumor on early postoperative imaging in the ALA group was 63.6 % vs. 37.6 % in the controls ($p < 0.0001$). Median residual tumor volume in the white-light group was 0.5 cm^3 vs. 0 cm^3 in the 5-ALA group ($p = 0.001$). Residual tumor was defined as a volume >0.175 cm^3 on contrast enhancement [90].

Since 2010, several prospective and retrospective single-center nonrandomized studies have been published [5, 10, 47]. Complete removal rates ranged from 60 to 100 % [3, 13, 20, 34, 63, 107–109]. In a report by Diez Valle of 36 patients, their mean preoperative tumor volume was 51.18 mL (range, 7.3–110 mL). Total resection was achieved in 83.3 % (30/36) of cases, while resection was >98 % of preoperative tumor volume in all cases, giving a mean resection rate of 99.8 %. The mean postoperative tumor volume in the six cases with remnants was 0.56 mL (range, 0.21–1.8 mL) [13]. In these recent reports, GTR rates were higher in the prospective Stummer study. In retrospect, several factors may explain the rates found in the earlier Stummer study: The majority of study centers had no experience with the new 5-ALA technology; several teams recruited only a few patients into the study; and neither navigation, mapping, nor monitoring was routinely used. In a recent analysis of the 5-ALA study results, the authors showed that, in up to two-thirds of cases with subtotal resection, the surgeon aborted tumor removal for various reasons and was always aware that the resection was incomplete [91, 92, 93].

To improve GTR rates, 5-ALA FGS in combination with 1.5-T iMRI was investigated in a retrospective study of 19 patients with gliomas (eight with WHO grade II/III and 11 with GBM) [103]. All patients also underwent postoperative 1.5-T MRI to confirm the EOR. In patients with 5-ALA-induced fluorescence-positive tumors, the average resection rate for patients undergoing 5-ALA-guided surgery alone vs. 5-ALA combined with 1.5-T iMRI was 91.8 % vs. 92.6 %, respectively. In patients with 5-ALA fluorescence-negative tumors (three GBMs), the average

resection rate was 89.2 % with combined 5-ALA fluorescence and iMRI but only 68.7 % with 5-ALA on its own. Thus, resection guided by 5-ALA fluorescence without the use of iMRI is sufficient for 5-ALA-positive glioma, which includes almost all malignant gliomas. Nevertheless, resection guided by 5-ALA fluorescence combined with iMRI is of interest for those rare patients with fluorescent-negative malignant gliomas and satellite lesions and/or no contrast enhancement on preoperative MRI [103].

Tumors in Functional Areas

Some studies have more precisely evaluated the possibilities of using FGS to increase GTR rates for malignant gliomas in eloquent areas despite the risks. Intraoperative mapping and/or preoperative multimodal functional imaging techniques and awake surgery have been combined with 5-ALA FGS to increase GTR of cortical malignant gliomas in eloquent areas with no postoperative surgical complications. Fiegls performed 25 procedures in 18 consecutive patients with primary malignant brain tumors in eloquent areas. GTR was achieved in 16 (64 %) of cases with preservation of all functional areas and fiber tracts [21]. Schucht included 66 patients with GBM in a prospective study, 53 of whom were eligible for complete resection of enhancing tumor (CRET) on early postoperative MRI, while 13 were CRET ineligible. The use of 5-ALA for both intraoperative fluorescence imaging and navigation was the surgical standard for all patients. Intraoperative monitoring (motor- and somatosensory-evoked potentials) and cortical and subcortical mapping, including awake surgery, were used in patients with tumors in or adjacent to a presumed eloquent area. In the entire surgical cohort (66 patients), CRET was achieved in 77 %. In the CRET-eligible patients only ($n=53$), CRET was achieved in 89 % of cases, in 97 % of those with preoperatively presumed non-eloquent tumor location, and in 74 % of those with preoperatively presumed eloquent tumor location [98].

Eyupoglu analyzed whether a dual intraoperative visualization approach combining 5-ALA FGS with iMRI would enable maximum possible resection of malignant gliomas in the vicinity of functional brain areas of 37 patients in a prospective study. All tumors in this series were classified according to Sawaya's functional grading system: grade I = located in non-eloquent brain areas, grade II = located in the vicinity of eloquent brain areas, and grade III = located in eloquent brain areas [79]. Also, all patients underwent preoperative functional diagnostics [magnetoencephalography (MEG) and/or fMRI]. In the subgroup with functional grade I ($n=9$), no statistical significance was found. The intended 100 % resection was achieved by surgery with 5-ALA alone and corroborated by iMRI. Patients belonging to the subgroup with function grade II ($n=12$) benefited significantly from dual intraoperative visualization. Tumor EOR was significantly increased with 5-ALA alone from 71.7 to 100 % with two modalities ($p<0.0002$). In the functional grade III group ($n=16$), iMRI in combination with functional neuronavigation was significantly superior to 5-ALA-guided surgery

alone. The EOR result with the latter was 57.6 %, whereas further tumor resection up to 71.2 % was achieved with the additional use of iMRI ($p < 0.0003$). The authors concluded that intraoperative evaluation of the EOR with fluorescence guidance led to a significantly higher rate of GTR with no postoperative neurological deficits, especially in cases of tumors lying close to functionally eloquent brain areas [20].

Early Postoperative MRI Accuracy in Assessing Tumor Resection

For clinical purposes, tissue enhanced by Gd in T1-weighted sequences is the best known surrogate marker for assessing malignant glioma volumes preoperatively and quality of resection postoperatively, despite a proven inability to show the entire tumor extent. This represents the limiting factor in evaluating the prognostic value of GTR in published series using early postoperative MRI alone. Studies suggest that 5-ALA fluorescence signals reach further than T1-weighted Gd-enhanced tissue [3, 33, 71, 91].

In Stummer's 2000 study of 52 patients, areas of residual contrast enhancement were identified by comparing early postoperative T1-weighted axial sequences with and without contrast enhancement. Of the 17 patients in whom complete removal of fluorescent tissue was achieved, 16 revealed no residual enhancement on postoperative images, while the remaining patient had a small region of residual enhancement. Postoperative MRI also showed no residual enhancement in 9/12 patients with vague fluorescence and in 8/23 patients with strong residual fluorescence. There is good evidence that PpIX fluorescence correlates with areas of Gd-enhanced tumor and that the complete resection of fluorescent tissue correlates with complete resection of enhancing areas [88]. Also, PpIX fluorescence may be more sensitive for evaluating residual tumor than Gd enhancement, as areas of low PpIX fluorescence fail to enhance at all on postoperative MRI despite containing areas of tumor [3, 71, 97]. Thus, contrast-enhanced MRI represents a macroscopic approach that leaves cellular transformation zones undetected, whereas 5-ALA appears to be superior in this respect, as it permits the identification and discrimination of this particular cellular zone, making it visible to the surgeon for more complete resection. To confirm this idea, Schucht demonstrated by volumetric means (quantifying the volume of fluorescing tissue by subtracting brain volume after surgery from brain volume prior to surgery and correcting for cerebrospinal flux spaces) that complete resection using 5-ALA fluorescence leads to significantly greater resection volumes compared with contrast-enhanced tumor, including non-Gd-enhanced tumor tissue, according to preoperative T1-weighted sequences. Furthermore, this study showed that a rim with a mean width of 6 mm was resected beyond the area of contrast enhancement [97].

Several groups of investigators have performed studies to correlate intraoperative 5-ALA fluorescence in tumors with preoperative ^{18}F-fluoroethyl-L-tyrosine ($^{18F\text{-}FET}$)–PET or ^{11}C-methionine (^{11}C-MET)–PET and T1-weighted contrast MRI uptake [4, 19, 22, 73, 83]. Independent of Gd enhancement, strong PpIX fluorescence

was seen in areas of maximum uptake with either ^{11}C-MET–PET or ^{18}F-FET–PET imaging. A preoperative FET–PET signal predicts intraoperative PpIX fluorescence with 87 % sensitivity and 94 % specificity [83]. Further characterization of combined PET and MRI with intraoperative PpIX fluorescence revealed that FET–PET was more sensitive than 5-ALA in detecting glioma tissue in general. In Ewelt's study of 17 PET-positive tumors histologically diagnosed as high-grade glioma, 14 were fluorescent and 13 were Gd enhancing. The authors concluded that FET–PET was more sensitive than 5-ALA in detecting glioma in general [19]. This result, however, is not supported by a recent study [73]. The correlation between intraoperative 5-ALA-positive tumor tissue left in the resection cavity after resection with postoperative ^{18}F-FET–PET and postoperative T1-weighted contrast MRI was determined in 10 patients with histologically verified GBM in eloquent brain regions who underwent 11 operations with neuronavigation and 5-ALA-assisted tumor resection. GTR was achieved in 45 % of cases according to postoperative T1-weighted contrast MRI, in 27 % of cases according to postoperative ^{18}F-FET–PET, and in none of the patients according to intraoperative ALA. The histology found at the 5-ALA-positive resection margins was infiltrating tumor tissue, whereas postoperative FET–PET failed to detect these residual ALA-positive tumors in most cases. 5-ALA fluorescence was more sensitive in the detection of GBM residual tumor compared with ^{18}F-FET uptake, whereas Tl-weighted contrast MRI was the least-sensitive postoperative imaging method for detecting residual tumor [73]. Recently, Arita assessed the association of 5-ALA and MET–PET uptake in gliomas by performing stereotactic biopsies at the beginning of resection but found no significant correlation between them, identifying both instead as independent indices of tumor cell density [4].

Progression-Free and Overall Survival

In Stummer's prospective 2000 study, 52 patients were stratified by residual tissue fluorescence. The survival time of patients with no fluorescence, vague fluorescence, and strong fluorescence was 101 ± 15 weeks, 79 ± 6 weeks, and 51 ± 3 weeks, respectively. Differences were significant between strong and no or vague residual fluorescence, but not between vague and no residual fluorescence, although the sample was too small to have any statistical power [88]. In Stummer's prospective randomized multicenter study comparing 5-ALA-induced FGS with conventional white-light surgery, 6-month progression-free surgery (PFS; no radiological progression of disease) was observed in 41 % vs. 21.1 % of patients in the ALA and white-light groups, respectively, a difference that was highly statistically significant ($p < 0.0003$). The PFS duration with 5-ALA was 5.1 months vs. 3.6 months with white light. Unfortunately, the trial failed to show a significant difference in overall survival (15.2 months for the 5-ALA group vs. 13.5 months for the white-light group). This result was disappointing, although there was a trend toward increased survival in the ALA group [90].

Various reasons might explain this result: The study was underpowered for proper analysis of the variable and was stopped early when primary end points were achieved; the percentage of GTR was high in the white-light group; and the absolute differences in residual tumor volume were not large, with a median residual volume of 0 cm^3 in 5-ALA patients and only 0.5 cm^3 in the control patients, making it difficult to prove any significant difference in overall survival. The cumulative incidence of repeat surgery was significantly lower, and the cumulative incidence of chemotherapy with temozolomide was marginally lower in the ALA patients, which may have led to a reduced beneficial effect on outcome in that group. Subsequent analysis of data from this phase III trial with patients restratified according to complete or incomplete resection, as revealed by early postoperative MRI irrespective of their initial study arm, showed that the two patient populations were similar except for younger age (<60 years) and less-frequent eloquent tumor location in the complete-resection arm. Improvement in overall survival was evident after adjusting for patient age and eloquent tumor location. Median patient survival time was significantly increased to 16.7 months in patients with complete resection compared with 11.8 months in those with partial resection ($p < 0.0001$) [91]. This effect was independent of the technique used to achieve complete resection, thus providing level IIb evidence (according to the Oxford Centre for Evidence-Based Medicine) that complete resection improves survival.

Recently, in retrospective study of 52 patients with newly diagnosed GBM and complete resection of enhancing tumor on early MRI, the effect of residual fluorescence in the surgical field on overall survival was studied. The median overall survival time was 27.0 months (95 % CI, 22.4–31.6) in patients without residual fluorescence ($n = 25$) vs. 17.5 months (95 % CI, 12.5–22.5) in those with residual fluorescence ($n = 27$; $p = 0.015$). The effect of residual fluorescence was also maintained in the multivariate analysis that included all covariables (HR, 2.5; $p = 0.041$) [3].

Conclusion

Several studies have proven the capability of 5-ALA FGS to increase the frequency of complete tumor resection. The technique is easy to use and has few side effects. The learning curve is short and its cost is limited. Compared with other methods currently being used, 5-ALA FGS does not interrupt the operation and results in a higher rate of complete tumor resection. At present, FGS with 5-ALA has become a standard part of the neuro-oncology armamentarium. In the future, its combined use with a miniaturized probe should allow real-time quantification of PpIX concentrations to improve the sensitivity of the method, thereby leading to optimal tumor resection.

Future Research

5-ALA FGS is safe and effective for increasing GTR rates, although further studies are needed to validate its impact on overall prognosis. Currently, 8 ongoing studies in 3 countries evaluate 5-ALA FGS (1 study in India, 6 studies in the USA, and 1 study in France) (https://clinicaltrials.gov).

A major limitation of 5-ALA FGS is the interobserver variability in correctly assessing low levels of fluorescence and the inability to detect PpIX concentrations below the threshold of visual detection. This phenomenon is partly responsible for the reduced sensitivity in detecting microscopic levels of malignancy and evaluating isolated tumor-cell infiltration not detected by enhanced MRI in GBM. Although new instrumentation enabling quantification and increased sensitivity to PpIX levels has been developed, further refinement of the techniques involved is still necessary. Haj-Hosseini has described a spectroscopy device for real-time feedback of the fluorescence signal that can improve the detection of tumor with no visible fluorescence [27]. However, the system is limited by its inability to accurately quantify absolute fluorescence that may be obscured by physical effects, such as variations in tissue optical properties. More recently, Valdes had reported on an intraoperative fiber-optic system that measures PpIX concentration levels in vivo. This probe can quantify absolute levels of PpIX in tissue by correcting for the spatially variable and distorting effects of tissue optical properties despite these variations [107–109]. Initial experience with intraoperative quantification of fluorescence probes has reportedly improved tumor resection accuracy, but, again, further refinement of the techniques involved is still needed. Hardware improvements such as more sensitive cameras and filters and stronger excitation light sources should also optimalize intraoperative fluorescence guidance.

The development of newer exogenous fluorophores with the ability to detect microinvasive disease and the improvement of detection technologies such as intraoperative confocal microscopy, which allows visualization of living tissue cytoarchitecture, are other research possibilities that may improve surgical tumor resection [47].

References

1. Acerbi F, Broggi M, Eoli M, Anghileri E, Cavallo C, Boffano C, Cordella R, Cuppini L, Pollo B, Schiariti M, Visintini S, Orsi C, La Corte E, Broggi G, Ferroli P (2014) Is fluorescein-guided technique able to help in resection of high-grade gliomas? Neurosurg Focus 36(2):E5. doi:10.3171/2013.11.FOCUS13487
2. Albert FK, Forsting M, Sartor K, Adams HP, Kunze S (1994) Early postoperative magnetic resonance imaging after resection of malignant glioma: objective evaluation of residual tumor and its influence on regrowth and prognosis. Neurosurgery 34:45–61

3. Aldave G, Tejada S, Pay E, Marigil M, Bejarano B, Idoate MA, Díez-Valle R (2013) Prognostic value of residual fluorescent tissue in glioblastoma patients after gross total resection in 5-aminolevulinic acid-guided surgery. Neurosurgery 72:915–920
4. Arita H, Kinoshita M, Kagawa N, Fujimoto Y, Kishima H, Hashimoto N, Yoshimine T (2012) ^{11}C-methionine uptake and intraoperative 5-aminolevulinic acid-induced fluorescence as separate index markers of cell density in glioma: a stereotactic image-histological analysis. Cancer 118:1619–1627
5. Babu R, Adamson C (2012) Fluorescence-guided malignant glioma resections. Curr Drug Discov Technol 9:1–12
6. Blake E, Curnow A (2010) The hydroxypyridinone iron chelator CP94 can enhance PpIX-induced PDT of cultured human glioma cells. Photochem Photobiol 86:1154–1160
7. Blake E, Allen J, Curnow A (2011) In vitro comparison of the effects of the iron-chelating agents, CP94 and Dexrazoxane, on protoporphyrin IX accumulation for photodynamic therapy and/or fluorescence guided resection. Photochem Photobiol 87:1419–1426
8. Chang SM, Parney IF, McDermott M, Barker FG 2nd, Schmidt MH, Huang W, Laws ER Jr, Lillehei KO, Bernstein M, Brem H, Sloan AE, Berger M, Glioma Outcomes Investigators (2003) Perioperative complications and neurological outcomes of first and second craniotomies among patients enrolled in the glioma outcome project. J Neurosurg 98:1175–1181
9. Colditz MJ, Jeffree RL (2012) Aminolevulinic acid (ALA)-protoporphyrin IX fluorescence guided tumour resection. Part 1: clinical, radiological and pathological studies. J Clin Neurosci 19:1471–1474
10. Colditz MJ, Kv L, Jeffree RL (2012) Aminolevulinic acid (ALA)-protoporphyrin IX fluorescence guided tumour resection. Part 2: theoretical, biochemical and practical aspects. J Clin Neurosci 19:1611–1616
11. Colliaud S, Juzeniene A, Moan J, Lange N (2004) On the selectivity of 5-Aminolevulinic acid-Induced protoporphyrin IX formation. Curr Med Chem Anticancer Agents 4: 301–316
12. Della Puppa A, De Pellegrin S, d'Avella E, Gioffrè G, Rossetto M, Gerardi A, Lombardi G, Manara R, Munari M, Saladini M, Scienza R (2013) 5-aminolevulinic acid (5-ALA) fluorescence guided surgery of high-grade gliomas in eloquent areas assisted by functional mapping. Our experience and review of the literature. Acta Neurochir 155:965–972
13. Díez Valle R, Tejada Solis S, Idoate Gastearena MA, García de Eulate R, Domínguez Echávarri P, Aristu Mendiroz J (2011) Surgery guided by 5- aminolevulinic fluorescence in glioblastoma: volumetric analysis of extent of resection in single-center experience. J Neurooncol 102:105–113
14. Divaris DX, Kennedy JC, Pottier RH (1990) Phototoxic damage to sebaceous glands and hair Follicles of mice after systemic administration of 5-Aminolevulinic acid correlates with localized protoporphyrin IX fluorescence. Am J Pathol 136:891–897
15. Ennis SR, Novotny A, Xiang J, Shakui P, Masada T, Stummer W, Smith DE, Keep RF (2003) Transport of 5-aminolevulinic acid between blood and brain. Brain Res 959:226–234
16. Ertl-Wagner BB, Blume JD, Peck D, Udupa JK, Herman B, Levering A, Schmalfuss IM, Members of the American College of Radiology Imaging Network 6662 Study Group (2009) Reliability of tumor volume estimation from MR images in patients with malignant glioma. Results from the American College of Radiology imaging network (ACRIN) 6662 Trial. Eur Radiol 19:599–609
17. European Medicines Agency (2007) Gliolan scientific discussion. Available from. http://www.ema.europa.eu/ema/index.jsp?curl=pages/medicines/human/medicines/000744/human_med_000807.jsp&murl=menus/medicines/medicines.jsp&mid=WC0b01ac058001d124. 21 July 2011
18. European Medicines Agency (2011) Gliolan – EPAR summary for the public Available from. http://www.ema.europa.eu/ema/index.jspcurl=pages/medicines/human/medicines/000744/human_med_000807.jsp&murl=menus/medicine/medicines.jsp&jsenabled=true. 29 July 2011
19. Ewelt C, Floeth FW, Felsberg J, Steiger HJ, Sabel M, Langen KJ, Stoffels G, Stummer W (2011) Finding the anaplastic focus in diffuse gliomas: the value of Gd-DTPA enhanced

MRI, FET-PET, and intraoperative, ALA-derived tissue fluorescence. Clin Neurol Neurosurg 113:541–547
20. Eyupoglu IY, Hore N, Savaskan N, Grummich P, Roessler K, Buchfelder M, Ganslandt O (2012) Improving the extent of malignant glioma resection by dual intraoperative visualisation approach. PLoS One 7(9):e44885. doi:10.1371/journal.pone.0044885
21. Feigl GC, Ritz R, Moraes M, Klein J, Ramina K, Gharabaghi A, Krischek B, Danz S, Bornemann A, Liebsch M, Tatagiba MS (2010) Resection of malignant brain tumors in eloquent cortical areas: a new multimodal approach combining 5-aminolevulinic acid and intraoperative monitoring. J Neurosurg 113:352–357
22. Floeth FW, Sabel M, Ewelt C, Stummer W, Felsberg J, Reifenberger G, Steiger HJ, Stoffels G, Coenen HH, Langen KJ (2011) Comparison of (18)F-FET PET and 5-ALA fluorescence in cerebral gliomas. Eur J Nucl Med Mol Imaging 238:731–741
23. Georgakoudi I, Keng PC, Foster TH (1999) Hypoxia significantly reduces aminolaevulinic acid-induced protoporphyrin IX synthesis in EMT6 cells. Br J Cancer 79:1372–1377
24. Gonda DD, Warnke P, Sanai N, Taich Z, Kasper EM, Chen CC (2013) The value of extended glioblastoma resection: insights from randomized controlled trials. Surg Neurol Int 4:1–10
25. Grant WE, Hopper C, MacRobert AJ, Speight PM, Bown SG (1993) Photodynamic therapy of oral cancer: photosensitisation with systemic aminolaevulinic acid. Lancet 17:147–148
26. Haglund MM, Berger MS, Hochman DW (1996) Enhanced optical imaging of human gliomas and tumor margins. Neurosurgery 38:308–317
27. Haj-Hosseini N, Richter J, Andersson-Engels S, Wårdell K (2010) Optical touch pointer for fluorescence guided glioblastoma resection using 5-aminolevulinic acid. Lasers Surg Med 42:9–14
28. Hardesty DA, Sanai N (2012) The value of glioma extent of resection in the modern neurosurgical era. Front Neurol 3:140
29. Hatiboglu MA, Weinberg JS, Suki D, Rao G, Prabhu SS, Shah K, Jackson E, Sawaya R (2009) Impact of intraoperative high-field magnetic resonance imaging guidance on glioma surgery: a prospective volumetric analysis. Neurosurgery 64:1073–1081; discussion 1081
30. Hebeda KM, Wolbers JB, Sterenborg HJCM, Kamorshot W, Van Gemert JJC, Van Alphen HAM (1995) Fluorescence localization in tumour and normal brain after intratumoral injection of hematoporphyrin derivative into brain tumor. J Photochem Photobiol B Biol 27:85–92
31. Hefti M, Von Campe G, Moschopulosa M, Siegnerb A, Looserc H, Landolt H (2008) 5-aminolevulinic acid induced protoporphyrin IX fluorescence in high-grade glioma surgery: a one-year experience at a single institution. Swiss Med Wkly 138:180–185
32. Hegi ME, Diserens AC, Gorlia T, Hamou MF, de Tribolet N, Weller M, Kros JM, Hainfellner JA, Mason W, Mariani L, Bromberg JE, Hau P, Mirimanoff RO, Cairncross JG, Janzer RC, Stupp R (2005) MGMT gene silencing and benefit from temozolomide in glioblastoma. N Engl J Med 10:997–1003
33. Idoate MA, Diez Valle R, Echeveste J, Tejada S (2011) Pathological characterization of the glioblastoma border as shown during surgery using 5-aminolevulinic acid induced fluorescence. Neuropathology 31:575–582
34. Jacquesson T, Ducray F, Maucourt-Bouch D, Armoiry X, Tisserand GL, Mbaye M, Pelissou-Guyotat I, Guyotat J (2013) Exérèse neurochirurgicale optimale des gliomes de haut grade guidée par fluorescence: mise au point à partir d'une série rétrospectivede 22 patients. Neurochirurgie 59:9–16
35. Johansson A, Palte G, Schnell O, Schnell O, Tonn JC, Herms J, Stepp H (2010) 5-Aminolevulinic acid-induced protoporphyrin IX levels in tissue of human malignant brain tumors. Photochem Photobiol 86:1373–1378
36. Keles GE, Anderson B, Berger MS (1999) The effect of extent of resection on time to tumor progression and survival in patients with glioblastoma multiforme of the cerebral hemisphere. Surg Neurol 52:371–379
37. Kelty CJ, Ackroyd R, Brown NJ, Brown SB, Reed MW (2004) Comparison of high- vs low-dose 5-aminolevulinic acid for photodynamic therapy of Barrett's esophagus. Surg Endosc 18:452–458

38. Kennedy JC, Pottier RH (1992) Endogenous protoporphyrin IX, a clinically useful photosensitizer for photodynamic therapy. J Photochem Photobiol B 14:275–292
39. Kowalczuk A, Macdonald RL, Amidei C, Dohrmann G 3rd, Erickson RK, Hekmatpanah J, Krauss S, Krishnasamy S, Masters G, Mullan SF, Mundt AJ, Sweeney P, Vokes EE, Weir BK, Wollman RL (1997) Quantitative imaging study of extent of surgical resection and prognosis of malignant astrocytomas. Neurosurgery 41:1028–1038
40. Krammer B, Plaetzer K (2008) ALA and its clinical impact, from bench to bedside. Photochem Photobiol Sci 7:283–289
41. Kriegmair M, Baumgartner R, Lumper W, Waidelich R, Hofstetter A (1996) Early clinical experience with 5-aminolevulinic acid for the photodynamic therapy of superficial bladder cancer. Br J Urol 77:667–671
42. Kubben PL, ter Meulen KJ, Schijns OE, ter Laak-Poort MP, van Overbeeke JJ, van Santbrink H (2011) Intraoperative MRI-guided resection of glioblastoma multiforme: a systematic review. Lancet Oncol 11:1062–1070
43. Kuhnt D, Becker A, Ganslandt O, Bauer M, Buchfelder M, Nimsky C (2011) Correlation of the extent of tumor volume resection and patient survival in surgery of glioblastoma multiforme with high-field intraoperative MRI guidance. Neuro Oncol 13:1339–1348
44. Lacroix M, Abi-Said D, Fourney DR, Gokaslan ZL, Shi W, DeMonte F, Lang FF, McCutcheon IE, Hassenbusch SJ, Holland E, Hess K, Michael C, Miller D, Sawaya R (2001) A multivariate analysis of 416 patients with glioblastoma multiforme: prognosis, extent of resection, and survival. J Neurosurg 95:190–198
45. Lenaburg HJ, Inkabi KE, Vitaz TW (2009) The use of intraoperative MRI for the treatment of glioblastoma multiforme. Technol Cancer Res Treat 8:159–162
46. Leunig A, Rick K, Stepp H, Gutmann R, Alwin G, Baumgartner R, Feyh J (1996) Fluorescence imaging and spectroscopy of 5-aminolevulinic acid induced protoporphyrin IX for the detection of neoplastic lesions in the oral cavity. Am J Surg 172:674–675
47. Li Y, Rey-Dios R, Roberts DW, Valdés PA, Cohen-Gadol AA (2014) Intraoperative fluorescence-guided resection of high-grade gliomas: a comparison of the present techniques and evolution of future strategies. World Neurosurg 82:175–185. pii: S1878-8750(13)00760-2. doi:10.1016/j.wneu.2013.06.014
48. Linuma S, Farshi SS, Ortel B, Hasan T (1994) A mechanistic study of cellular photodestruction with 5-aminolaevulinic acid-induced porphyrin. Br J Cancer 70:21–28
49. Malik Z, Lugacy H (1987) Destruction of erytholeukaemic cells by photoactivation of endogenous porphyrins. Br J Cancer 56:589–595
50. Mc Gillion FB, Thompson GG, Goldberg A (1975) Tissue uptake of d-aminolaevulinic acid. Biochem Pharmacol 24:299–301
51. McGirt MJ, Chaichana KL, Gathinji M, Attenello FJ, Than K, Olivi A, Weingart JD, Brem H, Quiñones-Hinojosa AR (2009) Independent association of extent of resection with survival in patients with malignant brain astrocytoma. J Neurosurg 110:156–162
52. Mirimanoff RO, Gorlia T, Mason W, Van den Bent MJ, Kortmann RD, Fisher B, Reni M, Brandes AA, Curschmann J, Villa S, Cairncross G, Allgeier A, Lacombe D, Stupp R (2006) Radiotherapy and temozolomide for newly diagnosed glioblastoma: recursive partitioning analysis of EORTC26981/22981-NCIC CE3 phase III randomized trial. J Clin Oncol 24: 2563–2569
53. Montcel B, Mahieu-Williame L, Armoiry X, Meyronet D, Guyotat J (2013) Two-peaked 5- ALA-induced PpIX fluorescence emission spectrum distinguishes glioblastomas from low grade gliomas and infiltrative component of glioblastomas. Biomed Opt Express 4:548–558
54. Moore GE, Peyton WT, Hunter SW, French L (1948) The clinical use of sodium fluorescein and radioactive diiodofluorescein in the localization of tumors of the central nervous system. Minn Med 31:1073–1076
55. Munakata H, Sun JY, Yoshida K, Nakatani T, Honda E, Hayakawa S, Furuyama K, Hayashi N (2004) Role of the heme regulatory motif in the heme-mediated inhibition of mitochondrial import of 5-aminolevulinate synthase. J Biochem 136:233–238

56. Murray KJ (1982) Improved surgical resection of human brain tumors: part 1 –a preliminary study. Surg Neurol 17:316–319
57. Nitta RT, Li G (2013) The invasive nature of glioblastoma. World Neurosurg 80:279–280
58. Novotny A, Stummer W (2003) 5-aminolevulinic acid and the blood – brain barrier- a review. Med Laser Appl 18:36–40
59. Ocheltree SM, Shen H, Hu Y, Xiang J, Keep RF, Smith DE (2004) Role of PEPT2 in the choroid plexus uptake of glycylsarcosine and 5-aminolevulinic acid: studies in wild-type and null mice. Pharm Res 21:1680–1685
60. Olson JJ, Ryken T (2008) Guidelines for the treatment of newly diagnosed glioblastoma: introduction. J Neurooncol 89:255–258
61. Okuda T, Yoshioka H, Kato A (2012) Fluorescence-guided surgery for glioblastoma multiforme using high-dose fluorescein sodium with excitation and barrier filters. J Clin Neurosci 19:1719–1722
62. Orringer D, Lau D, Khatri S, Zamora-Berridi G, Zhang K, Wu C, Chaudhary N, Sagher O (2012) Extent of resection in patients with glioblastoma: limiting factors, perception of resectability, and effect on survival. J Neurosurg 117:851–859
63. Panciani PP, Fontanella M, Schatlo B, Garbossa D, Agnoletti A, Ducati A, Lanotte M (2012) Fluorescence and image guided resection in high grade glioma. Clin Neurol Neurosurg 114: 37–41
64. Pastor J, Vega-Zelaya L, Pulido P, Garnés-Camarena O, Abreu A, Sola RG (2013) Role of intraoperative neurophysiological monitoring during fluorescence-guided resection surgery. Acta Neurochir (Wien) 155:2201–2213
65. Pichlmeier U, Bink A, Schackert G, Stummer W (2008) Resection and survival in glioblastoma multiforme: an RTOG recursive partitioning analysis of ALA study patients. Neuro Oncol 10:1025–1034
66. Pirotte BJ, Levivier M, Goldman S, Massager N, Wikler D, Dewitte O, Bruneau M, Rorive S, David P, Brotchi J (2009) Positron emission tomography-guided volumetric resection of supratentorial high-grade gliomas: a survival analysis in 66 consecutive patients. Neurosurgery 64:471–481 [discussion 81]
67. Pogue BW, Gibbs-Strauss S, Valdés PA, Samkoe K, Roberts DW, Paulsen KD (2010) Review of neurosurgical fluorescence imaging methodologies. IEEE J Sel Top Quantum Electron 16:493–505
68. Regula J, MacRobert AJ, Gorchein A, Buonaccorsi GA, Thorpe SM, Spencer GM, Hatfield AR, Bown SG (1995) Photosensitisation and photodynamic therapy of oesophageal, duodenal, and colorectal tumours using 5 aminolaevulinic acid induced protoporphyrin IX–a pilot study. Gut 36:67–75
69. Rimington C (1966) Porphyrin and haem biosynthesis and its control. Acta Med Scand 445:11–24
70. Ritz R, Daniels R, Noell S, Feigl GC, Schmidt V, Bornemann A, Ramina K, Mayer D, Dietz K, Strauss WS, Tatagiba M (2012) Hypericin for visualization of high grade gliomas: first clinical experience. Eur J Surg Oncol 38:352–360
71. Roberts DW, Valdés PA, Harris BT, Fontaine KM, Hartov A, Fan X, Ji S, Lollis SS, Pogue BW, Leblond F, Tosteson TD, Wilson BC, Paulsen KD (2011) Coregistered fluorescence-enhanced tumor resection of malignant glioma: relationships between δ-aminolevulinic acid-induced protoporphyrin IX fluorescence, magnetic resonance imaging enhancement, and neuropathological parameters. J Neurosurg 114:595–603
72. Roberts DW, Valdés PA, Harris BT, Hartov A, Fan X, Ji S, Leblond F, Tosteson TD, Wilson BC, Paulsen KD (2012) Glioblastoma multiforme treatment with clinical trials for surgical resection (aminolevulinic acid). Neurosurg Clin N Am 23:371–377
73. Roessler K, Becherer A, Donat M, Cejna M, Zachenhofer I (2012) Intraoperative tissue fluorescence using 5-aminolevolinic acid (5-ALA) is more sensitive than contrast MRI or amino acid positron emission tomography ((18)F-FET PET) in glioblastoma surgery. Neurol Res 34:314–317

74. Ryken TC, Frankel B, Julien T, Olson JJ (2008) Surgical management of newly diagnosed glioblastoma in adults: role of cytoreductive surgery. J Neurooncol 89:271–286
75. Rygh OM, Selbekk T, Torp SH, Lydersen S, Hernes TA, Unsgaard G (2008) Comparison of navigated 3D ultrasound findings with histopathology in subsequent phases of glioblastoma resection. Acta Neurochir (Wien) 150:1033–1041; discussion 1042
76. Shahar T, Nossek E, Steinberg DM, Rozovski U, Blumenthal DT, Bokstein F, Sitt R, Freedman S, Corn BW, Kanner AA, Ram Z (2012) The impact of enrollment in clinical trials on survival of patients with glioblastoma. J Clin Neurosci 19:1530–1534
77. Sanai N, Berger MS (2008) Glioma extent of resection and its impact on patient outcome. Neurosurgery 62:753–764; discussion 264–265
78. Sanai N, Polley MY, McDermott MW, Parsa AT, Berger MS (2011) An extent of resection threshold for newly diagnosed glioblastomas. J Neurosurg 115:3–8
79. Sawaya R, Hammoud M, Schoppa D, Hess KR, Wu SZ, Shi WM, Wildrick DM (1998) Neurosurgical outcomes in a modern series of 400 craniotomies for treatment of parenchymal tumors. Neurosurgery 42:1044–1055; discussion 1055–1056. Review
80. Senft C, Bink A, Franz K, Vatter H, Gasser T, Seifert V (2011) Intraoperative MRI guidance and extent of resection in glioma surgery: a randomised, controlled trial. Lancet Oncol 12:997–1003
81. Sroka R, Beyer W, Gossner L, Sassy T, Stocker S, Baumgartner R (1996) Pharmacokinetics of 5-aminolevulinic-acid-induced porphyrins in tumour-bearing mice. J Photochem Photobiol B 34:13–19
82. Stieglitz LH, Fichtner J, Andres R, Schucht P, Krähenbühl AK, Raabe A, Beck J (2013) The silent loss of neuronavigation accuracy: a systematic retrospective analysis of factors influencing the mismatch of frameless stereotactic systems in cranial neurosurgery. Neurosurgery 72:796–807
83. Stockhammer F, Misch M, Horn P, Koch A, Fonyuy N, Plotkin M (2009) Association of F18-fluoro-ethyl-tyrosin uptake and 5-aminolevulinic acid-induced fluorescence in gliomas. Acta Neurochir (Wien) 151:1377–1383
84. Stummer W, Götz C, Hassan A, Heimann A, Kempski O (1993) Kinetics of Photofrin II in perifocal brain edema. Neurosurgery 33:1075–1081; discussion 1081–1082
85. Stummer W, Stocker S, Wagner S, Stepp H, Fritsch C, Goetz C, Goetz AE, Kiefmann R, Reulen HJ (1998) Intraoperative detection of malignant gliomas by 5-aminolevulinic acid-induced porphyrin fluorescence. Neurosurgery 42:518–525; discussion 525–5266
86. Stummer W, Stepp H, Möller G, Ehrhardt A, Leonhard M, Reulen HJ (1998) Technical principles for protoporphyrin-IX-fluorescence guided microsurgical resection of malignant glioma tissue. Acta Neurochir (Wien) 140:995–1000
87. Stummer W, Stocker S, Novotny A, Heimann A, Sauer O, Kempski O, Plesnila N, Wietzorrek J, Reulen HJ (1998) In vitro and in vivo porphyrin accumulation by C6 glioma cells after exposure to 5-aminolevulinic acid. J Photochem Photobiol B 45:160–169
88. Stummer W, Novotny A, Stepp H, Goetz C, Bise K, Reulen HJ (2000) Fluorescence-guided resection of glioblastoma multiforme by using 5-aminolevulinic acid-induced porphyrins: a prospective study in 52 consecutive patients. J Neurosurg 93:1003–1013
89. Stummer W, Reulen HJ, Novotny A, Stepp H, Tonn JC (2003) Fluorescence-guided resections of malignant gliomas–an overview. Acta Neurochir Suppl 88:9–12
90. Stummer W, Pichlmeier U, Meinel T, Wiestler OD, Zanella F, Reulen HJ, ALA-Glioma Study Group (2006) Fluorescence-guided surgery with 5-aminolevulinic acid for resection of malignant glioma: a randomised controlled multicentre phase III trial. Lancet Oncol 7: 392–401
91. Stummer W, Reulen HJ, Meinel T, Pichlmeier U, Schumacher W, Tonn JC, Rohde V, Oppel F, Turowski B, Woiciechowsky C, Franz K, Pietsch T, ALA-Glioma Study Group (2008) Extent of resection and survival in glioblastoma multiforme: identification of and adjustment for bias. Neurosurgery 62:564–576; discussion 564–576
92. Stummer W, Van den Bent MJ, Westphal M (2011) Cytoreductive surgery of glioblastoma as the key to successful adjuvant therapies: new arguments in an old discussion. Acta Neurochir (Wien) 153:1211–1218

93. Stummer W, Tonn JC, Mehdorn HM, Nestler U, Franz K, Goetz C, Bink A, Pichlmeier U, ALA-Glioma Study Group (2011) Counterbalancing risks and gains from extended resections in malignant glioma surgery: a supplemental analysis from the randomized 5-aminolevulinic acid glioma resection study. J Neurosurg 114:613–623
94. Stummer W, Tonn JC, Goetz C, Ullrich W, Stepp H, Bink A, Pietsch T, Pichlmeier U (2014) 5-Aminolevulinic acid-derived tumor fluorescence: the diagnostic accuracy of visible fluorescence qualities as corroborated by spectrometry and histology and postoperative imaging. Neurosurgery 74:310–319; discussion 319–320
95. Stupp R, Mason WP, van den Bent MJ, Weller M, Fisher B, Taphoorn MJ, Belanger K, Brandes AA, Marosi C, Bogdahn U, Curschmann J, Janzer RC, Ludwin SK, Gorlia T, Allgeier A, Lacombe D, Cairncross JG, Eisenhauer E, Mirimanoff RO, European Organisation for Research and Treatment of Cancer Brain Tumor and Radiotherapy Groups, National Cancer Institute of Canada Clinical Trials Group (2005) Radiotherapy plus concomitant and adjuvant temozolomide for glioblastoma. N Engl J Med 352:987–996
96. Stupp R, Hegi ME, Mason WP, van den Bent MJ, Taphoorn MJ, Janzer RC, Ludwin SK, Allgeier A, Fisher B, Belanger K, Hau P, Brandes AA, Gijtenbeek J, Marosi C, Vecht CJ, Mokhtari K, Wesseling P, Villa S, Eisenhauer E, Gorlia T, Weller M, Lacombe D, Cairncross JG, Mirimanoff RO, European Organisation for Research and Treatment of Cancer Brain Tumour and Radiation Oncology Groups, National Cancer Institute of Canada Clinical Trials Group (2009) Effects of radiotherapy with concomitant and adjuvant temozolomide versus radiotherapy alone on survival in glioblastoma in a randomised phase III study: 5-year analysis of the EORTC-NCIC trial. Lancet Oncol 10:459–466
97. Schucht P, Knittel S, Slotboom J, Seidel K, Murek M, Jilch A, Raabe A, Beck J (2013) 5-ALA complete resections go beyond MR contrast enhancement: shift corrected volumetric analysis of the extent of resection in surgery for glioblastoma. Acta Neurochir (Wien) 156:305–312; discussion
98. Schucht P, Beck J, Abu-Isa J, Andereggen L, Murek M, Seidel K, Stieglitz L, Raabe A (2014) Gross total resection rates in contemporary glioblastoma surgery: results of an institutional protocol combining 5-ALA intraoperative fluorescence imaging and brain mapping. Neurosurgery. doi:10.1227/NEU.0b013e31826d1e6b
99. Takahashi K, Ikeda N, Nonoguchi N, Kajimoto Y, Miyatake S, Hagiya Y, Ogura S, Nakagawa H, Ishikawa T, Kuroiwa T (2011) Enhanced expression of coproporphyrinogen oxidase in malignant brain tumors: CPOX expression and 5-ALA-induced fluorescence. Neuro Oncol 13:1234–1243
100. Teng L, Nakada M, Zhao SG, Endo Y, Furuyama N, Nambu E, Pyko IV, Hayashi Y, Hamada JI (2011) Silencing of ferrochelatase enhances 5-aminolevulinic acid-based fluorescence and photodynamic therapy efficacy. Br J Cancer 104:798–807
101. Terr L, Weiner LP (1983) An autoradiographic study of delta-aminolevulinic acid uptake by mouse brain. Exp Neurol 79:564–568
102. Tonn JC, Stummer W (2008) Fluorescence-guided resection of malignant gliomas using 5-aminolevulinic acid: practical use, risks, and pitfalls. Clin Neurosurg 55:20–26
103. Tsugu A, Ishizaka H, Mizokami Y, Osada T, Baba T, Yoshiyama M, Nishiyama J, Matsumae M (2011) Impact of the combination of 5-aminolevulinic acid-induced fluorescence with intraoperative magnetic resonance imaging-guided surgery for glioma. World Neurosurg 76:120–127
104. Unsgaard G, Selbekk T, Brostrup Müller T, Ommedal S, Torp SH, Myhr G, Bang J, Nagelhus Hernes TA (2005) Ability of navigated 3D ultrasound to delineate gliomas and metastases–comparison of image interpretations with histopathology. Acta Neurochir (Wien) 147:1259–1269; discussion 1269
105. Utsuki S, Oka H, Sato S, Shimizu S, Suzuki S, Tanizaki Y, Kondo K, Miyajima Y, Fujii K (2007) Histological examination of false positive tissue resection using 5-aminolevulinic acid-induced fluorescence guidance. Neurol Med Chir 47:210–214
106. Valdés PA, Samkoe K, O'Hara JA, Roberts DW, Paulsen KD, Pogue BW (2010) Deferoxamine iron chelation increases delta-aminolevulinic acid induced protoporphyrin IX in xenograft glioma model. Photochem Photobiol 86:471–475

107. Valdés PA, Leblond F, Kim A, Harris BT, Wilson BC, Fan X, Tosteson TD, Hartov A, Ji S, Erkmen K, Simmons NE, Paulsen KD, Roberts DW (2011) Quantitative fluorescence in intracranial tumor: implications for ALA-induced PpIX as an intraoperative biomarker. J Neurosurg 115:11–17
108. Valdés PA, Kim A, Brantsch M, Valdés PA, Kim A, Brantsch M, Niu C, Moses ZB, Tosteson TD, Wilson BC, Paulsen KD, Roberts DW, Harris BT (2011) 5-aminolevulinic acid-induced protoporphyrin IX concentration correlates with histopathologic markers of malignancy in human gliomas: the need for quantitative fluorescence-guided resection to identify regions of increasing malignancy. Neuro Oncol 13:846–856
109. Valdés PA, Kim A, Leblond F, Conde OM, Harris BT, Paulsen KD, Wilson BC, Roberts DW (2011) Combined fluorescence and reflectance spectroscopy for in vivo quantification of cancer biomarkers in low- and high-grade glioma surgery. J Biomed Opt 16:116007–1160014
110. Valdés PA, Moses ZB, Kim A, Belden CJ, Wilson BC, Paulsen KD, Roberts DW, Harris BT (2012) Gadolinium- and 5-aminolevulinic acid-induced protoporphyrin IX levels in human gliomas: an ex vivo quantitative study to correlate protoporphyrin IX levels and blood-brain barrier breakdown. J Neuropathol Exp Neurol 71:806–813
111. Van den Boogert J, van Hillegersberg R, de Rooij FW, de Bruin RW, Edixhoven-Bosdijk A, Houtsmuller AB, Siersema PD, Wilson JH, Tilanus HW (1998) 5-Aminolaevulinic acid-induced protoporphyrin IX accumulation in tissues: pharmacokinetics after oral or intravenous administration. J Photochem Photobiol B 44:29–38
112. Webber J, Kessel D, Fromm D (1997) Plasma levels of protoporphyrin IX in humans after oral administration of 5-aminolevulinic acid. J Photochem Photobiol B 137:151–153
113. Webber J, Kessel D, Fromm D (1997) Side effects and photosensitization of human tissues after aminolevulinic acid. J Surg Res 68:31–37
114. Weller M, Felsberg J, Hartmann C, Berger H, Steinbach JP, Schramm J, Westphal M, Schackert G, Simon M, Tonn JC, Heese O, Krex D, Nikkhah G, Pietsch T, Wiestler O, Reifenberger G, von Deimling A, Loeffler M (2009) Molecular predictors of progression-free and overall survival in patients with newly diagnosed glioblastoma: a prospective translational study of the German Glioma Network. J Clin Oncol 27:5743–57450
115. Westphal M, Hilt DC, Bortey E, Delavault P, Olivares R, Warnke PC, Whittle IR, Jääskeläinen J, Ram Z (2003) A phase 3 trial of local chemotherapy with biodegradable carmustine (BCNU) wafers (Gliadel wafers) in patients with primary malignant glioma. Neuro Oncol 5:79–88
116. Widhalm G, Wolfsberger S, Minchev G, Woehrer A, Krssak M, Czech T, Prayer D, Asenbaum S, Hainfellner JA, Knosp E (2010) 5-Aminolevulinic acid is a promising marker for detection of anaplastic foci in diffusely infiltrating gliomas with non significant contrast enhancement. Cancer 116:1545–1552
117. Widhalm G, Kiesel B, Woehrer A, Traub-Weidinger T, Preusser M, Marosi C, Prayer D, Hainfellner JA, Knosp E, Wolfsberger S (2013) 5-Aminolevulinic acid induced fluorescence is a powerful intraoperative marker for precise histopathological grading of gliomas with non-significant contrast-enhancement. PLoS One 18:8
118. Willems PW, Taphoorn MJ, Burger H, Berkelbach van der Sprenkel JW, Tulleken CA (2006) Effectiveness of neuronavigation in resecting solitary intracerebral contrast-enhancing tumors: a randomized controlled trial. J Neurosurg 104:360–368
119. Willems PW, van der Sprenkel JW, Tulleken CA, Viergever MA, Taphoorn MJ (2006) Neuronavigation and surgery of intracerebral tumours. J Neurol 253:1123–1136
120. Wyld L, Reed MW, Brown NJ (1998) The influence of hypoxia and pH on aminolaevulinic acid-induced photodynamic therapy in bladder cancer cells in vitro. Br J Cancer 77:1621–1622
121. Wyld L, Tomlinson M, Reed MW, Brown NJ (2002) Aminolaevulinic acid-induced photodynamic therapy: cellular responses to glucose starvation. Br J Cancer 86:1343–1347
122. Zhao S, Wu J, Wang C, Liu H, Dong X, Shi C, Shi C, Liu Y, Teng L, Han D, Chen X, Yang G, Wang L, Shen C, Li H (2013) Intraoperative fluorescence-guided resection of high-grade malignant gliomas using 5-aminolevulinic acid-induced porphyrins: a systematic review and meta-analysis of prospective studies. PLoS One 28:8

Clinical Relevance of Prognostic and Predictive Molecular Markers in Gliomas

Tali Siegal

Contents

Abstract Sorting and grading of glial tumors by the WHO classification provide clinicians with guidance as to the predicted course of the disease and choice of treatment. Nonetheless, histologically identical tumors may have very different outcome and response to treatment. Molecular markers that carry both diagnostic and prognostic information add useful tools to traditional classification by redefining tumor subtypes within each WHO category. Therefore, molecular markers have become an integral part of tumor assessment in modern neuro-oncology and biomarker status now guides clinical decisions in some subtypes of gliomas. The routine assessment of *IDH* status improves histological diagnostic accuracy by differentiating diffuse glioma from reactive gliosis. It carries a favorable prognostic implication for all glial tumors and it is predictive for chemotherapeutic response in anaplastic oligodendrogliomas with codeletion of 1p/19q chromosomes. Glial tumors that con-

T. Siegal, MD
Center for Neuro-Oncology, Davidoff Institute of Oncology, Rabin Medical Center, Campus Beilinson, Petach Tikva 49100, Israel
e-mail: talisi1@clalit.org.il

J. Schramm (ed.), *Advances and Technical Standards in Neurosurgery,*
Advances and Technical Standards in Neurosurgery, Vol. 43,
DOI 10.1007/978-3-319-21359-0_4

tain chromosomal codeletion of 1p/19q are defined as tumors of oligodendroglial lineage and have favorable prognosis. *MGMT* promoter methylation is a favorable prognostic marker in astrocytic high-grade gliomas and it is predictive for chemotherapeutic response in anaplastic gliomas with wild-type IDH1/2 and in glioblastoma of the elderly. The clinical implication of other molecular markers of gliomas like mutations of *EGFR* and *ATRX* genes and *BRAF* fusion or point mutation is highlighted. The potential of molecular biomarker-based classification to guide future therapeutic approach is discussed and accentuated.

Keywords Molecular markers • Prognostic markers • Predictive markers • Low-grade glioma • High-grade glioma • MGMT • IDH mutation • Chromosomal deletion • EGFR • ATRX • BRAF

Introduction

Histological grading of gliomas according to the classification system of the World Health Organization (WHO) provides a basis for defining groups of tumors for clinical assessment. This grading also predicts the clinical behavior of the respective neoplasm with direct impact on the applied treatment regimen. Yet, within each defined histological tumor type and WHO grading, considerable variability in clinical course and response to therapy is well recognized. Traditionally, clinical characteristics such as patient age, performance status, tumor dimensions, extent of surgical resection, presumed histological cell of origin (oligodendroglial vs. astrocytic), and histological grading are used to identify prognostic subgroups of patients within each category of glial tumor. Accordingly, age and performance status are strong prognostic indicators in glioblastoma (GBM) but also in low-grade gliomas (LGG) [32, 55]. Obviously, conventional clinical classification has limitations to differentiate tumor subtypes with higher certainty that will allow for better characterization of tumor entities and variants. Molecular markers that carry both diagnostic and prognostic information add useful information to traditional classification and elucidate clinical observations by redefining tumor subtypes within each WHO category. Therefore, molecular markers have become an integral part of tumor assessment in modern neuro-oncology and biomarker status now guides clinical decisions in some subtypes of gliomas [76]. This review discusses the prognostic and predictive implication of current molecular classification of gliomas and highlights their potential to guide therapeutic approach.

What Are Prognostic and Predictive Biomarkers?

Characterization of malignant tumor is typically achieved by molecular analysis and by detection of tumor biomarkers. Two classes of biomarkers are recognized in oncology: *prognostic markers and predictive ones. Prognostic markers* inform

about likely disease outcome independent of the treatment received while *predictive markers* provide information about expected outcomes with application of specific interventions. Therefore, predictive markers can help select among two or more therapy options and they are particularly important for targeted therapy which is expected to benefit only patients whose tumors are characterized by the presence of the biomarker. For example, the GBM subtype containing the mutated variant of the epidermal growth factor receptor (EGFRvIII) possibly will respond to rindopepimut, a peptide vaccine, directed against the EGFRvIII antigenic domain. In that case, evaluation of the targeted therapy in a trial that enrolls only patients whose tumors are positive for that marker is appropriate. This type of trial design is called an enrichment design [24], and the marker is classified as an enrichment or selection marker. Currently, there are two ongoing studies that apply enrichment design for GBM. These studies are using EGFRvIII as a selection marker and aim to evaluate the therapeutic effect of rindopepimut in either newly diagnosed (NCT01480479) or recurrent (NCT01498328) GBM.

A biomarker is considered predictive if the efficacy of two treatments is different for the biomarker-positive patients than the biomarker-negative patients. The best setting in which to evaluate a predictive biomarker is a randomized clinical trial (RCT) of the selected therapy vs. a standard treatment, where the biomarker status is obtained but not used to direct treatment [25]. An example for such a trial is the German Neuro-Oncology Working Group (NOA) phase III trial in newly diagnosed elderly GBM patients (NOA-08). This trial compared radiotherapy alone (standard treatment for elderly GBM) vs. chemotherapy alone with the alkylating agent temozolomide (TMZ) [77]. The methylation status of the O^6-methylguanine-DNA methyltransferase (*MGMT*) promoter was evaluated, and the study established that *MGMT* promoter methylation is a very strong predictive biomarker for TMZ sensitivity in this patient population. Ideally, a biomarker would be assessed prospectively in an RCT. However, biomarker development often lags behind therapeutic development. Therefore, biomarker studies are frequently conducted retrospectively on archived specimen collections, sometimes several years after the therapy has been developed. An example for such setting is the practice-changing RCT of concurrent TMZ plus radiotherapy vs. radiotherapy alone for GBM [65] for which the biomarker *MGMT* methylation status was studied on a subset of the patients for whom tumor specimens and assay results were available ($n = 206$ patients of the 573 randomized) [31]. The analysis showed that *MGMT* methylation is a prognostic marker but the data did not provide sufficient evidence that *MGMT* status is predictive. Yet, with a careful prospective design, a retrospective analysis can still provide convincing evidence in support of a predictive biomarker [64].

The three molecular markers that are routinely assessed in clinical practice are isocitrate dehydrogenase 1 and 2 (*IDH1/2*) gene mutations, 1p and 19q chromosomal codeletions, and *MGMT* promoter methylation. They gained clinical relevance because they have diagnostic, prognostic, and, sometimes, predictive value (Table 1). Recently, additional markers were identified and they will be described in view of their interactions with the above extensively investigated three markers.

Table 1 Molecular biomarkers and their clinical relevance

	Molecular biomarkers					
Clinical relevance	*IDH1/2* mutation	1p/19q codeletion	*MGMT* promoter methylation	EGFRvIII	ATRX loss	BRAF fusion or point mutation
Frequency (%):						
Pilocytic astro	0	0	<10	0	0	50–70/10
PXA Diffuse astro	0 70–80	0 15	10–20 40–50	0 0	? 70	Rare/60–70 Rare
Oligo/oligoastro	70–80	30–60	60–80	0	14	Rare
Anapl. astro	50–70	15	50	0	60–80	Rare
Anapl. oligo/OA	50–70	50–80	70	0	5/30	Rare
GBM	5–10	<5	35	25–30	4	3–5
Biological implication	Linked to DNA and histone methylation, energy metabolism	Unclear biological role, linked to oligo morphology	Silencing and impairment of DNA damage repair	Constitutive activation of downstream pro-oncogenic pathways	Telomere dysfunction, genomic destabilization	Constitutive activation of BRAF downstream pathways
Diagnostic implication	D.D. between diffuse glioma and gliosis	Oligo lineage	None	Associated with GBM	Astrocytic lineage	Associated with pilocytic astro or PXA
Prognostic marker	Yes – all histologies	Yes – for oligo	Yes – astrocytic HGG	Probably	Yes	Unclear
	Favorable	Favorable	Favorable	Unfavorable	Favorable	
Predictive marker	Yes	Yes	Yes	Unclear	No	Unclear
	In AO with 1p/19q deletion for chemoTx response	In AO with *IDH*	Anapl. gliomas *IDH* wt; GBM ≥70 y	Selection marker for vaccination Tx		Selection marker for targeted Tx
	Selection marker for targeted Tx	For chemoTx response				

Prognostic marker: informs about likely disease outcome independent of the treatment received; predictive marker: provides information about expected outcomes with application of specific interventions

Astro astrocytoma, *Oligo* oligodendroglioma, *OA* oligoastrocytoma, *PXA* pleomorphic xanthoastrocytoma, *Tx*. therapy, *wt* wild type

IDH Mutations

The genome-wide sequencing effort of the Cancer Genome Atlas (TCGA) project in GBM discovered a new mutation in the *IDH* genes in 2008 [53]. In the initial report, mutation in the R132 position of the *IDH1* gene was observed in 12 % of GBM cases, and the mutations were enriched in patients with secondary GBM. Nearly all mutations in *IDH* are heterozygous somatic point mutations in which a single nucleotide change at codon 132 (*IDH1*) or 172 (*IDH2*) results in coding for a different amino acid than in the wild-type gene. Thus, almost 90 % of *IDH1* mutations result in an arginine to histidine substitutions with other mutations occurring less frequently. *IDH2* mutations are much less common (~3 %) and are associated with oligodendroglial histology [30, 84].

IDH is a catalytic enzyme with at least three isoforms – IDH1, IDH2, and IDH3. Mutations in IDH3 have not been observed in gliomas. IDH1 enzyme is located in the cytoplasm and its normal function is to catalyze the oxidative decarboxylation of isocitrate into alpha-ketoglutarate (alpha-KG) and nicotinamide adenine dinucleotide (NADPH). The identical reaction is carried out by IDH2 in the mitochondria [8]. The mutated IDH enzyme is unable to generate alpha-KG and instead converts isocitrate to 2-hydroxyglutarate (2-HG) which then accumulates considerably in gliomas [18]. This 2-HG metabolite has been proposed as a novel oncometabolite, but its exact mechanistic role in glioma genesis is still under active investigation. It should be noted that in addition to gliomas, *IDH* mutations are also observed in acute myeloid leukemia, in intrahepatic cholangiocarcinoma, and in chondrosarcoma [3, 9, 45]. Emerging data suggest that the accumulation of 2-HG generate competitive inhibition for enzymes which regulate DNA methylation and histone demethylases resulting in the evolution of glioma CpG island methylator phenotype (G-CIMP) (for more details, see next section) [67, 83]. The strong association between *IDH* mutations, G-CIMP phenotype, and some other genetic alterations clearly provides evidence that gliomas with *IDH* mutations have a distinct pathogenic origin.

Molecular classification of gliomas separates the tumors into *IDH* wild-type vs. *IDH*-mutant gliomas (Figs. 1 and 2). Distinct entities among the *IDH* wild-type gliomas are pediatric tumors like pilocytic astrocytomas, pleomorphic xanthoastrocytomas and ependymomas, and the most frequent tumor in adults – primary GBM. Conversely, most WHO grade II and III adult gliomas and secondary GBM share *IDH* mutations and carry a better prognosis than *IDH* wild-type tumors of the same histological grade [76]. The prognostic data have largely come from retrospective analysis of tissue banks obtained from clinical trials [29, 69, 70, 75, 79] and indicates that *IDH* mutation is a favorable prognostic marker in adult low- and high-grade gliomas (HGG) (Table 1).

IDH-mutated gliomas display a distinct clinical phenotype (Fig. 1). These patients are significantly younger than those with *IDH* wild-type gliomas across all tumor grades [30] and the mutation is rarely seen in the elderly population. Distinctive radiographic characteristics in *IDH*-mutant HGG include a predilection

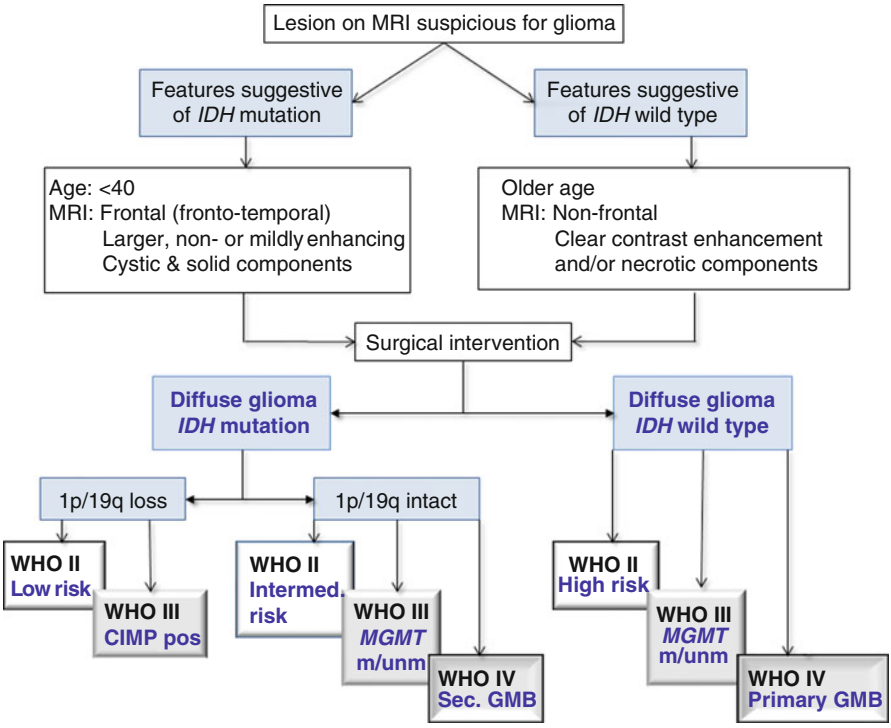

Fig. 1 Clinical features and histological and molecular classifications of adult gliomas. *CIMP* CpG island methylation phenotype, *m/unm* methylated/unmethylated

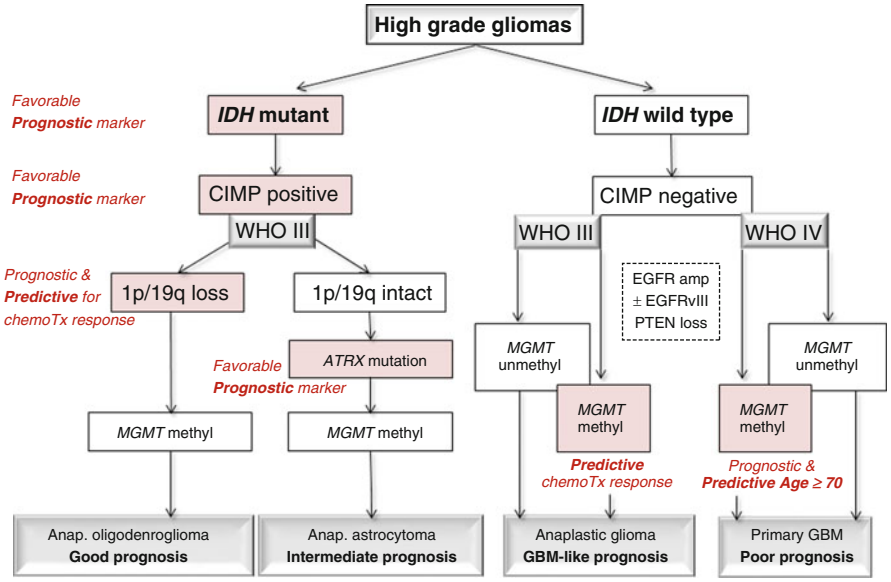

Fig. 2 Molecular classification of high-grade adult gliomas and prognostic and/or predictive implication of biomarkers. *CIMP* CpG island methylation phenotype, *methyl* methylated, *unmethyl* unmethylated

for frontal lobe location, large tumor size at diagnosis, more frequent nonenhancing tumor component and less contrast enhancement, reduced necrotic-appearing areas, and more prevalent cystic and diffuse components [30, 39]. Interestingly, a retrospective study of 335 HGG recently demonstrated that *IDH1* mutation may serve as a predictive molecular marker to guide aggressive surgical resection beyond the enhancing tumor margins (maximal resection of total tumor volume including the nonenhancing tumor) as it conferred additional survival benefit only in *IDH1-mutant* variants [6].

Diagnostic assessment of *IDH* status is performed on tissue sample and can be obtained either by immunohistochemistry (IHC) or by sequencing. IHC uses an antibody directed against the most prevalent *IDH*-mutant isoform (*IDH1* R132H substitution) which accounts for approximately 85 % of all *IDH* mutations in gliomas [30, 84]. Compared with sequencing, the sensitivity and specificity of IHC have been reported to be 94 % and 100 %, respectively [14]. Still, sequencing can identify those infrequent *IDH* mutations not identified by IHC. The routine use of IHC for assessment of *IDH1* status improved histological diagnosis in cases with limited sample availability helping to distinguish between diffuse glioma and pilocytic astrocytoma, ependymoma, and nonneoplastic reactive gliosis [14, 37]. Finally, noninvasive methods to detect *IDH1*-mutant tumors are under development, like magnetic resonance spectroscopy that can detect the abnormal accumulation of the oncometabolite 2-HG within the tumor. This technique has the potential to monitor treatment response but caution is currently needed as false-negative results may be frequent [4, 7].

IDH mutations separate gliomas into two genotype distinct groups (Fig. 2), but the presence of the mutation can also serve as a potential therapeutic target [38]. Recently, two compounds specifically targeting mutants IDH1 R132H (AGI 5198) [56] and IDH2 R140Q (AGI 6780) [73] have been developed. Although the potential clinical benefit of such inhibitors is not yet clear, their emergence raises new hope for the treatment of *IDH*-mutated tumors. Initial studies demonstrated that the targeted inactivation of IDH1 R132H by the inhibitor AGI 5198 impaired growth of *IDH1*-mutant glioma cells and mouse xenografts and promoted gliogenic differentiation [59]. Another potential approach is to directly target 2-HG production by inhibiting the conversion of glutamine to alpha-KG with siRNA or by a small molecular inhibitor [62]. This slows the growth rate of *IDH*-mutant glioma cells, suggesting that "starving" mutant *IDH1* cells of alpha-KG may have therapeutic benefit.

MGMT Promoter Methylation

DNA methylation is the covalent addition of a methyl group preferentially at the 5′-position of a cytosine or guanine nucleotide. The cytosine and guanine, separated by only one phosphate, tend to cluster to so-called CpG islands, located in the promoter regions of more than half of all human genes [66]. DNA methylation is mediated by the DNA methyltransferase family of enzymes and hypermethylation mostly occurs at the promoter CpG Island of genes and is closely associated with transcriptional inactivation. Interestingly, the methylation patterns differ between

gliomas of WHO grade II–IV [68]. As mentioned above, the TCGA project has identified a glioma CpG island methylation phenotype (G-CIMP) that correlated with younger age, a proneural gene expression profile [72], longer overall survival in GBM patients [51], and a high frequency of *IDH1* mutation which links metabolic alterations and epigenetic modification [83].

The *MGMT* gene is located at chromosome 10q26 and codes for the ubiquitously expressed DNA repair enzyme that removes alkyl adducts from the O^6-position of guanine [54]. MGMT enzyme protects normal cells from carcinogens, but it also repairs the lethal effects of alkylating chemotherapy such as TMZ. Methylation of *MGMT* promoter is found in 35–45 % of HGG and in about 80 % of LGG [13, 31] (Table 1). *MGMT* methylated and unmethylated GBM seem to differ in primary tumor location [19], pattern of contrast enhancement [41] and the apparent diffusion coefficient in MRI analysis [60], and the incidence of pseudoprogression observed after concurrent chemoradiation therapy [10, 52]. However, none of these differences allows for noninvasive determination of *MGMT* promoter status for the individual patient.

Several clinical studies have shown that *MGMT* promoter methylation is a strong and independent prognostic factor associated with prolonged progression-free and overall survival in HGG (Table 1) [26, 31, 78, 79]. However, most studies failed to prove that MGMT methylation is predictive for sensitivity to chemotherapy with TMZ. Recently, the predictive value of MGMT as a biomarker associated with benefit from treatment with alkylating agents has been demonstrated for some subgroups of HGG. The first group includes elderly patients with HGG randomized to treatment with either TMZ alone or radiotherapy alone as initial treatment [44, 77]. Subgroup analyses of both trials showed better outcome for chemotherapy in patients with *MGMT* promoter methylation but reduced survival for patients with unmethylated tumor. It should be noted that even though *MGMT* methylation frequency is age independent in HGG, tumors in elderly often lack other favorable prognostic markers established in younger GBM patients, which most likely contributes to the overall worse prognosis in that age group [81]. Still, the results of the RCT in the elderly strongly suggest that treatment strategy should be individualized per *MGMT* status in that age group. The second distinct group analysis explored anaplastic gliomas of patients enrolled to the NOA-04 trial [79] and evaluated whether *IDH1* status determines the prognostic vs. predictive role of *MGMT* promoter methylation [78]. It was found that *MGMT* promoter methylation is a predictive marker for benefit from alkylating agents only in patients with *IDH1* wild-type but not in *IDH1*-mutant tumors (Fig. 2). These findings need further prospective evaluation to establish the clinical utility of these biomarkers in anaplastic gliomas.

In clinical setting, there is no consensus about the most suitable technique for determination of the *MGMT* methylation status [13, 57]. A study that compared five different methods showed diverse levels of correlation between *MGMT* methylation status and overall survival in GBM patients [35]. Most tests are able to discriminate clearly methylated from evidently unmethylated cases that have association with gene silencing and prognostic value [15]. Nonetheless, there seems to be a category

of intermediate samples that are more challenging. A particular demanding point is the definition of a technically and clinically relevant cutoff between positive and negative test results. Another issue is whether the status of *MGMT* promoter methylation which is determined from a small-sized stereotactic biopsy can reliably carry clinical relevance. A study that examined 25 HGG by 2–4 biopsy specimens that were collected from different sites within each tumor demonstrated that the methylation profile constitutes a homogenous marker throughout the tumor [27]. Interestingly, it has also been demonstrated that in the majority of recurrent GBM (89 %), the *MGMT* promoter methylation status of the primary tumor is retained at recurrence [21].

Routinely, tumor DNA is extracted from the pathological specimen for *MGMT* status evaluation. A different approach is to determine the MGMT methylation status from free circulating DNA in serum/plasma of glioma patients [22, 40]. This noninvasive method may enable longitudinal monitoring. The methylation status in both tumor tissue and plasma proved to be highly concordant with a specificity of almost 100 % but the sensitivity of blood testing is still inferior for routine application of this testing.

1p and 19q Chromosomal Deletions

Combined loss of genetic material from chromosomal arms 1p (short arm of chromosome 1) and 19q (long arm of chromosome 19) has long been recognized as a typical molecular signature of oligodendroglial tumors [58]. This combined loss results from an unbalanced translocation that leads to the loss of one hybrid chromosome and thereby loss of heterozygosity [33]. 1p and 19q codeleted tumors carry a better prognosis than do histologically indistinguishable tumors of the same grade but without this codeletion [11, 71, 79]. While loss of 1p/19q is common in oligodendrogliomas, loss of 1p alone or 19q alone is sometimes seen in astrocytomas but it does not convey the same prognostic implication as the combined loss of 1p/19q in oligodendrogliomas. The prognostic implication for prolonged overall survival of 1p/19q codeleted tumor has been established in three RCT of anaplastic gliomas [11, 71, 79]. At extended follow-up, it became clear that 1p/19q codeletion status is a predictive marker for chemotherapy responsiveness in anaplastic oligodendrogliomas [11, 71]. Both studies (RTOG 9402 and EORTC 26951) compared chemotherapy with procarbazine, lomustine, and vincristine (PCV) in combination with radiation therapy to radiation therapy alone. Tumor tissues from study patients were retrospectively analyzed for codeletion status when possible. Survival curves separated after the median survival had been reached for the study cohort, and significantly more patients lived for 10 years or longer after the initial combined chemoradiation therapy than after radiotherapy alone. The median survival of the subgroup of patients with 1p/19q codeleted tumors doubled following the initial treatment with chemoradiation therapy when compared to treatment with radiotherapy alone, establishing the predictive value of 1p/19q biomarker. Based on the

results of these RCT, it is not surprising that the NCCN treatment guidelines recommend 1p/19q codeletion as the only molecular biomarker to be used for therapeutic stratification in anaplastic oligodendroglioma and mixed gliomas [49]. Recently, a retrospective analysis of 228 patients with anaplastic gliomas that included the cohort of the NOA-04 study [74] established a molecular classification scheme which integrates *IDH1* status, G-CIMP, and 1p/19q deletion (Fig. 2). This scheme was demonstrated to translate into clinical relevant survival differences better than histological classification [82].

Assessment of 1p/19q deletion is most frequently performed either by fluorescent in situ hybridization (FISH) or by loss of heterozygosity analysis (PCR-based microsatellite analysis) on tumor sample. Newer techniques, such as array comparative genomic hybridization and single nucleotide polymorphism array, are becoming available for clinical use [50]. The choice of technique depends on laboratory expertise, equipment available for testing, and the clinician and pathologist's preference.

EGFR Mutation

The *EGFRvIII* is a mutant of *EGFR* that is expressed in approximately 20–30 % of GBM (Table 1). EGFRvIII expression typically occurs in the presence of wild-type EGFR overexpression which is detected in about 50 % of GBM [42]. EGFRvIII is most common in primary GBM and rare in secondary GBM.

EGFR is a transmembrane glycoprotein which contains an extracellular ligand-binding domain and a cytoplasmatic domain containing a tyrosine kinase [5]. The activation of this receptor turns on oncogenic pathways. The mutated receptor of the EGFRvIII has a truncated extracellular domain due to deletion of 267 amino acids and it results in constitutive tyrosine kinase activity and pro-oncogenic effects such as enhancing proliferation, radio- and chemotherapeutic resistance, and migration with inhibition of apoptosis [48]. Yet, its prognostic relevance is controversial, but long-term survival might be worse in patients whose tumor carries this mutation. As EFGRvIII is not expressed on normal tissues, it is an effective target for immunotherapy [5]. For that reason, vaccination strategies based on this unique peptide sequence have been developed and have been tested in various phase II trials. Currently, two studies evaluate the therapeutic effect of the EGFRvIII-directed vaccine, rindopepimut, in either newly diagnosed (NCT01480479) or recurrent (NCT01498328) GBM.

Methods to detect EGFR overexpression and presence of EGFRvIII include IHC, FISH, and reverse transcriptase PCR (RT-PCR) [20, 50] which all show high concordance between these tests [20]. A noninvasive method is based on the fact that EGFRvIII-positive cells are able to secrete membrane-derived microvesicles containing EGFRvIII mRNA. These microvesicles merge with the plasma membrane of negative cells conferring the oncogenic advantage associated with the mutant variant [2]. Hence, EGFRvIII mRNA is detected in microvesicles in the

serum of EGFRvIII-positive GBM patients indicating that it could be a biomarker to monitor either tumor response or a relapse [63].

ATRX Mutation

The *alpha-thalassemia/mental retardation syndrome X-linked* (*ATRX*) gene is located on chromosome Xq21.1, and physiologically, ATRX protein is ubiquitously expressed in cell nuclei. Mutations in the ATRX gene result in a loss of nuclear protein expression in tumor cells, but not in non-tumor cells. ATRX loss of function leads to telomere dysfunction and to a phenotype called alternative lengthening of telomeres (ALT) along with more widespread genomic destabilization [1, 16]. Mutations of *ATRX* have been recently reported in both pediatric and adult astrocytic gliomas [61, 76, 80, 82] (Table 1), and a recent study of 214 astrocytomas found that ALT phenotype is highly associated with loss of ATRX protein expression in high-grade pediatric and adult astrocytomas [1]. The mutations are also highly associated with other mutations such as *IDH1* and *TP53* and they are almost mutually exclusive with 1p/19q codeletion [34]. Therefore, ATRX loss is considered a very specific marker for astrocytic lineage tumors including diffuse and anaplastic astrocytoma and a subset of oligoastrocytoma [34, 80, 82]. Two studies found that patients with *ATRX* mutation with *IDH* mutation tended to be younger and survived significantly longer [34, 80].

Studies that analyzed adult anaplastic gliomas found that ATRX loss refines the molecular classification of these tumors and identifies a subgroup of *IDH*-mutant astrocytic tumors with better prognosis [80, 82] (Fig. 2). Thus, in the clinical setting, the combination of routine 1p/19q deletion and ATRX assessment (by IHC) could help to guide the diagnosis within the spectrum of *IDH*-mutant gliomas. It should be noted that in contrast to gliomas of adult patients, *ATRX* mutations are far less common in pediatric anaplastic gliomas and LGG and have to date never been found in pilocytic astrocytoma [1, 43, 61] (Table 1).

Molecular Markers in Low-Grade Gliomas

Although the diagnosis of LGG has traditionally been made on the basis of histology, molecular abnormalities known to occur in these tumors have been evolving as supportive markers to assist diagnostics and patient management [75]. The markers that have been mostly investigated are *IDH* mutation, *MGMT* methylation, 1p/19q deletions, v-RAF murine sarcoma viral oncogene homolog B1 (BRAF) alterations, and *TP53* mutation which are common in low-grade astrocytomas. Current understanding of the likely molecular pathogenesis of LGG assumes that *IDH* mutations are early events [74] which give rise to the formation of oligodendroglial tumors in the face of 1p/19q codeletions. Otherwise, *IDH mutation* leads to the evolution of

astrocytoma particularly in face of *PT53* mutations. *IDH* wild-type tumors are less well understood and share a less favorable prognosis, irrespective of histology (Tables 1) [28, 75].

Widely accepted clinical prognostic factors in LGG are age at diagnosis, tumor size, and presence or absence of symptomatic disease including intractable seizures. The overall analysis of the distribution of molecular changes and outcome in LGG leads to the distinction of three subgroups of patients as specified above (Table 1). Despite this molecular distinction, it should be noted that no marker has yet been validated in LGG to guide a decision between chemotherapy and radiotherapy which means that no predictive value has been found. In fact, the level of independence between *IDH*, 1p/19q deletions, and *MGMT* status is still a matter of controversy and so far, no known biomarker is of any relevance for the postoperative course of the disease in the absence of a genotoxic treatment. Although the prognostic significance (regarding overall survival) of *IDH* mutation was noted by several studies [28, 46, 75], it seems that none of the molecular markers are sensitive prognostic indicator in LGG patients who do not receive radiotherapy or chemotherapy after surgery. An exception may be the case of BRAF alterations which may serve as selection markers for a targeted therapy.

BRAF Fusion or Point Mutation

BRAF is a major component of RAS/RAF/MEK/MAPK signaling pathway that functions to transmit extracellular signals from the cytoplasmatic membrane to the nucleus. Various alterations in BRAF are associated with brain tumors [36]. These mutations are rare in adult gliomas whereas more than 85 % of all pediatric LGG have one or two abnormalities in BRAF (Table 1). Pediatric HGG possess BRAF mutations in approximately 20 % of patients and the mutations are also occasionally observed in adults. Many tumors with point mutations contain a single nucleotide substitution that constitutively activates BRAF as a monomer (instead of the typical dimer signal). These point mutations are potential targets for treatment with BRAF inhibitors, with BRAFV600E mutation being the most investigated one [17]. Such point mutations are observed in approximately 20 % of fibrillary astrocytomas, 50 % of gangliogliomas, 75 % of pleomorphic xanthoastrocytomas, and 5 % of pilocytic astrocytoma.

Some pediatric LGG have truncated fusion mutations of BRAF rather than the point mutation. This happens when there is a translocation that duplicates the *BRAF* activation domain but at the same time have deletion of the N-terminal inhibitory domain. This places the *BRAF* gene under the control of the promoter of *KIAA1549* (a gene of unknown function) and results in an expression of a mutant protein. The latter is typically found in pilocytic astrocytomas and most commonly in tumors of the posterior fossa [23]. It is predicated that binding of BRAF inhibitors to the one side of the dimer, which is a constituent of the mutant fusion protein, will result in

a feedback loop that will further activate the pathway, rather than inhibiting it. In that case, downstream inhibitors such as MEK, ERK, and, possibly, mTOR might be more appropriate agents for therapeutic intervention. Finally, *KIAA1549-BRAF* gene fusions are an important diagnostic marker to distinguish pilocytic astrocytomas from high-grade astrocytic tumors – a distinction that can be both challenging and therapeutically relevant since pilocytic astrocytomas and GBM share the morphological feature of microvascular proliferation.

Coexistence and Interaction of Various Molecular Markers

Largely, glial tumors can be divided into two groups based on presence or absence of *IDH* mutations (Figs. 1 and 2). These two groups probably differ in the genesis of the related tumors. The currently recognized molecular markers (*IDH* mutation, 1p/19q deletion, and *MGMT* promoter methylation) are not entirely independent of each other. The *IDH* mutations induce the G-CIMP glioma phenotype, which almost always have *MGMT* methylation and often also 1p/19q codeletion, and apparently have better prognosis than *IDH* wild-type G-CIMP-negative tumors. It is therefore not surprising that a recent retrospective analysis of the RTOG 9402 trial, which demonstrated a significant survival advantage in anaplastic oligodendrogliomas with up-front chemoradiation therapy, found that the benefit is associated with *IDH* mutation [12]. As expected, another study in GBM tumors demonstrated that combination of *IDH1* mutations and *MGMT* methylation status predict survival better than either one of the markers alone [47]. Currently, studies in both GBM and anaplastic gliomas suggest that MGMT methylation has prognostic value when it comes together with *IDH* mutation [47, 78]. However, in the absence of *IDH* mutations, it is becoming increasingly evident that *MGMT* promoter methylation is predictive for response to treatment with alkylating agents [44, 77, 78]. This has been demonstrated both in elderly GBM patients and recently in anaplastic gliomas (Fig. 2). Finally, *ATRX* mutation which is a hallmark of astrocytic lineage carries a favorable prognostic implication in anaplastic gliomas but it is mostly restricted to *IDH*-mutant tumors which are largely G-CIMP positive [80, 82].

In Conclusion

- Routine evaluation of the status of 1p/19q chromosomes, *MGMT* promoter methylation, and expression of *IDH* and *ATRX* mutations has direct clinical implications.
- This evaluation refines classification of gliomas as it combines traditional histological subtypes and staging together with contemporary molecular classification.

- The combination of molecular classification with traditional histology informs the clinician on both prognostic outlook and preferred management algorithm.
- Furthermore, progress in molecular diagnostics will help to improve the design of future RCT because it is a tool that enriches patient populations and thus may reform the selection of appropriate therapeutic measures.

References

1. Abedalthagafi M, Phillips JJ, Kim GE, Mueller S, Haas-Kogen DA, Marshall RE et al (2013) The alternative lengthening of telomere phenotype is significantly associated with loss of ATRX expression in high-grade pediatric and adult astrocytomas: a multi-institutional study of 214 astrocytomas. Mod Pathol Off J U S A Can Acad Pathol Inc 26:1425–1432
2. Al-Nedawi K, Meehan B, Micallef J, Lhotak V, May L, Guha A et al (2008) Intercellular transfer of the oncogenic receptor EGFRvIII by microvesicles derived from tumour cells. Nat Cell Biol 10:619–624
3. Amary MF, Bacsi K, Maggiani F, Damato S, Halai D, Berisha F et al (2011) IDH1 and IDH2 mutations are frequent events in central chondrosarcoma and central and periosteal chondromas but not in other mesenchymal tumours. J Pathol 224:334–343
4. Andronesi OC, Rapalino O, Gerstner E, Chi A, Batchelor TT, Cahill DP et al (2013) Detection of oncogenic IDH1 mutations using magnetic resonance spectroscopy of 2-hydroxyglutarate. J Clin Invest 123:3659–3663
5. Babu R, Adamson DC (2012) Rindopepimut: an evidence-based review of its therapeutic potential in the treatment of EGFRvIII-positive glioblastoma. Core Evid 7:93–103
6. Beiko J, Suki D, Hess KR, Fox BD, Cheung V, Cabral M et al (2014) IDH1 mutant malignant astrocytomas are more amenable to surgical resection and have a survival benefit associated with maximal surgical resection. Neuro Oncol 16:81–91
7. Bertolino N, Marchionni C, Ghielmetti F, Burns B, Finocchiaro G, Anghileri E et al (2014) Accuracy of 2-hydroxyglutarate quantification by short-echo proton-MRS at 3 T: a phantom study. Phys Med PM Int J Devot Appl Phys Med Biol Off J Ital Assoc Biomed Phys 30:702–707
8. Bolduc JM, Dyer DH, Scott WG, Singer P, Sweet RM, Koshland DE Jr et al (1995) Mutagenesis and Laue structures of enzyme intermediates: isocitrate dehydrogenase. Science 268:1312–1318
9. Borger DR, Tanabe KK, Fan KC, Lopez HU, Fantin VR, Straley KS et al (2012) Frequent mutation of isocitrate dehydrogenase (IDH)1 and IDH2 in cholangiocarcinoma identified through broad-based tumor genotyping. Oncologist 17:72–79
10. Brandes AA, Franceschi E, Tosoni A, Blatt V, Pession A, Tallini G et al (2008) MGMT promoter methylation status can predict the incidence and outcome of pseudoprogression after concomitant radiochemotherapy in newly diagnosed glioblastoma patients. J Clin Oncol Off J Am Soc Clin Oncol 26:2192–2197
11. Cairncross G, Wang M, Shaw E, Jenkins R, Brachman D, Buckner J et al (2013) Phase III trial of chemoradiotherapy for anaplastic oligodendroglioma: long-term results of RTOG 9402. J Clin Oncol Off J Am Soc Clin Oncol 31:337–343
12. Cairncross JG, Wang M, Jenkins RB, Shaw EG, Giannini C, Brachman DG et al (2014) Benefit from procarbazine, lomustine, and vincristine in oligodendroglial tumors is associated with mutation of IDH. J Clin Oncol Off J Am Soc Clin Oncol 32:783–790
13. Cankovic M, Nikiforova MN, Snuderl M, Adesina AM, Lindeman N, Wen PY et al (2013) The role of MGMT testing in clinical practice: a report of the association for molecular pathology. J Mol Diagn JMD 15:539–555
14. Capper D, Weissert S, Balss J, Habel A, Meyer J, Jager D et al (2010) Characterization of R132H mutation-specific IDH1 antibody binding in brain tumors. Brain Pathol 20:245–254

15. Christians A, Hartmann C, Benner A, Meyer J, von Deimling A, Weller M et al (2012) Prognostic value of three different methods of MGMT promoter methylation analysis in a prospective trial on newly diagnosed glioblastoma. PLoS One 7:e33449
16. Clynes D, Jelinska C, Xella B, Ayyub H, Taylor S, Mitson M et al (2014) ATRX dysfunction induces replication defects in primary mouse cells. PLoS One 9:e92915
17. Dahiya S, Emnett RJ, Haydon DH, Leonard JR, Phillips JJ, Perry A et al (2014) BRAF-V600E mutation in pediatric and adult glioblastoma. Neuro Oncol 16:318–319
18. Dang L, White DW, Gross S, Bennett BD, Bittinger MA, Driggers EM et al (2009) Cancer-associated IDH1 mutations produce 2-hydroxyglutarate. Nature 462:739–744
19. Ellingson BM, Cloughesy TF, Pope WB, Zaw TM, Phillips H, Lalezari S et al (2012) Anatomic localization of O6-methylguanine DNA methyltransferase (MGMT) promoter methylated and unmethylated tumors: a radiographic study in 358 de novo human glioblastomas. Neuroimage 59:908–916
20. Faulkner C, Palmer A, Williams H, Wragg C, Haynes HR, White P et al (2014) EGFR and EGFRvIII analysis in glioblastoma as therapeutic biomarkers. Br J Neurosurg 1–7
21. Felsberg J, Thon N, Eigenbrod S, Hentschel B, Sabel MC, Westphal M et al (2011) Promoter methylation and expression of MGMT and the DNA mismatch repair genes MLH1, MSH2, MSH6 and PMS2 in paired primary and recurrent glioblastomas. Int J Cancer J Int du Cancer 129:659–670
22. Fiano V, Trevisan M, Trevisan E, Senetta R, Castiglione A, Sacerdote C et al (2014) MGMT promoter methylation in plasma of glioma patients receiving temozolomide. J Neurooncol 117:347–357
23. Forshew T, Tatevossian RG, Lawson AR, Ma J, Neale G, Ogunkolade BW et al (2009) Activation of the ERK/MAPK pathway: a signature genetic defect in posterior fossa pilocytic astrocytomas. J Pathol 218:172–181
24. Freidlin B, McShane LM, Korn EL (2010) Randomized clinical trials with biomarkers: design issues. J Natl Cancer Inst 102:152–160
25. Freidlin B, Sun Z, Gray R, Korn EL (2013) Phase III clinical trials that integrate treatment and biomarker evaluation. J Clin Oncol Off J Am Soc Clin Oncol 31:3158–3161
26. Gilbert MR, Wang M, Aldape KD, Stupp R, Hegi ME, Jaeckle KA et al (2013) Dose-dense temozolomide for newly diagnosed glioblastoma: a randomized phase III clinical trial. J Clin Oncol Off J Am Soc Clin Oncol 31:4085–4091
27. Grasbon-Frodl EM, Kreth FW, Ruiter M, Schnell O, Bise K, Felsberg J et al (2007) Intratumoral homogeneity of MGMT promoter hypermethylation as demonstrated in serial stereotactic specimens from anaplastic astrocytomas and glioblastomas. Int J Cancer J Int du Cancer 121:2458–2464
28. Hartmann C, Hentschel B, Tatagiba M, Schramm J, Schnell O, Seidel C et al (2011) Molecular markers in low-grade gliomas: predictive or prognostic? Clin Cancer Res Off J Am Assoc Cancer Res 17:4588–4599
29. Hartmann C, Hentschel B, Wick W, Capper D, Felsberg J, Simon M et al (2010) Patients with IDH1 wild type anaplastic astrocytomas exhibit worse prognosis than IDH1-mutated glioblastomas, and IDH1 mutation status accounts for the unfavorable prognostic effect of higher age: implications for classification of gliomas. Acta Neuropathol 120:707–718
30. Hartmann C, Meyer J, Balss J, Capper D, Mueller W, Christians A et al (2009) Type and frequency of IDH1 and IDH2 mutations are related to astrocytic and oligodendroglial differentiation and age: a study of 1,010 diffuse gliomas. Acta Neuropathol 118:469–474
31. Hegi ME, Diserens AC, Gorlia T, Hamou MF, de Tribolet N, Weller M et al (2005) MGMT gene silencing and benefit from temozolomide in glioblastoma. N Engl J Med 352: 997–1003
32. Ho VK, Reijneveld JC, Enting RH, Bienfait HP, Robe P, Baumert BG et al (2014) Changing incidence and improved survival of gliomas. Eur J Cancer 50:2309–2318
33. Jenkins RB, Blair H, Ballman KV, Giannini C, Arusell RM, Law M et al (2006) A t(1;19)(q10;p10) mediates the combined deletions of 1p and 19q and predicts a better prognosis of patients with oligodendroglioma. Cancer Res 66:9852–9861

34. Jiao Y, Killela PJ, Reitman ZJ, Rasheed AB, Heaphy CM, de Wilde RF et al (2012) Frequent ATRX, CIC, FUBP1 and IDH1 mutations refine the classification of malignant gliomas. Oncotarget 3:709–722
35. Karayan-Tapon L, Quillien V, Guilhot J, Wager M, Fromont G, Saikali S et al (2010) Prognostic value of O6-methylguanine-DNA methyltransferase status in glioblastoma patients, assessed by five different methods. J Neurooncol 97:311–322
36. Kieran MW (2014) Targeting BRAF in pediatric brain tumors. Am Soc Clin Oncol Educ Book/ASCO. Am Soc Clin Oncol. Meeting. e436–e440. PMID: 24857135
37. Korshunov A, Meyer J, Capper D, Christians A, Remke M, Witt H et al (2009) Combined molecular analysis of BRAF and IDH1 distinguishes pilocytic astrocytoma from diffuse astrocytoma. Acta Neuropathol 118:401–405
38. Krell D, Mulholland P, Frampton AE, Krell J, Stebbing J, Bardella C (2013) IDH mutations in tumorigenesis and their potential role as novel therapeutic targets. Future Oncol 9:1923–1935
39. Lai A, Kharbanda S, Pope WB, Tran A, Solis OE, Peale F et al (2011) Evidence for sequenced molecular evolution of IDH1 mutant glioblastoma from a distinct cell of origin. J Clin Oncol Off J Am Soc Clin Oncol 29:4482–4490
40. Lavon I, Refael M, Zelikovitch B, Shalom E, Siegal T (2010) Serum DNA can define tumor-specific genetic and epigenetic markers in gliomas of various grades. Neuro Oncol 12: 173–180
41. Levner I, Drabycz S, Roldan G, De Robles P, Cairncross JG, Mitchell R (2009) Predicting MGMT methylation status of glioblastomas from MRI texture. Med Image Comput Computer Assist Interv MICCAI … Int Conf Med Image Comput Comput Assist Interv 12:522–530
42. Liu L, Backlund LM, Nilsson BR, Grander D, Ichimura K, Goike HM et al (2005) Clinical significance of EGFR amplification and the aberrant EGFRvIII transcript in conventionally treated astrocytic gliomas. J Mol Med 83:917–926
43. Liu XY, Gerges N, Korshunov A, Sabha N, Khuong-Quang DA, Fontebasso AM et al (2012) Frequent ATRX mutations and loss of expression in adult diffuse astrocytic tumors carrying IDH1/IDH2 and TP53 mutations. Acta Neuropathol 124:615–625
44. Malmstrom A, Gronberg BH, Marosi C, Stupp R, Frappaz D, Schultz H et al (2012) Temozolomide versus standard 6-week radiotherapy versus hypofractionated radiotherapy in patients older than 60 years with glioblastoma: the Nordic randomised, phase 3 trial. Lancet Oncol 13:916–926
45. Mardis ER, Ding L, Dooling DJ, Larson DE, McLellan MD, Chen K et al (2009) Recurring mutations found by sequencing an acute myeloid leukemia genome. N Engl J Med 361: 1058–1066
46. Metellus P, Coulibaly B, Colin C, de Paula AM, Vasiljevic A, Taieb D et al (2010) Absence of IDH mutation identifies a novel radiologic and molecular subtype of WHO grade II gliomas with dismal prognosis. Acta Neuropathol 120:719–729
47. Molenaar RJ, Verbaan D, Lamba S, Zanon C, Jeuken JW, Boots-Sprenger SH et al (2014) The combination of IDH1 mutations and MGMT methylation status predicts survival in glioblastoma better than either IDH1 or MGMT alone. Neuro Oncol 16:1263–1273
48. Nagane M, Coufal F, Lin H, Bogler O, Cavenee WK, Huang HJ (1996) A common mutant epidermal growth factor receptor confers enhanced tumorigenicity on human glioblastoma cells by increasing proliferation and reducing apoptosis. Cancer Res 56:5079–5086
49. NCCN (2013) Clinical practice guidelines in oncology. Central nervous system cancers, Version 2. http://www.nccn.org
50. Nikiforova MN, Hamilton RL (2011) Molecular diagnostics of gliomas. Arch Pathol Lab Med 135:558–568
51. Noushmehr H, Weisenberger DJ, Diefes K, Phillips HS, Pujara K, Berman BP et al (2010) Identification of a CpG island methylator phenotype that defines a distinct subgroup of glioma. Cancer Cell 17:510–522
52. Park CK, Kim J, Yim SY, Lee AR, Han JH, Kim CY et al (2011) Usefulness of MS-MLPA for detection of MGMT promoter methylation in the evaluation of pseudoprogression in glioblastoma patients. Neuro Oncol 13:195–202

53. Parsons DW, Jones S, Zhang X, Lin JC, Leary RJ, Angenendt P et al (2008) An integrated genomic analysis of human glioblastoma multiforme. Science 321:1807–1812
54. Pegg AE (2000) Repair of O(6)-alkylguanine by alkyltransferases. Mutat Res 462:83–100
55. Pignatti F, van den Bent M, Curran D, Debruyne C, Sylvester R, Therasse P et al (2002) Prognostic factors for survival in adult patients with cerebral low-grade glioma. J Clin Oncol Off J Am Soc Clin Oncol 20:2076–2084
56. Popovici-Muller J, Saunders JO, Salituro FG, Travins JM, Yan S, Zhao F et al (2012) Discovery of the first potent inhibitors of mutant IDH1 that lower tumor 2-HG in vivo. ACS Med Chem Lett 3:850–855
57. Quillien V, Lavenu A, Sanson M, Legrain M, Dubus P, Karayan-Tapon L et al (2014) Outcome-based determination of optimal pyrosequencing assay for MGMT methylation detection in glioblastoma patients. J Neurooncol 116:487–496
58. Reifenberger J, Reifenberger G, Liu L, James CD, Wechsler W, Collins VP (1994) Molecular genetic analysis of oligodendroglial tumors shows preferential allelic deletions on 19q and 1p. Am J Pathol 145:1175–1190
59. Rohle D, Popovici-Muller J, Palaskas N, Turcan S, Grommes C, Campos C et al (2013) An inhibitor of mutant IDH1 delays growth and promotes differentiation of glioma cells. Science 340:626–630
60. Romano A, Calabria LF, Tavanti F, Minniti G, Rossi-Espagnet MC, Coppola V et al (2013) Apparent diffusion coefficient obtained by magnetic resonance imaging as a prognostic marker in glioblastomas: correlation with MGMT promoter methylation status. Eur Radiol 23:513–520
61. Schwartzentruber J, Korshunov A, Liu XY, Jones DT, Pfaff E, Jacob K et al (2012) Driver mutations in histone H3.3 and chromatin remodelling genes in paediatric glioblastoma. Nature 482:226–231
62. Seltzer MJ, Bennett BD, Joshi AD, Gao P, Thomas AG, Ferraris DV et al (2010) Inhibition of glutaminase preferentially slows growth of glioma cells with mutant IDH1. Cancer Res 70:8981–8987
63. Shao H, Chung J, Balaj L, Charest A, Bigner DD, Carter BS et al (2012) Protein typing of circulating microvesicles allows real-time monitoring of glioblastoma therapy. Nat Med 18:1835–1840
64. Simon RM, Paik S, Hayes DF (2009) Use of archived specimens in evaluation of prognostic and predictive biomarkers. J Natl Cancer Inst 101:1446–1452
65. Stupp R, Mason WP, van den Bent MJ, Weller M, Fisher B, Taphoorn MJ et al (2005) Radiotherapy plus concomitant and adjuvant temozolomide for glioblastoma. N Engl J Med 352:987–996
66. Suzuki MM, Bird A (2008) DNA methylation landscapes: provocative insights from epigenomics. Nat Rev Genet 9:465–476
67. Turcan S, Rohle D, Goenka A, Walsh LA, Fang F, Yilmaz E et al (2012) IDH1 mutation is sufficient to establish the glioma hypermethylator phenotype. Nature 483:479–483
68. Uhlmann K, Rohde K, Zeller C, Szymas J, Vogel S, Marczinek K et al (2003) Distinct methylation profiles of glioma subtypes. Int J Cancer J Int du Cancer 106:52–59
69. van den Bent MJ, Hartmann C, Preusser M, Strobel T, Dubbink HJ, Kros JM et al (2013) Interlaboratory comparison of IDH mutation detection. J Neurooncol 112:173–178
70. van den Bent MJ, Dubbink HJ, Marie Y, Brandes AA, Taphoorn MJ, Wesseling P et al (2010) IDH1 and IDH2 mutations are prognostic but not predictive for outcome in anaplastic oligodendroglial tumors: a report of the European Organization for Research and Treatment of Cancer Brain Tumor Group. Clin Cancer Res Off J Am Assoc Cancer Res 16:1597–1604
71. van den Bent MJ, Brandes AA, Taphoorn MJ, Kros JM, Kouwenhoven MC, Delattre JY et al (2013) Adjuvant procarbazine, lomustine, and vincristine chemotherapy in newly diagnosed anaplastic oligodendroglioma: long-term follow-up of EORTC brain tumor group study 26951. J Clin Oncol Off J Am Soc Clin Oncol 31:344–350
72. Verhaak RG, Hoadley KA, Purdom E, Wang V, Qi Y, Wilkerson MD et al (2010) Integrated genomic analysis identifies clinically relevant subtypes of glioblastoma characterized by abnormalities in PDGFRA, IDH1, EGFR, and NF1. Cancer Cell 17:98–110

73. Wang F, Travins J, DeLaBarre B, Penard-Lacronique V, Schalm S, Hansen E et al (2013) Targeted inhibition of mutant IDH2 in leukemia cells induces cellular differentiation. Science 340:622–626
74. Watanabe T, Nobusawa S, Kleihues P, Ohgaki H (2009) IDH1 mutations are early events in the development of astrocytomas and oligodendrogliomas. Am J Pathol 174:1149–1153
75. Weiler M, Wick W (2012) Molecular predictors of outcome in low-grade glioma. Curr Opin Neurol 25:767–773
76. Weller M, Pfister SM, Wick W, Hegi ME, Reifenberger G, Stupp R (2013) Molecular neuro-oncology in clinical practice: a new horizon. Lancet Oncol 14:e370–e379
77. Wick W, Platten M, Meisner C, Felsberg J, Tabatabai G, Simon M et al (2012) Temozolomide chemotherapy alone versus radiotherapy alone for malignant astrocytoma in the elderly: the NOA-08 randomised, phase 3 trial. Lancet Oncol 13:707–715
78. Wick W, Meisner C, Hentschel B, Platten M, Schilling A, Wiestler B et al (2013) Prognostic or predictive value of MGMT promoter methylation in gliomas depends on IDH1 mutation. Neurology 81:1515–1522
79. Wick W, Hartmann C, Engel C, Stoffels M, Felsberg J, Stockhammer F et al (2009) NOA-04 randomized phase III trial of sequential radiochemotherapy of anaplastic glioma with procarbazine, lomustine, and vincristine or temozolomide. J Clin Oncol Off J Am Soc Clin Oncol 27:5874–5880
80. Wiestler B, Capper D, Holland-Letz T, Korshunov A, von Deimling A, Pfister SM et al (2013) ATRX loss refines the classification of anaplastic gliomas and identifies a subgroup of IDH mutant astrocytic tumors with better prognosis. Acta Neuropathol 126:443–451
81. Wiestler B, Claus R, Hartlieb SA, Schliesser MG, Weiss EK, Hielscher T et al (2013) Malignant astrocytomas of elderly patients lack favorable molecular markers: an analysis of the NOA-08 study collective. Neuro Oncol 15:1017–1026
82. Wiestler B, Capper D, Sill M, Jones DT, Hovestadt V, Sturm D et al (2014) Integrated DNA methylation and copy-number profiling identify three clinically and biologically relevant groups of anaplastic glioma. Acta Neuropathol
83. Xu W, Yang H, Liu Y, Yang Y, Wang P, Kim SH et al (2011) Oncometabolite 2-hydroxyglutarate is a competitive inhibitor of alpha-ketoglutarate-dependent dioxygenases. Cancer Cell 19:17–30
84. Yan H, Parsons DW, Jin G, McLendon R, Rasheed BA, Yuan W et al (2009) IDH1 and IDH2 mutations in gliomas. N Engl J Med 360:765–773

Part II
Standards

Spinal Dural Arteriovenous Fistula: A Review

Shimon Maimon, Yehudit Luckman, and Ido Strauss

Contents

S. Maimon, MD (✉) • I. Strauss
Department of Neurosurgery, Sourasky Hospital Tel Aviv Medical Center,
Tel Aviv, Israel

Sackler Faculty of Medicine, Tel Aviv University, Tel Aviv, Israel
e-mail: shimonm@tlvmc.gov.il; maimonsm50@gmail.com

Y. Luckman
Department of Neuroradiology, Rabin Medical Center,
Beilinson Campus, Petach Tikva, Israel

Sackler Faculty of Medicine, Tel Aviv University, Tel Aviv, Israel

J. Schramm (ed.), *Advances and Technical Standards in Neurosurgery*,
Advances and Technical Standards in Neurosurgery, Vol. 43,
DOI 10.1007/978-3-319-21359-0_5

Abstract Spinal dural arteriovenous fistula (SDAVF) is a rare disease, the etiology of which is not entirely clear. It is the most common vascular malformation of the spinal cord, comprising 60–80 % of the cases. The clinical presentation and imaging findings may be nonspecific and misleading, often mistaking it for other entities like demyelinating or degenerative diseases of the spine.

This chapter describes the imaging findings, clinical signs, and symptoms of this disease and also the available treatment options according to the current literature.

Angiography is still considered the gold standard for diagnosis; however, MRI/MRA is increasingly used as a screening tool. Modern endovascular techniques are becoming increasingly more effective in treating SDAVF offering a less invasive treatment option; however, they still lag behind surgical success rates which approach 100 %. The outcome of both treatment options is similar if complete obliteration of the fistula is obtained and depends mainly on the severity of neurological dysfunction before treatment.

Heightened awareness by radiologists and clinicians to this rare entity is essential to make a timely diagnosis of this treatable disease. A multidisciplinary treatment approach is required in order to make appropriate treatment decisions.

Keywords Spinal dural arteriovenous fistula • SDAVF • Spinal venous congestion • Radicular artery • Radicular vein • Medullary artery • Spinal cord edema • Spinal angiography

Introduction

Spinal dural arteriovenous fistula (SDAVF) is a rare and enigmatic disease. Its structural and clinical features have been recognized since the first description by Foix and Alajouanine in 1926; however, the essentials of treatment were first described only in 1974 [1]. Several years later, Kendall and Logue [2], in an elegant study, showed that the fistula does not lie on the cord surface but rather within the dural root sleeve. Nevertheless, the etiology remains unclear [2–5].

SDAVF is part of a heterogenous group of spinal vascular malformations. Of the various classifications proposed to date for these anomalies, the most widely used one [6] divides them into four groups and is based on the anatomic location of the fistula and the arterial vessels involved [4–8], as follows:

Type 1 – SDAVFs, also known as dorsal intradural AVFs, are located mostly near or within the nerve root sleeve dura, connecting one or more of the radiculodural branches with an intradural radicular vein that drains into extramedullary intradural veins (Fig. 1).

Type 2 – Congenital intramedullary arteriovenous malformations (AVMs), also termed glomus AVMs, are fed by the spinal artery branches.

Type 3 – Juvenile AVMs, also known as intra- and extramedullary AVMs or metameric AVMs, are complex spinal and extraspinal malformations.

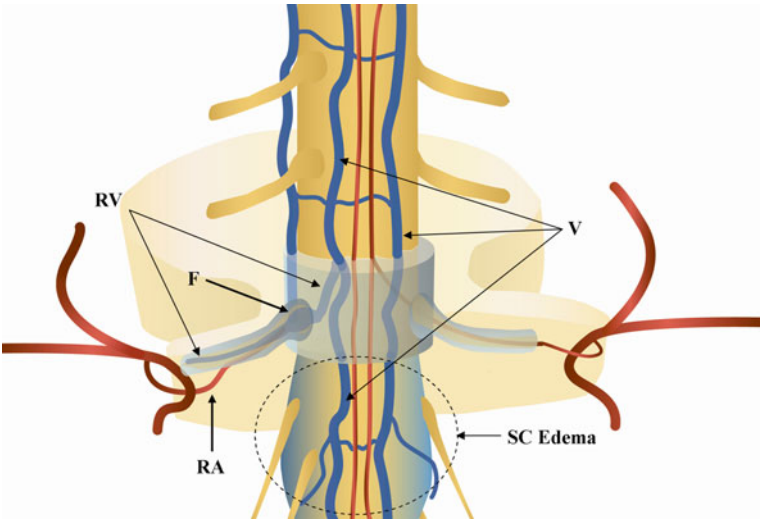

Fig. 1 A diagram showing the vascular anatomy of SDAVF. The radicular artery (RA) is connected to the radicular vein (RV) at the fistula point (F) on the dura of the nerve sleeve. The intradural veins (V) are congested and the spinal cord (SC) is swollen due to cord edema

Type 4 – Perimedullary fistulas, also known as pial or spinal cord AVFs, are intradural extramedullary AVFs that connect pial arterial branches with pial veins in the subarachnoid space.

This classification does not include epidural fistulas, which normally do not drain into the dural space and rarely cause myelopathic signs [4, 7].

Alternatively, Bicetre's classification divides spinal vascular lesions into three main groups: (1) genetic hereditary lesions that are caused by a genetic disorder affecting the vascular germinal cells (e.g., spinal vascular malformation in hereditary hemorrhagic telangiectasia), (2) those caused by a genetic nonhereditary vascular disorder affecting the same metamer (e.g., Cobb syndrome), and (3) single lesions that may affect the cord, nerve root, or filum terminale. The last group includes most spinal vascular lesions [4, 9].

The more comprehensive classification of Spetzler et al. [10] divides all types of vascular lesions into three groups: neoplastic vascular lesions (hemangioblastoma, "cavernoma"), aneurysms, and arteriovenous lesions. The third group is further divided into AVMs and AVFs, and the AVFs are further divided into extradural and intradural types. Intradural AVFs may be ventral or dorsal. Ventral AVFs are synonymous with perimedullary fistulas (i.e., type 4 of the anatomical classification), and dorsal AVFs are synonymous with SDAVFs (i.e., type 1 of the anatomical classification).

Dorsal AVFs with one feeder are categorized as type A (Fig. 2), and with multiple feeders, as type B (Fig. 3). This classification has implications for surgical treatment options and was developed for that purpose.

This chapter focuses on the epidemiology, pathophysiology, clinical and imaging manifestations, treatment, and outcome of SDAVFs (i.e., anatomically type 1, spinal

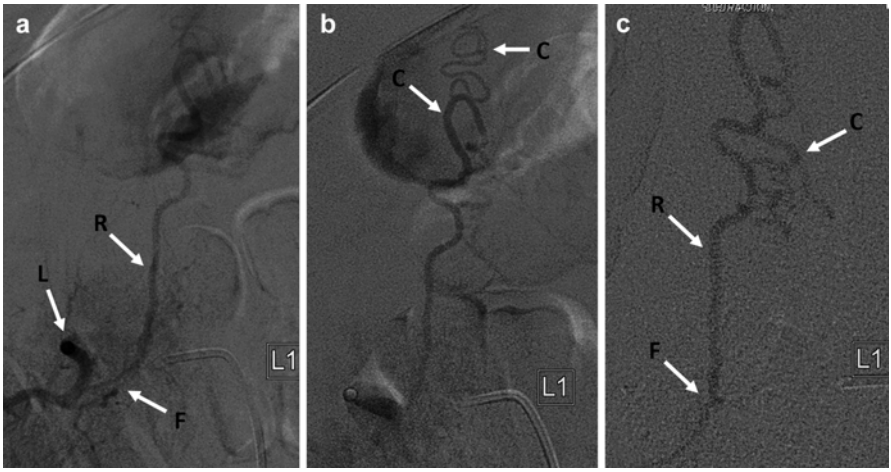

Fig. 2 Demonstrated is a SDAVF at the foraminal level of the *right* L1–L2 vertebra, in a 60-year-old male with long-standing progressive myelopathy. (**a**, **b**) – Injection to the first *right* lumbar artery (L). Marked on the image are the point of fistula (F) and radicular vein (R). Retrograde flow in the radicular vein into the coronal veins(C). (**c**) Injection from a microcatheter in wedge position showing the fistula (F) and the radicular vein (R) drained into the coronal vein (C)

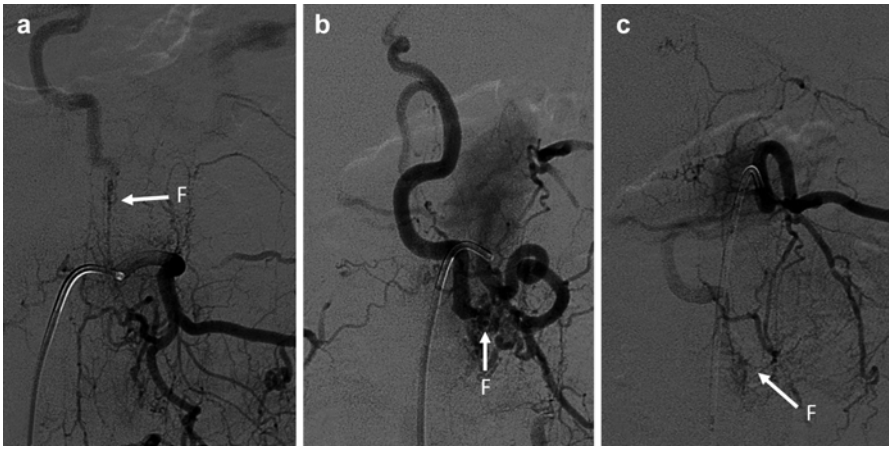

Fig. 3 Shown is a SDAVF with multiple feeders (treatment of the same SDAVF using glue is shown in Fig. 9). The *arrows* labeled with "F" mark the different arterial feeders of the fistula – from the first *left* lumbar artery in (**a**), from the *left* D12 intercostal artery in (**b**), and from the intercostal artery of D11 (**c**). Also demonstrated are early filling of the radicular vein and connections to coronal veins

vascular malformations), with special attention to recent technological and therapeutic innovations. The clinical and radiologic distinctions of SDAVFs (the most common lesion) from perimedullary fistula (type 4a, low-flow shunt type) [3, 4, 7, 11], the least common malformation, are discussed under the appropriate sections due to the many similar features.

Epidemiology

SDAVF is an acquired treatable disease with an estimated annual incidence of 5–10 per million population [12] mostly affecting middle age and elderly men [4, 7, 11]. It accounts for 60–80 % of all cases of vascular spinal malformations and tends to be located in the mid thoracic to the upper lumbar spine [2, 4, 7, 11, 13, 14]. Patient ages range from 18 to 83 years; the reported mean age in different studies is 54–63 years for both males and females [4, 7, 11, 15, 16]. Men are affected more than women (male:female ratio, 6:1), and elderly individuals more than young ones [4, 5, 11, 17–19]; only 1–4 % of cases occur in the under-30-year age group [4, 11]. Except for one patient in the series of Wang et al. [11], no patients younger than 20 years were reported [4].

Anatomy

Anatomically, spinal vascular anomalies located inside or on the cord or at the proximal nerve root are fed by pial (radiculomedullary, medullary) arteries, whereas those located on the dura are fed by radiculodural (radiculomeningeal) arteries. Knowing the angio-architecture of these lesions is crucial to understanding their pathophysiology, presentation, indications for treatment, and treatment [4, 7, 8].

The formation of the neural tube is a complex process. Between days 22 and 27, the intrinsic vascular system of the spinal cord is established. Two longitudinal collector veins form in the subarachnoid space dorsal and ventral to the cord, later joining the epidural space via radicular (bridging) veins. Part of the spinal blood drains into the epidural system via the bridging veins and part travels into the intracranial system [20], to the vertebral plexus and posterior fossa sinuses [4]. The collector veins give rise to the anterior and posterior median veins.

The blood supply to the spine (including bony elements, soft tissue, dura, and nerves) is by segmental arteries originating at each level: from the vertebral artery and ascending cervical artery at the cervical spine, the intercostal and lumbar arteries at the thoracic and lumbar spine, and the iliolumbar branches, mainly the middle and lateral sacral arteries, at the sacral region [21]. The segmental arteries give rise to the anterior and posterior central branches that supply the bony spine and dura and give rise to the radicular (radiculodural) arteries at every level, which supply the nerve root and the dura nearby. *These radiculodural arteries are the vessels involved in SDAVF* [4]. At some levels, the radicular arteries give rise to the radiculomedullary (=radiculopial) arteries that follow the nerve roots and the anterior and posterior spinal divisions, entering the subarachnoid space to supply the cord, pia, and arachnoid. In contrast to the radiculodural branches that arise at each level, the locations of these radiculomedullary branches are not predictable [4]. The radiculomedullary branches that follow the anterior nerve roots join the anterior spinal artery at the median sulcus of the cord; the radiculomedullary branches that follow the posterior

nerve roots join one of the two (one on each side) paramedian posterior longitudinal spinal arteries. Those from the left branches join the left posterior spinal artery, and those from the right branches join the right posterior spinal artery [22].

The anterior spinal artery originates classically from the V4 segment of the two vertebral arteries and runs in the median sulcus of the anterior cord to the conus medullaris. The two posterior spinal arteries originate from the posterior inferior cerebellar artery or the intradural segments of the vertebral arteries (V4 segment). They run in the posterior paramedian part of the cord, between the cord and the pia. These two systems are connected at the spinal conus (like a "circle of Willis" of the brain). As mentioned above, these longitudinal vessels are connected at some spinal levels, to radiculomedullary arteries that assist in cord nourishment [22]. The locations of these radiculomedullary arteries are not predictable and have to be specifically searched for. The radiculomedullaris magna (artery of Adamkiewicz) is the largest and best known radiculomedullary artery. It arises from the lower intercostal or upper lumbar arteries (more frequently from the left). The anterior radiculomedullary arteries connect in a typical way to the anterior spinal artery at the midline, with a hairpin curve at the connection point in the anterior fissure [18].

These three longitudinal intradural subpial arteries supply the cord and give rise to branches at each level; they also have small horizontal branches that connect the two systems (rami perforantes of the vasocorona) at each level and supply that cord segment (Fig. 2) [23]. The cord drains through radial intrinsic and superficial small veins which in turn drain into the longitudinal spinal cord veins, the anterior and posterior median spinal veins that runs in close proximity to the spinal arteries (Fig. 4). There are many connections between these longitudinal veins, including transmedullary anastomosis. The radicular veins drain the longitudinal median veins into the extradural space, mostly following the nerve roots. They have a one-directional "valve" system in the dura to prevent reflux into the intradural venous system.

Pathophysiology

The pathological arteriovenous shunt in SDAVF is located within the dura mater, between the radiculodural artery(ies) and the intradural radicular vein. It usually lies at the posterior wall of the spinal nerve root sleeve, within the intervertebral foramen where the radicular veins pass the dura at the dorsal wall of the dural root sleeve adjacent to the radicular artery [7, 16, 19, 24]. Sometimes, the shunt lies along the dura between two adjacent nerve roots [7]. We have noted the latter finding in several of the 40 patients with SDAVF operated by our group in the last 15 years (unpublished observation). Normally, blood from the spinal cord drains through the medullary veins and venous plexus, usually (80–90 % of healthy people) in a dorsal direction and in some in a combination of ventral and dorsal directions [7]. The presence of a shunt leads to arterialization of the radicular vein and a reversal of the blood flow to the cord venous system, into the perimedullary venous

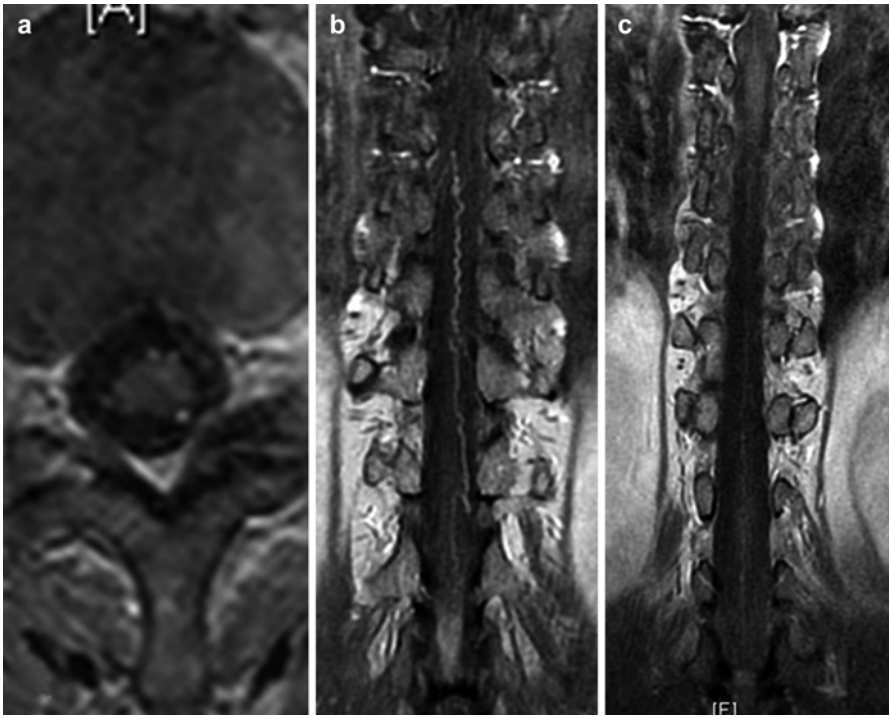

Fig. 4 (**a**) Axial view, T1 with gad, showing the posterior and anterior longitudinal veins. (**b**, **c**) High-resolution T1 with gad coronal views showing the posterior (**b**) and anterior (**c**) part of the canal with the posterior and anterior longitudinal veins (mildly enlarged), respectively

plexus. This, together with the reduced outflow by the other radicular veins due to partial thrombosis [12, 14], leads to venous engorgement and intradural venous hypertension, and, consequently, cord edema and ischemia [4, 7, 11, 14, 18, 19], causing chronic hypoxia, loss of normal functions, and progressive myelopathy [7, 15, 16, 18, 21, 25]. In 1983, 6 years after Kendall and Logue [2] reported the correct location of the fistula, researchers showed that the fistula can be occluded by disconnecting the radicular vein from the dura at the shunt location [3, 7, 26]. This has since become the standard treatment and can be achieved by surgery or endovascular route [4, 7, 11, 12, 18, 27].

According to angiography studies, nearly 80 % of SDAVF lesions are found between T6 and L2; only 4 % are sacral and 2 % are high cervical near the foramen magnum, while low cervical are extremely rare [7, 18, 28–30]. Rarely do patients have more than one fistula (0.5–4 % of cases) [11, 18, 31, 32]. In their large study of 326 patients, Donghai et al. [11] found that 82.5 % of the lesions were located at T5 to L5. The most common locations were T7 (12.6 %), T6 (9.8 %), T5 and T9 (8.6 % each), and L1 (8.3 %). Only 6 % were found in the upper thoracic region and 3.5 % in the cervical region. In the Toronto Western Hospital series, 94 % of the fistulas were located between T5 and S1; most were at T7, with a left side (70 %) propensity [18].

Upper extremity involvement is a localizing sign. It develops only in patients with fistulae in the cervical spine; presentation with SAH is very rare (1.8 % of cases) and it develops only in SDAVF at the level of the foramen magnum [11, 18, 33].

In the evaluation of SDAVF, two factors must be taken into consideration: the rate of flow (low/high) at the fistula and the number of thrombosed/occluded radicular veins. The relationship between these two factors affects the development and the degree of edema, which, in turn, predicts the severity of the clinical disease [7, 24]. The higher the flow at the fistula and/or the greater the number of nonfunctional radicular veins, the less efficient the drainage of the intradural space and the greater the risk of cord edema and dysfunction. This is the explanation for the wide spectrum of MRI findings, ranging from no edema to whole cord edema and for the variable clinical picture, from incidental finding to quadriparesis.

The 15-year experience of our group with 40 patients with SDAVF suggests that as in cranial dural AVF [34], the venous impairment is the most important factor and controls the disease process (unpublished observation). This is supported by data in both recent and older articles [18, 24, 35] and from the extrapolation of data on intracranial AVF.

The progression of the edema is usually from the posterior cord, mainly from the conus caudally (Fig. 5), in cephalad direction. This phenomenon is probably attributable to the fewer venous drainage channels in the lower thoracic spinal canal than in the cervical spine [36], making the lower thoracic spine more vulnerable to congestion and a rise in intradural venous pressure [7, 37]. Accordingly, symptoms may be due to conus myelopathy even though the shunt itself is remote from the conus. Support for this theory was provided by studies reporting conus involvement in more than 90 % of cases [7, 11, 38]. However, in the large series of Wang et al. [11], only 26 % of patients had edema in the conus. Others showed that focal edema does not always reach the conus, with about 10 % of patients having no cord edema at all [11, 38].

Houdart et al. in 2001 [39], in a good example of the natural history of SDAVF, described an incidental finding of SDAVF in a patient 2 years before the appearance of symptoms of progressive bilateral leg weakness and micturition difficulties. Researchers speculate that the co-occurrence of asymptomatic or non-edema-related spinal dural shunt/fistula concomitant with mild venous drainage impairment due to few radicular vein malfunction most likely represents the early stage of the disease process, and ultimately, due to deterioration in the function of the radicular veins, cord impairment developed [7]. This theory is supported by the recent and very important study of Hetts et al. [24] which showed a clear correlation between severity of the cord edema, the clinical findings, and the length of the intradural draining veins from the fistula to the point of drainage to the extradural venous system. The extent and length of these engorged veins are functions of the severity of the radicular vein occlusion. The drainage ability of the cord to the extradural system decreases with an increase in the number of dysfunctional radicular draining veins.

Along the same lines, studies have shown that pressure on the venous side of the fistula may be as high as 74 % of the systemic arterial mean pressure [15, 40]. Accordingly, some patients report symptom exacerbation after physical activities

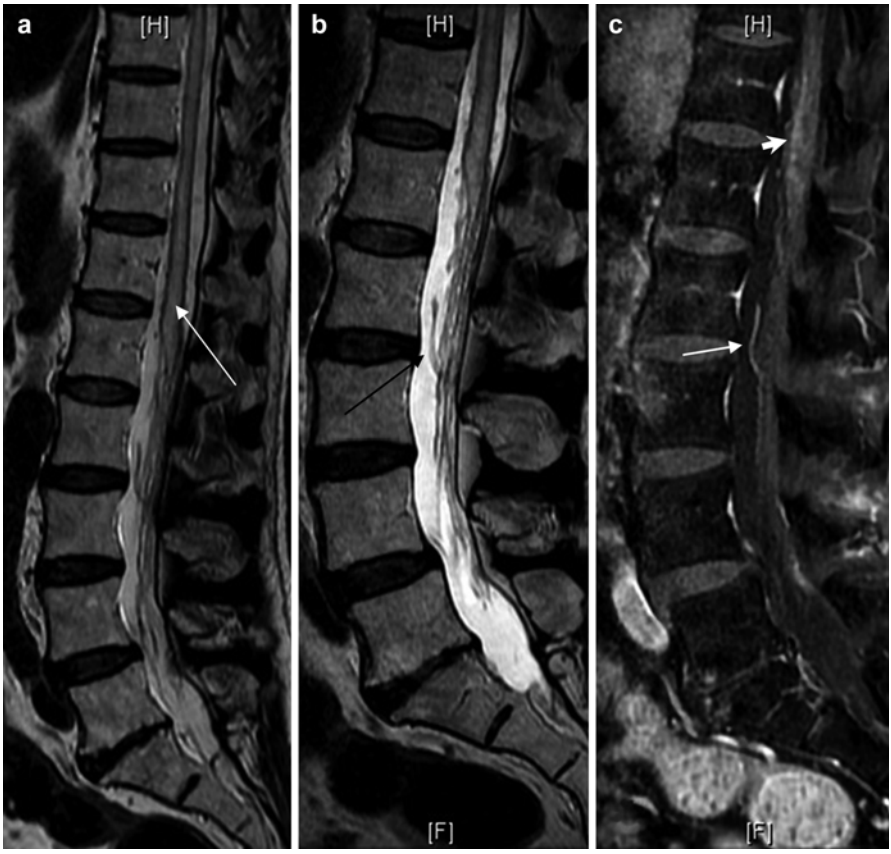

Fig. 5 Cord edema, enlarged vessels, and enhancement of the conus in a patient with a long-standing history of spinal dural AV fistula. (**a**, **b**) T2 sagittal view of the thoracolumbar spinal cord showing cord edema (*white arrow* in **a**) and enlarged vessels (*black arrow* in **b**). (**c**) T1 sagittal view with fat suppression showing conus enhancement (*arrow head*) and large enhanced vessel (*white arrow*)

known to cause increase in blood arterial pressure. This is probably attributable to congestion caused by the increased flow within the fistula and the consequent increase in intradural venous pressure in the presence of a lack of change in drainage.

The difficult distinction between SDAVF and perimedullary fistula is highlighted by the 1926 report of Foix and Alajouanine. The authors describe two men aged 29 and 37 years old who presented with ascending myelopathy and died 33 and 11 months, respectively, after disease onset [7]. Postmortem examination revealed extensive necrosis of the cord, mainly the lower cord, more gray than white matter, involvement of the anterior and posterior roots, and degeneration of the long tracts. Interestingly, increased thickness of the intra- and extramedullary vessel walls was noted, with lumen dilatation and marked tortuosity. The vascular changes are now

recognized to represent a long-standing increase in vessel flow and pressure with venous congestion due to arterialization. The findings within the cord represent subacute necrotizing myelopathy, which has been described in several other diseases as well [7]. These cases have traditionally been considered the first documentation of SDAVF in the medical literature. However, SDAVF (type 1) has many clinical features in common with perimedullary fistula (type 4a), probably because of the same underlying mechanism of spinal damage. The clinical deficit in perimedullary fistula has also been attributed to intradural venous congestion and, in some cases, to subacute necrotizing myelopathy. Therefore, it is possible that the patients described by Foix and Alajouanine had a perimedullary fistula (type 4a), and not SDAVF, especially given the difficulty in differentiating the two entities without angiography [38]. Furthermore, all large series of SDAVF published since 2004 report that less than 1 % of cases occur in patients less than 30 years old [7]. Therefore, it is highly unlikely to have two young patients with SAVDF in one small series.

The radicular vein dysfunction in SDAVF had not been described in perimedullary spinal fistula. However, the currently available knowledge on vascular AVMs/AVFs within the central nervous system suggests that part of the symptoms of perimedullary spinal fistula are due to venous changes/occlusion/malfunction.

Etiology

The etiology of SDAVF is unknown. Based on findings that intracranial dural fistulas are attributable to cerebral vein thrombosis and associated with factor V (Leiden) deficiency [7], researchers have suggested that SDAVF may be due to a reopening of a thrombosed radicular vein. The study of Merland et al. [14] implied that radicular vein occlusion/thrombosis is part of the disease. However, an association of SDAVF with thrombophilia has not been directly documented [7].

Clinical Findings

SDAVF is an underdiagnosed disease often misdiagnosed [41]. The presenting symptoms consist of sensory and/or motor deficits ascending from the feet and mimicking polyneuropathy/radiculopathy. This is mostly due to venous congestion and cord edema. The initial symptoms can be mild, are often nonspecific, and include gait difficulties, symmetrical or asymmetrical sensory deficit, diffuse or patchy sensory loss, and radicular pain [17]. Moreover, signs of mild myelopathy may be present without imaging evidence of spinal cord edema [4, 7, 42, 43]. The motor weakness is unilateral in 24 % of cases and bilateral in the remainder; the sensory disturbances tend to be bilateral and asymmetrical [11]. Patients often have a combination of symptoms and signs of upper and lower motor neuron deficits

[2, 4, 5, 7, 18], which may be misleading during diagnosis [11, 18, 33, 44]. Paresthesia occurs at no clear level, with or without lower back pain, similar to degenerative disease [33]. On the rare occasions when the edema involves the cervical spine, the upper extremities may be affected [18]. The neurologic deficit progresses at a different rate in different patients; it can be stepwise or acutely worsen to paraplegia and incontinence [7, 37] and, as noted above, can be after physical activity, prolonged standing, exercise, and changes in posture. In most cases, bowel and bladder incontinence and sexual dysfunction appear late in the course of disease [7] and are signs of severe cord damage. There are also instances in which the disease starts acutely with late stabilization and then progresses. In part of cases, sensory symptoms are the first or dominant symptoms. Pain has been reported in 50–60 % of patients but is rarely the only presenting symptom [7, 18, 33].

Additional rare signs and symptoms are hemorrhage into the spinal subarachnoid space (1.8 % of patients) [4, 11, 18], attributable to a cervical location of the fistula, mainly near the foramen magnum [7, 11, 18], and headaches due to intracranial subarachnoid hemorrhage [7]. Bleeding or an aneurysm in the feeding artery or at the fistula site [4] is much less common than in perimedullary fistula. In our experience of the last 15 years, only one of our 40 patients had a small aneurysm in the feeding artery of a left T5 fistula with relatively high flow.

Diagnosis

The interval from symptom onset to diagnosis varies from several days (for acute presentations) to many years (for slow-flow and unaggressive fistulas) [4, 7, 11, 18]. The nonspecific nature of the symptoms, the mixed presentation sometimes including signs of both upper and lower motor neuron deficits (60 % of cases) [11, 18, 33, 44], the variable disease course [4, 11, 14], and misleading findings on imaging studies can lead to a delayed or missed diagnosis. This problem is exacerbated by the presence of spinal degenerative, prostatic, or vascular insufficiency comorbidities, given the generally older age of the patients and lack of awareness of SDAVF among neurosurgeons, neurologists, orthopedic surgeons, and radiologists [4, 11, 15, 33, 45]. Indeed, many patients undergo unnecessary invasive interventions such discectomy and laminectomy or fusion, prostatic surgery, or biopsies before the correct diagnosis is made [7, 11, 14]. It is important that clinicians distinguish SDAVF from poly(radiculo)neuropathy by involvement of the upper extremities (rare in SDAVF), presence of sensory sacral involvement (very rare in polyneuropathy), and presence of upper neuron signs (rare in polyneuropathy) [7]. Additionally, any sensory or motor leg deficits are usually asymmetric in SDAVF and symmetric in poly(radiculo)neuropathy. Myelitis may be associated with “engorged” veins in MRI examination that can mimic the finding in SDAVF. Both SDAVF and enlarged prostate may cause bladder incontinence and micturition difficulties. Careful neurologic examination is important to rule out this entity, the SDAVF.

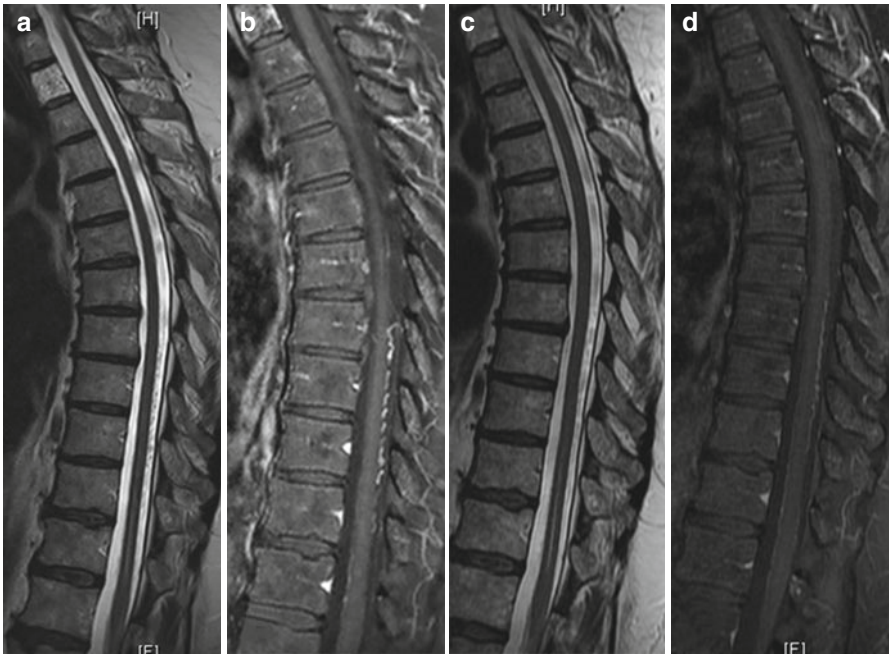

Fig. 6 Myelitis mimicking a spinal fistula. A 50-year-old female who presented 6 months earlier with an acute attack of myelopathy with mild progression since. MRI disclosed high signal on T2 images at the center of the cord (**a**) and some "abnormal vessels" in the thecal sac (*arrow* in **b**). (**c**) Follow-up MRI showing improvement in the T2 changes. Now, it looks more like a syrinx. Also seen are CSF flow artifacts behind the cord. (**d**) Fewer vessels are seen on sagittal T1 post GAD

Owing to diagnostic delay, many patients have severe motor/sensory, sexual, and sphincteric dysfunction already at diagnosis; 10–30 % are confined to a wheelchair at the time of diagnosis [4, 7, 11, 33]. In the largest series of patients with SDAVF reported to date, Wang et al. [11] found that the most common initial symptoms were lower extremity motor weakness (71.8 %), sensory deficit (70.2 %), and sphincter disturbance (26.7 %). At the time of diagnosis, because of propagation of the disease, the prevalence rates of these symptoms were 80.8 %, 85.6 %, and 52.5 %, respectively [11]. The rate of initial misdiagnosis was 81 %, and of erroneous treatment, 62 %. The main misdiagnoses were degenerative spinal disease (50 % of cases), myelitis (22 %; Figs. 6 and 7), prostatic disease (5 %), and intermedullary tumor (4.5 %) [11]. This is unfortunate because some of the potentially treatable clinical deficits may become irreversible if caught too late [4, 7, 11, 18].

This trend may be improving, however. Our review of the literature suggested that in the more recent studies, more patients were diagnosed while asymptomatic or with only mild disease relative to earlier studies. This is probably due to increasing efforts to alert physicians to SDAVF, increased availability of MRI, and advances in diagnostic modes.

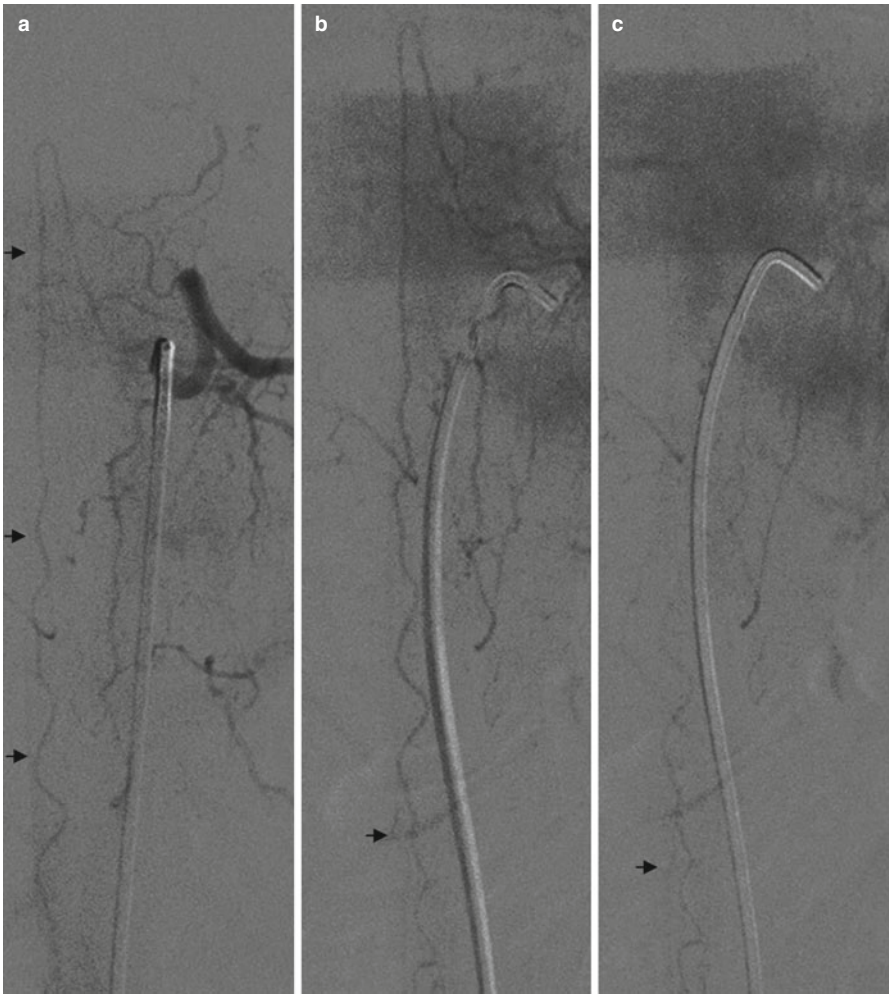

Fig. 7 Normal spinal angiography with no evidence of a fistula (same case presented in Fig. 6). The anterior spinal artery seen in (**a**) (*short arrows*) has a normal appearance without a delay in the venous phase washout (*arrows* in **b**, **c**). Blush of the vertebra is seen in the upper part of (**b**, **c**), as a sign for the good quality of the run

Imaging

The definitive diagnostic mode of SDAVF is spinal angiography (Fig. 2); however, magnetic resonance imaging (MRI) is today the first tool in searching the disease (Fig. 8). Myelography or CT myelography can be used in rare cases where MRI is contraindicated.

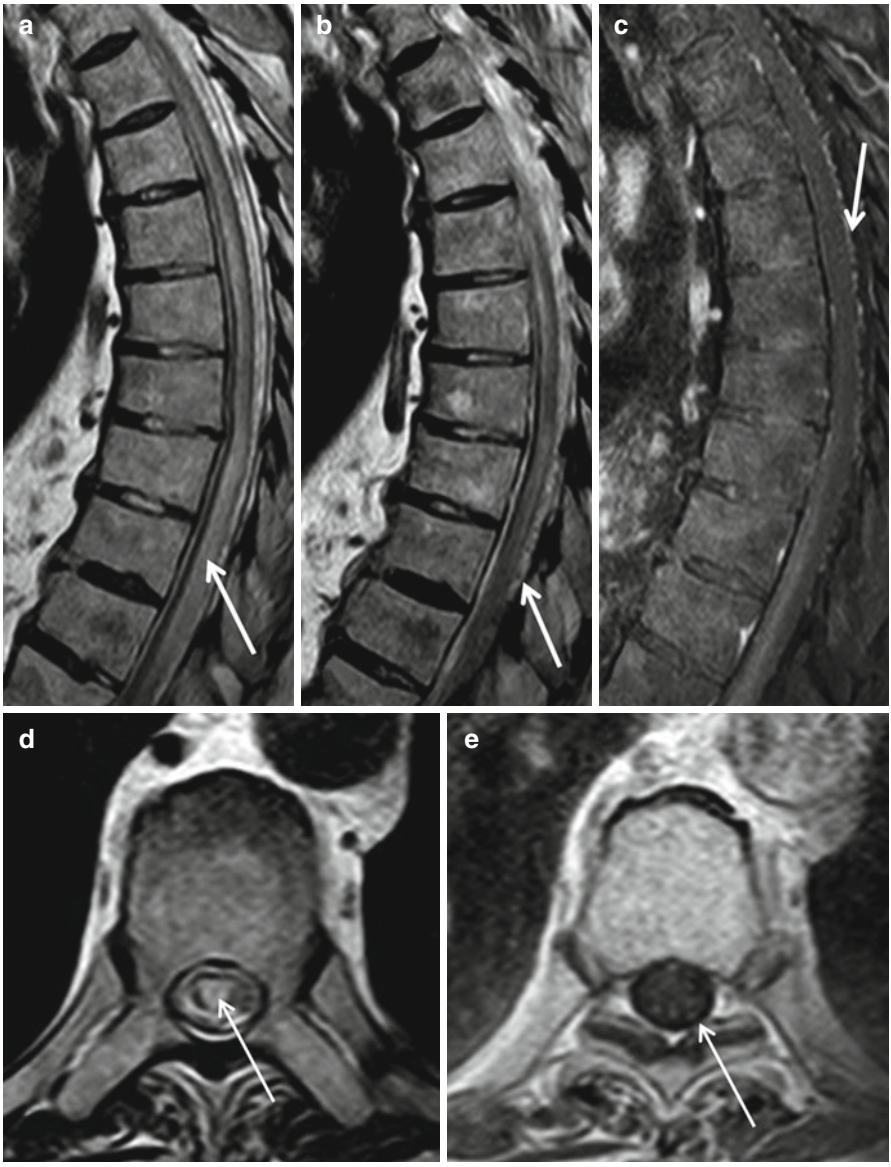

Fig. 8 MRI of a patient with SDAVF that had symptoms for more than a year, showing the classical findings of cord swelling and high signal at the center of the cord (*arrow* in **a**, **d**). Multiple enlarged veins in the subarachnoid space can be seen as flow voids in (**b**) (*arrow*) and as enhanced serpentine vessels in (**c**, **d**) (*arrow*). (**a**, **b,** sagittal TSE-T2; **c**, sagittal T1, fat suppuration with gadolinium; **d**, axial TSE-T2; **e,** axial SE-T1 with gadolinium)

MRI Findings

The presence of a SDAVF is classically characterized by a triad of findings on routine MRI [4, 7, 11, 45]. (a) A cord hyperintensity signal on T2-weighted images, mainly centrally, is suggestive of cord edema (Fig. 8a, d), present in 90 % of cases [7, 11, 38]. The cord edema may be focal or encompass multiple, continuous segments; rarely, whole cord edema is found. Cord expansion may be seen as well. (b) T2 findings of enlarged pial flow voids around the cord, especially dorsal to the cord within the subarachnoid space (Fig. 8b), represent engorged veins [4, 7], present in nearly 80 % of cases [11, 38] on routine MRI. Enlarged veins in the subarachnoid space can be better detected on heavy T2-weighted sequences, such as constructive interference in steady-state (CISS) or fast imaging employing steady-state acquisition (FIESTA),owing to the myelographic effect. The vessels appear as serpentine-filling defects. However, these sequences are less sensitive to the T2 changes within the cord. Sometimes, the void is visible only on T1 contrast-enhanced images because of the slow flow in the fistula [4]. Flow voids are more prevalent in recent studies, possibly reflecting advances in MRI technology [7]. (c) Enhancement within the cord on T1 postcontrast images may be due to venous engorgement and disruption of the blood-brain barrier [43, 46]. It usually develops at a late stage in the course of the disease and is suggestive of an aggressive course and a damaged cord. Later in the disease course, the cord might show atrophy [4, 14, 19, 47].

Routine MRI findings of cord edema together with abnormal intratracheal vessels have a high sensitivity and 97 % specificity for a diagnosis of spinal fistula [38]. The addition of heavily T2-weighted CISS and FIESTA sequences may increase the diagnostic sensitivity if abnormal vessels are suspected on regular spinal MRI [4]. However, cord edema is not visualized in about 10 % of cases and vessel dilatation in about 20 % [11, 38]. Furthermore, in the early disease stages before damage to the blood-brain barrier, the cord does not appear to be enhanced [4, 11]. Since there are fewer venous outflow channels within the lower thoracic and upper lumbar regions, researchers propose that the venous congestion is likely to appear first within the conus medullaris and move caudally as congestion worsens [4, 7, 14]. However, Wang et al. [11], in the largest series of SDAVF, reported conus edema in only 26 % of cases. In 6 % of patients, no changes are visible on routine MRI [11, 13, 19] despite the presence of symptoms of radicular pain and clinical signs of mild myelopathy [4, 7, 11, 16]. In these cases, the fistula was found later, on angiography or during surgery [11]. The introduction of high-tesla MRI machines and new sequences (e.g., CISS and FIESTA) may help to reduce these rates [4].

Some fistulas might be detected on MRI incidentally when a patient is still asymptomatic or only has mild symptoms [16]. Multiple engorged veins are seen within the subarachnoid space, without an abnormal signal within the cord parenchyma [16]. Jellema et al. [7] described an incidental finding of a radicular artery-to-vein fistula on postmortem study of subjects without myelopathy. The

hyperintense signal in the cord is sometimes difficult to interpret, mainly in patients without clearly abnormal vessels, and can suggest other cord diseases such as spinal infection or myelitis [4, 5, 7, 11, 42]. This problem may be partly solved with use of the newer, higher-quality MRI machines where cord signal changes and configuration are better visualized and interpreted. At the same time, clinicians should be aware that in some healthy patients, the new machines and sequences can visualize the median veins, mainly the posterior ones (Fig. 4) [48–50]. This normal "variant" can sometimes lead to a false-positive MRI diagnosis of fistula and to unneeded spinal angiography.

MRI rarely identifies the location of the lesion because there is no correlation between the fistula level, the T2 signal changes, and the perimedullary dilated vessels [4, 11]. First-pass magnetic resonance angiography (MRA) with gadolinium enhancement may depict the early filing of the radicular veins, thereby identifying the lesion level [4, 11, 38, 51, 52]. This increases the sensitivity of MRI by differentiating SDAVF from perimedullary fistula, which involves different feeding vessels, and helps guide the neurointerventional team during spinal digital subtraction angiography (DSA), limiting the number of levels that need to be screened [50, 53] and thereby reducing procedural time and radiation dose [21, 50–53]. MRA should be performed on a good-quality machine by an experienced team using 3D gradient echo volume acquisition with a dynamic injection in the arterial phase in the sagittal or coronal planes, followed by maximum intensity projection reconstruction [50]. Some studies reported a nearly 100 % sensitivity of MRA for SDAVF, whereas others had lower rates of around 80–90 % and also some false-positives [38, 50, 51, 54]. MRA and MRI may aid in posttreatment follow-up studies, in the evaluation of residual or successfully treated SDAVFs [18, 53].

Computed tomography angiography (CTA) has similar potential to MRA. However, when the level of the fistula cannot be determined on routine MRI, the entire spine would need to be scanned by CTA, exposing patients to a very high radiation dose [4, 7]. The recent high-quality 128- and 256-multidetector CT devices, which decrease the whole-body radiation time and dose, may solve this problem. So far, experience with this tool is too sparse to recommend it for this purpose.

Myelography or CT myelography is used today for the diagnosis of SDAVF only when MRI/MRA is contraindicated. The presence of atherosclerotic changes and orifice feeder occlusion is a case where CT myelography could be useful to locate fistulas that could not be detected angiographically [7, 55].

Angiography

Conventional spinal angiography is still considered the diagnostic gold standard for spinal fistulas, including SDAVF. However, it is available only in specialized centers [38] and the procedure is invasive and demanding owing mainly to the generally older age of the patients and the common presence of atherosclerotic changes in the aorta that make catheterization of the segmental vessels difficult. When the level of

the fistula cannot be determined by CTA or MRA, or when routine MRI clearly suggests the presence of a fistula, we prefer angiography under general anesthesia so that embolization can be continued directly, if feasible. In older patients or patients with a low level of cooperation, angiography is also performed under general anesthesia; the lesser patient movement and better breathing control allow for better quality images and more patient comfort during the long procedure. When the pre-angiography diagnosis is not clear-cut and the patient is young and cooperative, we use local anesthesia.

If the fistula level is unknown or the diagnosis is unclear, all segmental spinal feeders should be screened, starting at D5 and descending level by level to the lower lumbar and mid-sacral spine and then the two common and internal iliac arteries. Most SDAVF are located at the mid–lower thoracic spine (70–80 %) so it is searched first [7, 11, 56]. If the fistula is still not revealed, the upper thoracic segmental vessels are visualized, and the subclavian arteries and their branches are explored. The two vertebral and two common and external carotid arteries are inoculated also selectively to explore any fistula that fed by them. To avoid missing a very slow-flow fistula, we use a low frame rate with two images for 4 s and then one image for 15 s. This also reduces the radiation dose and prevents tube heating. Once the fistula is located, we perform runs at higher speed in different angulations at that level to explore the lesion's angiographic architecture for the option of embolization. A good-quality run is defined as the presence of a hemi-vertebral blush following injection of contrast medium into the segmental artery (Figs. 2a, 3b, 7b, c, and 9c). The blush indicates that enough contrast medium has reached the meningeal branches that involved when a fistula exists. If the run is poor, the catheter is repositioned and the run repeated.

The angiographic hallmark of a SDAVF is early filling of an enlarged radicular vein running into the middle and then filling of multiple enlarged serpentine draining veins, the coronal veins, in an ascending or descending direction (Figs. 2 and 3). These veins then drain into other radicular veins, if open, or up into the intracranial space or down to the sacral area. The anterior spinal artery, if found, is characterized by slow flow and stasis due to the cord edema and venous congestion. The dural fistula may be supplied from the same segmental artery but also from contralateral arteries or segmental arteries at levels above or below the fistula. These feeders can be used for embolization.

DSA is an invasive procedure requiring a high level of expertise. On the one hand, some authors recommend that it should not be performed if the MRI study is totally negative or that it should be limited to cases in which there are some findings on MRI and a high clinical suspicion of SDAVF [38, 57]. On the other hand, in the large series of Wang et al. [11], 10 % of patients with SDAVF had no MRI findings. Saraf-Lavi et al. [50] also reported a 10 % rate of SDAVF in the absence of findings on both routine MRI and first-pass MRA. Given that the absence of conus edema, or of other imaging findings on MRI/MRA, does not rule out fistula and that some patients have only one of the known findings, we believe, contrary to Toossi et al. [38], that continued evaluation with spinal angiography is needed when clinical suspicion is high.

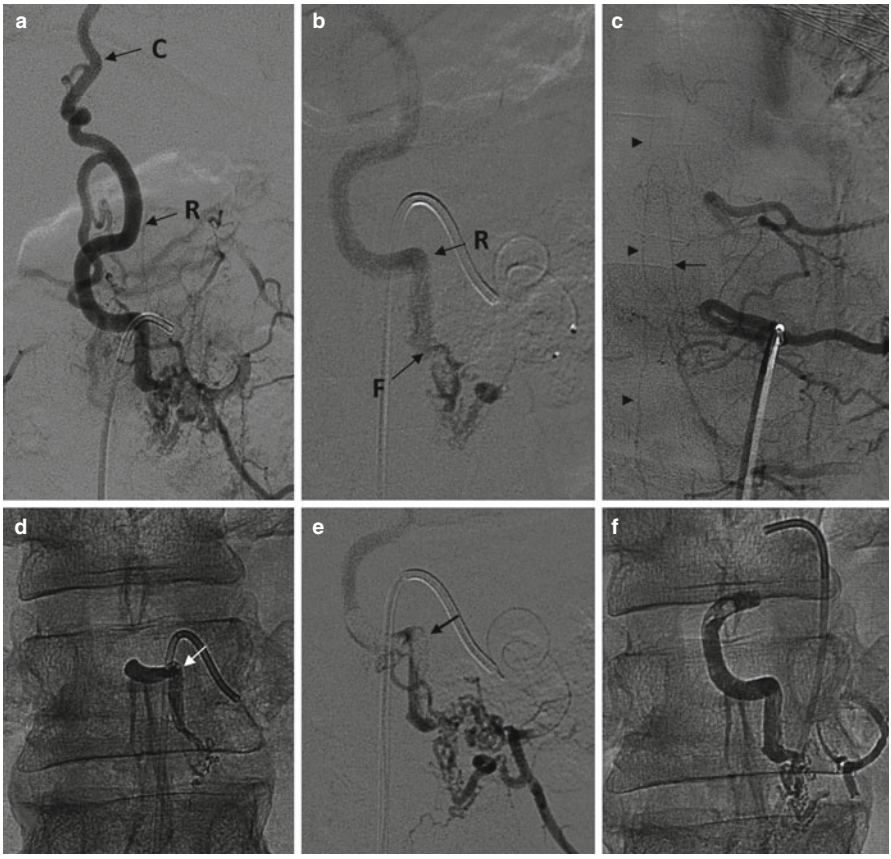

Fig. 9 Treatment of a SDAVF with multiple feeders using glue (same case presented in Fig. 3). (**a**) The fistula is located at the *left* D12–L1 foraminal level. The radicular vein (R) and coronal veins (C). (**b**) Selective injection from the microcatheter in a wedge position showing the point of the fistula in the dura (F) and the retrograde drainage in the radicular vein (R). (**c**) The radiculomedullary magna artery (Adamkiewicz artery, *arrow*) arising from the *left* D8 intercostal artery feeding the anterior spinal artery (*arrow heads*), before embolization of the fistula. (**d**) Non-subtracted image of D12 after the first injection of diluted glue (18 %) into the fistula, showing the glue cast in the radicular vein (*arrow*). (**e**) Contrast injection showed incomplete occlusion of the fistula and filling from a second branch due to incomplete obliteration of the venous side (*arrow* points at the filling defect in the vein). This remnant was occluded with a second glue injection. This is demonstrated in part **f** showing a non-subtracted image of the fistula and the venous part fully obliterated with glue. At this stage, the fistula was cured

SDAVF is ruled out angiographically if no fistula is found and the radiculomedullary injection shows good anterior spinal artery flow with no spinal venous delay (seen best near the conus) (Fig. 7) [21]. In suspected cases in which a fistula is not identified, all runs should be re-read before a final conclusion is reached. Some studies have reported identifying a lesion on the second reading [50]. In some cases (3 %), a second or third angiogram needs to be performed, and rarely, if the fistula

is with very low flow or the patient's aorta is severely diseased due to atherosclerotic changes with segmental artery occlusion, exploratory surgery is necessary to find and treat the fistula [7, 11, 18]. Studies show that in 3 % of patients, diagnostic angiography itself causes acute clinical deterioration warranting immediate treatment. These cases need to be distinguished from deterioration due to a rare, undetected second fistula [4, 11, 18]. There are several reports describing the use of 3-dimensional angiography in the evaluation of spinal lesions and the correct work position to reach the fistula [42].

The differentiation of perimedullary fistula from SDAVF is very difficult by MRI. Therefore, the diagnosis also takes the clinical signs and symptoms into account, together with gadolinium-enhanced three-dimensional MRA or CTA findings [4, 18, 21]. On conventional spinal angiography, like SDAVFs, perimedullary fistulas drain into the intradural veins; however, in contrast to SDAVF, they are supplied by pial arterial branches due to the location of the fistula at the subpial space. By contrast to SDAVFs, flow increases in the pial arteries (anterior or posterior or both spinal arteries) owing to the flow demand by the pial fistula; an increase in pial venous flow is observed (due to the abnormal arteriovenous pial connection) and no clear sign for interference/occlusion of the radicular veins. There is no clear explanation for the venous drainage impairment in SDAVF.

Treatment

The spontaneous occlusion of a SDAVF is very rare [7, 56]. Treatment is directed at halting the progression of symptoms or even reversing them [7, 8, 21]. There are two main options: endovascular treatment and open surgery, alone or in combination [4, 7, 11, 18, 45, 58]. Both involve disconnecting the draining radicular veins at the fistula at the point of dural attachment, to eliminate the source of congestion in the intradural venous system [4, 5, 7, 18, 26, 27, 45] and thereby decrease the edema [3, 4, 18, 59]. However, the reduced venous drainage due to the malfunction of the radicular veins cannot be resolved with the tools available. Whether treatment is necessary in patients with asymptomatic fistulas remains controversial [16], as symptoms may appear even 2 years after an incidental finding of SDAVF [39]. We believe asymptomatic patients, if left untreated, should be closely followed clinically and with serial MRIs and be treated immediately when any new relevant clinical signs appear.

Endovascular Treatment

In endovascular surgery for SDAVF, a liquid embolic material (glue or Onyx) is injected to permanently occlude the venous side of the fistula. Prior to the embolization, a diagnostic angiography is performed. Exploration must include all the

segmental arteries at the level of the fistula and also one level above and below on both sides in order to have a complete understanding of the vasculature anatomy around the lesion and chose the best feeder to approach and embolize the fistula. These vessels should be checked again at the end of embolization to rule out any fistula remnants. It is essential to completely fill the proximal part of the radicular vein in order to prevent recanalization (Fig. 9) [3, 4, 7, 16, 18, 44, 59]. Particles are insufficient because they tend to occlude only the arterial side (feeders) and not the draining vein – the fistula side [4, 5, 7, 18, 35]. If the fistula is not completely filled, any clinical improvement will be temporary, and recanalization will eventually occur by recruitment of flow from nearby dural vessels [4, 5, 7, 18, 27, 60].

When using glue, the microcatheter should be placed in a wedge position near the lesion. To do so, the microcatheter must be the same size as the feeding artery, so the flow distal to its tip depends only on the pressure and flow in the catheter. This allows the invasive neuroradiologist to maintain full control over the lesion with a very low risk of reflux of the injected material. The glue is injected after holding respiration to prevent patient motion. The proper concentration of glue is determined by the rate of flow at the fistula, the location of the microcatheter relative to the fistula, successful placement of the catheter in the wedge position, and the location and configuration of the radicular vein connection to the spinal coronal veins. In most of our cases, the concentration ranges between 18 % and 25 %. The glue should not reach the coronal veins, and the microcatheter should not stick to the vessel wall due to a too-long injection. We prefer to perform the injection using a zero roadmap and not on a run.

When the liquid embolic material reaches the venous side and fills its first few centimeters, the fistula is considered cured (Fig. 9f) [5, 18, 27, 61, 62]. If this does not occur, the patient should be referred for surgery [4, 11] immediately. Definitive treatment should not be delayed based on the transient clinical improvement. The two main reasons for treatment failure are failure to place the microcatheter in the wedge position and placement of the microcatheter too far from the lesion due to difficulties in navigation.

Onyx was introduced about 15 years ago for use in the treatment of brain AVMs and dural fistulas. It has proven to have a high success rate in intracranial dural fistula surgery [63] and has been used by some groups for spinal dural fistulas as well [11]. We have had some experience with Onyx in patients with SDAVF, but not enough to recommend its use. Most of the reported studies are from centers that found glue to be associated with a low rate of recanalization [4, 7, 18, 27] and it is the favor material to be used till now.

In general for both glue and Onyx, if the radiculomedullary branch (including the radiculomedullary magna – artery of Adamkiewicz) arises from the same segmental branch as the fistula, surgery is preferred over endovascular treatment to avoid their accidental embolization [4, 7, 11, 18, 27]. However, we have found that if a wedge position can be achieved sufficiently far from the origin of the nearby radiculomedullary artery, meticulous injection of glue without reflux may be performed. Surgery is also preferred in patients with tortuous feeders that cannot be safely catheterized close enough to the fistula.

Surgical Treatment

Surgical occlusion of the SDAVF is simple and safe. It involves hemilaminectomy with exposure of the dura, opening the dura to identify the radicular vein, following the vein to its dural attachment and the fistula point [3, 11, 18], and coagulating/clipping the vein at its attachment to separate it from the dura. Effective occlusion of the dura is indicated by an immediate change in color (to blue) of the arterialized intradural veins. Some surgeons also coagulate the small feeders on the outer side of the dural wall, although we believe this is not necessary and can damage the radiculomedullary branch if it is running nearby, causing cord infarction. The only location in which surgical occlusion is difficult is the sacral region [52].

There have not been direct prospective randomized comparisons between open surgery and endovascular embolization. A meta-analysis performed by Steinmetz et al. (2004) found the success rate of open surgery in SDAVF to be 98 % [64], and of endovascular embolization 46 %. However, with the introduction of technological improvements in angio suites and microcatheters and growing experience with the technique, reported rates of successful endovascular surgery have been rising up to 70–80 % (Table 1) [5, 18, 27]. The morbidity associated with endovascular surgery when performed by an experienced team is very low [5, 7, 11, 18, 27].

According to our experience, and in agreement with several studies [11, 18], because endovascular treatment is less invasive, the postoperative course is less painful than after open surgery, and the hospital stay is shorter. An attempt of

Table 1 The main publications regarding surgical and endovascular treatments of SDAVF

	Period	# of cases	Success
Symon et al. [65]	1952–1982	Surgery 55	85 %
Mourier et al. [66]	1978–1988	Embolization 63 Surgery 30	64 % 97 %
Niimi [27]	1980–1995	Embolization 49	80 %
Westphal and Koch [67]	1990–1998	Embo 35 Surgery 37	42 % Not specified
Song et al. [68]	1985–1999	Embolization 23 Surgery 14	70 % 100 %
Van Dijk et al. [44]	1986–2001	Embolization 44 Surgery 35	25 % 100 %
Steinmetz et al. [64]	1995–2004	Surgery 18	100 %
Ruiz-Jureschke et al. [69]	1995–2007	Embolization 9 Surgery 10	55.6 % 90 %
Su et al. [70]	1992–2012	Embolization 66 Surgery 24	60 % Not specified
Kirsch et al. [71]	1992–2012	Embolization 61 Surgery 31	77 % Not specified
Muralidharan et al. [72]	1985–2008	Surgery 154	94.8 %
Gokhale [73]	1993–2013	Embolization 10 Surgery 17	70 % 100 %

embolization during angiography [18] is acceptable if the lesion is found to be suitable. If the embolization fails, then the glue or Onyx that was injected can serve as a marker for fluoroscopic localization of the fistula, before the skin is cut at surgery [4, 27]. However, in some centers, owing to the high cure rate of surgery relative to embolization, patients are sent directly to open surgery [11].

Follow-Up and Prognosis

The edema and vessel engorgement have to regress after complete closure of the fistula [59]. Postoperative recovery depends on the severity of the disease (clinical and imaging features) at the time of treatment [4, 7, 11]. In our experience, the duration of the disease before treatment is also an important factor. A long segment of severe edema and cord enhancement, severe neurologic deficit, and sphincteric malfunction are bad prognostic signs [4, 7, 11, 14, 24]. Around 80 % of patients have some clinical (motor and sensory) improvement; the rest do not improve at all or even show clinical deterioration (4.5–11 %) despite fistula occlusion [4, 7, 11]. The motor deficits tend to regress more (70 % of cases) than the sensory deficits (33 % of cases), and sphincter disturbances can persist or improve mildly. Sexual dysfunction is seldom reversible in patients with long-term disease. Pain, especially foot pain, often persists [4, 7, 11, 74]. The mechanism underlying postoperative failure to improve symptoms or prevent their deterioration is unknown.

In the past, we performed follow-up angiography routinely in all patients after surgery or embolization for SDAVF. In the last 6 years, we have relied on a clinical examination and MRI scan done 3–6 months after treatment. If the patient shows clinical improvement and the MRI shows less cord edema and less vessel engorgement, we continue with follow-up 6 months later. If there is no clinical improvement or no changes on MRI from the pretreatment scan, we perform urgent spinal angiography to rule out reopening of the fistula or to reveal a second one as can be found in 3 % of patients [11, 18, 32]. In addition, our experience has shown that in some patients who deteriorate in an acute fashion, sometimes to paraplegia and sphincter dysfunction, an urgent treatment may lead to dramatic improvement within days.

Summary

SDAVF is a rare underdiagnosed disease with a known clinical- and imaging-based differential diagnosis. Search for a fistula is prompted clinically by signs or symptoms of ascending motor or sensory disease combined with lower upper and motor neuron signs, particularly in middle-aged patients. MRI is the main diagnostic tool, with the aid of MRA or CTA to identify the lesion location. The spinal angiography is the definitive diagnostic mode and needs experienced team. The spectrum of clinical and imaging findings varies with the extent of impairment of intradural

venous drainage to the extradural veins at the level of the radicular vein in the spinal canal. The tools available today do not allow for treatment of the drainage impairment itself, while the fistula can be successfully eliminated in a high percentage of patients with the tool we have today. We believe if embolization can be done safely, it should be pursued. Endovascular surgery, performed by experienced teams with modern techniques and equipment, has a success rate of 70–80 %. This is lower than the reported rate of surgery, although surgery is more invasive. Clinicians should be alerted to the possibility of SDAVF because early treatment can improve prognosis and prevent the symptoms from worsening to the point of irreversibility.

Main Points

- SDAVF and perimedullary fistula type A have several clinical features in common. Both cause intradural venous congestion leading to cord dysfunction. They can be diagnosed and differentiated by noninvasive imaging (MRA/CTA) although DSA remains the gold standard.
- Incidental SDAVF can be found in asymptomatic patients, representing the early stage of the disease process.
- Early evaluation, diagnosis, and treatment improve prognosis [5, 22, 52].
- An acute exacerbation may develop at any time without warning signs and lead to severe disability. Therefore, when SDAVF is suspected, definitive diagnosis and treatment should be pursued on an urgent basis.
- When evaluating routine spinal MRI with enlarged subarachnoid vessels even if no conus/cord edema is present [11, 38], SDAVF or perimedullary fistula must be included in the differential diagnosis.

References

1. Aminoff MJ, Barnard RO, Logue V (1974) The pathophysiology of spinal vascular malformations. J Neurol Sci 23(2):255–263
2. Kendall BE, Logue V (1977) Spinal epidural angiomatous malformations draining into intrathecal veins. Neuroradiology 13(4):181–189
3. Afshar JK, Doppman JL, Oldfield EH (1995) Surgical interruption of intradural draining vein as curative treatment of spinal dural arteriovenous fistulas. J Neurosurg 82(2):196–200
4. Krings T, Geibprasert S (2009) Spinal dural arteriovenous fistulas. AJNR Am J Neuroradiol 30(4):639–648
5. Lev N, Maimon S, Rappaport ZH, Melamed E (2001) Spinal dural arteriovenous fistulae–a diagnostic challenge. Isr Med Assoc J 3(7):492–496
6. Rosenblum B, Oldfield EH, Doppman JL, Di Chiro G (1987) Spinal arteriovenous malformations: a comparison of dural arteriovenous fistulas and intradural AVM's in 81 patients. J Neurosurg 67(6):795–802
7. Jellema K, Tijssen CC, van Gijn J (2006) Spinal dural arteriovenous fistulas: a congestive myelopathy that initially mimics a peripheral nerve disorder. Brain 129(Pt 12):3150–3164
8. Patsalides A, Knopman J, Santillan A, Tsiouris AJ, Riina H, Gobin YP (2011) Endovascular treatment of spinal arteriovenous lesions: beyond the dural fistula. AJNR Am J Neuroradiol 32(5):798–808

9. Rodesch G, Hurth M, Alvarez H, Tadié M, Lasjaunias P (2002) Classification of spinal cord arteriovenous shunts: proposal for a reappraisal–the Bicêtre experience with 155 consecutive patients treated between 1981 and 1999. Neurosurgery 51(2):374–379; discussion 379–380
10. Spetzler RF, Detwiler PW, Riina HA, Porter RW (2002) Modified classification of spinal cord vascular lesions. J Neurosurg 96(2 Suppl):145–156
11. Donghai W, Ning Y, Peng Z, Shuo X, Xueen L, Peng Z, Bin H, Xingang L (2013) The diagnosis of spinal dural arteriovenous fistulas. Spine. doi:10.1097/BRS.0b013e31828a38c4
12. Thron A (2001) Spinal dural arteriovenous fistulas. Radiologe 41(11):955–960
13. Gilbertson JR, Miller GM, Goldman MS, Marsh WR (1995) Spinal dural arteriovenous fistulas: MR and myelographic findings. AJNR Am J Neuroradiol 16(10):2049–2057
14. Merland JJ, Riche MC, Chiras J (1980) Intraspinal extramedullary arteriovenous fistulae draining into the medullary veins. J Neuroradiol 7(4):271–320
15. Hassler W, Thron A, Grote EH (1989) Hemodynamics of spinal dural arteriovenous fistulas. An intraoperative study. J Neurosurg 70(3):360–370
16. Van Rooij WJ, Nijenhuis RJ, Peluso JP, Sluzewski M, Beute GN, van der Pol B (2012) Spinal dural fistulas without swelling and edema of the cord as incidental findings. AJNR Am J Neuroradiol 33(10):1888–1892
17. Heros RC, Debrun GM, Ojemann RG, Lasjaunias PL, Naessens PJ (1986) Direct spinal arteriovenous fistula: a new type of spinal AVM. Case report. J Neurosurg 64(1):134–139
18. Medel R, Crowley RW, Dumont AS (2009) Endovascular management of spinal vascular malformations: history and literature review. Neurosurg Focus 26(1), E7
19. Muralidharan R, Saladino A, Lanzino G, Atkinson JL, Rabinstein AA (2011) The clinical and radiological presentation of spinal dural arteriovenous fistula. Spine 36(25):E1641–E1647
20. Groen RJM, Grobbelaar M, Muller CJF, van Solinge G, Verhoof O, du Toit DF, Hoogland PVJM (2005) Morphology of the human internal vertebral venous plexus: a cadaver study after latex injection in the 21-25-week fetus. Clin Anat 18(6):397–403
21. Krings T, Lasjaunias PL, Hans FJ et al (2007) Imaging in spinal vascular disease. Neuroimaging Clin N Am 17(1):57–72
22. Lasjaunias P, Berenstein A, Ter Brugge K (2001) Surgical neuroangiography: clinical vascular anatomy and variations. Springer, Berlin
23. Thron AK (1988) Vascular anatomy of the spinal cord: neuroradiological investigations and clinical syndromes. Springer, Vienna
24. Hetts SW, Moftakhar P, English JD, Dowd CF, Higashida RT, Lawton MT, Douglas VC, Halbach VV (2012) Spinal dural arteriovenous fistulas and intrathecal venous drainage: correlation between digital subtraction angiography, magnetic resonance imaging, and clinical findings. J Neurosurg Spine 16(5):433–440
25. Kataoka H, Miyamoto S, Nagata I, Ueba T, Hashimoto N (2001) Venous congestion is a major cause of neurological deterioration in spinal arteriovenous malformations. Neurosurgery 48(6):1224–1229; discussion 1229–1230
26. Oldfield EH, Di Chiro G, Quindlen EA, Rieth KG, Doppman JL (1983) Successful treatment of a group of spinal cord arteriovenous malformations by interruption of dural fistula. J Neurosurg 59(6):1019–1030
27. Niimi Y, Berenstein A, Setton A, Neophytides A (1997) Embolization of spinal dural arteriovenous fistulae: results and follow-up. Neurosurgery 40(4):675–682; discussion 682–683
28. Geibprasert S, Pongpech S, Jiarakongmun P, Krings T (2009) Cervical spine dural arteriovenous fistula presenting with congestive myelopathy of the conus. J Neurosurg Spine 11(4): 427–431
29. Reinges MH, Thron A, Mull M, Huffmann BC, Gilsbach JM (2001) Dural arteriovenous fistulae at the foramen magnum. J Neurol 248(3):197–203
30. Schaat TJ, Salzman KL, Stevens EA (2002) Sacral origin of a spinal dural arteriovenous fistula: case report and review. Spine 27(8):893–897
31. Krings T, Coenen VA, Weinzierl M, Reinges MHT, Mull M, Thron A, Rohde V (2006) Spinal dural arteriovenous fistula associated with a spinal perimedullary fistula: case report. J Neurosurg Spine 4(3):241–245

32. Krings T, Mull M, Reinges MHT, Thron A (2004) Double spinal dural arteriovenous fistulas: case report and review of the literature. Neuroradiology 46(3):238–242
33. Jellema K, Canta LR, Tijssen CC, van Rooij WJ, Koudstaal PJ, van Gijn J (2003) Spinal dural arteriovenous fistulas: clinical features in 80 patients. J Neurol Neurosurg Psychiatry 74(10):1438–1440
34. Brunereau L, Gobin YP, Meder JF, Cognard C, Tubiana JM, Merland JJ (1996) Intracranial dural arteriovenous fistulas with spinal venous drainage: relation between clinical presentation and angiographic findings. AJNR Am J Neuroradiol 17(8):1549–1554
35. Hall WA, Oldfield EH, Doppman JL (1989) Recanalization of spinal arteriovenous malformations following embolization. J Neurosurg 70(5):714–720
36. Tadié M, Hemet J, Freger P, Clavier E, Creissard P (1985) Morphological and functional anatomy of spinal cord veins. J Neuroradiol 12(1):3–20
37. Koenig E, Thron A, Schrader V, Dichgans J (1989) Spinal arteriovenous malformations and fistulae: clinical, neuroradiological and neurophysiological findings. J Neurol 236(5):260–266
38. Toossi S, Josephson SA, Hetts SW, Chin CT, Kralik S, Jun P, Douglas VC (2012) Utility of MRI in spinal arteriovenous fistula. Neurology 79(1):25–30
39. Houdart E, Redondo A, Saint-Maurice JP, Merland JJ (2001) Natural history of an incidentally discovered spinal dural arteriovenous fistula. Neurology 57(4):742–743
40. Hassler W, Thron A (1994) Flow velocity and pressure measurements in spinal dural arteriovenous fistulas. Neurosurg Rev 17(1):29–36
41. Grandin C, Duprez T, Stroobandt G, Laterre EC, Mathurin P (1997) Spinal dural arteriovenous fistula: an underdiagnosed disease? Acta Neurol Belg 97(1):17–21
42. Suh DC, Kim HS, Baek H-J, Park JW, Kim KK, Rhim SC (2012) Angioarchitecture of spinal dural arteriovenous fistula – evaluation with 3D rotational angiography. Neurointervention 7(1):10–16
43. Terwey B, Becker H, Thron AK, Vahldiek G (1989) Gadolinium-DTPA enhanced MR imaging of spinal dural arteriovenous fistulas. J Comput Assist Tomogr 13(1):30–37
44. Van Dijk JMC, Ter Brugge KG, Willinsky RA, Farb RI, Wallace MC (2002) Multidisciplinary management of spinal dural arteriovenous fistulas: clinical presentation and long-term follow-up in 49 patients. Stroke 33(6):1578–1583
45. Saladino A, Atkinson JLD, Rabinstein AA, Piepgras DG, Marsh WR, Krauss WE, Kaufmann TJ, Lanzino G (2010) Surgical treatment of spinal dural arteriovenous fistulae: a consecutive series of 154 patients. Neurosurgery 67(5):1350–1357; discussion 1357–1358
46. Chen CJ, Chen CM, Lin TK (1998) Enhanced cervical MRI in identifying intracranial dural arteriovenous fistulae with spinal perimedullary venous drainage. Neuroradiology 40(6):393–397
47. Huffmann BC, Spetzger U, Reinges M, Bertalanffy H, Thron A, Gilsbach JM (1998) Treatment strategies and results in spinal vascular malformations. Neurol Med Chir (Tokyo) 38(Suppl): 231–237
48. Bowen BC, Pattany PM (2000) Contrast-enhanced MR angiography of spinal vessels. Magn Reson Imaging Clin N Am 8(3):597–614
49. Bowen BC, Saraf-Lavi E, Pattany PM (2003) MR angiography of the spine: update. Magn Reson Imaging Clin N Am 11(4):559–584
50. Saraf-Lavi E, Bowen BC, Quencer RM, Sklar EML, Holz A, Falcone S, Latchaw RE, Duncan R, Wakhloo A (2002) Detection of spinal dural arteriovenous fistulae with MR imaging and contrast-enhanced MR angiography: sensitivity, specificity, and prediction of vertebral level. AJNR Am J Neuroradiol 23(5):858–867
51. Farb RI, Kim JK, Willinsky RA, Montanera WJ, terBrugge K, Derbyshire JA, van Dijk JMC, Wright GA (2002) Spinal dural arteriovenous fistula localization with a technique of first-pass gadolinium-enhanced MR angiography: initial experience. Radiology 222(3):843–850
52. Krings T, Mull M, Gilsbach JM, Thron A (2005) Spinal vascular malformations. Eur Radiol 15(2):267–278
53. Bowen BC, Fraser K, Kochan JP, Pattany PM, Green BA, Quencer RM (1995) Spinal dural arteriovenous fistulas: evaluation with MR angiography. AJNR Am J Neuroradiol 16(10): 2029–2043

54. Luetmer PH, Lane JI, Gilbertson JR, Bernstein MA, Huston J 3rd, Atkinson JLD (2005) Preangiographic evaluation of spinal dural arteriovenous fistulas with elliptic centric contrast-enhanced MR Angiography and effect on radiation dose and volume of iodinated contrast material. AJNR Am J Neuroradiol 26(4):711–718
55. Oldfield EH, Bennett A 3rd, Chen MY, Doppman JL (2002) Successful management of spinal dural arteriovenous fistulas undetected by arteriography. Report of three cases. J Neurosurg 96(2 Suppl):220–229
56. Meder JF, Devaux B, Merland JJ, Frédy D (1995) Spontaneous disappearance of a spinal dural arteriovenous fistula. AJNR Am J Neuroradiol 16(10):2058–2062
57. Hartman J, Rabinstein AA (2012) Can we rule out a spinal arteriovenous fistula using only MRI? Yes, we can. Neurology 79(1):15–16
58. Narvid J, Hetts SW, Larsen D, Neuhaus J, Singh TP, McSwain H, Lawton MT, Dowd CF, Higashida RT, Halbach VV (2008) Spinal dural arteriovenous fistulae: clinical features and long-term results. Neurosurgery 62(1):159–166; discussion 166–167
59. Kaufmann TJ, Morris JM, Saladino A, Mandrekar JN, Lanzino G (2011) Magnetic resonance imaging findings in treated spinal dural arteriovenous fistulas: lack of correlation with clinical outcomes. J Neurosurg Spine 14(4):548–554
60. Nichols DA, Rufenacht DA, Jack CR Jr, Forbes GS (1992) Embolization of spinal dural arteriovenous fistula with polyvinyl alcohol particles: experience in 14 patients. AJNR Am J Neuroradiol 13(3):933–940
61. Jellema K, Sluzewski M, van Rooij WJ, Tijssen CC, Beute GN (2005) Embolization of spinal dural arteriovenous fistulas: importance of occlusion of the draining vein. J Neurosurg Spine 2(5):580–583
62. Sherif C, Gruber A, Bavinzski G, Standhardt H, Widhalm G, Gibson D, Richling B, Knosp E (2008) Long-term outcome of a multidisciplinary concept of spinal dural arteriovenous fistulae treatment. Neuroradiology 50(1):67–74
63. Maimon S, Nossek E, Strauss I, Blumenthal D, Frolov V, Ram Z (2011) Transarterial treatment with Onyx of intracranial dural arteriovenous fistula with cortical drainage in 17 patients. AJNR Am J Neuroradiol 32(11):2180–2184
64. Steinmetz MP, Chow MM, Krishnaney AA, Andrews-Hinders D, Benzel EC, Masaryk TJ, Mayberg MR, Rasmussen PA (2004) Outcome after the treatment of spinal dural arteriovenous fistulae: a contemporary single-institution series and meta-analysis. Neurosurgery 55(1):77–87; discussion 87–88
65. Symon L, Kuyama H, Kendall B (1984) Dural arteriovenous malformations of the spine. Clinical features and surgical results in 55 cases. J Neurosurg 60(2):238–247
66. Mourier KL, Gelbert F, Rey A, Assouline E, George B, Reizine D, Merland JJ, Cophignon J (1989) Spinal dural arteriovenous malformations with perimedullary drainage. Indications and results of surgery in 30 cases. Acta Neurochir (Wien) 100(3–4):136–141
67. Westphal M, Koch C (1999) Management of spinal dural arteriovenous fistulae using an interdisciplinary neuroradiological/neurosurgical approach: experience with 47 cases. Neurosurgery 45(3):451–457; discussion 457–458
68. Song JK, Vinuela F, Gobin YP, Duckwiler GR, Murayama Y, Kureshi I, Frazee JG, Martin NA (2001) Surgical and endovascular treatment of spinal dural arteriovenous fistulas: long-term disability assessment and prognostic factors. J Neurosurg 94(2 Suppl):199–204
69. Ruiz-Juretschke F, Perez-Calvo JM, Castro E, García-Leal R, Mateo-Sierra O, Fortea F, Iza B, Garbizu JM, Villoria F (2011) A single-center, long-term study of spinal dural arteriovenous fistulas with multidisciplinary treatment. J Clin Neurosci 18(12):1662–1666
70. Su I-C, Ter Brugge KG, Willinsky RA, Krings T (2013) Factors determining the success of endovascular treatments among patients with spinal dural arteriovenous fistulas. Neuroradiology 55(11):1389–1395
71. Kirsch M, Berg-Dammer E, Musahl C, Bäzner H, Kühne D, Henkes H (2013) Endovascular management of spinal dural arteriovenous fistulas in 78 patients. Neuroradiology 55(3):337–343

72. Muralidharan R, Mandrekar J, Lanzino G, Atkinson JL, Rabinstein AA (2013) Prognostic value of clinical and radiological signs in the postoperative outcome of spinal dural arteriovenous fistula. Spine 38(14):1188–1193
73. Gokhale S, Khan SA, McDonagh DL, Britz G (2014) Comparison of surgical and endovascular approach in management of spinal dural arteriovenous fistulas: a single center experience of 27 patients. Surg Neurol Int 5:7
74. Cenzato M, Versari P, Righi C, Simionato F, Casali C, Giovanelli M (2004) Spinal dural arteriovenous fistulae: analysis of outcome in relation to pretreatment indicators. Neurosurgery 55(4):815–822; discussion 822–823

Intracranial Meningiomas: A 30-Year Experience and Literature Review

H. Maximilian Mehdorn

Contents

H.M. Mehdorn, MD, PhD
Department of Neurosurgery, University Clinics of Schleswig-Holstein Campus Kiel,
Arnold Heller Str 3 Hs 41, 24105 Kiel, Germany
e-mail: mehdorn@nch.uni-kiel.de

J. Schramm (ed.), *Advances and Technical Standards in Neurosurgery,*
Advances and Technical Standards in Neurosurgery, Vol. 43,
DOI 10.1007/978-3-319-21359-0_6

Abstract Intracranial meningiomas are tumors arising from the covering cells of the arachnoid layer of the dura mater or from the intraventricular choroid plexus. While mostly benign tumors, they still represent a major challenge to neurosurgeons and other medical disciplines involved in their diagnostic and therapeutic management. Although this review intends to give some state-of-the-art information from the literature, it is mainly based on personal experiences since more than 30 years caring for more than 1500 meningioma patients and point to a few new strategies to further improve on patient outcome.

Diagnostics are based on magnetic resonance imaging which shows the relationship between tumor and surrounding intracranial structures, particularly the brain but also the vasculature and to some extent the cranial nerves. Furthermore, it may suggest the grading of the tumor and is very helpful in the postoperative diagnosis of complications and later follow-up course.

Surgery still is the main treatment with the aim to completely remove the tumor; also in cases of recurrence, other additional options include radiotherapy and radiosurgery for incompletely removed or recurrent meningiomas. Postoperative chemotherapy has not been shown to provide substantial benefit to the patient especially in highly malignant meningiomas.

All therapy options should be intended to provide the patient with the best possible functional outcome. Patients' perspective is not always equivalent to surgeons' perspectives. Neuropsychological evaluation and additional guidance of patients harboring meningiomas have proven to be important in modern neurosurgical intracranial tumor treatment. Their help beyond neurosurgical care facilitates the patients to lead an independent postoperative life.

Keywords Intracranial meningioma • Surgery • Magnetic resonance imaging • Neuropsychology

Introduction

Intracranial meningiomas have been a challenge to neurosurgeons, both from a technical and an emotional point of view. Their usually benign histology and the inherent long-term course make, according to data from the USA [33], meningioma

the most prevalent intracranial tumor (50.4 per 100,000 inhabitants), although meningiomas are discovered at an incidence rate of 3.7–4.5 per 100,000 inhabitants per year ([33] CBTRUS 2005). This rate needs to be compared to that of neuroepithelial tumors – an incidence rate of 6.5/year per 100,000 inhabitants and an estimated prevalence rate of 28.5 per 100,000 [33]. An autopsy study [107] reported an incidence of 2.3 % cases of asymptomatic meningiomas in 10,033 autopsies performed between 1950 and 1982, and 8.2 % of the autopsied meningioma subjects harbored multiple meningiomas, all without stigmata of neurofibromatosis. The female to male ratio was 3 to 1.

Excellent multi-authored textbooks have been published in recent years on all problems encountered when treating meningiomas [4, 83, 116]. This article however is intended to summarize, on the basis of personal experiences accumulated over more than 30 years, some of the recent surgically relevant advances in diagnosing and treating these tumors, with particular reference to advances over the last 20 years. Both a review of the literature and personal experience form the basis of this report. The challenge has remained basically unchanged since Cushing's times although techniques have much improved but also patients' expectations and society's demands have increased ever since.

Patient Population

The mean age of the population in western countries and subsequently also that of our patients have steadily increased over the recent years. In the book of P. Bailey on intracranial meningiomas translated into German and published in 1951, the peak of age distribution for intracranial meningiomas was 45 years and the series stopped at age 65. In contrast, the author has reviewed the surgical series starting in 1968 in the Dept. of Neurosurgery at Essen University, continued since 1991 at Kiel University and followed until now: this series of more than 1500 patients shows that initially the patients over age 70 accounted for 2 % of the patients operated upon for intracranial meningiomas in the period 1968 until 1973, and this percentage steadily increased over time, reaching a plateau of approx. 25 % in recent years (Fig. 1). The gender distribution has remained constant with a 3.3 to 1 preponderance of female to male patients in our population, similar to other reports.

Initial Clinical Presentation

The clinical symptoms which led to the diagnosis have not really changed over the last decades. It had been hoped that the introduction and ready availability of modern imaging techniques would have led to earlier diagnosis of meningiomas, thereby reducing the size of the average tumor.

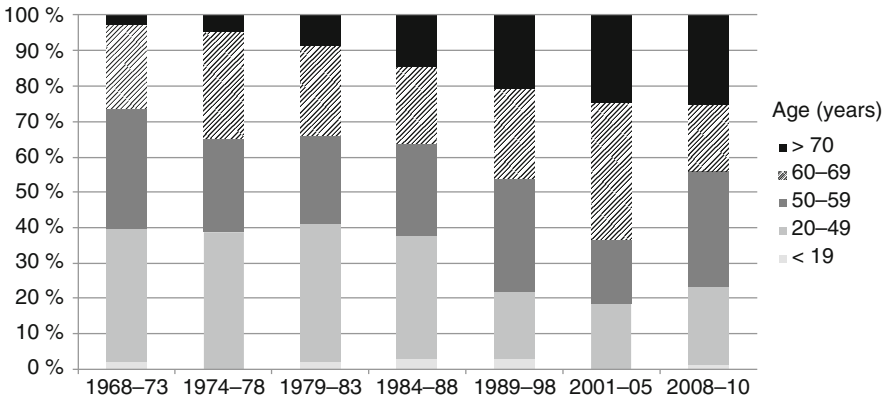

Fig. 1 Aging meningioma population Essen 1968–1989 and Kiel 1991–2010: steady rise of percentage of older patients, particularly over 70 years up to 25 % of the surgical population

In our clinical experience, this has not been the case for all presenting symptoms, but this may vary from region to region. Seizures usually rapidly lead to diagnostic steps, but often symptoms develop only gradually. More important than modern imaging techniques would still be that relatives, doctors, and the patients alike take notice of subtle clinical alterations. This awareness can and needs to be trained to some degree. Already slight changes e.g. of personality occurring in a relative resp. a patient who may additionally complain, e.g., of "some kind of visual disturbances" or headaches should be considered as early symptoms. It seems obvious that the earlier the diagnosis can be ascertained, the better surgical outcome should be. This may be true and helpful for tumors both in adults and in children [39].

To take retro-orbital tumors as example from our clinical experience, the interval between first visual problems and diagnosis ranged, for these tumors in the Essen area reviewed from 1977 until 1989, from a few days to 85 months (mean 24.8 + 22.9 months), while in Kiel region it was, for the time span from 1984 until 1992, still up to 240 months (mean 48.6 + 77.9 months). This may have been related to educating the public and the doctors alike.

The latter data correspond well to even recently reported ranges of preoperative symptoms from 10 days to 35 years in Chinese population [170] for suprasellar meningioma involving the optic pathways.

There are other meningiomas however, which, upon first clinical presentation, have to be considered untreatable with a reasonable survival period, and yet one is usually inclined "to do something for the patient" (Fig. 2a, b) although one feels that life span for this particular patient is not long despite all possible therapies [2, 120].

On the other hand, liberal and frequent cranial imaging for other symptoms including nonspecific symptoms and in the event of suspected brain injury has led to a higher number of asymptomatic meningiomas being discovered, which require a treatment algorithm different from that of symptomatic meningiomas.

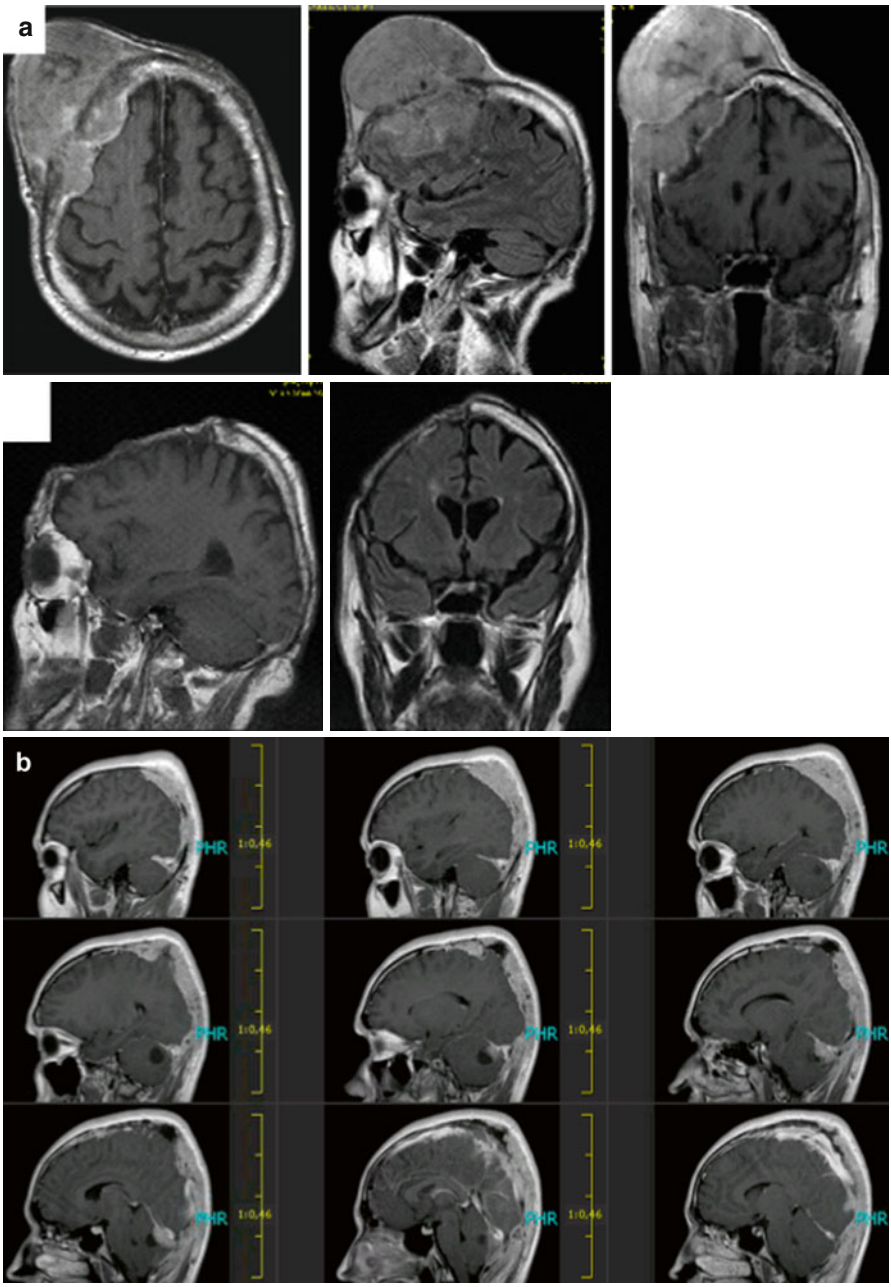

Fig. 2 (**a**) Patient who comes too late to be reasonably treatable. Rapidly growing and protruding malignant meningioma – Why does a patient come so late for treatment? Surgical total removal was followed by radiotherapy; nevertheless the patient showed multifocal intracranial recurrence 5 months after first surgery and died shortly thereafter. (**b**) Patient who comes some weeks after initial symptoms has been noticed but is impossible to cure – highly malignant destructive meningioma extending over more than half of the scalp, later with cervical spine and pulmonary metastases from which he/she eventually died

Histology and Molecular Biology

Modern histological evaluation of meningiomas is summarized in the WHO classifications of 1993 by Kleihus et al. and most recently in 2007 by Louis et al. [89, 90] which describe 19 classes of meningiomas, attributing 15 of them to grades I–III, leaving 4 variants of undefined grading and differentiating the hemangiopericytoma as a separate entity. Compared to 1993, the new classification includes more grade II meningiomas, taking into account the clinical picture as well. In addition to the grading, histological features rapidly available and important to the clinician are the mitotic index; also well-defined cell proliferation markers, e.g., Ki67 and MIB-1; and the growth pattern. It should be noted that the neurosurgeon can help the neuropathologist to establish the full diagnosis by providing fresh samples of tumor tissue in addition to conventionally preserved tissue blocks. The surgeon should also pay particular attention to the tumor–brain tissue interface possibly including some surrounding tissue in the histological specimen.

Molecular biology variants in meningiomas have been recognized in meningiomas in the late 1980s [41, 95, 160] as in other tumors, and their specific diagnosis will certainly play a role in the future. Molecular genetics have shown that alterations of chromosome 22 (monosomy 22) and the NF-2 tumor suppressor gene are important for the meningioma [32]. The importance of TGF-alpha in the career of meningioma recurrence was well shown by [87] in that a lower score matched with better survival for the patients. The distribution of steroid hormone and growth factor receptors in human meningioma tissue specimen and in tissue culture was reviewed by Black et al. [16] in order to clarify their possible implications in therapy. Scarpelli et al. [140] pointed to the importance of TP53 gene mutation as marker for malignant transformation of a benign meningioma.

Molecular biology also may help to explain why multiple meningiomas may occur without anatomical bridges: Stangl et al. [165] pointed to the clonality of multiple meningiomas. Reviews summarizing details of the WHO classification including molecular biology are given by Lamszus [82], Lusis and Gutmann [91], as well as Ragel and Jensen [122] and Campbell et al. [24]. Further research aims to better classify meningiomas by adding molecular genetics to histology of meningiomas [94] with the intention to provide targeted therapeutic strategies.

Furthermore, other groups have applied molecular biology studies to better understand mobility of meningioma cells [118], cell survival, and angiogenesis in meningioma [81]. This group has furthermore studied NDRG4 and its role in tumor invasion, as has done our group [86] for the transmembrane chemokines CXL16 and CX3CL1. So far, however, these data are only based on ex vivo tumor tissue examination. Preoperative and not yet available in vivo tumor examination may in the future become helpful in preoperatively tailoring surgical details.

Radiological Evaluation

CT

In most instances, computed tomography scanning (CT) without contrast enhancement is nowadays reserved for emergency imaging after seizures, acute neurological deficits, and disturbance of consciousness to differentiate, in a first step, the underlying intracranial pathology. Furthermore, high-resolution CT may be used in selected patients to better define the bony structures in the vicinity of a meningioma, often pointing to its origin. In some cases angio-CT may be helpful to clarify the patency or compression/occlusion of the sinus system and the larger draining veins, although this information can also be obtained using MRI scanning.

MRI

Magnetic resonance imaging (MRI), usually in a 1.5 T machine, is the method of choice to diagnose intracranial pathology such as meningiomas. The full spectrum of sequences may become necessary although usually the standard sequences are sufficient to obtain surgically relevant informations.

T1 imaging without and with gadolinium contrast enhancement defines the tumor with regard to its size, anatomical relationships, particularly its origin and compression or displacement effects toward adjacent brain tissue and cerebral vasculature, while the extent of edema is best seen in T2 or FLAIR imaging. The border zone between a meningioma and the brain is highly relevant to surgical strategy and ease of tumor removal as is the border between the tumor and intracranial vessels. From a surgeon's perspective, as will be discussed later, most important is the arachnoid plane if present in normal anatomy and next the pial plane. Taoka et al. [168] have investigated the role of brain surface motion imaging by obtaining a subtraction image of pulse-gated heavily T2-weighted images on different phases of the cardiac cycle. They found a 76.5 % agreement between preoperative MRI prediction concerning brain-meningioma interface from a single acquisition mode and surgical findings. The anatomical correlation between meningioma, particularly its border zone, and the arteries is of importance, both in meningiomas in difficult location such as the petroclival [133, 135–137, 146, 147] in any (larger) meningioma. Kashimura et al. [71] have combined magnetic resonance angiography and magnetic resonance imaging. By fusing the 3D time of flight (TOF) dataset and the 3D spoiled gradient-recalled (SPGR) dataset in a newly developed volume registration and visualization software, they improved on clarifying the 3D relationship between the meningioma and the surrounding vasculature. While details of the tumor–brain tissue border can be predicted to some extent by the degree of edema [132] based on CT [67] and MRI [167], the functional–anatomical correlation between meningio-

mas and arteries/veins is more difficult if not impossible to predict even in MRI. T1 imaging as well as MR angiography may help to define a compression/narrowing of the vessel diameter by the meningioma, but the definition of a virtual space between the meningioma surface and the outer vessel wall may be surgically more relevant. This is true for vessels of all diameters; however, this has not been evaluated systematically so far. Figure 3a, b may serve as an example. Angiography may help concerning the brain-tumor interface as has been shown by Sindou and coworkers [3, 154, 156].

The consistency of a meningioma influences surgical maneuverability and risks of tumor removal as well. Early studies by Yamaguchi et al. [175] showed usefulness of T2 imaging to predict consistency, hyperintensity being correlated to a soft

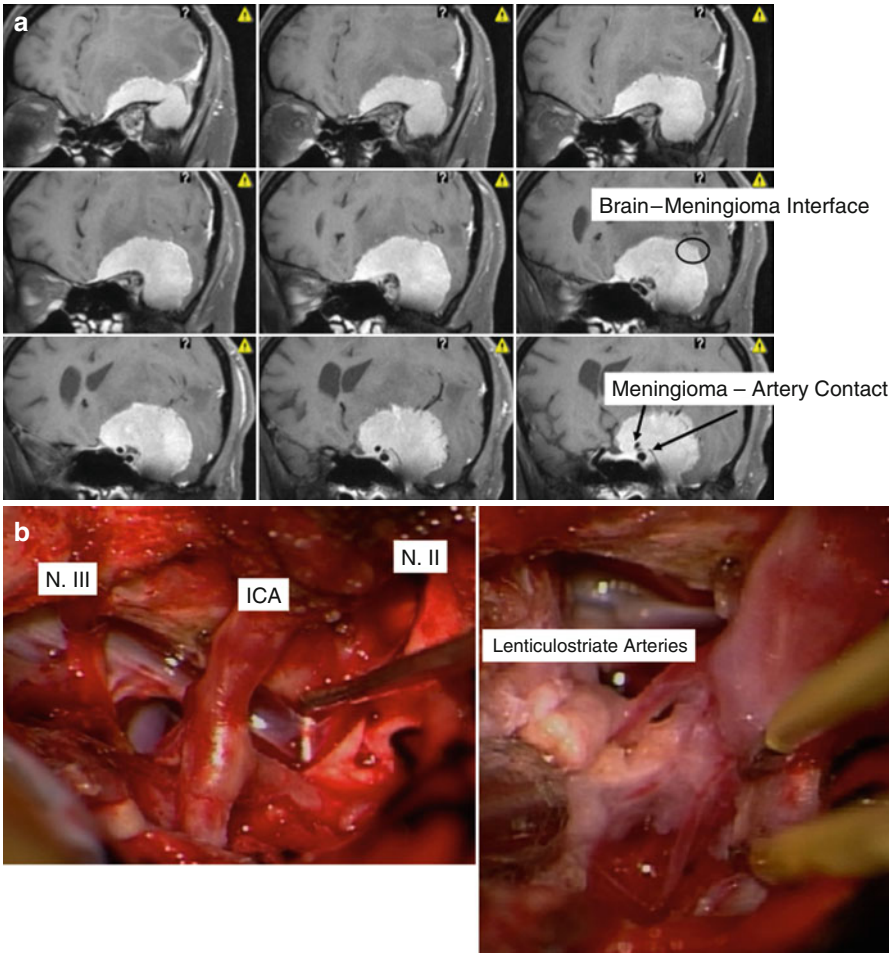

Fig. 3 (**a**) Surgeon's questions to MRI: Tumor interfaces with brain, nerves, and vessels. Neuroradiology can only partially help. (**b**) Surgeons' view: The tumor is easily peeled off the internal caroid artery (ICA) and nerves I–II but not from perforators

tumor, while Yoneoka et al. [177] showed that T2R images with shorter T2 value are helpful to correlate with collagen-rich fibrous tissue. Kashimura et al. [71], in a small series of meningiomas, showed that fractional anisotropy from preoperative diffusion tensor (DT) MR could predict meningioma consistency as well. Recent studies by Hoover et al. [63] and Sitthinamsuwan et al. [158] have shown that most (predictability in the range of 90 %) meningiomas presenting as hyperintense on T2 and T1 hypointense in FLAIR were softer and therefore easier to remove than those with hypointense imaging.

Another study that was concerned with the stiffness of the meningioma and the surrounding brain tissue as it influences surgical maneuverability was recently published by Murphy et al. [104]. They have evaluated the value of 3D magnetic resonance elastography (MRE) using a single-shot spin-echo planar pulse sequence on a 3 T machine. They correlated the results obtained by this technique in a group of 12 patients with meningiomas to the surgical findings and found an even better correlation to the surgical impression of the tumor being harder or softer than with T1- and T2-weighted imaging.

While most meningiomas are benign, well-circumscribed tumors, some are not. The character of a meningioma is conventionally evaluated using the aspects of meningioma shape and homogeneity on T1 and T2 images, including calcified spots, contrast homogeneity, configuration of the border to the brain – smooth or irregular – and abnormally draining veins surrounding the meningioma. The preoperative evaluation regarding tumor growth over some time may help to decide for or against surgery particularly in the situation of an old or high-risk patient.

MR spectroscopy (MRS) is now widely used in intrinsic brain tumors and has been examined by some groups in meningiomas as well. Our group has examined the possibilities and limitations of MRS in a 1.5T and a 3T machine in 2 series of meningiomas [22, 97]. After some initial enthusiasm, we came to the conclusion that the information obtained by MR spectroscopy does not warrant its routine clinical use. The time requirement for 2 spectra is in the range of 15 min which is added to regular scanning time. Too many details need to be taken into consideration to place the region of interest: it should not be too close to the bone, to the vasculature, and to the edema zone to give reliable results. Furthermore, details of scanning need to be considered as well: a short echo time should be used not to underestimate the lipids and low-weight proteins which serve as indicator of tumor grading; 3T MRS is preferred to 1.5T. The Tokyo group, examining 100 consecutive patients harboring intracranial meningiomas, concluded that 1H-MRI spectroscopy helps to identify meningiomas with high proliferative activity but did not add more information in malignant meningiomas [28]. Furthermore, it does not help to identify the potential future tumor growth, but it may help to grade a meningioma as found also by these authors. The dural reaction (“tail”) which might be good to know prior to surgery to plan the extension of craniotomy cannot be distinguished by spectroscopy, and only to some extent, the effect of the meningiomas upon the arachnoid border can be evaluated. Also, Kimura et al. [74] have discussed that glutamate may serve as an indicator of functional integrity of glial matrix adjacent to the meningioma.

Functional (f)MRI studies are not as important in meningioma surgery as in glioma surgery. In selected patients these studies can be performed with the intention to better define the access, e.g., to a parasagittal or falcine meningioma, sparing exposure of the motor cortex; on the other hand, the access strategy is usually more defined by structural features such as the relationship between tumor location, particularly meningioma origin, vein displacement, etc., than correlation to motor cortex. Only in deep-seated, e.g., ventricular meningioma [21], fMRI studies including fiber tracking may help to identify the best way to the tumor – the shortest way is usually considered to be the best in order to keep the access-related neuropsychological deficit as minimal as possible.

Main differential diagnosis of meningiomas in the intracranial cavity is metastasis; meningiomas have long been thought to be distinguished by the dural tail sign but this is no reliable indicator [66, 163]. Fibroma or fibrosarcoma may be included in the supratentorial differential diagnosis. In the posterior fossa, a neurinoma needs also to be included and can mostly be ruled out by the clinical symptoms and the shape of the tumor, not so well by its effect on the bony structures. Furthermore, high-grade glioma, lymphoma, osteoma, and others may be included in the differential diagnosis. Usually, however, the diagnosis of a meningioma is rather straightforward, and from a surgical point of view, the location and extent of a space-occupying lesion are more important for the patient than to rule out all other possibilities.

Scintigraphy

When MRI was not yet as fully developed as of today, many studies have been performed using scintigraphy as imaging modality. Also our group [17, 18, 76] has evaluated the use of somatostatin receptor scintigraphy (SRS) in view of receptor status and to detect recurrence, differentiating it from scar, e.g., dural graft materials. A limitation of this receptor scintigraphy was also described in patients harboring SRS-negative meningiomas which obviously are not detected using this method [96].

Subtraction Angiography Versus MRI Angiography

Conventional subtraction angiography does not play anymore the important role as previously reported. Angiography helps to define the blood supply to the meningioma, its degree of vascularization, and its effect on the surrounding vasculature of the brain incl. the sinus system. As is well known and will be discussed later, the "cleavage" between meningioma and the surrounding brain tissue plays an important role for the surgical ease. Sindou's group [3, 154, 156] has identified the pial supply of the tumor as separate predictor for prognosis with regard to postoperative hemorrhage, due to the possibility of extra- or subpial dissection.

Nowadays, MRI angiography [84, 124, 125] is able to define vascular supply to the meningioma as well as the veins involved in the meningioma and the surrounding brain. Sometimes details concerning vascular supply of a meningioma can be obtained better through selective arterial spin labeling techniques ([172, 173] and unpublished personal data from our group). These may be particularly helpful in some instances to decide for or against preoperative embolization and to direct the surgeon to various compartments of meningiomas with different vascularization sources.

Preoperative embolization has been introduced to reduce blood loss and is still strongly advocated in many centers [40], particularly in highly vascularized tumor or when the tumor supply through the nidus can be reached surgically only late during tumor removal, e.g., in petroclival meningiomas. Many techniques and materials have been suggested [60, 169], incl. intratumoral puncture and injection of Onyx ® [42]. The time interval between embolization and surgical tumor removal also has been considered to play an important role: the timing of surgery being influenced by the development of necrosis in the tumor as visualized by MRI [13]. It may only be an effective help to the surgeon when the tumor is completely embolized [12]. However, even using modern embolizing materials such as Onyx® and intratumoral injection, embolization rates of only up to 87 % have been recently reported [42]; otherwise the benefit for the surgeon is not convincing and can be outweighed by the risks, particularly in areas such as the posterior fossa where the vascular supply of cranial nerves is often the same as that of the meningioma. Also, rapid hemorrhage following embolization has been reported as severe risk [178]. On the other hand, embolization as sole therapy for intracranial meningioma with subsequent MRI controls has been published as well [11]. We have seen only extremely rarely an indication for preoperative embolization for the following reasons: in convexity meningiomas, the surgeon has rapid access to the vascular supply; in basal meningiomas, embolization is rarely effective for the abovementioned reason; and costs of the procedure need to be weighted against costs of blood transfusion and should not be underestimated.

Nevertheless it may still be considered necessary to perform angiography with regard to sinus configuration and functional obliteration, particularly in the regions of the superior sagittal sinus and the transverse sinus. Also, collateral venous outflow circulation around an occluded area of sinus can be shown in more detail using subtraction angiography, particularly its functional importance when including the time course of filling of collateral circulation (which can to some degree also be shown by 4D CT angiography). On the other hand, sometimes it is, from a surgical perspective, better to be able to include the imaging data of an occluded sinus into neuronavigation, which is possible using CT angio, and reduce the imaging quality than to have optimal imaging by angiography, which usually must be interpreted as stand-alone images.

Functional Diagnostics

Neurological and neuro-ophthalmological examination of the patients is extended by neuropsychological evaluation and support. This helps to identify subtle alterations of patients' brain functions preoperatively, to overcome anxiety, and to suggest

further treatment options postoperatively to integrate the patient rapidly into his normal environment back to an active, possibly fully functional position [55]. As will be discussed later in the chapter, an excellent postoperative MRI exam does not necessarily relate to an excellent clinical outcome with "100 % functionality in daily life."

Surgical Thoughts

Indication for/Against Surgery

Indications for meningioma surgery depend on a combination of various factors. While surgical indication for symptomatic meningioma surgery seems appropriate in most instances, this is more complicated in asymptomatic meningioma patients. Liberal use of imaging in patients for other problems – e.g., after minor trauma or with headaches of unknown origin – has brought forward an increasing number of patients with asymptomatic meningiomas. This is understandable since the incidence of meningiomas in autopsy series has been reported in the range of 2 % with multiple meningiomas in 8.2 % [107] and is higher in older patients.

Many factors need to be included into the discussion with the patient and his/her family: patient's clinical presentation, prospective length of survival – his/her biological age – more than chronological age, and, more importantly, tumor size, concomitant edema and its effect on cerebral structures, presumed histological grading and surgical risks based on size and location, as well as patient's expectations of surgical results. These factors need to be discussed weighing for a wait-and-see attitude, for surgery or other treatment options. Therefore it is important to know the natural history of meningioma, the risks of surgery, and the prognosis of the key clinical symptoms after surgery.

Natural History of Meningioma

Few data are available concerning the spontaneous course of patients harboring a symptomatic meningioma. In our own series, we have followed, in 1989, 16 patients who had become symptomatic with a meningioma but were refused to undergo surgery, mainly for anesthesiological reasons. More than 1/3 of these patients died within 90 days after diagnosis [98, 99]. Additional 3 patients died within follow-up times up to 90 months. Seven survivors could be followed for up to 240 months (average 72 months). Similar experiences have been published by other authors, as well:

Firsching et al. [46] had followed incidental meningiomas in 17 patients and found an annual growth rate between 1 and 21 %, and Nakamura et al. [106]

detected annual growth rates in the same but wider range (0.48–72.8 %). Lower growth rates were found in calcified meningiomas. Abeloos and Lefranc [1] reviewed the literature and calculated that approx. 60 % of incidental meningiomas would not grow. More specifically, Rubin et al. [129] studied 56 patients with 63 meningiomas mostly discovered incidentally and followed over 65 ± 34 months; they found an annual growth rate of 4 mm per year. This is consistent with other reports in the literature which give annual growth rates in the range of 1–21 % and 2.4 mm up to 4.4 mm per year. Niiro et al. [110] reported on 40 patients over 70 years of age who were followed for a mean follow-up of 41.8 months during which time 5 became symptomatic.

Meningiomas in patients who do not undergo surgery for a variety of reasons may present, according to Chamoun et al. [27], with three different growth patterns: The tumor may remain unchanged, grow in a linear fashion, or grow exponentially. The problem is that the initial presentation (Fig. 4) does not predict the future growth pattern, hence the idea to look for parameters indicating the presumed further course as has been discussed above. The question is how often and in which intervals a patient should be controlled by MRI scan; in our practice we found annual controls usually sufficient and refrain from further controls when the meningioma remains unchanged over 3 years and no clinical signs develop. This policy is particularly maintained if the meningioma is asymptomatic or if the patient is reluctant to undergo surgery.

It has been agreed upon that asymptomatic meningiomas presenting without functional contact to the brain ("innocent or incidental meningioma") may be considered for a wait-and-see strategy [46]; Nakamura et al. [106], while others which present with edema reaction of the surrounding brain should be suggested for surgical removal on the assumption that the tumor–brain barrier would be disrupted [132] and further tumor progress and compression against the brain would only lead to further damage of the surrounding structures.

The risks of the natural course of the disease – a possibly growing space-occupying tumor – need to be weighed against the surgical risks in order to give a sound patient-oriented clinical advice. Once the diagnosis of a meningioma is ascertained, e.g., strongly suspected on the basis of imaging, the patient should obtain good neurosurgical consultation in order to evaluate the best possibilities for his/her future course. This needs to be done by the surgeon alone or possibly by an interdisciplinary tumor board in which the surgeon plays the dominant role.

Radicality of Surgery

Radical meningioma removal at the first surgery as has been performed successfully for the first time by Prof. Pecchioli in 1835 (cited from Giuffre [51]) with aggressive search for meningioma remnants offers the best chances for a recurrence free survival. This has been shown statistically for the first time by Simpson [153] and has been experienced by many neurosurgeons [30] to the point that it

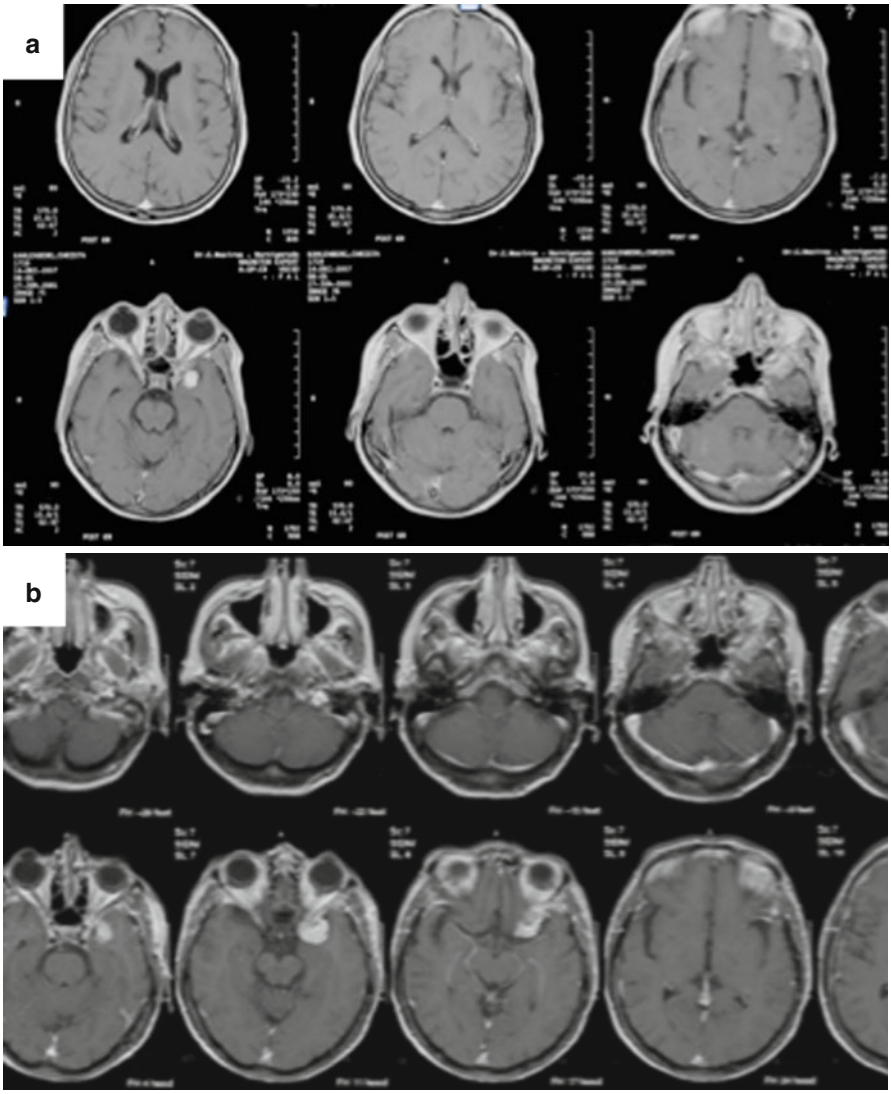

Fig. 4 Spontaneous course of a meningioma in 5-year interval – first, headaches and then visual problems due to close connection to optic nerve. (**a**) 2001: Only one axial MRI slice in which the meningioma is seen; (**b**) 2006: 3 axial slices depicting the grown meningioma

has been suggested to perform a grade 0 resection [75], meaning a more than 2 cm margin of dura to be removed around the meningioma. This concept is supported by Kamitani et al. [70] who found microscopic evidence of meningioma cells in the thick arachnoid membranes surrounding meningioma sites. However the risk of surgical damage may outweigh the benefit of radical resection which may be seen only later in life as "prevented recurrence." A long debate weighs both

advantages and disadvantages of radical surgery, and the decision needs to be individualized in every single case preoperatively and during surgery, leading to a less radical attitude in recent years again. Simpson grade I removal has been reported in larger series only in 27 % of posterior petrous bone meningiomas [8], 36 % of tentorial meningiomas [9], while grade I and II resections were achieved in 57 % on parasellar meningiomas [134, 138] and in 90 % in tuberculum sellae meningiomas [7]. Radical surgery had been advocated in the 1980s of the last century even in such areas as the cavernous sinus and the petroclival region [56, 72] where the meningioma is mostly growing invasively around and encasing the cranial nerves and the carotid and basilar artery. Modifications of this aggressive approach have been suggested by several authors [117, 151]. In our series, we have usually taken an intermediate approach being careful to preserve the cranial nerves as much as possible and to determine carefully which part of the meningioma is the larger specifically the clinically more relevant one – the intracavernous or the intradural one. The relatively low ratio of complete meningioma removal in the literature points to the necessity to discuss adjuvant therapies which will be described later and to follow the patient subsequently in certain intervals to check for recurrence.

In our Kiel series from 1991 until 2002 [166], we have seen that after initial surgery in 463 patients in 16 % the meningioma recurred, the first recurrence would occur at an average of 65 months postsurgery but the second recurrence would already occur 34 months after second surgery.

Surgical Techniques and Complications

Many data concerning technical details have been compiled and published over the years, as treatment skills have steadily developed. As has been shown in our consecutive series from Essen and Kiel including more than 1500 patients as well as in many other larger series covering a longer time span, mortality has dramatically declined over the last 45 years (Fig. 5a).

It needs to be noted, however, that mortality is still higher in older patients than in younger ones (Fig 5b).

This risk reduction can be attributed to a number of possible factors: the tumors may be diagnosed earlier, so they may tend to have damaged the brain to a lesser degree; their preoperative imaging – starting with computed tomography (CT) scanning in 1972 and evolving to MRI imaging in recent years – has given more details concerning the anatomical relationship to various structures as discussed earlier. This enabled microsurgical techniques as introduced into the broad neurosurgical community in the early 1970s of the last century to be used wisely and routinely and be taught to all residents and staff members. This went parallel with the development of knowledge of microsurgical anatomy, important basically anywhere in neurosurgery but particularly important on the skull base [176].

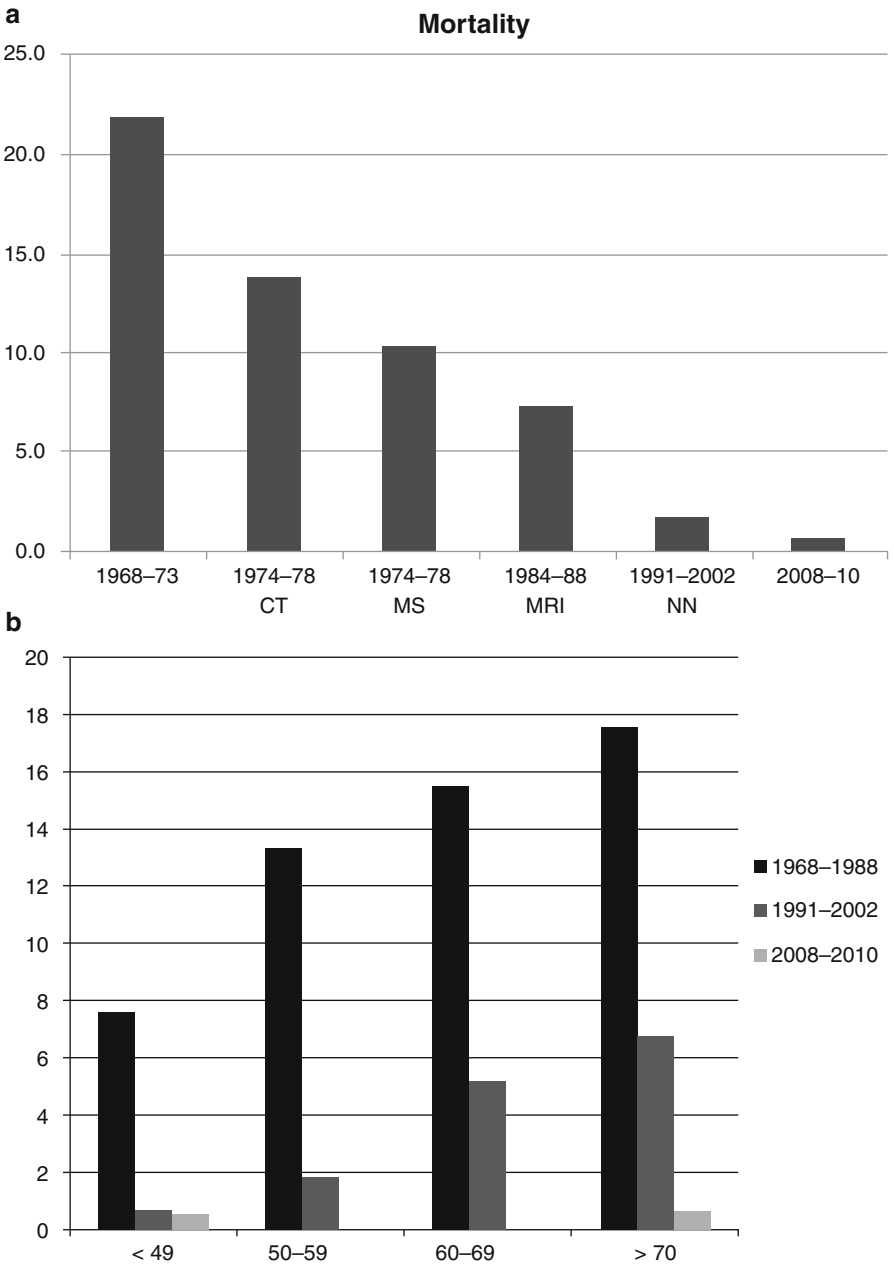

Fig. 5 (**a**) Development of mortality. Introduction of new techniques into neurosurgery and improvement of surgical skills led to improved outcome. *CT* computed tomography, *MS* routine microsurgery, *MRI* widespread introduction of MRI as primary diagnostic step; *NN* neuronavigation. (**b**) Age dependency of mortality: Age is still an important factor for perioperative mortality despite improved preoperative evaluation of patients, surgery, and anesthesiological and postoperative management

Craniotomy – patient positioning, size, and placement of craniotomy. Patient positioning for intracranial surgery has been discussed since many years, and many very elaborate positions have been suggested [14, 112, 127, 150, 164]. The main goal is always to allow for easy access to the tumor, and supine and prone, sitting, and mixed positions have been suggested. Besides allowing for easy access to the tumor, also the surgeons' ease and comfort should be considered, particularly when long hours of tedious dissection are expected. Therefore, in our routine, most patients are positioned in the supine position, sometimes in the parkbench and prone positions; rarely only the sitting position is used, e.g., in meningiomas located deep near the midline and approached through a posterior parafalcine approach, since the latter requires the surgeon to work hands and arms upward.

Craniotomy is planned very precisely taking the expected anatomy, e.g., draining veins into consideration and using neuronavigation or other computer planning tools. Positioning of the head with help of a 3-pin headholder is oriented so that the surgical target area is above the cardiac valve level in order to allow venous outflow. The head should be turned in such a direction that the approach to the meningioma is as perpendicular as possible to make brain retraction unnecessary and subsequent damage of overlapping brain tissue unlikely; in posterior fossa meningioma surgery, the head should be positioned so that the cerebellum falls away, meaning a not perpendicular approach; when turning the head, one should still keep in mind that the venous outflow must not be hampered. For this purpose sometimes it may be better to turn the entire table with the patient well attached to it instead of turning the head into an awkward position.

Neuronavigation and Skull Base Approaches

Neuronavigation as brought into the neurosurgical theater was initially thought to better orient the surgeon during the procedure [48, 61, 100, 115, 161]. Of course, neuronavigation does not replace profound neuroanatomical knowledge as has only recently been pointed out again correctly [152]. Neuronavigation and improved understanding of surgical patient placement [150] lead to less damage of the surrounding brain which is ideally not – even not gently – pushed away nor retracted [164] but falls away from the surgical field. Additionally, skull base approaches have been, developed by many groups with the intention to gain access to the meningiomas while not touching the brain e.g., leaving the surgical site seemingly untouched if viewed from the brain but with the meningioma being completely removed. Often, interdisciplinary teamwork with maxillofacial surgeons and/or ENT colleagues may be helpful not only to share the responsibility of excellent surgery but also to improve and expand on technical skills incl. techniques of reconstruction, use of new instruments, etc. [38, 45, 68, 103]. Brain shift does not play the role in meningioma surgery as it does in glioma surgery, so it should be more appropriate to use neuronavigation in meningioma surgery. With more and more clinical access to and routine use of neuronavigation, it has been established that it is very

helpful to identify the optimal approach to the tumor. During surgery itself, its limitations have become obvious: Bone surgery can be aided and performed more precisely using neuronavigation as well as reconstruction of the skull base using implants (Fig. 6). But tumor removal itself can only minimally be helped by neuronavigation: its accuracy for defining the relationship between a surgical instrument such as knife, ultrasonic aspirator, or bipolar forceps and vital structures such as the carotid or other arteries or intracranial nerves is limited, and real-time combination of neuronavigation with the tools – neuronavigated tools – is rarely if ever performed because of two reasons: inherently inaccurate due to velocity of instrument movements which need to be transferred to the computer and imaged on its screen and the necessity for the surgeon to look to the neuronavigation and check for the geometrical correlation between instrument and the structure in question. This has

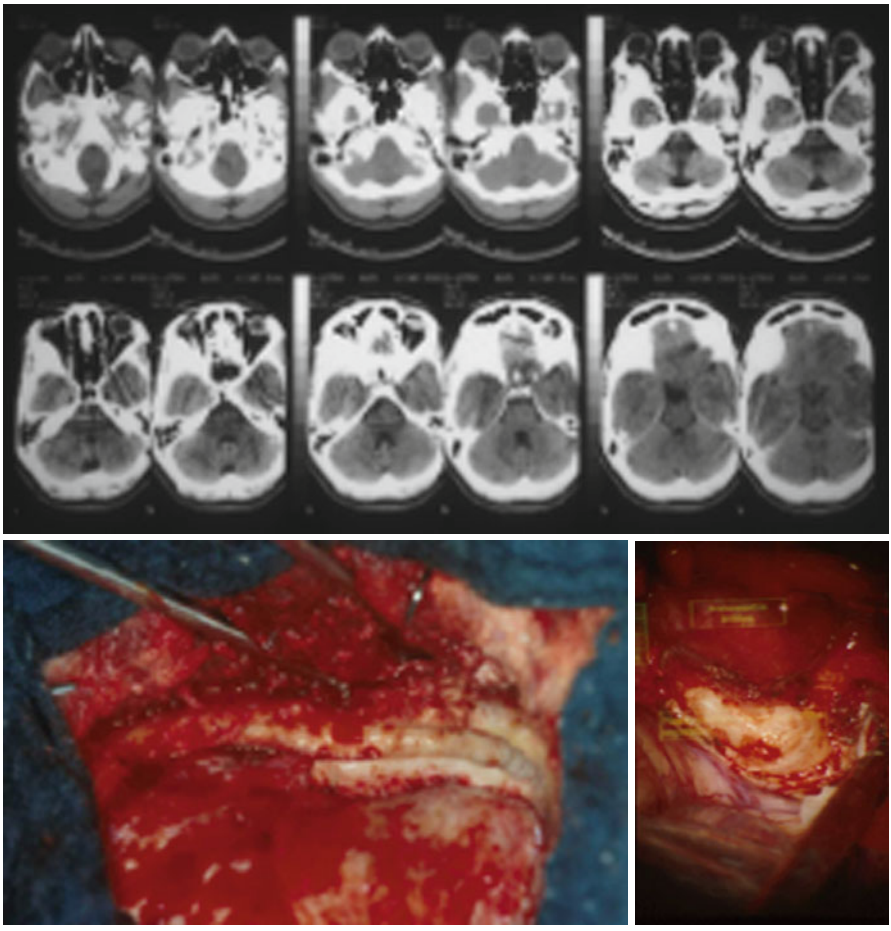

Fig. 6 Neuronavigation as important support tool to remove a sphenoid wing meningioma and reconstruct the lateral orbital wall. Although anatomical landmarks guide the surgeon in the skull base, neuronavigation helps to obtain complete tumor removal and a good cosmetic reconstruction of the lateral orbital wall

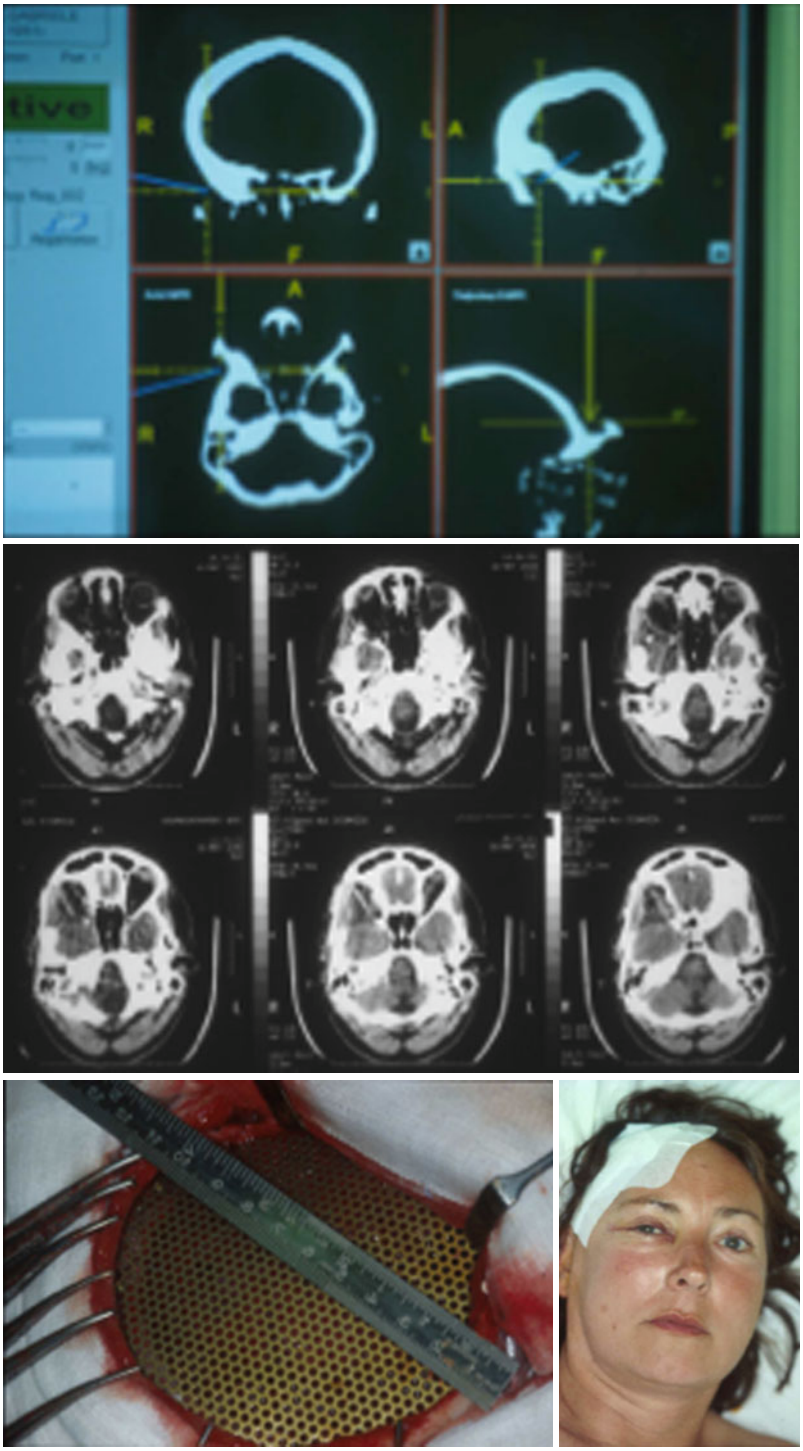

Fig. 6 (continued)

been overcome to a certain degree by modern faster computer machines and the integration of an area of interest into the optical pathway, the focus point of the microscope being equivalent to the edge of the surgical instrument or the pointer (Fig. 7). When endoscopy is used in meningioma surgery, neuronavigation is considered extremely helpful, e.g., in patients with intraventricular meningiomas, but its value has also been questioned for tumors in this region [152].

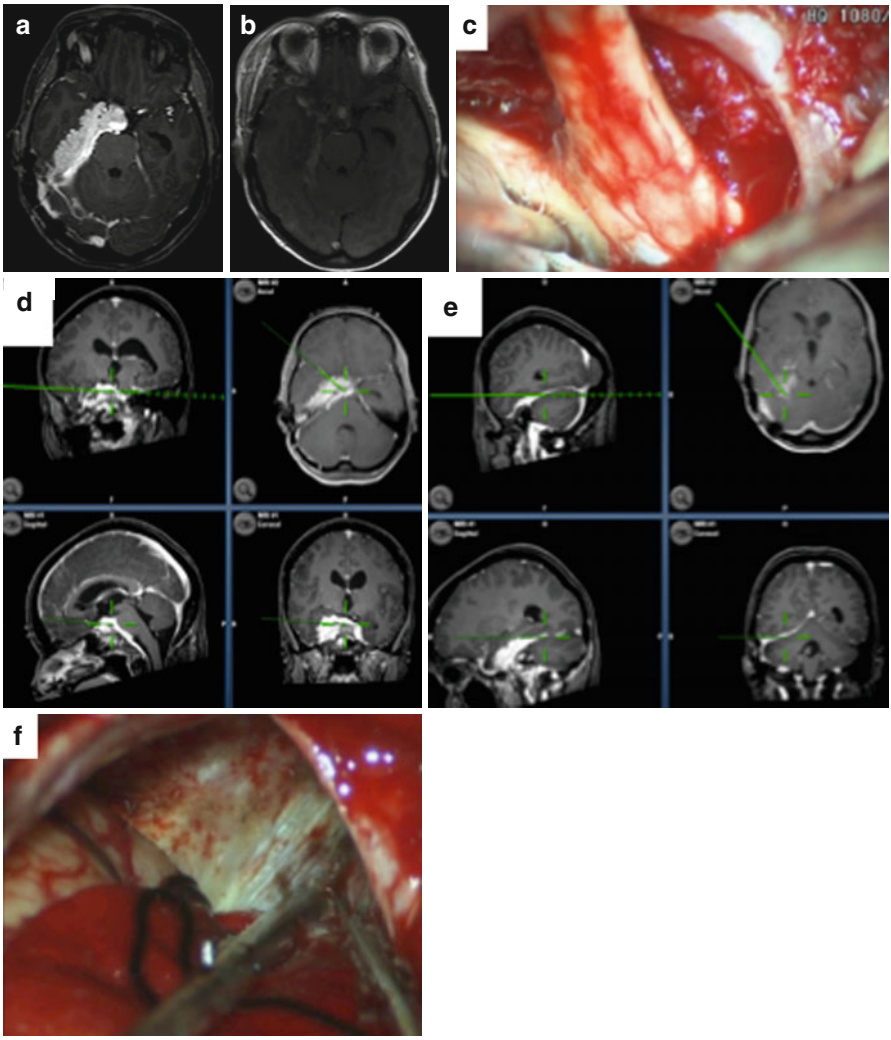

Fig. 7 Neuronavigation in skull base meningiomas supports radical surgery in intradural space: combined frontotemporal and subtemporal approach to completely remove the intradural part of a petroclival meningioma. (**a**, **b**) Pre- and postoperative MRI scan; (**c**) 2 intraoperative view of neuronavigation in the region of the optic chiasm, tumor under the chiasm; (**d**) pointer at chiasmal region after tumor removal; (**e**) pointer in the posterior part of tumor extension as shown in the right portion of fig (**f**)

Taking these limitations into consideration, we have shown in the early 1990s in our series shortly after introduction of neuronavigation that the length of stay in the intensive care unit was reduced from 2.6 to 2 days (taken as surrogate measure for quality of surgery) for meningioma patients undergoing navigated surgery compared to meningioma patients who for logistical reasons had undergone meningioma surgery in the same period without the aid of neuronavigation. Similarly and more precisely, Paleologos et al. [115] have performed a cost-effectiveness analysis and found that, taking everything into account, the costs of standard meningioma surgery were 20 % higher compared to navigated meningioma surgery. Therefore we nowadays use neuronavigation routinely in our dept. for patients with convexity meningiomas, particularly those close to the midline structures, e.g., the sinus, to define the skin incision, the bone flap, and the dural resection – circumcision – with a safety margin of possibly 1 cm in order to achieve Simpson grade 1 removal (Fig. 8). Skull base meningiomas are operated with the aid of neuronavigation in selected cases when one has to define precisely the approach area and the angle of surgical direction or for teaching purposes and to better orient oneself about the degree of resection. Large meningiomas do not necessarily lend themselves more to neuronavigation because here also a certain degree of brain shift will diminish surgical anatomical accuracy at a time when it would be desired to have more information.

Furthermore, long-term outcome in meningioma patients may improve when neuronavigation is used by both the neurosurgeon and the radiation oncologist in an interdisciplinary fashion by defining "surgically easily resectable" areas of meningiomas and thereby making them "radiotherapeutically easily treatable" on the basis of the same imaging platform.

It remains to be seen in the future whether intraoperative MRI as advocated by some groups [144] may help to reduce the remaining complication rate. We have available intraoperative high-field MRI (ioMRI) in a short-bore magnet since 2005 and used it only initially in meningioma surgery to prove the concept. In our opinion, as long as its use will require some compromise in positioning the patient and as long as it will not be able to repeatedly study, e.g., the precise localization of relevant arteries within meningiomas or edema development during surgery in a

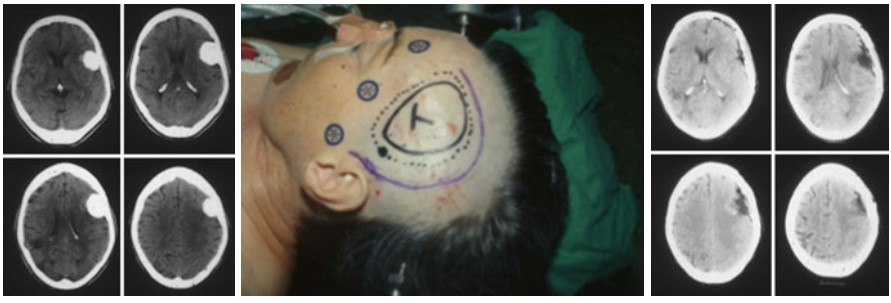

Fig. 8 Neuronavigation – planning and teaching the access for a left frontal meningioma and the result, 1 day after surgery: note the safety margin of the well-centered craniotomy

reasonable time frame, ioMRI will not be part of the neurosurgical armamentarium for removing meningiomas; a useful indication would be if one could easily foresee intraoperative complications using repeat ioMRI scans such as distant hemorrhage.

Preoperative dexamethasone treatment reduces the risk of postoperative brain swelling. The importance of improved anesthesiological techniques and ICU or intermediate care management should not be underestimated in the optimization process which has been achieved over recent years.

While initially mortality has been considered the primary measure for quality of surgery, in recent years this has become a minor issue. Nevertheless the patients need to be informed about an inherent lethal risk in any kind of surgical maneuver [49] even if not expected in the vast majority of operations anymore.

Nowadays, postoperative quality of life is gaining more and more importance and is being asked for. This points to the increasing importance of neuropsychology in the management of meningioma patients as will be discussed later in the chapter.

Endoscopy

Endoscopy has become a routine method in neurosurgery in recent years, initially in the ventricular system and later in tumor surgery. As it has extended the use of microscope-based transbasal approaches to pituitary tumors by benefitting from angled views into the sellar region, it has also been used to improve the extradural approach to anterior skull base meningiomas originating from, e.g., the tuberculum sella, the olfactory groove, and even further down to the clivus [114].

The advantage of not touching the brain and basal nerves and vessels at all or only in a very late phase of surgery has been reported to relate to similar or better clinical outcome, e.g., in regard to visual improvement after endoscopic removal of tuberculum sella [171], but needs to be weighted against the risk of postoperative leakage of cerebrospinal fluid which has been reported up to 34.6 % even in recent years even when using refined multilayer closure techniques [79].

Our group has not yet applied endoscopy to a larger extent in skull base surgery, particularly not in meningioma surgery as some groups [34, 85] have advocated, mainly for fear of CSF leakage [79].

Particular Craniotomies

While most craniotomies are performed in routine fashion, according to the surgeons' preference as free flap or as bone flap with muscle still attached, some craniotomies may carry particular difficulties and therefore should be studied in the cadaver laboratory before going into surgery: extended craniotomies including

orbital dissection, as well as keyhole trans- and supraorbital approaches [15, 23, 47, 102, 162] which may be used in conjunction with or instead of the transsylvian approach to reach deep-seated meningiomas, the approach to petroclival meningiomas, or craniotomies crossing the sinus, especially when the sinus is functionally vital.

One example is demonstrated here: a female patient, age 47, with a "bump" which her hairdresser had seen in the top of the calvarium without any complaints. MRI showed a hyperostotic meningioma originating in the midline from the convexity dura and the falx, compromising the superior sagittal sinus (SSS) at its middle third (Fig. 9). Additionally she harbored a left temporal hyperostotic meningioma and an en plaque sphenoid wing meningioma.

Surgery was suggested to the patient, and she agreed. Craniotomy was planned as a "double craniotomy": first an inner circle of bone was drilled out using high-speed craniotome; this circle was based on the neuronavigation and intended to cover the entire hyperostotic area which needed to be discarded plus some extra bone. In order to be able to mobilize the bone flap, a second circle of bone was drilled at approx. 2 cm away from the first craniotomy circle. This distance was used to mobilize the first bone flap by subperiosteally moving the dura away from the bone without damage to the underlying brain parenchyma and to the draining veins entering the superior sagittal sinus (SSS). Applying this technique, the rostral and the posterior margins of the tumor in the midline and the open lumen of the SSS could be identified and the tumor was removed totally after the dura had been circumferentially excised. Finishing complete tumor removal with particular attention to save the relevant draining veins, the convexity dura was replaced with fascia lata. Depending on the overall situation, the outer ring of bone was also discarded and a

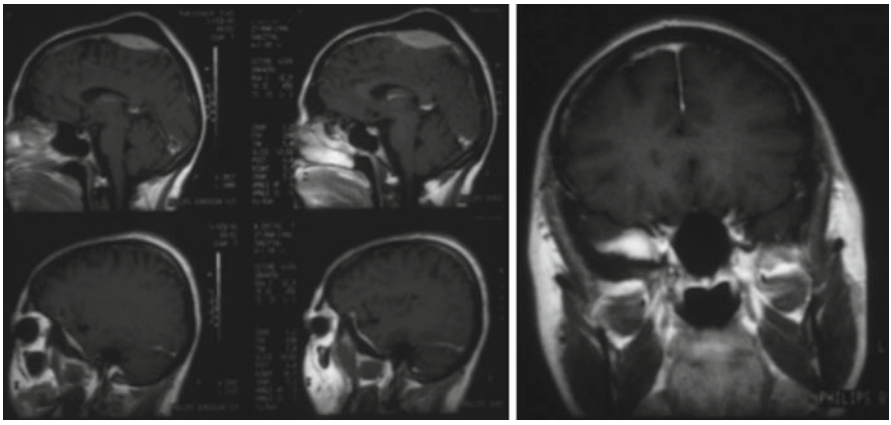

Fig. 9 Multiple meningiomas – first the falcine meningioma is removed as described in the text. No local recurrence

methyl methacrylate plastic was adapted to the convexity with excellent cosmetic results. The patient made an uneventful recovery and underwent further surgery for the left temporal meningioma at a later stage as well. Her en plaque sphenoid wing meningioma was treated using hydroxyurea in 1998 and has been stable ever since, and she continued life fully working as teacher until retirement 15 years after first surgery and further on, functioning normally. Radiotherapy was thought inappropriate due to her young age at initial presentation and the multiple meningiomas. In posterior fossa approach to petrous bone meningiomas, the open transverse sinus needs not always to be occluded but the bone can safely be drilled away with a high-speed craniotome. Combined approaches both to the posterior and middle fossa have been suggested in order to completely remove appropriate tumors [80]. However, already Zentner et al. [180] had questioned the necessity of radical removal of petroclival meningiomas. An exemplary patient who underwent staged resection of his/her petroclival meningioma in 1992 using the retromastoid and frontotemporal approaches is presented in Fig. 10. He/she remained well and without recurrence over 15 years until his/her death from cardiac reasons.

Surgical Strategy

The major goal of surgical strategy should always be to initially gain rapid control over the tumor. To achieve this goal the surgeon has several options: one may approach the tumor either extradurally by drilling away parts of bone, e.g., the

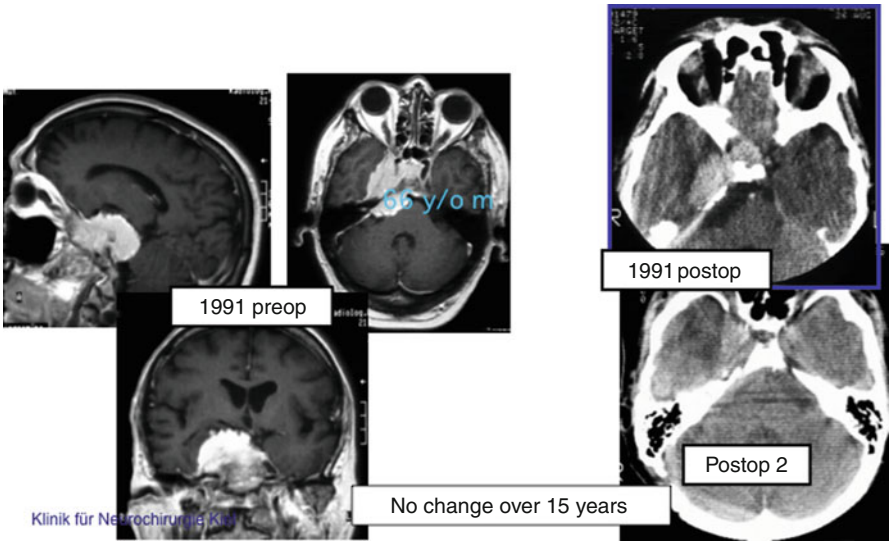

Fig. 10 Petroclival meningioma in a 66 y/o m – staged resection – first the infratentorial part is removed and next the supratentorial rest without opening the cavernous sinus, good clinical course over 15 years

sphenoid wing in case of sphenoid wing meningiomas, or one should, following craniotomy for convexity meningioma, cut the dura circumferentially. By doing so the arterial blood supply to the tumor is reduced leaving only the feeders coming from the surrounding brain tissue. Reducing blood supply in the same time reduces tumor volume and allows for better handling of the meningioma. Particularly in tuberculum sellae meningiomas, its hyperostotic bony origin needs to be dealt with at first, and drilling the bony canals of the feeding arteries with a diamond drill without irrigation allows for a much easier way of removing the devascularized tumor than first decompressing the still vascularized meningioma and at a later stage arriving at its origin (Fig. 11). However, one has to be careful in these instances and check on the preoperative MRI scans for the course of intratumoral arteries coming from the anterior cerebral artery complex which may take part in the tumor vascularization. This technique can also be applied in posterior fossa – petroclival tumors. In this location, it is obvious that one has to consider carefully the preoperative MRI and CT images to define the exact location of the tumor origin which needs to be taken care of at first, if possible (Fig. 12).

The surgeon has to be aware of the obstacles which he/she will encounter on his/her way to the tumor origin, i.e., cranial nerves and major vessels, which he/she needs to work around diligently. The possibility of attacking primarily the tumor origin is somewhat limited in case of increased local or general intracranial pressure. If one foresees this situation due to the extent of space occupation/requirement, it may be wise to preoperatively administer antiedematous medication, e.g.,

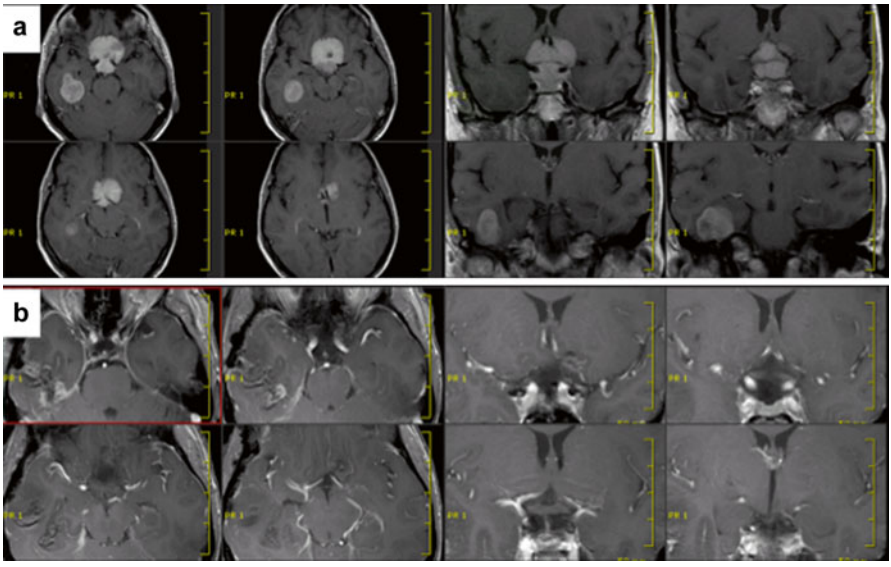

Fig. 11 Progressive tuberculum sellae meningioma + right temporal meningioma removed in single frontotemporal approach. Patient finally decided to undergo surgery when visual problems became more evident – and they disappeared after surgery (**a**) preop MRI, (**b**) postop MRI the day after surgery, improved visual function

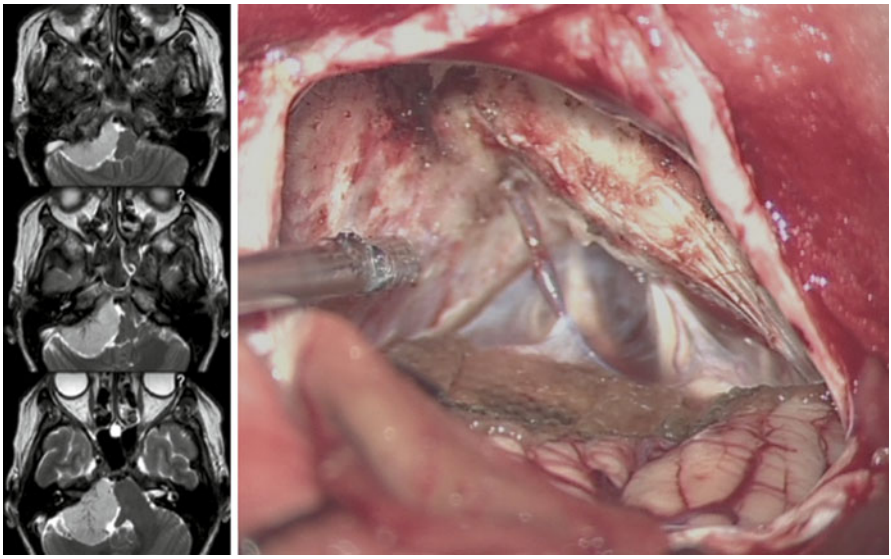

Fig. 12 Petrous meningioma extending anterior to the inner auditory canal but respecting the arachnoid planes. Postop no deficit

mannitol, in addition to dexamethasone phosphate. If deemed useful, one may also use a lumbar drainage in order to relieve intracranial local pressure by voiding the cisterns, which we have used only exceptionally for fear of downward herniation.

When attacking the meningioma, it is important to visualize what one has seen on preoperative MRI scans with regard to the border between the meningioma and the brain. The presence or absence of an arachnoid plane makes surgery easy or extremely difficult, particularly in the posterior fossa. The situation which one sees at the beginning of surgery may change as surgery progresses but is basically defined by the natural behavior of the meningiomas as expressed by its receptor status. A meningioma which respects the arachnoid layer in the supratentorial cavities resp. the arachnoid membranes in the posterior fossa will also most probably respect the integrity, e.g., of cranial nerves or the vessels.

Therefore, with steady bipolar coagulation of the dura in the area surrounding the tumor origin, one can devascularize the tumor to some extent while approaching the primary tumor navel, e.g., at the medial part of the sphenoid wing or at the petrous bone anterior to the inner auditory meatus. In these locations, it may be difficult to achieve immediate bleeding control over the meningeal arteries. Often it is necessary to use high-speed diamond drilling to close the sometimes rather active feeding arteries perforating through the bone to the dura. Once the meningioma has been devascularized to a major extent, it shrinks and can be removed in a piecemeal fashion with larger pieces to be given for histology and molecular biology examinations; once enough tissue has been preserved for examination, the rest can be removed using ultrasound aspirator (CUSA ® or SONOCA®). These instruments have been refined over the last 20 years to a perfection with various tips and strength levels allowing elegantly removing the tumor – first reducing the stroma and leaving

the fibrous tissue next to be completely resected with scissors and/or bipolar coagulation and also being able to remove bone itself.

When one removes a larger meningioma in the posterior fossa, one will also come close to or meet the basilar artery and its branches which need to be dealt with great care, similarly to the cranial nerves. Here again the same principle applies: when the meningioma has respected the arachnoid plane, it will most probably also respect the adventitial tissue of the arteries. But, pulling on the meningioma tissue will also risk to put strain on the arachnoid tissue which will then affect/stretch the smaller arteries and nerves, particularly the sixth nerve which is well enveloped in its arachnoid plane and takes a long curved course before entering Dorello's canal. Therefore the risk of some degree of usually transient palsy is quite high particularly for the sixth nerve.

The Arteries/Veins

The arterial supply and the venous drainage nearly always get into contact with the meningioma. One should be prepared to work the tumor off the vessels by pulling gently or dissecting it sharply. Perforating arteries should be preserved if possible by any means. Often this is the most tedious and time-consuming part of surgery but it is worthwhile to prevent neurological deficits. They are more difficult if not impossible to dissect from the meningioma, since often they drain also the tumor and even if the meningioma gets into intimate contact with the venous tissue adhering firmly to it. In such instances it may become necessary to coagulate the vein and dissect it in order to achieve complete tumor removal – if this is possible in other attachment areas as well; if not, the small remnant may as well stay on the vein to prevent the risk of intracerebral damage due to edema or hemorrhage; in such an instance one should consider further therapy – radiotherapy – or watchful waiting.

The Nerves

As has been earlier mentioned, the cranial nerves may also pose significant problems when dissecting the meningioma away from. This is true for all nerves. The nerve itself will be stretched already by the meningioma to a certain extent as will be its supplying vessels, which may also be affected by the meningioma. Therefore, one has to make sure not to overextend the nerves nor to damage them applying heat to them or their vasculature during coagulation of the meningioma. This may happen easily particularly when removing, e.g., a larger frontobasal (planum sphenoidale or tuberculum sellae meningioma) lifting the optic chiasm; when working at the optic nerve, its tiny feeding arteries coming from below may be damaged when pulling on the tumor capsule causing a well-circumscribed ischemic lesion in the nerve (Fig 13).

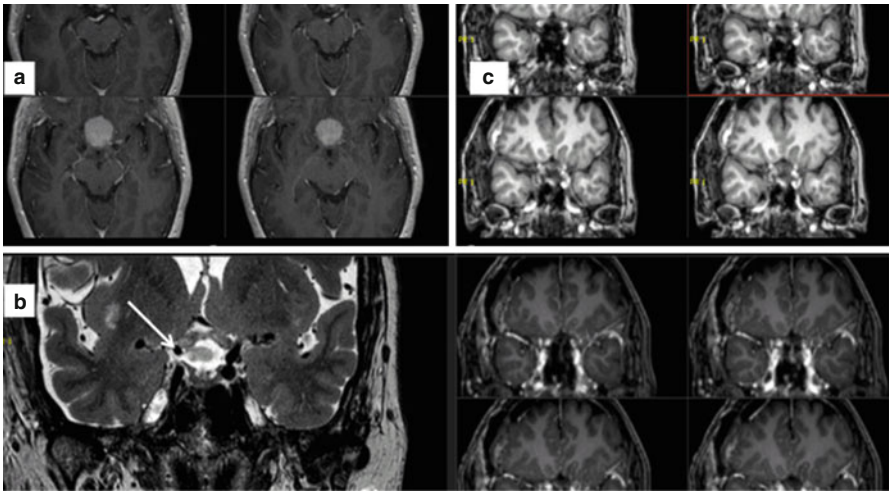

Fig. 13 Tuberculum sellae meningioma – postop further worsening of preoperatively severely affected vision right ON due to focal ischemia (s. *arrow*) due to small terminal optic nerve arteries (**a**) preop MRI; (**b**, **c**) postop MRI

Often, it has been suggested to use electrophysiological monitoring during surgery for tumors in close vicinity to cranial nerves or other important structures [5, 19, 77, 92, 105, 126, 128, 141], even in a multimodal fashion, but there may be limitations to the extent with which it can performed in a practical way, i.e., the number of cranial nerve which can monitored simultaneously. Also, one always has to weigh the benefit of electrophysiological monitoring over the burden of observing these nerves reacting during surgery, which usually requires trained personnel. Furthermore, electrophysiological monitoring during dissection of cranial nerves may be a useful adjunct in that one learns to be gentle with the nerves until this memorizer may not be required anymore, at a late stage of competence. In analogy to awake craniotomy for intrinsic brain tumors in eloquent areas, awake craniotomy for a large foramen magnum meningioma, in addition to monitoring evoked potentials, has also been performed [35] but should certainly be reserved to particular indications.

Adjuncts for Radical Tumor Removal

At the first intervention, microsurgical meningioma removal offers the best chance to be radical. However one has to make sure that the tumor, its border zone, and its origin are completely removed. If by any means possible, one should remove a safety margin on the dura of approx. 1 cm. Often one sees some vascular blush extending on the dura from the tumor origin, and histology usually shows some meningioma cells spreading along the vessels. So this dura should be removed or at least be coagulated carefully. Still, even with these precautions, one cannot

guarantee a 100 % complete removal without recurrence. Fluorescence as used successfully in glioma surgery (aminolevulinic acid – ALA) has been tried by some groups in single cases or small groups of patients [10, 29, 69] during meningioma surgery in order to increase radicality, but no controlled studies showing a benefit for radicality and long-term recurrence free survival are available until now.

Replacement of Removed Dura and Bone

Since in most instances radical surgery should be tried to achieve, a substitute is required for the dura resected with a safety margin in convexity meningioma to achieve Simpson I resection and in skull base meningioma to prevent CSF leakage. The best dural substitute is temporalis muscle fascia in patients with sphenoid wing meningioma; in convexity meningiomas usually it is best to use the inner layer of the galea; this needs to be considered when planning the craniotomy and the tissue has to be taken care of while removing the meningioma. If no sufficient amount of galea is available, other substitutes are required. Having used all sorts of dural substitutes, we have found that TachoSil ® is the most suitable substitute even for closing larger defects. This graft material may be laid out over a number of sutures crossing the dural defect in a mesh-like fashion in order to keep it on the dural level. Once in place after soaking it a bit with wet sponges, it will adhere rapidly to the dural rims. Since this material became available to us, we have, in the majority of patients, preferred it even to fascia lata which we had previously used to cover larger dural defect.

Covering bony defects is only necessary when a cosmetic problem may be envisioned, e.g., in the temporal or orbital area [20, 43–45, 62] or when a large defect would leave a larger area of brain vulnerable to outside forces. In these instances we prefer the tabula interna of the craniotomy flap or use titanium mesh or a combination of both materials which will be fixed to the remaining bone using titanium mini-plates and screws. Rarely only do we need methyl methacrylate cranioplasty to cover large bone defects. When one has drilled away a major part of the bone to gain atraumatic access to the meningioma, it may be wise to fill the space using fat graft to reduce the risk of CSF leakage.

Placement of a lumbar drainage postoperatively may be used in a liberal fashion but it should be removed as early as possible when CSF is not demonstrated on later postoperative CT or MRI scan in the surgical cavity in order to prevent its risks and not to extend unnecessarily the patients' stay in the hospital.

Particular Locations of Meningiomas

Midline meningiomas always pose a special risk to the patient and challenge to the surgeon. This is true particularly in the cranial convexity, i.e., around the superior sagittal sinus (SSS). In order to remove the meningioma completely, even if the SSS

seems completely occluded on MRI scanning, careful evaluation of cerebral hemispheric drainage is mandatory, if possible by MR angiography or 4-D CT angiography taking the time sequence of draining the brain additionally into consideration. Otherwise one might overlook small but clinically relevant draining parasinus systems which even may run transdurally and lead, through osseous channels, to larger subcutaneous draining veins. Neuronavigation may help to identify them prior to and during surgery and save them from being cut inadvertently, with the need of coagulation and obliteration, and the risk of reducing the draining system of the hemispheres.

Radical resection of a stenosed or occluded SSS is possible, with the aim to completely remove the meningioma; in such an instance, the falx needs to be resected completely as well, down to the level of the inferior sagittal sinus which may be saved if not in close vicinity to the meningioma. Being doubtful whether it would be safe to resect a not completely occluded SSS, in some cases we have measured the intrasinusoidal venous pressure prior to opening it an after test occlusion. The finding of unchanged pre–post-occlusion intrasinusoidal pressure helped us to decide for obliteration and complete resection of the infiltrated sinus segment. Other authors have recommended SSS reconstruction using different techniques and published case reports or larger series [36, 37, 58, 148, 155, 157]; we have used this technique in some instances only and preferred postoperative local radiotherapy for tumor remnants in the sinus wall.

Recurrent Meningiomas

As has been pointed out earlier, meningioma may recur locally in a certain percentage, depending on the radicality of initial surgery and their grading or may develop additional meningiomas distant from the first one. Calculating a rule of thumb from the old numbers of Simpson [153], one can estimate a 1 % per year recurrence rate in grade I meningiomas, a 2 % rate in grade II meningiomas, and 3 % in grade III meningiomas. The true “rate of recurrence” also depends on the intensity of postoperative follow-up of patients. There is no evidence-based suggestion how often a patient should be controlled by MRI postoperatively, in order to maintain the “good postoperative status.” From a clinical and health economics-based perspective, one may wonder whether it would be sufficient to perform imaging studies when new symptoms occur. The argument against this wait-and-see attitude may be that a recurring meningioma may cause new symptoms only when it has filled out an old resection cavity or grown into other directions irritating previously unaffected brain or nervous structures and thus has become more difficult to operate on.

Surgery is usually indicated when recurrence has been detected within a reasonably short time interval after first surgery independent of clinical symptoms or when new clinical symptoms occur after a longer time interval. Surgery for recurrent meningiomas is usually more difficult and less rewarding with regard to the clinical results for a variety of reasons: The new craniotomy needs to be extended usually

over the old one with the direction of regrowth in mind, so passing over the borders may require crossing scar formations extradurally and subsequently and more important intradurally. While the arachnoid plane may be initially present, in a recurrence situation it is usually no longer respected so the tumor is more difficult to dissect against the vessels and the brain surface risking more damage. Closure of the dura and the craniotomy site may be more technically more demanding than in virgin meningioma surgery causing more CSF leakage but is possible using modern substitutes such as TachoSil® and fibrin glue.

Taken all this together, the patient should be advised to undergo repeat surgery for a recurrent meningioma when his/her biological age warrants several more years to live, and even several repeat surgeries may become necessary as has been pointed out already many years ago by Cushing, e.g., in the case of the young violin player [31]. In our series the highest number of operations performed in a single patient for recurrences was 11 operations. This was a patient who had initially been operated elsewhere in 1992 for a parasagittal meningioma and came to us 1 year later with a recurrent meningioma which turned out to be malignant, and further surgeries were required because of clinical symptoms like seizures and finally subcutaneous metastases developing before pulmonary metastases terminated his/her life in 1996 which until shortly before his/her death had been of decent quality.

Adjuvant Therapy

Radiotherapy

When a meningioma cannot be completely removed incl. its adjacent dura ("Simpson grade 0"), the future carries the risk of recurrence. Accordingly it needs to be extensively discussed with the patient whether immediate radiotherapy or radiosurgery needs to be applied in a useful fashion.

While the benefit of radiosurgery used in the modality of Gamma Knife therapy is derived from its excellent isodose distribution, neurosurgeons using the Gamma Knife are very careful about the vicinity of the meningioma to radiosensitive structures like the optic tract, the pituitary gland, and the brain stem. Surgical–radiosurgical and radiotherapeutical discussion in tumor boards is the ideal way to have the patient benefit the most from combined therapies, and the surgeon should be integral part when planning the field of radiation.

Timing of radiotherapy as related to surgery however is a question of debate: While it has been shown early [6] that radiotherapy following first surgical resection is better able to control meningioma growth than after second surgery, some surgeons like to defer patients after incomplete resection with a wait-and-see attitude. This is certainly possible in older patients and in very firm, presumably slowly growing menigiomas, but younger patients or patients harboring soft and yet incompletely removed meningiomas should be advised to undergo radiosurgery within a

planned interval of a few months ("soon" [78]) after surgery; the interval is deemed helpful to let cranial nerves and small vessels recover from surgical trauma.

Maximum surgical resection of skull base meningiomas and adjuvant stereotactic radiosurgery shows the best results with a 97 % control rate over a longer period of time [65]. Excellent control rates of up to 94 % and 10-year control rate of 84 % [179] and 91.6 % [159] have been published in the radiosurgical and radiotherapeutical literature with minor risks such as peritumoral edema [50, 113] amenable to dexamethasone therapy. For large (i.e. >4 cm maximum diameter) meningiomas, fractionated stereotactic conformal radiotherapy has been suggested with a 3-year and 5-year progression-free survival of 96 % and 93 %, respectively [101]. The patient should be controlled, however, over a longer period of time in order not to overlook late progression [101, 159]. Also the patient needs, before being sent to radiotherapy and radiosurgery, to be informed about the risk albeit small of late (interval of more than 10 years) secondary malignancies [93, 111] or the occlusion of vessels in the radiation field, e.g., the internal carotid artery. We have experienced such a complication with severe clinical problems: a few years after surgical debulking and radiotherapy of a left-sided cavernous sinus meningioma, the patient came again to our attention with minor strokes due to severely impaired left hemispheric circulation, on the basis of a progressive narrowing to occlusion of the left carotid artery, and in the situation of an isolated left hemisphere. The superficial temporal artery having been occluded during initial surgery, a high-flow extra-intracranial bypass was suggested to the patient, but it occluded shortly after surgery, leaving the patient with her unchanged misery perfusion status for the left hemisphere. In such instances it may be advisable in the future to consider endovascular placement of an intraluminal stent to keep the carotid or other major arteries patent despite post-radiation media hyperplasia or progressive tumor growth.

Chemotherapy

Since meningiomas are, as has been pointed out, fraught with the risk of recurrence, early on it has been suggested to treat them with chemotherapy in addition to radiotherapy. However, conventional chemotherapy which has been used in gliomas such as PCV has brought no benefit to the patient. The following regimens have been proposed over the last 20 years until more recently [59, 73, 142, 143, 149]: hydroxyurea, somatostatin, and temozolomide [145], tyrosine kinase inhibitor imatinib mesylate [64], VEGF receptor inhibitor bevacizumab [88, 109], and trabectedin [119]. Most of these drugs were used in very small patient groups of a variety of high-grade recurrences or in single-patient experiences. Only hydroxyurea has been used in a more extended fashion by several groups, and the results have been reported in a retrospective fashion [25]. This author presented a series of 35 patients with recurrent grade II meningioma who had progressed after prior reoperation and radiotherapy and treated them with median 2 cycles of hydroxyurea 1000 m/m^2 orally divided twice per day. Overall progression-free survival (PFS) was 3 % at 6 months

(median PFS 2 months). Reardon's group [123] has reported on a series of 21 patients with recurrent grade I–III meningiomas treated with a combination therapy of imatinib (400 mg/day) and hydroxyurea (500 mg twice a day). Best radiographic response was stable disease over 6 months which was observed in 14 patients (67 %). They concluded that the combination therapy is well tolerated but has only modest antitumor activity, less in high-grade meningiomas than in grade I meningiomas. We had gained similar experience and have refrained from using HU in a regular fashion; only the abovementioned patient with a low-grade multiple meningioma has been on HU for more than 15 years now and has a stable disease (Fig. 9).

Chamberlain and Barnholtz-Sloan [26] have previously summarized the disappointing results presented in the literature concerning "targeted approach" and pointed to the guidelines for inoperable and radiation-refractory meningiomas which are limited to hydroxyurea, IFN-α, and Sandostatin LAR, a somatostatin analogue. Most of these data supporting some beneficial effect of medical treatment on meningiomas rely on case reports or smaller series. In our own early experience [130, 131], we had a young patient who was treated under compassionate use with octreotide with an intra- and suprasellar tumor suggestive at this time for a pituitary adenoma with good results for his/her visual field defects. When octreotide came on the market, it was too expensive for the patient, and we advised surgical excision of the tumor what had been rejected previously due to coagulation disorders. As it turned out during uneventful surgery, it was a tuberculum sellae meningioma which could be removed completely with permanent improvement of visual field defects.

Hormonal

On the basis of the finding of receptors binding a variety of hormones such as progesterone and others and based on laboratory research results, it has been suggested to use antihormonal therapy (mifepristone RU-486) in otherwise therapy refractory meningiomas [57, 139]. Only anecdotal reports have been presented at meetings, probably due to the not yet sufficiently evaluated variability of receptors in various meningiomas [174].

Outcome

Clinical Evaluation

The best result for a patient simply is the result which he/she desires from surgery: to be kept alive and well in order to lead an independent life for as long time as possible. This desire helps him/her to overcome preoperative fears and anxieties, which everyone has in view of undergoing craniotomy, to a very variable extent. However, reality may often turn out differently for the patient and his/her relatives. The

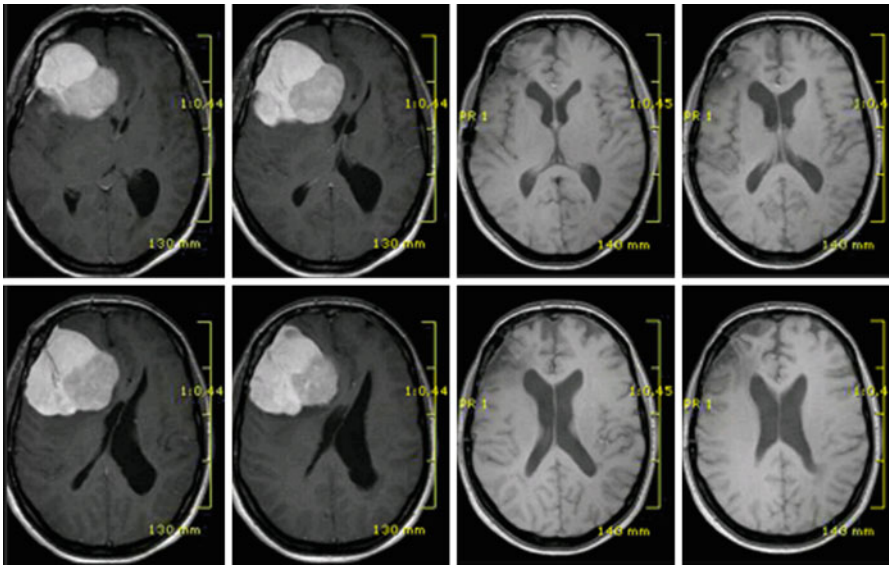

Fig. 14 Severe long-standing misdiagnosed neuropsychological problems in a female patient improve only slowly postoperatively, although the patient had understood how well she was "objectively" doing. (**a**) Preop MRI; (**b**) postop MRI scan shows nearly normal brain with only minor scar right frontal region, 6 months postop

surgeon therefore should extensively and responsibly discuss with the patient about his/her situation and his/her expectations. This should include the possibility of worsening of clinically guiding symptoms, the non-subsidance of previous symptoms, and others.

Often enough patient's perceptions both of an impending surgery and of results of surgery differ from surgeons' perception. From a neurosurgeon's perspective, formal neurological testing, e.g., for cranial nerve functions, seems adequate, but often other problems may be more important to the patient (Fig. 14). In this regard, our neuropsychology group, being a major integral part of our neurosurgical team, has extensively evaluated some of the problems involved in this complex.

Patient Performance and Perception: The importance of Neuropsychology

Several problems need to be addressed. Comorbid mental disorders in both the patients and their relatives are not infrequent: In one study [53] using structured clinical interviews for DISM-IV (SCID-IV) in patients and their relatives within 3 months after discovery of a brain tumor, 38 % of the patients and 47 % of the partners suffered from a psychiatric disorder, in the majority of elevated psychosocial stress.

Interestingly, partners were even more affected than patients themselves, particularly by the fear of surgical outcomes. This points clearly to the necessity that patients and partners should be counseled carefully – the better they are informed, the more relaxed they can cope with surgery. This stress is basically independent of the grade of tumor.

In order to better identify, even in a busy neurosurgical setting, patients suffering particularly from elevated psychosocial stress, the National Comprehensive Cancer Network's (NCCN) Distress Thermometer (DT) was evaluated in a group of 150 patients harboring primary intracranial tumors [54]. The single-item DT was shown to be a valid and practicable screening instrument for assessment of levels of distress in neurosurgical patients, comparable to the conventionally used hospital anxiety and depression scale (HADS). It is noteworthy that again the grading of tumor did not interfere with the level of distress.

Since it could be possible that preoperative stress level might affect neuropsychological test performance, in another study, we evaluated 172 patients preoperatively using a comprehensive test battery including the HADS and the Acute Stress Disorder Scale (ASDS) as more general measures of an emotional state and the Amsterdam Preoperative Anxiety and Information Scale (APAIS) as more specifically related to the neurosurgical procedure. After age and education adjustment, affect did not alter cognitive performance in any of the cognitive domains in the whole patient sample [52].

Furthermore, it became evident [55] that "acute stress disorder (ASD)" is a severe psychiatric comorbidity in patients with brain tumors which needs to be taken care of in the early phase of treatment.

Fortunately enough for meningioma patients, they seem to fare slightly better than patients with intrinsic brain tumors, as was shown in a comparative evaluation of two patient groups [52]: in the meningioma group, preoperative anxiety was higher compared to glioma patients, who, after the diagnosis had been communicated to them and their partners, understandably showed high levels of anxiety with increasing levels of depression. But in the follow-up evaluation, meningioma patients showed great relief about positive surgical course. Interestingly, an earlier study [121] had shown similarly high preoperative anxiety levels in meningioma patients as we have found; these authors attributed their finding to the high female proportion, which was not present in our group of patients. This study confirmed that overall physical and functional status was significantly related to the patients' emotional status, as was impaired memory associated with depression after 6 months. These findings support the need for routine preoperative neuropsychological assessment of patients with intracranial tumors in order to help improve in the postoperative functional status.

Postoperative Neurological Deficits

While most neurological deficits, e.g., paresis or sensory or speech disturbances, are relatively well tolerated by the patient and have a chance to improve over time, cranial nerve deficits pose a major often permanent problem to both the patient and

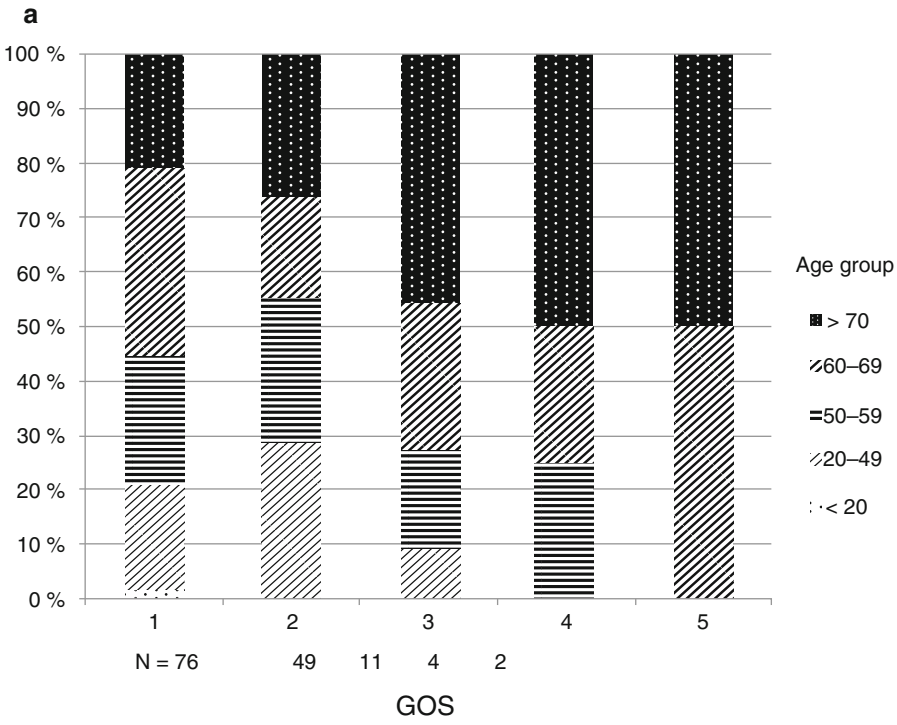

b

GOS	2	3	4	5
• Cranial Nerve Deficit	20	2	1	
• Rhinoliquorrhea	7		1	
• Epilpsy	5			
• Wound problems	4		1	
• Postop hemorrhage/infarction	3	5	3	
• Peripheral deficit Hemiparesis	4	3		
• Gait disturbances	2			
• Mental disturb.	2	1		
• Others				2

GOS: 1: normal – 5 dead

Fig. 15 (**a**) Quality of life in meningiomas postop (GOS) – age-related (note: GOS is read such as 1 means excellent and 5 means dead; only slight age relationship in 148 patients period 2008–2011). (**b**) Reasons for GOS >1 (in $N=148$), multiple reasons possible: cranial nerve deficit as major problem for patients to completely rehabilitate

his/her treating surgeon alike. This also certainly explains why the attitude toward radical meningioma removal even in the cavernous sinus suggested in the 1970s/early 1980s of the last century has been abandoned a few years later again. We have analyzed our own data concerning functional outcome as roughly measured using the Glasgow Outcome Score (GOS) with particular attention to postoperative cranial nerve deficits recently and have been disappointed about the number of longer-lasting nerve dysfunctions as given in Fig. 15. These data do not favorably compare with some published data. However, they depend to a large extent on the distribution of meningioma location: in a recent series of petroclival meningioma surgery, even 44 % new cranial nerve neuropathies were reported [108]; these figures may serve as a baseline for further improvement of surgical techniques in a teaching hospital.

Conclusion

Modern techniques have greatly improved the fate for meningioma patients, but many problems influencing long-term prognosis still need to be taken care of in the future. The full spectrum of ancillary diagnostic and therapeutic options from modern molecular biology to neuropsychology will help to further improve treatment strategies which should be guided by a technically well-trained and socially highly conscious academic neurosurgeon.

References

1. Abeloos L, Lefranc F (2011) What should be done in the event of incidental meningioma? Neurochirurgie 57(2):78–81
2. Ahmeti H, Maslehaty H, Petridis AK, Doukas A, Mahvash M, Barth H, Mehdorn HM (2013) Extensive growth of an anaplastic meningioma. Case Rep Neurol Med 2013:527184. doi:10.1155/2013/527184, Epub 2013 Oct 31
3. Alaywan M, Sindou M (1993) Prognostic factors in the surgery for intracranial meningioma. Role of the tumoral size and arterial vascularization originating from the pia mater. Study of 150 cases. Neurochirurgie 39(6):337–347
4. Al-Mefty O (1998) Operative atlas of meningiomas. Lippincott-Ravens, Philadelphia
5. Atalay A, Atalay B, Yemisci OU, Karatas M, Altinors N (2007) Intraoperative monitoring of a patient with craniovertebral junction meningioma. Turk Neurosurg 17(2):109–111
6. Barbaro NM, Gutin PH, Wilson CB, Sheline GE, Boldrey EB, Wara WM (1987) Radiation therapy in the treatment of partially resected meningiomas. Neurosurgery 20(4):525–528
7. Bassiouni H, Asgari S, Stolke D (2006) Tuberculum sellae meningiomas: functional outcome in a consecutive series treated microsurgically. Surg Neurol 66(1):37–44; discussion 44–35
8. Bassiouni H, Hunold A, Asgari S, Stolke D (2004) Meningiomas of the posterior petrous bone: functional outcome after microsurgery. J Neurosurg 100(6):1014–1024
9. Bassiouni H, Hunold A, Asgari S, Stolke D (2004) Tentorial meningiomas: clinical results in 81 patients treated microsurgically. Neurosurgery 55(1):108–116; discussion 116–118

10. Bekelis K, Valdes PA, Erkmen K, Leblond F, Kim A, Wilson BC, Harris BT, Paulsen KD, Roberts DW (2011) Quantitative and qualitative 5-aminolevulinic acid-induced protoporphyrin IX fluorescence in skull base meningiomas. Neurosurg Focus 30(5):E8
11. Bendszus M, Martin-Schrader I, Schlake HP, Solymosi L (2003) Embolisation of intracranial meningiomas without subsequent surgery. Neuroradiology 45(7):451–5
12. Bendszus M, Rao G, Burger R, Schaller C, Scheinemann K, Warmuth-Metz M, Hofmann E, Schramm J, Roosen K, Solymosi L (2000) Is there a benefit of preoperative meningioma embolization? Neurosurgery 47(6):1306–1311; discussion 1311–1312
13. Bendszus M, Warmuth-Metz M, Klein R, Bartsch AJ, Krone A, Tonn JC, Solymosi L (2002) Sequential MRI and MR spectroscopy in embolized meningiomas: correlation with surgical and histopathological findings. Neuroradiology 44(1):77–82
14. Benjamin V, Russell SM (2005) The microsurgical nuances of resecting tuberculum sellae meningiomas. Neurosurgery 56(2 Suppl):411–417; discussion 411–417
15. Beretta F, Andaluz N, Chalaala C, Bernucci C, Salud L, Zuccarello M (2010) Image-guided anatomical and morphometric study of supraorbital and transorbital minicraniotomies to the sellar and perisellar regions: comparison with standard techniques. J Neurosurg 113(5):975–981
16. Black P, Carroll R, Zhang J (1996) The molecular biology of hormone and growth factor receptors in meningiomas. Acta Neurochir Suppl 65:50–53
17. Bohuslavizki KH (2001) Somatostatin receptor imaging: current status and future perspectives. J Nucl Med 42(7):1057–1058
18. Bohuslavizki KH, Brenner W, Braunsdorf WE, Behnke A, Tinnemeyer S, Hugo HH, Jahn N, Wolf H, Sippel C, Clausen M, Mehdorn HM, Henze E (1996) Somatostatin receptor scintigraphy in the differential diagnosis of meningioma. Nucl Med Commun 17(4):302–310
19. Bosnjak R, Benedicic M (2008) Direct epidural electrical stimulation of the optic nerve: a new method for intraoperative assessment of function. J Neurosurg 109(4):647–653
20. Brusati R, Biglioli F, Mortini P, Raffaini M, Goisis M (2000) Reconstruction of the orbital walls in surgery of the skull base for benign neoplasms. Int J Oral Maxillofac Surg 29(5):325–330
21. Buhl R, Huang H, Gottwald B, Mihajlovic Z, Mehdorn HM (2005) Neuropsychological findings in patients with intraventricular tumors. Surg Neurol 64(6):500–503
22. Buhl R, Nabavi A, Wolff S, Hugo HH, Alfke K, Jansen O, Mehdorn HM (2007) MR spectroscopy in patients with intracranial meningiomas. Neurol Res 29(1):43–46
23. Bumpous J, Janecka IP (1995) Transorbital approaches to the cranial base. Clin Plast Surg 22(3):461–481
24. Campbell BA, Jhamb A, Maguire JA, Toyota B, Ma R (2009) Meningiomas in 2009: controversies and future challenges. Am J Clin Oncol 32(1):73–85
25. Chamberlain MC (2012) Hydroxyurea for recurrent surgery and radiation refractory high-grade meningioma. J Neurooncol 107(2):315–321
26. Chamberlain MC, Barnholtz-Sloan JS (2011) Medical treatment of recurrent meningiomas. Expert Rev Neurother 11(10):1425–1432
27. Chamoun R, Krisht KM, Couldwell WT (2011) Incidental meningiomas. Neurosurg Focus 31(6):E19
28. Chernov MF, Kasuya H, Nakaya K, Kato K, Ono Y, Yoshida S, Muragaki Y, Suzuki T, Iseki H, Kubo O, Hori T, Okada Y, Takakura K (2011) (1)H-MRS of intracranial meningiomas: what it can add to known clinical and MRI predictors of the histopathological and biological characteristics of the tumor? Clin Neurol Neurosurg 113(3):202–212
29. Coluccia D, Fandino J, Fujioka M, Cordovi S, Muroi C, Landolt H (2010) Intraoperative 5-aminolevulinic-acid-induced fluorescence in meningiomas. Acta Neurochir (Wien) 152(10):1711–1719
30. Condra KS, Buatti JM, Mendenhall WM, Friedman WA, Marcus RB Jr, Rhoton AL (1997) Benign meningiomas: primary treatment selection affects survival. Int J Radiat Oncol Biol Phys 39(2):427–436
31. Cushing H, Eisenhardt L (1938) Meningiomas: their classification, regional behaviour, life history and surgical end results. Charles C Thomas, Springfield

32. Dalrymple SJ, Jenkins RB (1994) Molecular genetics of astrocytomas and meningiomas. Curr Opin Neurol 7(6):477–483
33. Davis FG, Kupelian V, Freels S, McCarthy B, Surawicz T (2001) Prevalence estimates for primary brain tumors in the United States by behavior and major histology groups. Neuro Oncol 3(3):152–158
34. de Divitiis E, Esposito F, Cappabianca P, Cavallo LM, de Divitiis O, Esposito I (2008) Endoscopic transnasal resection of anterior cranial fossa meningiomas. Neurosurg Focus 25(6):E8. doi:10.3171/FOC.2008.25.12.E8
35. Deipolyi AR, Han SJ, Sughrue ME, Litt L, Parsa AT (2011) Awake far lateral craniotomy for resection of foramen magnum meningioma in a patient with tenuous motor and somatosensory evoked potentials. J Clin Neurosci 18(9):1254–6. doi:10.1016/j.jocn.2010.12.046, Epub 2011 Jul 7
36. Desse N, Malikov S, Fuentes S, Pech-Gourg G, Graillon T, Dufour H (2013) Superior sagittal sinus reconstruction using a femoral venous graft after total removal of a meningioma. Case report. Neurochirurgie 59(1):43–46
37. DiMeco F, Li KW, Casali C, Ciceri E, Giombini S, Filippini G, Broggi G, Solero CL (2004) Meningiomas invading the superior sagittal sinus: surgical experience in 108 cases. Neurosurgery 55(6):1263–1272; discussion 1272–1274
38. Donovan MG, Ondra SL, Illig JJ, Dickerson NC (1993) Combined transmandibular-zygomatic approach and infratemporal craniotomy for intracranial skull base tumors. J Oral Maxillofac Surg 51(7):754–758
39. Dorner L, Fritsch MJ, Stark AM, Mehdorn HM (2007) Posterior fossa tumors in children: how long does it take to establish the diagnosis? Childs Nerv Syst 23(8):887–890
40. Dowd CF, Halbach VV, Higashida RT (2003) Meningiomas: the role of preoperative angiography and embolization. Neurosurg Focus 15(1):E10
41. el-Azouzi M, Black PM (1989) The concept of suppressor genes in the molecular biology of central nervous system tumors. Neurochirurgie 35(4):201–208
42. Elhammady MS, Peterson EC, Johnson JN, Aziz-Sultan MA (2012) Preoperative onyx embolization of vascular head and neck tumors by direct puncture. World Neurosurg 77(5–6):725–730
43. Eufinger H, Wehmoller M, Machtens E, Heuser L, Harders A, Kruse D (1995) Reconstruction of craniofacial bone defects with individual alloplastic implants based on CAD/CAM-manipulated CT-data. J Craniomaxillofac Surg 23(3):175–181
44. Eufinger H, Wittkampf AR, Wehmoller M, Zonneveld FW (1998) Single-step fronto-orbital resection and reconstruction with individual resection template and corresponding titanium implant: a new method of computer-aided surgery. J Craniomaxillofac Surg 26(6): 373–378
45. Evans BT, Neil-Dwyer G, Lang D (1994) Reconstruction following extensive removal of meningioma from around the orbit. Br J Neurosurg 8(2):147–155
46. Firsching RP, Fischer A, Peters R, Thun F, Klug N (1990) Growth rate of incidental meningiomas. J Neurosurg 73(4):545–547
47. Fliss DM, Abergel A, Cavel O, Margalit N, Gil Z (2007) Combined subcranial approaches for excision of complex anterior skull base tumors. Arch Otolaryngol Head Neck Surg 133(9):888–896
48. Fronda C, Miller D, Kappus C, Bertalanffy H, Sure U (2008) The benefit of image guidance for the contralateral interhemispheric approach to the lateral ventricle. Clin Neurol Neurosurg 110(6):580–586
49. Gaoyu C, Hua F, Kaizhi L, Yanli G, Yi H (2008) Intraoperative fatal pulmonary embolism during resection of a parasagittal meningioma. Anaesth Intensive Care 36(5):753
50. Girvigian MR, Chen JC, Rahimian J, Miller MJ, Tome M (2008) Comparison of early complications for patients with convexity and parasagittal meningiomas treated with either stereotactic radiosurgery or fractionated stereotactic radiotherapy. Neurosurgery 62(5 Suppl):A19–A27; discussion A27–28
51. Giuffre R (1984) Successful radical removal of an intracranial meningioma in 1835 by Professor Pecchioli of Siena. J Neurosurg 60(1):47–51

52. Goebel S, Mehdorn HM (2011) Measurement of psychological distress in patients with intracranial tumours: the NCCN distress thermometer. J Neurooncol 104(1):357–364
53. Goebel S, Kaup L, Mehdorn HM (2011a) Measuring preoperative anxiety in patients with intracranial tumors: the Amsterdam preoperative anxiety and information scale. J Neurosurg Anesthesiol 23(4):297–303
54. Goebel S, Stark AM, Kaup L, von Harscher M, Mehdorn HM (2011b) Distress in patients with newly diagnosed brain tumours. Psychooncology 20(6):623–630
55. Goebel S, Strenge H, Mehdorn HM (2012) Acute stress in patients with brain cancer during primary care. Support Care Cancer 20(7):1425–1434
56. Goel A, Muzumdar DP, Nitta J (2001) Surgery on lesions involving cavernous sinus. J Clin Neurosci 8(Suppl 1):71–77
57. Grunberg SM (1994) Role of antiprogestational therapy for meningiomas. Hum Reprod 9(Suppl 1):202–207
58. Guclu B, Sindou M (2010) Reconstruction of vein of Labbe in temporo-occipital meningioma invading transverse sinus: technical report. Acta Neurochir (Wien) 152(6):941–945; discussion 945
59. Hahn BM, Schrell UM, Sauer R, Fahlbusch R, Ganslandt O, Grabenbauer GG (2005) Prolonged oral hydroxyurea and concurrent 3d-conformal radiation in patients with progressive or recurrent meningioma: results of a pilot study. J Neurooncol 74(2):157–165
60. Hart JL, Davagnanam I, Chandrashekar HS, Brew S (2011) Angiography and selective microcatheter embolization of a falcine meningioma supplied by the artery of Davidoff and Schechter. Case report. J Neurosurg 114(3):710–713
61. Hassfeld S, Zoller J, Albert FK, Wirtz CR, Knauth M, Muhling J (1998) Preoperative planning and intraoperative navigation in skull base surgery. J Craniomaxillofac Surg 26(4):220–225
62. Heufelder MJ, Sterker I, Trantakis C, Schneider JP, Meixensberger J, Hemprich A, Frerich B (2009) Reconstructive and ophthalmologic outcomes following resection of spheno-orbital meningiomas. Ophthal Plast Reconstr Surg 25(3):223–226
63. Hoover JM, Morris JM, Meyer FB (2011) Use of preoperative magnetic resonance imaging T1 and T2 sequences to determine intraoperative meningioma consistency. Surg Neurol Int 2:142
64. Horak P, Wohrer A, Hassler M, Hainfellner J, Preusser M, Marosi C (2012) Imatinib mesylate treatment of recurrent meningiomas in preselected patients: a retrospective analysis. J Neurooncol 109(2):323–330
65. Ichinose T, Goto T, Ishibashi K, Takami T, Ohata K (2010) The role of radical microsurgical resection in multimodal treatment for skull base meningioma. J Neurosurg 113(5):1072–1078
66. Ikeda D, Chiocca EA (2012) Editorial: dural tail sign. J Neurosurg 117(4):643–644
67. Ildan F, Tuna M, Gocer AP, Boyar B, Bagdatoglu H, Sen O, Haciyakupoglu S, Burgut HR (1999) Correlation of the relationships of brain-tumor interfaces, magnetic resonance imaging, and angiographic findings to predict cleavage of meningiomas. J Neurosurg 91(3):384–390
68. Jung SH, Ferrer AD, Vela JS, Granados FA (2011) Spheno-orbital meningioma resection and reconstruction: the role of piezosurgery and premolded titanium mesh. Craniomaxillofac Trauma Reconstr 4(4):193–200
69. Kajimoto Y, Kuroiwa T, Miyatake S, Ichioka T, Miyashita M, Tanaka H, Tsuji M (2007) Use of 5-aminolevulinic acid in fluorescence-guided resection of meningioma with high risk of recurrence. Case report. J Neurosurg 106(6):1070–1074
70. Kamitani H, Masuzawa H, Kanazawa I, Kubo T (2001) Recurrence of convexity meningiomas: tumor cells in the arachnoid membrane. Surg Neurol 56(4):228–235
71. Kashimura H, Inoue T, Ogasawara K, Arai H, Otawara Y, Kanbara Y, Ogawa A (2007) Prediction of meningioma consistency using fractional anisotropy value measured by magnetic resonance imaging. J Neurosurg 107(4):784–787

72. Kawase T, Shiobara R, Toya S (1994) Middle fossa transpetrosal-transtentorial approaches for petroclival meningiomas. Selective pyramid resection and radicality. Acta Neurochir (Wien) 129(3–4):113–120
73. Kim MS, Yu DW, Jung YJ, Kim SW, Chang CH, Kim OL (2012) Long-term follow-up result of hydroxyurea chemotherapy for recurrent meningiomas. J Korean Neurosurg Soc 52(6):517–522
74. Kimura T, Ohkubo M, Igarashi H, Kwee IL, Nakada T (2007) Increase in glutamate as a sensitive indicator of extracellular matrix integrity in peritumoral edema: a 3.0-tesla proton magnetic resonance spectroscopy study. J Neurosurg 106(4):609–613
75. Kinjo T, al-Mefty O, Kanaan I (1993) Grade zero removal of supratentorial convexity meningiomas. Neurosurgery 33(3):394–399; discussion 399
76. Klutmann S, Bohuslavizki KH, Tietje N, Kroger S, Behnke A, Brenner W, Mester J, Henze E, Clausen M (1999) Clinical value of 24-hour delayed imaging in somatostatin receptor scintigraphy for meningioma. J Nucl Med 40(8):1246–1251
77. Kombos T, Suess O, Kern BC, Funk T, Pietila T, Brock M (2000) Can continuous intraoperative facial electromyography predict facial nerve function following cerebellopontine angle surgery? Neurol Med Chir (Tokyo) 40(10):501–505; discussion 506–507
78. Kondziolka D, Flickinger JC, Perez B (1998) Judicious resection and/or radiosurgery for parasagittal meningiomas: outcomes from a multicenter review. Gamma Knife Meningioma Study Group. Neurosurgery 43(3):405–413; discussion 413–414
79. Kong DS, Kim HY, Kim SH, Min JY, Nam DH, Park K, Dhong HJ, Kim JH (2011) Challenging reconstructive techniques for skull base defect following endoscopic endonasal approaches. Acta Neurochir (Wien) 153(4):807–813. doi:10.1007/s00701-011-0941-5, Epub 2011 Jan 16
80. Konig SA, Spetzger U (2012) Surgical strategies for supra- and infratentorially grown occipital meningeomas. J Neurol Surg A Cent Eur Neurosurg 73(2):79–83
81. Kotipatruni RP, Ferraro DJ, Ren X, Vanderwaal RP, Thotala DK, Hallahan DE, Jaboin JJ (2012) NDRG4, the N-Myc downstream regulated gene, is important for cell survival, tumor invasion and angiogenesis in meningiomas. Integr Biol (Camb) 4(10):1185–1197
82. Lamszus K (2004) Meningioma pathology, genetics, and biology. J Neuropathol Exp Neurol 63(4):275–286
83. Lee JH (ed) (2009) Meningiomas: diagnosis, treatment, and outcome. Springer, London. ISBN 978-1-84628-784-8
84. Lee KJ, Joo WI, Rha HK, Park HK, Chough JK, Hong YK, Park CK (2008) Peritumoral brain edema in meningiomas: correlations between magnetic resonance imaging, angiography, and pathology. Surg Neurol 69(4):350–355; discussion 355
85. Lee JY, Barroeta JE, Newman JG, Chiu AG, Venneti S, Grady MS (2013) Endoscopic endonasal resection of anterior skull base meningiomas and mucosa: implications for resection, reconstruction, and recurrence. J Neurol Surg A Cent Eur Neurosurg 74(1):12–17
86. Li G, Hattermann K, Mentlein R, Mehdorn HM, Held-Feindt J (2013) The transmembrane chemokines CXCL16 and CX3CL1 and their receptors are expressed in human meningiomas. Oncol Rep 29(2):563–570
87. Linggood RM, Hsu DW, Efird JT, Pardo FS (1995) TGF alpha expression in meningioma – tumor progression and therapeutic response. J Neurooncol 26(1):45–51
88. Lou E, Sumrall AL, Turner S, Peters KB, Desjardins A, Vredenburgh JJ, McLendon RE, Herndon JE 2nd, McSherry F, Norfleet J, Friedman HS, Reardon DA (2012) Bevacizumab therapy for adults with recurrent/progressive meningioma: a retrospective series. J Neurooncol 109(1):63–70
89. Louis DN, Ohgaki H, Wiestler OD, Cavenee WK (eds) (2007) WHO classification of tumors of the central nervous system. IARC, Lyon
90. Louis DN, Ohgaki H, Wiestler OD, Cavenee WK, Burger PC, Jouvet A, Scheithauer B, Kleihues P (2007) The 2007 WHO classification of tumor of the central nervous system. Acta Neuropathol 114:97–109

91. Lusis E, Gutmann DH (2004) Meningioma: an update. Curr Opin Neurol 17(6):687–692
92. Ma HL, Yu CL, Chang CN (1995) Intraoperative somatosensory evoked potentials for localization in excision of recurrent parasagittal meningioma – a case report. Acta Anaesthesiol Sin 33(4):237–240
93. Malone JP, Levin RJ (2002) Second malignant tumors after treatment of nasopharyngeal carcinoma: four case reports and literature review. Skull Base 12(2):87–91
94. Mawrin C, Perry A (2010) Pathological classification and molecular genetics of meningiomas. J Neurooncol 99(3):379–391
95. McDonald JD, Dohrmann GJ (1988) Molecular biology of brain tumors. Neurosurgery 23(5):537–544
96. Meewes C, Bohuslavizki KH, Krisch B, Held-Feindt J, Henze E, Clausen M (2001) Molecular biologic and scintigraphic analyses of somatostatin receptor-negative meningiomas. J Nucl Med 42(9):1338–1345
97. Mehdorn HM, Buhl R, Riedel C (2008) MR spectroscopy in meningiomas. 6th international congress on meningiomas and cerebral venous system, Boston, 3–6 Sept 2008. www.TheMeningiomaConference2008.org
98. Mehdorn HM, Holtz R, Husemann M, Reinhardt V, Grote W (1984) Long-term follow-up after operations on intracranial meningeomas – the indications for operation in old age. Adv Neurosurg 12:164–171
99. Mehdorn HM, Kusatz B, Grote W (1989) Spontanverlauf bei Patienten mit nicht-operierten intra-kraniellen Meningeomen und Operationsindikation im Altersbezug. In: Fischer HC (Hsg) Verhdl Dt Ges f Neurologie 5. Springer, Berlin/Heidelberg/New York, pp 306–309
100. Mehdorn HM, Schrader B, Nabavi A, Hempelmann R (2000) Neuronavigation in the region of the skull base. Laryngorhinootologie 79(7):404–411
101. Minniti G, Clarke E, Cavallo L, Osti MF, Esposito V, Cantore G, Cappabianca P, Enrici RM (2011) Fractionated stereotactic conformal radiotherapy for large benign skull base meningiomas. Radiat Oncol 6:36
102. Mishra A (2011) Transorbital approach to infratemporal fossa: novel technique. J Laryngol Otol 125(6):638–642
103. Mohr C, Mehdorn HM, Heesen J, Schettler D (1990) Microsurgical flap anastomosis for defect coverage in the orbital roof – indications and alternatives. Fortschr Kiefer Gesichtschir 35:90–93
104. Murphy MC, Huston J 3rd, Glaser KJ, Manduca A, Meyer FB, Lanzino G, Morris JM, Felmlee JP, Ehman RL (2013) Preoperative assessment of meningioma stiffness using magnetic resonance elastography. J Neurosurg 118(3):643–648
105. Nakamura M, Roser F, Dormiani M, Samii M, Matthies C (2005) Intraoperative auditory brainstem responses in patients with cerebellopontine angle meningiomas involving the inner auditory canal: analysis of the predictive value of the responses. J Neurosurg 102(4):637–642
106. Nakamura M, Roser F, Michel J, Jacobs C, Samii M (2003) The natural history of incidental meningiomas. Neurosurgery 53(1):62–70; discussion 70–71
107. Nakasu S, Hirano A, Shimura T, Llena JF (1987) Incidental meningiomas in autopsy study. Surg Neurol 27(4):319–322
108. Nanda A, Javalkar V, Banerjee AD (2011) Petroclival meningiomas: study on outcomes, complications and recurrence rates. J Neurosurg 114(5):1268–1277
109. Nayak L, Iwamoto FM, Rudnick JD, Norden AD, Lee EQ, Drappatz J, Omuro A, Kaley TJ (2012) Atypical and anaplastic meningiomas treated with bevacizumab. J Neurooncol 109(1):187–193
110. Niiro M, Yatsushiro K, Nakamura K, Kawahara Y, Kuratsu J (2000) Natural history of elderly patients with asymptomatic meningiomas. J Neurol Neurosurg Psychiatry 68(1):25–28
111. Nishio S, Morioka T, Inamura T, Takeshita I, Fukui M, Sasaki M, Nakamura K, Wakisaka S (1998) Radiation-induced brain tumours: potential late complications of radiation therapy for brain tumours. Acta Neurochir (Wien) 140(8):763–770

112. Nishizaki T, Ikeda N, Nakano S, Okamura T, Abiko S (2009) Occipital interhemispheric approach for lateral ventricular trigone meningioma. Acta Neurochir (Wien) 151(12):1717–1721
113. Nundkumar N, Guthikonda M, Mittal S (2013) Peritumoral edema following Gamma Knife radiosurgery as the primary treatment for intraventricular meningiomas. J Clin Neurosci 20(4):616–618
114. Ogawa Y, Tominaga T (2012) Extended transsphenoidal approach for tuberculum sellae meningioma – what are the optimum and critical indications? Acta Neurochir (Wien) 154(4):621–626. doi:10.1007/s00701-011-1266-0, Epub 2012 Jan 10
115. Paleologos TS, Wadley JP, Kitchen ND, Thomas DG (2000) Clinical utility and cost-effectiveness of interactive image-guided craniotomy: clinical comparison between conventional and image-guided meningioma surgery. Neurosurgery 47(1):40–47; discussion 47–48
116. Pamir NM, Black PM, Fahlbusch R (2011) Meningiomas – a comprehensive text. Saunders Elsevier, Philadelphia. ISBN 978-1-4557-0878-9
117. Pamir MN, Kilic T, Bayrakli F, Peker S (2005) Changing treatment strategy of cavernous sinus meningiomas: experience of a single institution. Surg Neurol 64(Suppl 2):S58–S66
118. Petermann A, Haase D, Wetzel A, Balavenkatraman KK, Tenev T, Guhrs KH, Friedrich S, Nakamura M, Mawrin C, Bohmer FD (2011) Loss of the protein-tyrosine phosphatase DEP-1/PTPRJ drives meningioma cell motility. Brain Pathol 21(4):405–418
119. Preusser M, Spiegl-Kreinecker S, Lotsch D, Wohrer A, Schmook M, Dieckmann K, Saringer W, Marosi C, Berger W (2012) Trabectedin has promising antineoplastic activity in high-grade meningioma. Cancer 118(20):5038–5049
120. Petridis AK, Doukas A, Mahvash M, Dörner L, Hugo HH, Mehdorn HM (2009). A case of rapid-growing anaplastic meningiomas. BMJ Case Rep. pii: bcr05.2009.1862. doi:10.1136/bcr.05.2009.1862. Epub 2009 Aug 19
121. Pringle AM, Taylor R, Whittle IR (1999) Anxiety and depression in patients with an intracranial neoplasm before and after tumour surgery. Br J Neurosurg 13(1):46–51
122. Ragel BT, Jensen RL (2005) Molecular genetics of meningiomas. Neurosurg Focus 19(5):E9
123. Reardon DA, Norden AD, Desjardins A, Vredenburgh JJ, Herndon JE 2nd, Coan A, Sampson JH, Gururangan S, Peters KB, McLendon RE, Norfleet JA, Lipp ES, Drappatz J, Wen PY, Friedman HS (2012) Phase II study of Gleevec(R) plus hydroxyurea (HU) in adults with progressive or recurrent meningioma. J Neurooncol 106(2):409–415
124. Reinacher P, Reinges MH, Simon VA, Hans FJ, Krings T (2007) Dynamic 3-D contrast-enhanced angiography of cerebral tumours and vascular malformations. Eur Radiol 17(Suppl 6):F52–F62
125. Reinacher PC, Stracke P, Reinges MH, Hans FJ, Krings T (2007) Contrast-enhanced time-resolved 3-D MRA: applications in neurosurgery and interventional neuroradiology. Neuroradiology 49(Suppl 1):S3–S13
126. Reithmeier T, Krammer M, Gumprecht H, Gerstner W, Lumenta CB (2003) Neuronavigation combined with electrophysiological monitoring for surgery of lesions in eloquent brain areas in 42 cases: a retrospective comparison of the neurological outcome and the quality of resection with a control group with similar lesions. Minim Invasive Neurosurg 46(2):65–71
127. Romani R, Silvasti-Lundell M, Laakso A, Tuominen H, Hernesniemi J, Niemi T (2011) Slack brain in meningioma surgery through lateral supraorbital approach. Surg Neurol Int 2:167
128. Romstock J, Strauss C, Fahlbusch R (2000) Continuous electromyography monitoring of motor cranial nerves during cerebellopontine angle surgery. J Neurosurg 93(4):586–593
129. Rubin G, Herscovici Z, Laviv Y, Jackson S, Rappaport ZH (2011) Outcome of untreated meningiomas. Isr Med Assoc J 13(3):157–160
130. Runzi MW, Jaspers C, Windeck R, Benker G, Mehdorn HM, Reinhardt V, Reinwein D (1989) Successful treatment of meningioma with octreotide. Lancet 1(8646):1074
131. Runzi MW, Jaspers C, Windeck R, Benker G, Mehdorn M, Reinhardt V, Reinwein D (1989) Treatment of meningioma with octreotide. Lancet 2(8656):217–218

132. Salpietro FM, Alafaci C, Lucerna S, Iacopino DG, Todaro C, Tomasello F (1994) Peritumoral edema in meningiomas: microsurgical observations of different brain tumor interfaces related to computed tomography. Neurosurgery 35(4):638–641; discussion 641–642
133. Samii M, Ammirati M (1988) The combined supra-infratentorial pre-sigmoid sinus avenue to the petro-clival region. Surgical technique and clinical applications. Acta Neurochir (Wien) 95(1–2):6–12
134. Samii M, Ammirati M, Mahran A, Bini W, Sepehrnia A (1989) Surgery of petroclival meningiomas: report of 24 cases. Neurosurgery 24(1):12–17
135. Samii M, Gerganov V, Giordano M, Samii A (2010) Two step approach for surgical removal of petroclival meningiomas with large supratentorial extension. Neurosurg Rev 34(2):173–179
136. Samii M, Gerganov VM (2011) Petroclival meningiomas: quo vadis? World Neurosurg 75(3–4):424
137. Samii M, Tatagiba M (1992) Experience with 36 surgical cases of petroclival meningiomas. Acta Neurochir (Wien) 118(1–2):27–32
138. Samii M, Tatagiba M, Monteiro ML (1996) Meningiomas involving the parasellar region. Acta Neurochir Suppl 65:63–65
139. Sartor O, Figg WD (1996) Mifepristone: antineoplastic studies. Clin Obstet Gynecol 39(2):498–505
140. Scarpelli M, Mazzucchelli R, Colanzi P (1997) Meningioma: the impact of new techniques for the diagnosis and prognosis. Adv Clin Path 1(2):149–153
141. Schramm J, Mokrusch T, Fahlbusch R, Hochstetter A (1985) Intra- and perioperative acoustic evoked brain stem potentials in cerebellopontile angle operations. HNO 33(11):495–498
142. Schrell UM, Rittig MG, Anders M, Kiesewetter F, Marschalek R, Koch UH, Fahlbusch R (1997) Hydroxyurea for treatment of unresectable and recurrent meningiomas. I. Inhibition of primary human meningioma cells in culture and in meningioma transplants by induction of the apoptotic pathway. J Neurosurg 86(5):845–852
143. Schrell UM, Rittig MG, Anders M, Koch UH, Marschalek R, Kiesewetter F, Fahlbusch R (1997) Hydroxyurea for treatment of unresectable and recurrent meningiomas. II. Decrease in the size of meningiomas in patients treated with hydroxyurea. J Neurosurg 86(5):840–844
144. Schulder M, Salas S, Brimacombe M, Fine P, Catrambone J, Maniker AH, Carmel PW (2006) Cranial surgery with an expanded compact intraoperative magnetic resonance imager. Technical note. J Neurosurg 104(4):611–617
145. Scorsetti M, Alongi F, Clerici E, Navarria P, Simonelli M, Rognone E, Santoro A (2012) Temozolomide combined with radiotherapy in the treatment of recurrent cranial meningioma previously treated with multiple surgical resections and two sessions of radiosurgery: a case report and literature review. Tumori 98(3):67e–71e
146. Seifert V (2010) Clinical management of petroclival meningiomas and the eternal quest for preservation of quality of life: personal experiences over a period of 20 years. Acta Neurochir (Wien) 152(7):1099–1116
147. Seifert V, Raabe A, Zimmermann M (2003) Conservative (labyrinth-preserving) transpetrosal approach to the clivus and petroclival region – indications, complications, results and lessons learned. Acta Neurochir (Wien) 145(8):631–642; discussion 642
148. Sekhar LN, Chanda A, Morita A (2002) The preservation and reconstruction of cerebral veins and sinuses. J Clin Neurosci 9(4):391–399
149. Sherman WJ, Raizer JJ (2012) Chemotherapy: what is its role in meningioma? Expert Rev Neurother 12(10):1189–1195; quiz 1196
150. Shevach I, Cohen M, Rappaport ZH (1992) Patient positioning for the operative approach to midline intracerebral lesions: technical note. Neurosurgery 31(1):154–155
151. Shrivastava RK, Sen C, Costantino PD, Della Rocca R (2005) Sphenoorbital meningiomas: surgical limitations and lessons learned in their long-term management. J Neurosurg 103(3):491–497

152. Silva DO, Matis GK, Costa LF, Kitamura MA, Birbilis TA, Azevedo Filho HR (2011) Intraventricular trigonal meningioma: neuronavigation? No, thanks! Surg Neurol Int 2:113
153. Simpson D (1957) The recurrence of intracranial meningiomas after surgical treatment. J Neurol Neurosurg Psychiatry 20(1):22–39
154. Sindou M, Alaywan M (1994) Role of pia mater vascularization of the tumour in the surgical outcome of intracranial meningiomas. Acta Neurochir (Wien) 130(1–4):90–93
155. Sindou M, Auque J, Jouanneau E (2005) Neurosurgery and the intracranial venous system. Acta Neurochir Suppl 94:167–175
156. Sindou MP, Alaywan M (1998) Most intracranial meningiomas are not cleavable tumors: anatomic-surgical evidence and angiographic predictability. Neurosurgery 42(3):476–480
157. Sindou MP, Alvernia JE (2006) Results of attempted radical tumor removal and venous repair in 100 consecutive meningiomas involving the major dural sinuses. J Neurosurg 105(4):514–525
158. Sitthinamsuwan B, Khampalikit I, Nunta-aree S, Srirabheebhat P, Witthiwej T, Nitising A (2012) Predictors of meningioma consistency: a study in 243 consecutive cases. Acta Neurochir (Wien) 154(8):1383–1389
159. Skeie BS, Enger PO, Skeie GO, Thorsen F, Pedersen PH (2010) Gamma knife surgery of meningiomas involving the cavernous sinus: long-term follow-up of 100 patients. Neurosurgery 66(4):661–668; discussion 668–669
160. Smith DA, Cahill DW (1994) The biology of meningiomas. Neurosurg Clin N Am 5(2):201–215
161. Solheim O, Selbekk T, Lindseth F, Unsgard G (2009) Navigated resection of giant intracranial meningiomas based on intraoperative 3D ultrasound. Acta Neurochir (Wien) 151(9):1143–1151
162. Sonig A, Nanda A (2012) Transorbital approach to the anterior cranial skull base. World Neurosurg 80(6):810–812
163. Sotoudeh H, Yazdi HR (2010) A review on dural tail sign. World J Radiol 2(5):188–192
164. Spetzler RF, Sanai N (2012) The quiet revolution: retractorless surgery for complex vascular and skull base lesions. J Neurosurg 116(2):291–300
165. Stangl AP, Wellenreuther R, Lenartz D, Kraus JA, Menon AG, Schramm J, Wiestler OD, von Deimling A (1997) Clonality of multiple meningiomas. J Neurosurg 86(5):853–858
166. Strassner C, Buhl R, Mehdorn HM (2009) Recurrence of intracranial meningiomas: did better methods of diagnosis and surgical treatment change the outcome in the last 30 years? Neurol Res 31(5):478–482
167. Takeguchi T, Miki H, Shimizu T, Kikuchi K, Mochizuki T, Ohue S, Ohnishi T (2003) Prediction of tumor-brain adhesion in intracranial meningiomas by MR imaging and DSA. Magn Reson Med Sci 2(4):171–179
168. Taoka T, Yamada S, Sakamoto M, Akashi T, Miyasaka T, Ochi T, Wada T, Uchikoshi M, Nakase H, Kichikawa K (2012) Accuracy for predicting adhesion between meningioma and the brain by using brain surface motion imaging: comparison between single and double acquisition methods. Neuroradiology 54(12):1313–20. doi:10.1007/s00234-012-1054-4, Epub 2012 Jun 23
169. Wakhloo AK, Juengling FD, Van Velthoven V, Schumacher M, Hennig J, Schwechheimer K (1993) Extended preoperative polyvinyl alcohol microembolization of intracranial meningiomas: assessment of two embolization techniques. AJNR Am J Neuroradiol 14(3): 571–582
170. Wang CW, Li YY, Zhu SG, Yang Y, Wang HW, Gong J, Liu YG (2011) Surgical management and evaluation of prognostic factors influencing postoperative visual outcome of suprasellar meningiomas. World Neurosurg 75(2):294–302
171. Wang Q, Lu XJ, Ji WY, Yan ZC, Xu J, Ding YS, Zhang J (2010) Visual outcome after extended endoscopic endonasal transsphenoidal surgery for tuberculum sellae meningiomas. World Neurosurg 73(6):694–700

172. Werner R, Alfke K, Schaeffter T, Nabavi A, Mehdorn HM, Jansen O (2004) Brain perfusion territory imaging applying oblique-plane arterial spin labeling with a standard send/receive head coil. Magn Reson Med 52(6):1443–1447
173. Werner R, Norris DG, Alfke K, Mehdorn HM, Jansen O (2005) Continuous artery-selective spin labeling (CASSL). Magn Reson Med 53(5):1006–1012
174. Wolfsberger S, Doostkam S, Boecher-Schwarz HG, Roessler K, van Trotsenburg M, Hainfellner JA, Knosp E (2004) Progesterone-receptor index in meningiomas: correlation with clinico-pathological parameters and review of the literature. Neurosurg Rev 27(4):238–245
175. Yamaguchi N, Kawase T, Sagoh M, Ohira T, Shiga H, Toya S (1997) Prediction of consistency of meningiomas with preoperative magnetic resonance imaging. Surg Neurol 48(6):579–83
176. Yasargil MG (1984–1998) Microneurosurgery, vols I–IV. Thieme, Stutgart
177. Yoneoka Y, Fujii Y, Takahashi H, Nakada T (2002) Pre-operative histopathological evaluation of meningiomas by 3 0T T2R MRI. Acta Neurochir (Wien) 144(10):953–957; discussion 957
178. Yu SC, Boet R, Wong GK, Lam WW, Poon WS (2004) Postembolization hemorrhage of a large and necrotic meningioma. AJNR Am J Neuroradiol 25(3):506–508
179. Zada G, Pagnini PG, Yu C, Erickson KT, Hirschbein J, Zelman V, Apuzzo ML (2010) Long-term outcomes and patterns of tumor progression after gamma knife radiosurgery for benign meningiomas. Neurosurgery 67(2):322–328; discussion 328–329
180. Zentner J, Meyer B, Vieweg U, Herberhold C, Schramm J (1997) Petroclival meningiomas: is radical resection always the best option? J Neurol Neurosurg Psychiatry 62(4):341–345

Arteries and Veins of the Sylvian Fissure and Insula: Microsurgical Anatomy

Matthieu Delion, Philippe Mercier, and Gilles Brassier

Contents

M. Delion (✉) • P. Mercier
Department of Neurosurgery, Angers Teaching Hospital, Angers 49933, France

Anatomy Laboratory, Medical Faculty, rue haute de Reculée, Angers 49045, France
e-mail: matthieudelion@yahoo.com

G. Brassier
Department of Neurosurgery, Rennes Teaching Hospital, Rennes 35033, France

J. Schramm (ed.), *Advances and Technical Standards in Neurosurgery*,
Advances and Technical Standards in Neurosurgery, Vol. 43,
DOI 10.1007/978-3-319-21359-0_7

Abstract We present a vascular anatomical study of the arteries and veins of the sylvian fissure and insula.

A good knowledge of the sylvian fissure, the insula, and their vascular relationship would seem mandatory before performing surgery in this area, whatever the type of surgery (aneurysms, arteriovenous malformations, insular tumors).

We start with the sylvian fissure and insula morphology, followed by the MCA description and its perforators, with special attention paid to the insular perforators. We demonstrate that the long insular perforators penetrating in the superior part of the posterior short gyrus and long gyri vascularize, respectively, the corticonuclear and corticospinal fasciculi. We particularly insist too on three anatomical constants regarding the vascularization of the insula, already described in the literature: The superior periinsular sulcus is the only sulcus on the lateral surface of the brain without an artery along its axis; the superior branch of the MCA supplies the anterior insular pole and both the anterior and middle short gyri in 100 % of cases; in at least 90 % of cases, the artery that supplied the central insular sulcus continued on to become the central artery.

We end with the anatomical study of the veins and cisterns.

Keywords Sylvian fissure • Insula • MCA • Perforators • Insular perforators • Insular vein • Cisterns

Introduction

Surgery of the insula represents a technical challenge because of the great vascular density (arteries and veins) and because of the proximity of the internal capsule.

A good knowledge of the sylvian fissure, the insula, and their vascular relationship would seem mandatory before performing surgery in this area, whatever the type of surgery (aneurysms, arteriovenous malformations, insular tumors).

We start with the sylvian fissure and insula morphology, followed by the MCA description and its perforators, with special attention paid to the long insular perforators, and end with the veins and cisterns.

Materials and Methods

Twenty-five formalin-fixed human heads were perfused (arteries (20) and arteries and veins (5) with colored latex). The brain was removed some days later, and the sylvian fissure and insula were examined using a Wild Leitz surgical microscope with a D80 Nikon photographic attachment set. The sylvian fissure was opened wide using microsurgical methods, and the arachnoid membranes and cisterns

identified. Then we examined the MCA main trunk, the MCA bifurcation, and the perforators; the insula supply was studied, using the removal of some operculae, and particularly the perforators arising from M2. The insular venous pattern of drainage and its connection to the superficial sylvian vein or the deep sylvian vein were identified. Additional fixed, but non-injected, brains were used for cortex study.

Description

The Sylvian Fissure [25, 27, 31] (Figs. 1, 2, and 3)

The sylvian fissure is the most distinct landmark on the lateral surface of the cerebrum; it separates the frontal and parietal lobes from the temporal lobe and extends from the anterior perforated substance to the supramarginal gyrus; the insula forms its floor. The sylvian fissure provides passage to the MCA and its branches and is a surgical gateway connecting the cerebral surface to the anterior part of the basal surface of the brain and skull base.

The sylvian fissure is divided into anterior (stem) and posterior (insulo-opercular compartments). The stem originates inferiorly at the anterior perforated substance located at the level of the ambiens gyrus of uncus and extends laterally between the orbital gyri and the temporal pole (Fig. 2). The temporal incisura and the fronto-orbital limb are two side branches of the sylvian stem. As the stem reaches the lateral surface of the brain, it divides into the horizontal, ascending, and posterior rami, and the confluence of which is named: the sylvian point.

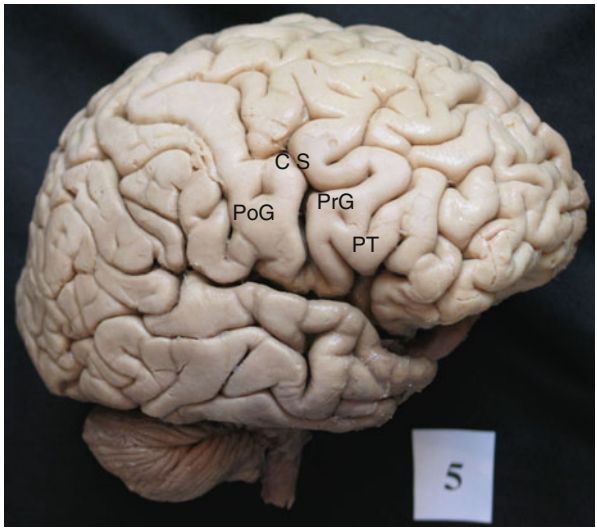

Fig. 1 Right lateral view of a cadaveric brain. The natural upward retraction of the apex of the pars triangularis creates the largest natural opening in the sylvian fissure. *PT* pars triangularis, *PrG* precentral gyrus, *PoG* postcentral gyrus, *CS* central sulcus

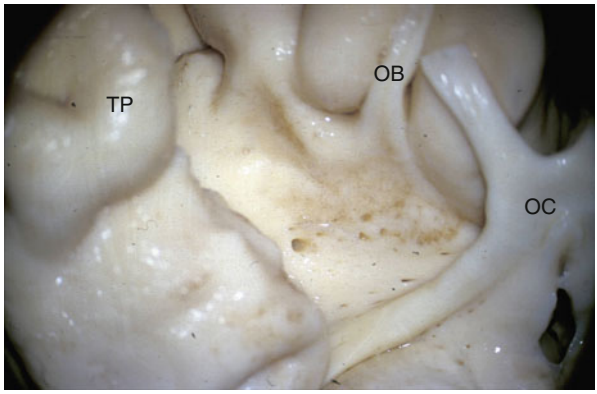

Fig. 2 Right inferior cerebral view of the APS (anterior perforated substance). *TP* temporal pole, *OB* olfactory bulb, *OC* optic chiasm. The APS is classically defined anteriorly by the olfactive bulb division, medially and posteriorly by the chiasm and the optic tract, and medially by the temporal pole

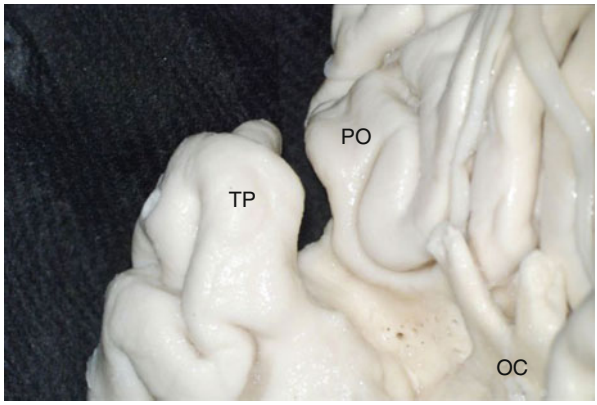

Fig. 3 Right inferior cerebral view of the limen insulae. *TP* temporal pole, *PO* pars orbitalis, *OC* optic chiasm

The horizontal and ascending rami divide the inferior frontal gyrus into pars orbitalis, triangularis, and opercularis. The posterior ramus separates the frontal and parietal lobes from the temporal lobe and forms the sylvian line. The posterior ramus is composed of the diagonal sulcus, the anterior and posterior subcentral sulci, and the terminal ascending and descending limbs, as well as the side branch of the transverse temporal sulcus. The horseshoe-shaped supramarginal gyrus drapes over the superior boundary of the posterior ramus. The floor of the sylvian stem constitutes the preinsular sulcus (sylvian vallecula) which corresponds to the anterior perforated substance (APS). The floor of the posterior ramus of the sylvian fissure is composed of the insula and post-insular sulcus.

Insula *[1, 19, 27, 33, 35] (Figs. 4, 5, and 6)*

The insula lies within the depths of the sylvian fissure, covered by the frontal, parietal, and temporal opercula and overlying the deep basal nuclei (claustrum and putamen of the lentiform nucleus); it has a trapezoid shape and is separated from the

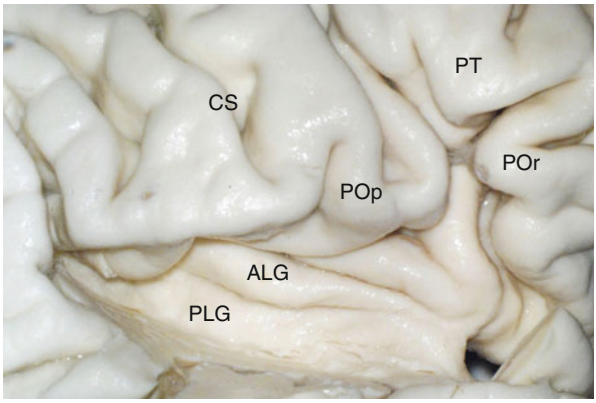

Fig. 4 Right lateral view of the insula after temporal operculae removal. *PT* pars triangularis, *POr* pars orbitalis, *POp* pars opercularis, *ALG* anterior long gyrus, *PLG* posterior long gyrus, *CS* central sulcus

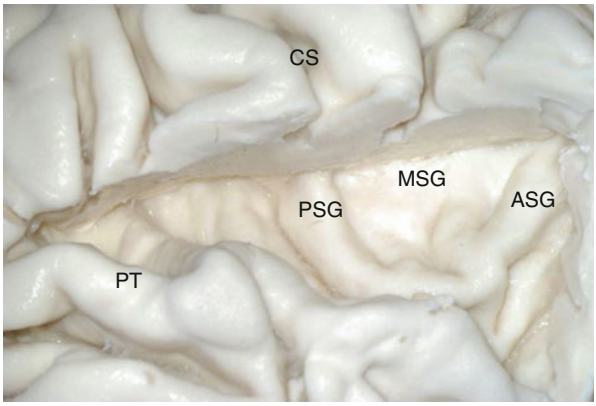

Fig. 5 Right lateral view of the insula after frontal and parietal operculae removal. *CS* central sulcus, *PT* planum temporale, *ASG* anterior short gyrus, *MSG* middle short gyrus, *PSG* posterior short gyrus. The middle short gyrus is here underdeveloped and slightly convex

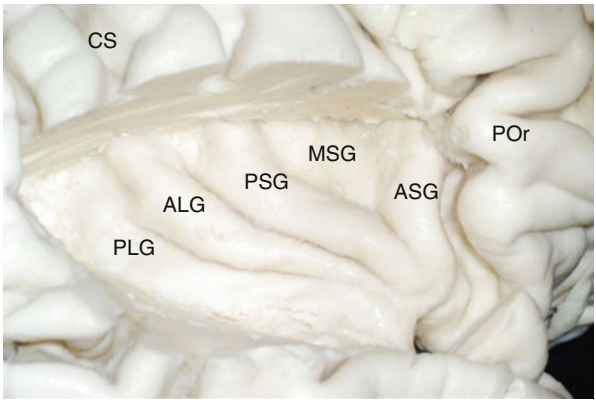

Fig. 6 Right lateral view of the insula after frontal, parietal, and temporal operculae removal. *CS* central sulcus, *POr* pars orbitalis, *ASG* anterior short gyrus, *MSG* middle short gyrus, *PSG* posterior short gyrus, *ALG* anterior long gyrus, *PLG* posterior long gyrus

opercula by the anterior, superior, and inferior periinsular sulci, which are located, respectively, beneath the fronto-orbital, frontoparietal, and temporal operculae. The limen insulae is the entranceway into the insula and forms the lateral limit of the sylvian vallecula.

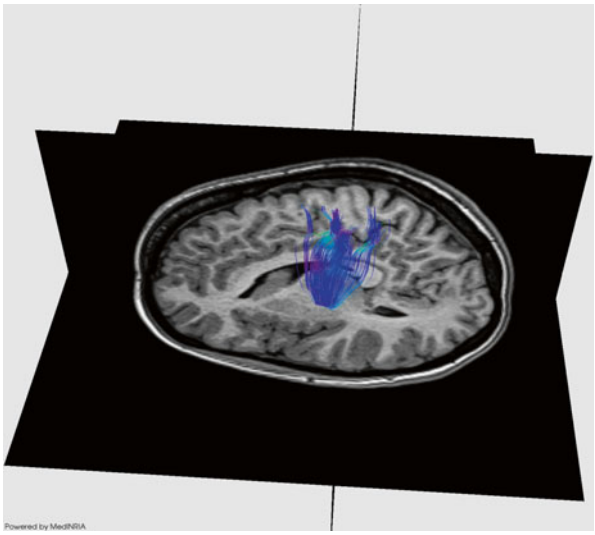

Fig. 7 Left lateral view of the brain by MR imaging with DTI tractography of the corticospinal tract. Medinria software. We can see the corticospinal tract running through the posterior limb of the internal capsule, which is projected over the long gyri of the insula

The central insular sulcus traverses the insula from the superior periinsular sulcus to the limen insulae and divides it into anterior and posterior portions:

- The anterior insula is composed of the transverse and accessory insular gyri and three principal short gyri (anterior, middle, and posterior). The transverse and accessory insular gyri form the insular pole which is located at the most anteroinferior aspect of the insula. The transverse gyrus acts as a junction between the inferior portion of the anterior insula and the posterior fronto-orbital region; the accessory insular gyrus extends from the anterior portion of the anterior short gyrus and is located beneath the fronto-orbital operculum on the superior aspect of the transverse insular gyrus. The anterior, middle, and post short insular gyri fuse to form the insular apex. In 50 % of cases, the precentral gyrus separating the middle and posterior short gyri is merely a shallow depression, and the middle short gyrus is underdeveloped and slightly convex (Fig. 6).
- The posterior insula consists of the anterior and posterior long insular gyri which are separated by the postcentral insular sulcus.
- In 60 % of cases, the superior extremity of the central insular sulcus is in direct continuity with the inferior extremity of the cerebral central sulcus.

The operculum of the precentral gyrus covers the middle third and the anterior portion of the posterior third of the insula. The corticonuclear fibers at the level of the genu of the internal capsule project over the middle third of the insula which responds to the posterior short gyrus, and the posterior limb of the internal capsule with the corticospinal fibers is projected over the long anterior and posterior gyri (Figs. 7 and 8).

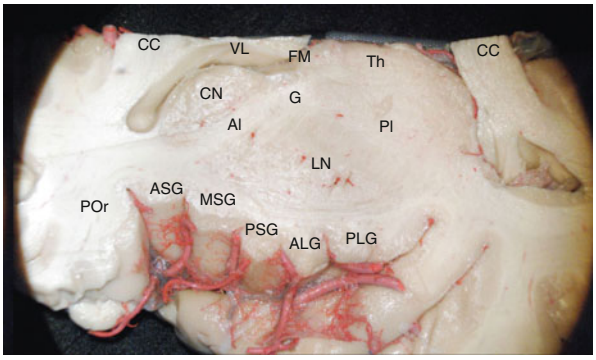

Fig. 8 Superolateral view of a left insula; the frontoparietal operculae have been removed using a transverse cut along the superior limiting sulcus to show the relationships between the insula and the deeper structures. The foramen of Monro is located deep to the middle portion of the middle short gyrus, and the lentiform nucleus extends from the midportion of the middle short gyrus to the middle part of the posterior long gyrus; the knee of the internal capsule and also the corticonuclear tract are projected over the middle third of the insula which responds to the posterior short gyrus. The posterior limb of the internal capsule is projected over the long gyri of the insula. *POr* pars orbitalis, *ASG* anterior short gyrus, *MSG* medial short gyrus, *PSG* posterior short gyrus, *ALG* anterior long gyrus, *PLG* posterior long gyrus, *CN* caudate nucleus, *CC* corpus callosum, *LN* lentiform nucleus, *Th* thalamus, *AL* anterior limb, *G* genu, *PL* posterior limb, *LV* lateral ventricle, *FM* foramen of Monro

Arteries

MCA [7, 12, 13, 24, 26, 35] (Figs. 9, 10, 11, and 12)

The MCA, the youngest and surely the most variable of all cerebral vessels, can be divided into four segments. The M1 (sphenoidal) extends from the ICA bifurcation to the main MCA division which is located adjacent to the limen insulae. The M2 (insular segments) extends from the MCA division to the periinsular sulci and the M3 segments (opercular) from the periinsular sulci to the surface of the brain along the sylvian fissure. The M4 (cortical) segments located on the parasylvian surface of the brain are extended over the cortical surface of the cerebral hemisphere.

The MCA originates at the division of the internal carotid artery lateral to the optic chiasm and courses laterally under the anterior perforated space to reach the end of the sylvian fissure. At this point, the artery turns, crosses over the limen insulae, and enters the insular area at the level of the insular apex where it forms a genu. The main division of the MCA is usually found before, or at the level of, the limen. The secondary trunks resulting from the division (frontal and temporal branches) will course over the surface of the insular cortex giving rise to the cortical branches.

The main trunk of the M1 ends in a bifurcation in 78 % of the specimens, a trifurcation in 12 %, and a quadrifurcation (or multiple branches arising from a single

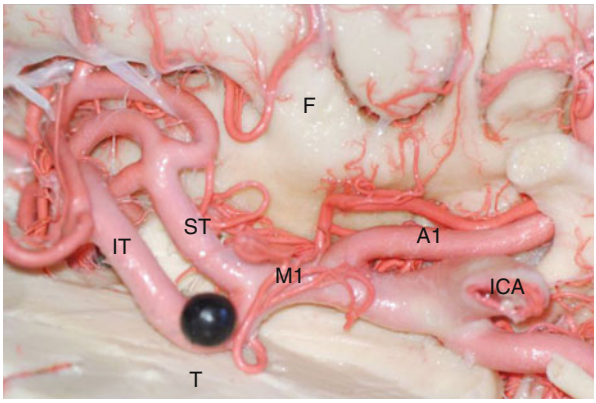

Fig. 9 Right inferior view after removal of the temporal pole; there is a very short M1 dividing at the sylvian fissure entrance in superior and inferior trunks. *OC* optic chiasm, *A1* first part of the anterior cerebral artery, *M1* first part of the middle cerebral artery, *ICA* internal cerebral artery, *F* frontal lobe, *T* temporal lobe, *ST* superior trunk, *IT* inferior trunk

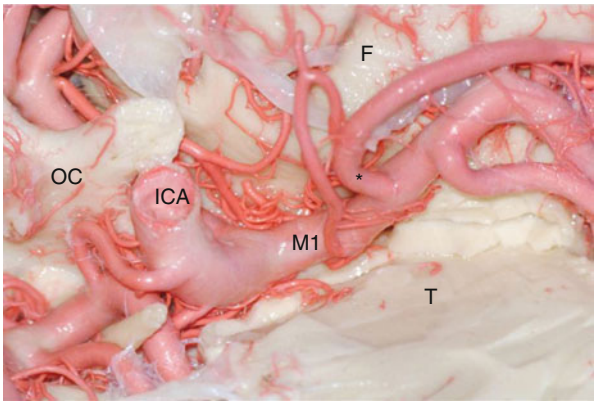

Fig. 10 Left inferior view after removal of the temporal pole; there is a false bifurcation with a strong frontal branch (*) mimicking the main division. *Abbreviations*: see caption 9

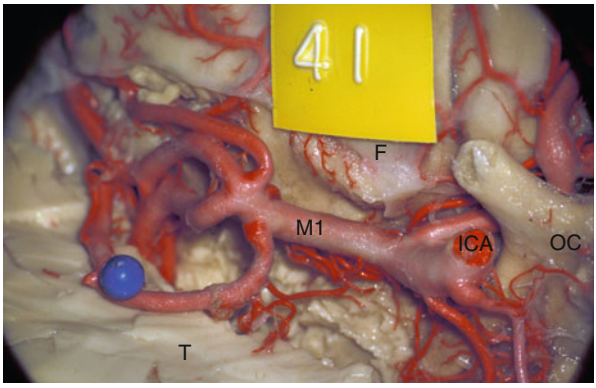

Fig. 11 Right inferior view after removal of the temporal pole; there is an MCA quadrifurcation (less than 10 % of cases). *Abbreviations*: see caption 9

trunk [29]) in 10 % (fig). In about 10 %, there is a strong frontal or temporal branch mimicking the main division and named [34] a false bifurcation (Fig), and in 80 %, small cortical arteries can arise from the main trunk before the main division [26]. In 20 % of cases, we found one uncal artery supplying the piriform cortex with, in some cases, an additional supply coming from the ICA or the anterior choroidal artery.

M1 Perforators [7, 9, 14, 15, 28, 32] (Figs. 13, 14, 15, 16, 17, and 18)

Based on their morphological and topographical features, the perforating arteries are classically divided into three groups: medial, middle, and lateral.

The medial group, the most numerous, arose from the MCA just distal to the carotid bifurcation and the origin of the anterior choroidal artery; they have to be differentiated from the two perforators arising from the ICA bifurcation. Concerning their territory, they are in balance with the recurrent artery of Heubner [12, 16, 20].

The middle group arose from the mid-third of M1 directly from the main MCA's main trunk or from a cortical branch, separately, or from a common stem.

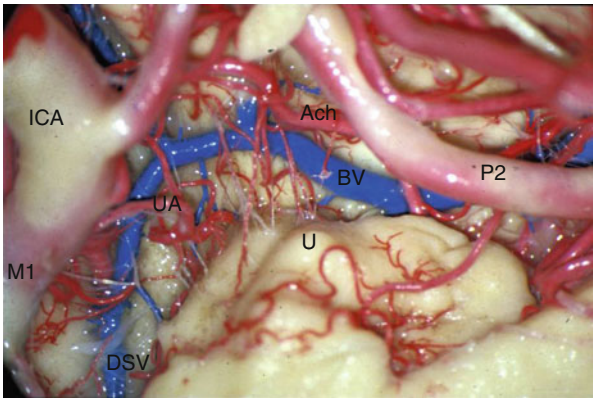

Fig. 12 Right inferior view (the frontal lobe is on the left, and the brainstem is up): There is an uncal artery supplying the uncus and the piriform cortex. *DSV* deep sylvian vein, *U* uncus, *BV* basal vein, *Ach* anterior choroidal artery. *M1* first part of the middle cerebral artery, *ICA* internal cerebral artery, *P2* second segment of the posterior cerebral artery, *UA* uncal artery

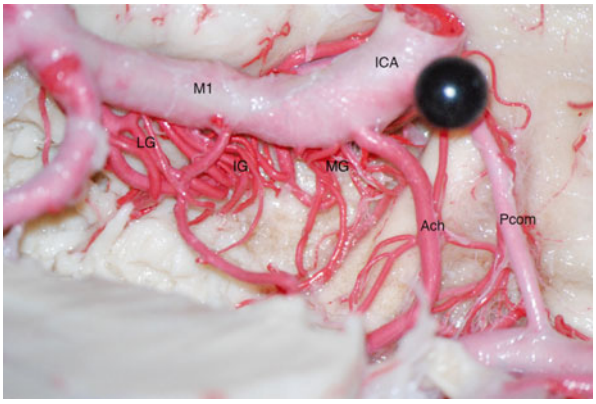

Fig. 13 Right inferior view after temporal pole removal; there are three groups of perforators merging from M1. *M1* first part of the middle cerebral artery, *Pcom* posterior communicating artery, *LS* lenticulostriate arteries, *MG* medial group of LS, *IG* intermediate group of LS, *LG* lateral group of LS, *H* Heubner artery, *OC* optic chiasm, *Acha* anterior choroidal artery, *ICA* internal carotid artery

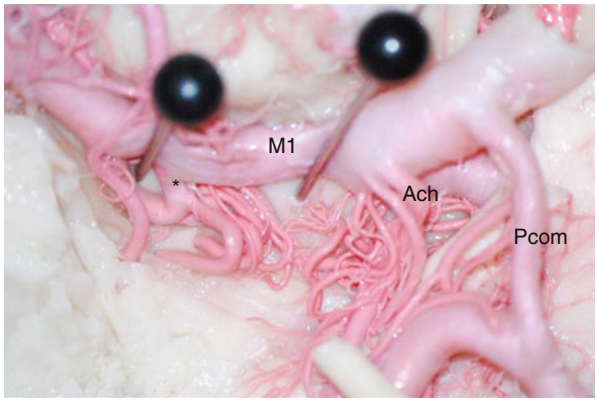

Fig. 14 Right inferior view after temporal pole removal; the medial group of perforators is missing; the lateral group (lenticulostriate arteries) is arising from a common trunk (*). *M1* first part of the middle cerebral artery; *Pcom* posterior communicant artery; *Ach* anterior choroidal artery

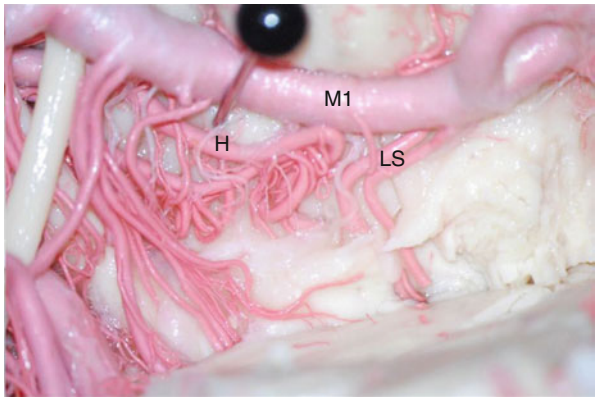

Fig. 15 Left inferior view after temporal pole removal; the medial and middle groups of perforators are missing and replaced by the Heubner. *Abbreviations*: see caption 13

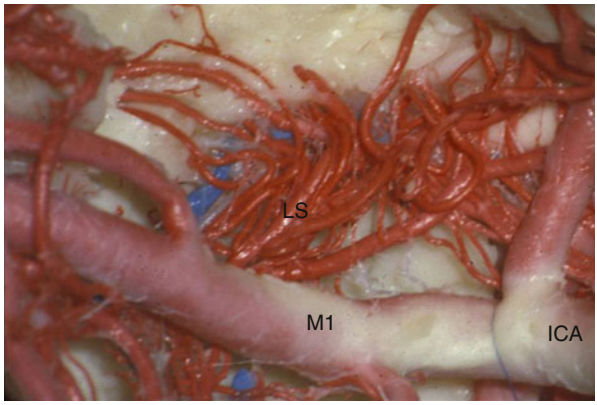

Fig. 16 Right inferior view after temporal pole removal; the medial group of perforators is missing; the lateral group (lenticulostriate arteries) is arising separately from M1. *Abbreviations*: see caption 13

The lateral group, also named the lenticulostriate arteries, is well developed with a larger diameter. They have a classical “S” shape and can arise separately or from a common trunk or a cortical branch; if they arise from the MCA, they arise classically from its dorsal aspect, but it’s not uncommon to find a rostral, caudal, or

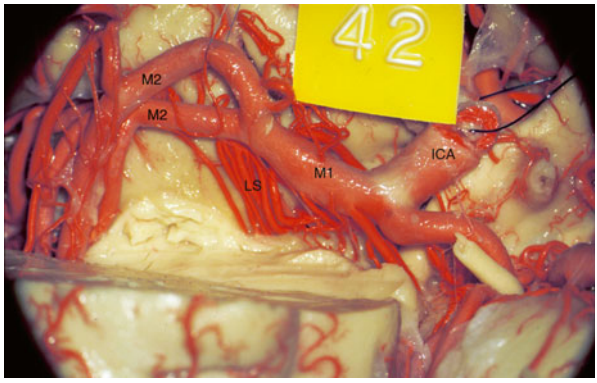

Fig. 17 Right inferior view after temporal pole removal; the lateral group (lenticulostriate arteries) is arising from M2. *M1* first part of the middle cerebral artery, *M2* second segment of middle cerebral artery, *LS* lenticulostriate arteries, *ICA* internal carotid artery

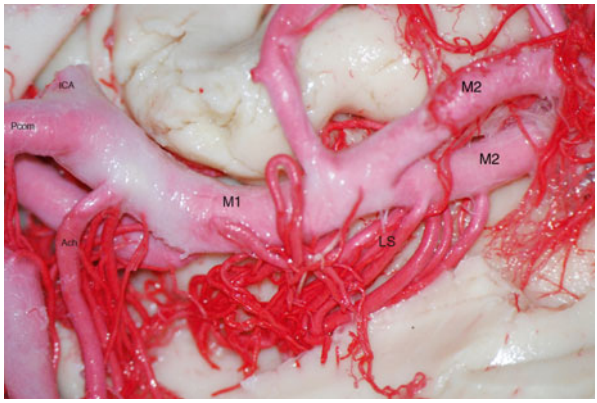

Fig. 18 Left inferior view after temporal pole removal; the lateral group (lenticulostriate arteries) is arising from M2. *ICA* internal carotid artery, *M1* first part of the middle cerebral artery, *LS* lenticulostriate arteries, *Pcom* posterior communicant artery, *M2* second segment of the middle cerebral artery, *Ach* anterior choroidal artery

ventral origin. The most important point is their origin from M2 in 14–30 % of cases. They supply the caudate nucleus, the putamen, the globus pallidus, the internal capsule, and the corona radiata [3].

M2 Branches (Fig. 19)

The cortical distribution supplied by the MCA included the majority of the lateral surface of the hemisphere, all of the insular and opercular surface, the lateral part of the orbital surface of the frontal lobe, the temporal lobe, and the lateral part of the inferior surface of the temporal lobe.

The fronto-orbital, prefrontal, precentral, and central arteries usually arose from the superior trunk. The temporopolar, temporo-occipital, angular and anterior, middle, and posterior temporal arteries usually arose from the inferior trunk. The anterior and posterior parietal arteries usually arose from the main trunk.

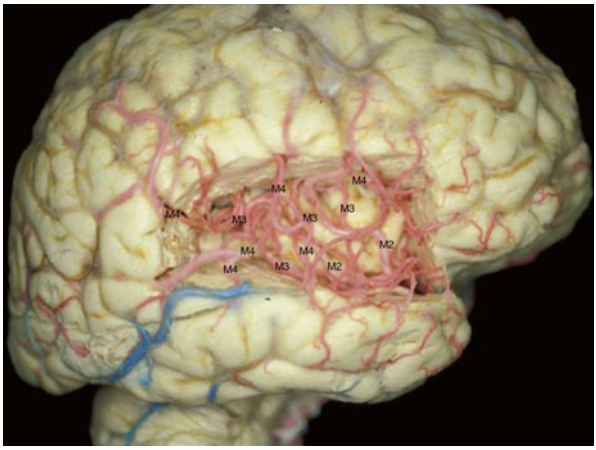

Fig. 19 Lateral right hemisphere view after frontal, parietal, and temporal operculae removal showing the M2, M3, and M4 MCA parts, *M2* second segment of the middle cerebral artery, *M3* third segment of the middle cerebral artery, *M4* fourth segment of the middle cerebral artery

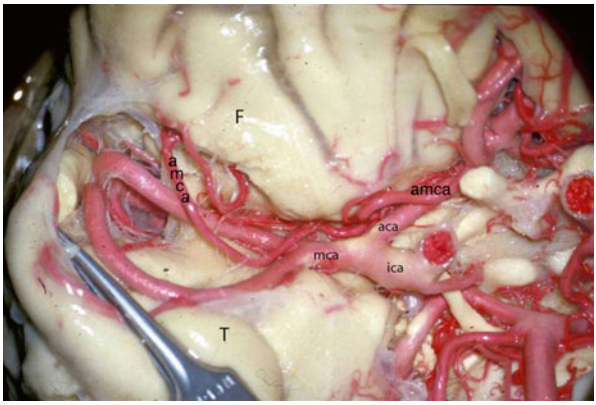

Fig. 20 Right inferior view of the right sylvian sulcus showing a small accessory middle cerebral artery (amca). *F* frontal lobe, *T* temporal lobe, *ica* internal carotid artery, *aca* anterior cerebral artery, *mca* middle cerebral artery

Accessory Middle Cerebral Artery [12, 29] (Figs. 20 and 21)

An accessory MCA was found in two hemispheres; in both specimens, the origin was the ACA at the level of the A1-A2-AcoA junction (A1 first segment of the anterior cerebral artery, A2 second segment of the anterior cerebral artery, AcoA communicant artery), and the course was parallel to that of MCA. The cortical distribution was in the territory of the fronto-orbital and precentral artery in one specimen and in the territory of the fronto-orbital, precentral, and central artery in the other. Both accessory arteries supplied perforating branches entering the APS, including the recurrent artery of Heubner; in the second case, there was a second Heubner arising from the proximal A2 segment of the ACA.

Insular Supply (Figs. 22, 23, 24, 25, 26, 27, and 28)

The MCA, the largest, youngest, and most complex of the cerebral arteries, provides the sole supply to the insula but predominantly from M2.

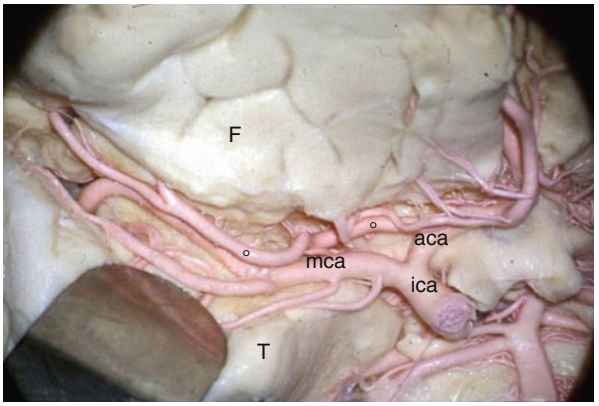

Fig. 21 Right inferior view of the right sylvian sulcus showing a huge, large accessory middle cerebral artery (°). *F* frontal lobe, *T* temporal lobe, *ica* internal carotid artery, *aca* anterior cerebral artery, *mc*a middle cerebral artery

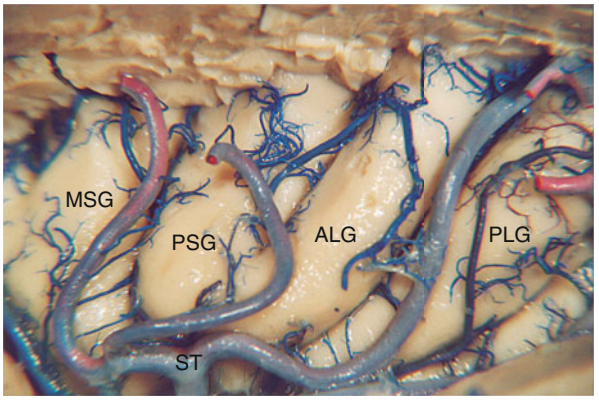

Fig. 22 Lateral view of a left insula (injection with blue Indian ink). The superior trunk supplies the anterior part of the insula and gives off perforators. *MSG* medial short gyrus, *PSG* posterior short gyrus, *ALG* anterior long gyrus, *PLG* posterior long gyrus, *ST* superior trunk. The artery that supplies the central insular sulcus continues on to become the central artery

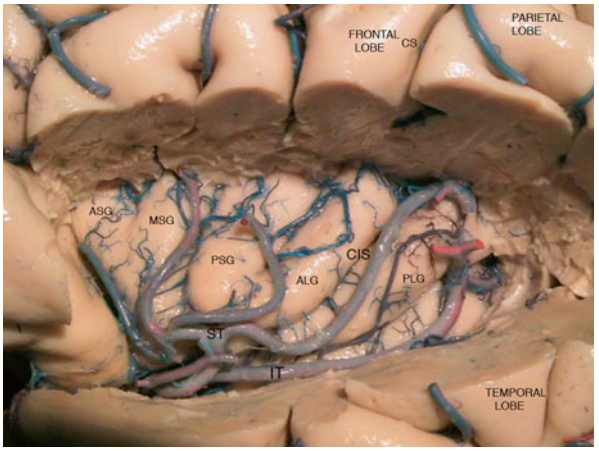

Fig. 23 Lateral view of a left insula (injection with blue Indian ink) after frontal, parietal, and temporal operculae removal. *ASG* anterior short gyrus, *MSG* medial short gyrus, *PSG* posterior short gyrus, *ALG* anterior long gyrus, *PLG* posterior long gyrus, *ST* superior trunk, *IT* inferior trunk, *CS* central sulcus, *CIS* central insular sulcus. The artery that supplies the central insular sulcus continues on to become the central artery

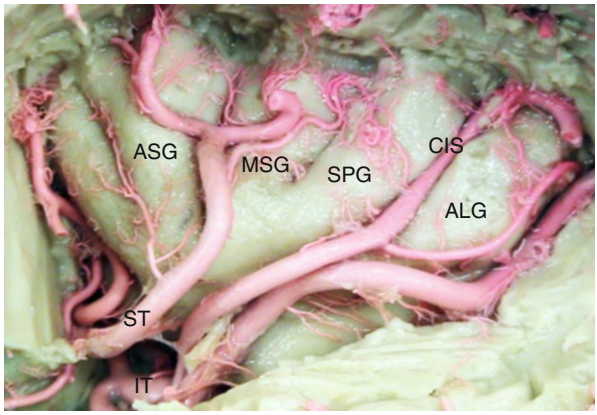

Fig. 24 Lateral view of a left insula (injection with red latex) after frontal, parietal, temporal and operculae removal. *Abbreviations*: see caption 23

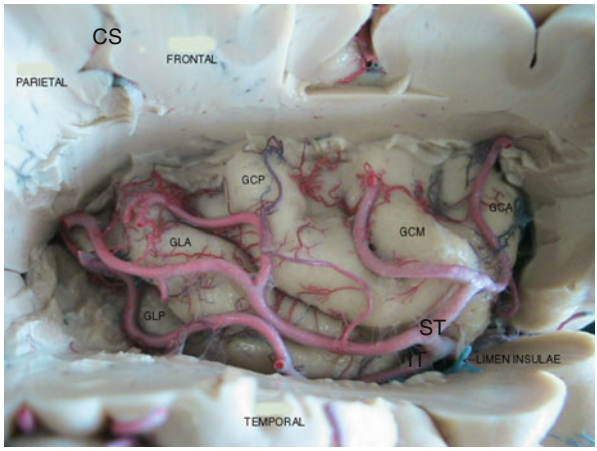

Fig. 25 Lateral view of a right insula (injection with red latex) after frontal, parietal, and temporal operculae removal. *LI* limen insulae. *GLA* anterior long gyrus, *GCP* anterior short gyrus, *GLP* posterior long gyrus, *GCM* middle short gyrus, *GCA* anterior short gyrus. *Other abbreviations*: see caption 23

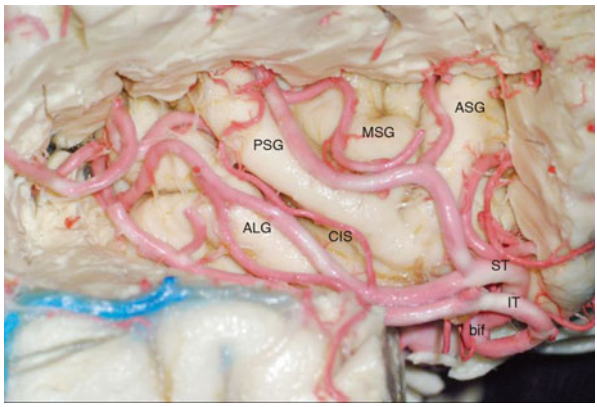

Fig. 26 Lateral view of a right insula (injection with red latex) after frontal, parietal, and temporal operculae and temporal pole removal. *bif* MCA bifurcation. *Other abbreviations*: see caption 23

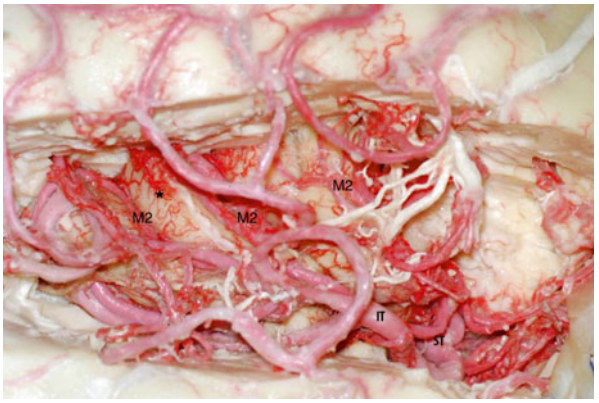

Fig. 27 Lateral view of a right insula; the pial plan of the insular cortex has been respected illustrating the short insular arteries arising from M2 and creating a pial network on the insula cortex. These arteries vascularize only the insular cortex and don't penetrate in the subcortical white matter. *ST* superior trunk, *IT* inferior trunk, *M2* segment M2 of the MCA, *pial network

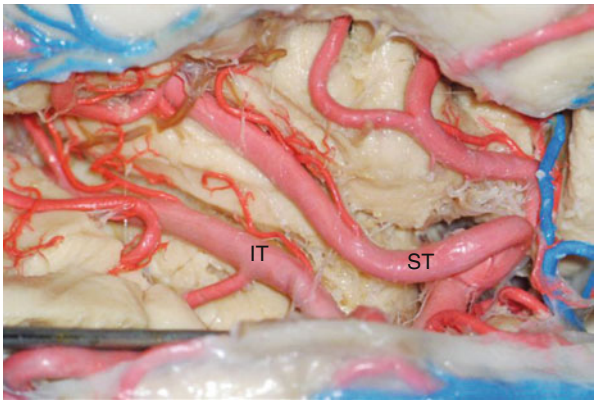

Fig. 28 Lateral view of a right insula showing the insular arteries arising from M2. *ST* superior trunk, *IT* inferior trunk

The only constant arterial relationships identified in our study were that the anterior and middle short gyri which were always supplied by the superior trunk of the MCA, and, in 50 % of cases, the insula is totally supplied by the superior trunk. No insular cortex was supplied exclusively by the inferior trunk; the central artery is a branch of the superior trunk in the majority of cases and supplies the central insular sulcus; the angular artery is always a branch of the inferior trunk and in 50 % of cases does not supply the insula.

An examination of 50 hemispheres (25 brains) revealed an average of 85 insular arteries originating from M2; in 50 % of cases, some insular arteries can arise from M1, but they only supply the limen insulae. In 20 % of cases, branches can arise from M3 and supply the periinsular sulcus. The average diameter was 0.3 mm; an average of 8.5 insular arteries in each hemisphere resembled the perforator arteries, and their distribution occasionally reached as far as the corona radiata. Approximately 85–90 % of insular arteries were short and supplied the insular cortex and extreme capsule; 10 % was medium sized and also supplied the claustrum and external capsule; 3–5 % of insular arteries were long and supplied the deep structures.

Insular Perforators *(Figs. 29, 30, 31, 32, 33, 34, 35, and 36)*

We described these insular perforators precisely in a very recent publication about 20 formalin-fixed cadaver hemispheres [2]. We named perforators as the long insular arteries (3–5 % of insular arteries) that extended as far as the corona radiata. They were mostly located in the posterior region of the insula; their diameter is equal or superior to 0.3 mm and equal to or larger than 0.5 mm in 61.5 % of cases (0.5–0.8 mm). The average number of perforators in each hemisphere was 4.55 (3–11) arising from the superior trunk in 72.5 %, from the inferior trunk in 19.8 %, and from the middle trunk (trifurcation) in 7.7 %. These long insular arteries arose from M2 in 51.6 %, from the junction M2–M3 in 37.4 %, and from M3 in 11 %.

Concerning now the origin of the cortical branches, the long arteries most commonly arose from the precentral artery (13.2 %), from the central artery (17.6 %), from the anterior parietal artery (26.4 %), and from the posterior parietal artery (17.6 %).

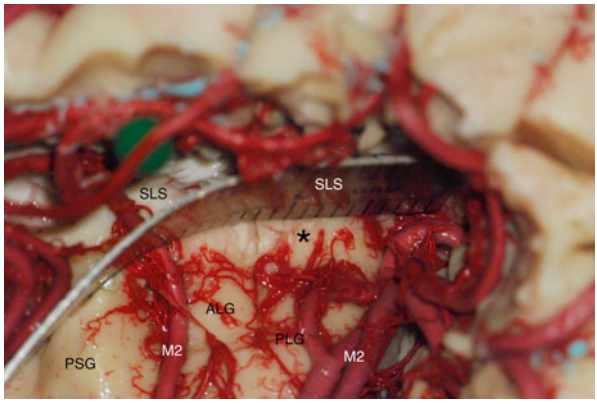

Fig. 29 Lateral view of a posterior half part of a left insula showing a 0.5 mm caliber insular perforating artery penetrating into the superior part of the posterior long gyrus (*). *SLS* superior limiting sulcus, *M2* M2 segment of the middle cerebral artery, *PSG* posterior short gyrus, *ALG* anterior long gyrus, *PLG* posterior long gyrus

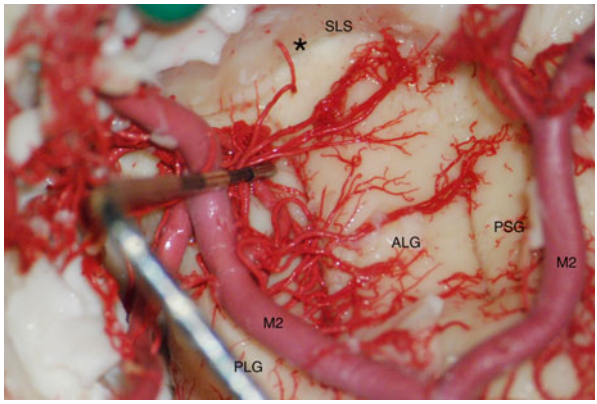

Fig. 30 Lateral view of a posterior half part of a right insula showing an insular perforating artery penetrating into the superior limiting sulcus adjacent to the anterior long gyrus*. *SLS* superior limiting sulcus, *M2* M2 segment of the middle cerebral artery, *PSG* posterior short gyrus, *ALG* anterior long gyrus, *PLG* posterior long gyrus

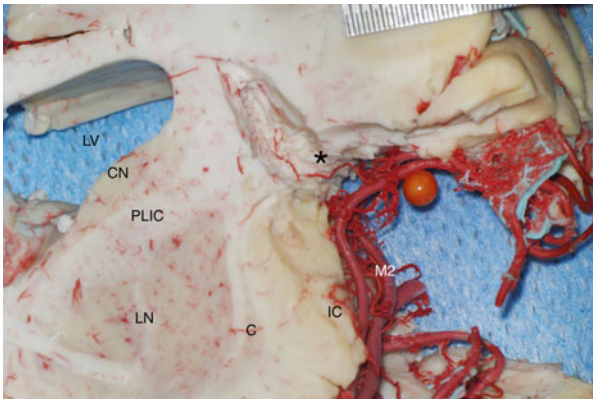

Fig. 31 Photography of a coronal section passing through the posterior limb of the internal capsule. The perforating artery* stops in the lateral part of the corona radiata. It probably supplies the external part of the corticospinal tract and the arcuate fasciculus. *M2* M2 segment of the middle cerebral artery, *IC* insular cortex, *C* claustrum, *LN* lenticular nucleus, *PLIC* posterior limb of internal capsule, *CN* caudate nucleus, *LV* lateral ventricle (Delion and Mercier [2])

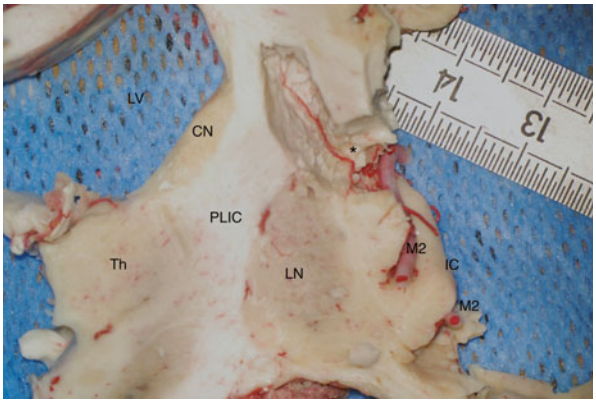

Fig. 32 Photography of a coronal section passing through the posterior limb of the internal capsule. The perforating artery* penetrates through the lateral part of the corona radiata and stops in the middle of the fibers of the corona radiata. It probably supplies a most important part of the corticospinal tract than on the precedent (Fig. 31). *M2* M2 segment of the middle cerebral artery, *IC* insular cortex, *Th* thalamus, *LN* lenticular nucleus, *PLIC* posterior limb of internal capsule, *CN* caudate nucleus, *LV* lateral ventricle

In one third of the cases, these arteries penetrate in the area of the central insula (superior part of the insular posterior short gyrus, superior limiting sulcus (SLS) adjacent to the posterior short gyrus, and SLS adjacent to the posterior short sulcus); in another third of the cases, they penetrate in the insular long gyri and in the SLS adjacent to the insular long gyri; in the last third of the cases, they penetrate in the anterior part of the insula.

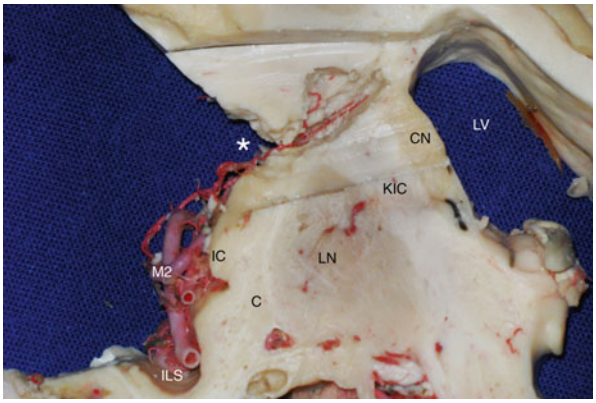

Fig. 33 Photography of a coronal section passing through the knee of the internal capsule. The perforating artery* seems to vascularize the totality of the corona radiata. It probably supplies the corticonuclear tract. *M2* M2 segment of the middle cerebral artery, *IC* insular cortex, *C* claustrum, *LN* lenticular nucleus, *KIC* knee of internal capsule, *CN* caudate nucleus, *LV* lateral ventricle, *ILS* inferior limiting sulcus (Delion and Mercier [2])

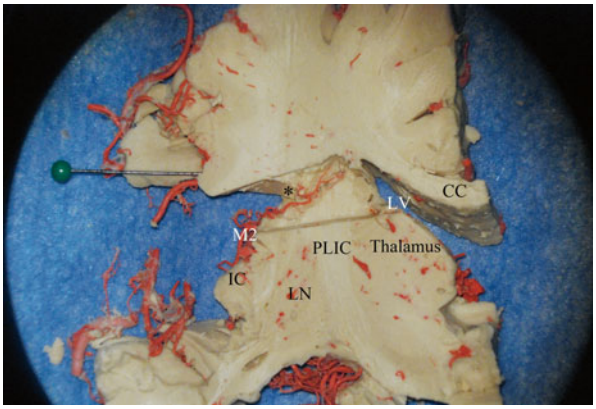

Fig. 34 Photography of a coronal section passing through the posterior limb of the internal capsule, illustrating the subcortical course of a long perforating artery*. It probably supplies the corticospinal tract. *M2* M2 segment of the middle cerebral artery, *IC* insular cortex, *C* claustrum, *LN* lenticular nucleus, *PLIC* posterior limb of internal capsule, *CN* caudate nucleus, *LV* lateral ventricle, *CC* corpus callosum (Delion and Mercier [2])

The subcortical course of these arteries was orthogonal to the plan of the insula and lightly ascending to the lateral ventricular body. They reached the oval center of Vieussens. We differentiated three groups of arteries according to their length: In 36 % of cases, these arteries ended in the corona radiata or deeper than the fibers of the corona radiata (some of them crossed the fibers of the corona radiata and joined the ependym of the lateral ventricular body). In 27 % of the cases, they stopped their course at the lateral aspect of the corona radiata, and in 30 %, they

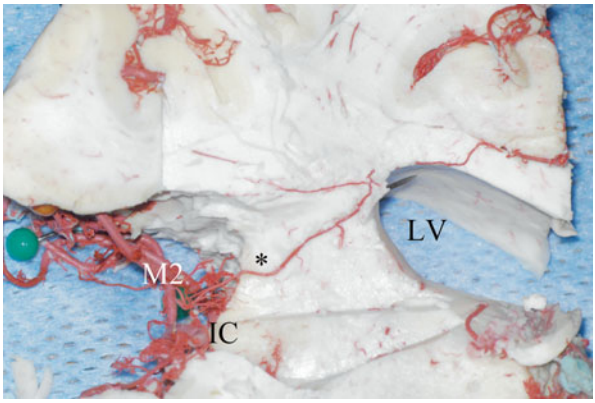

Fig. 35 Coronal section illustrating the subcortical course of a large insular perforating artery*. This perforating artery went beyond the fibers of the corona radiata and goes all the way to the ependym of the body of the lateral ventricle. It probably supplies the corona radiata and the occipitofrontal tract. *M2* M2 segment of the middle cerebral artery, *LV* lateral ventricle, *IC* insular cortex (Delion and Mercier [2])

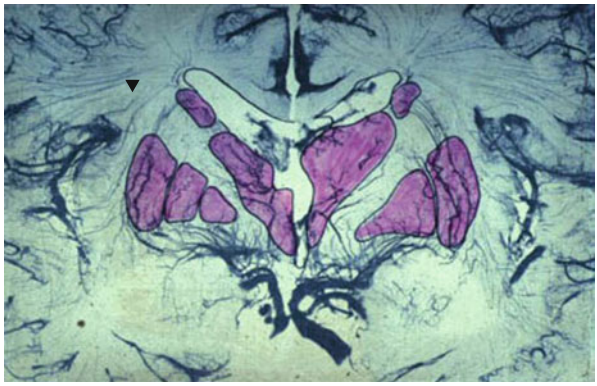

Fig. 36 Coronal X-ray front view. Vascular cerebral arterial injection with black Indian ink. The deep nuclei are colored in purple. A long perforator reaches the corona radiata (*black arrowhead*)

terminated their course between the sagittal plan of the claustrum and the lateral fibers of the corona radiata, corresponding to the area of the arcuate fasciculus. According to the anatomic work of Wen [33] and to our dissection (Fig. 8), the knee of the internal capsule and also the corticonuclear tract are projected over the middle third of the insula which responds to the posterior short gyrus. Considering the length, the cortical penetration, and the rotation of the motor fibers above the internal capsule, we believe that the insular perforators penetrating into the superior part of the posterior short gyrus supply the corticonuclear fibers of the corona radiata in 91 % of cases.

According to the same author [33] and to our dissection (Fig. 8), the posterior limb of the internal capsule is projected over the long gyri of the insula. Considering the length and the cortical penetration of the perforating arteries and the obliqueness

of the precentral gyrus, we think that the perforators penetrating into the superior part of the long gyri supply the corticospinal fibers of the corona radiata in 45 % of cases and just the external part of it in 45 %. It means that 90 % of them supply the corticospinal tract.

Veins

Insular Venous Drainage [25, 31] (Figs. 37, 38, 39, 40, 41, 42, and 43)

The venous anatomic features of the insula are mostly variable and asymmetrical; but, classically, the anterior lobe (short gyri) is draining upward to the superficial sylvian vein, while the posterior lobe (long gyri) and the apex are draining downward to the deep sylvian vein.

The superficial sylvian vein, the largest vein draining along the posterior ramus of the sylvian fissure, usually courses on the temporal side, then turns medially at the anterior end of the sylvian fissure, and empties into the sphenoparietal vein in the majority of cases, but also in the cavernous sinus, the sphenopetrosal sinus, or the deep sylvian vein.

The deep sylvian vein is the predominant vein draining the insula formed by the union of insular veins near the limen insulae; it passes medially across the anterior perforated substance where it joins the anterior cerebral vein to form the first segment of the basal vein [12] or continues and empties into the sphenoparietal sinus.

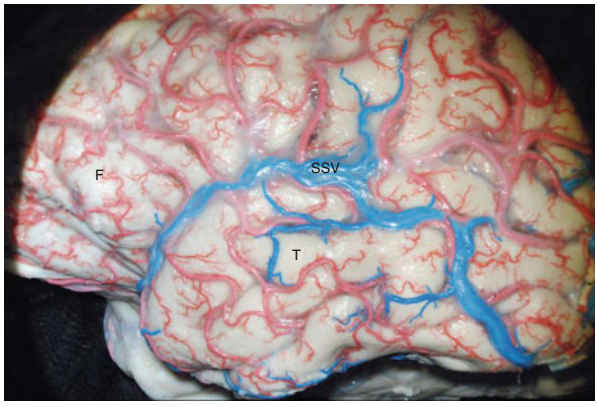

Fig. 37 Left lateral view of a brain hemisphere: the superficial sylvian vein is covered by the outer arachnoid membrane. *SSV* superficial sylvian vein, *DSV* deep sylvian vein, *F* frontal lobe, *T* temporal lobe. *SSM* superficial sylvian membrane, *OC* optic chiasm, *BV* basal vein. *M1* first part of the middle cerebral artery

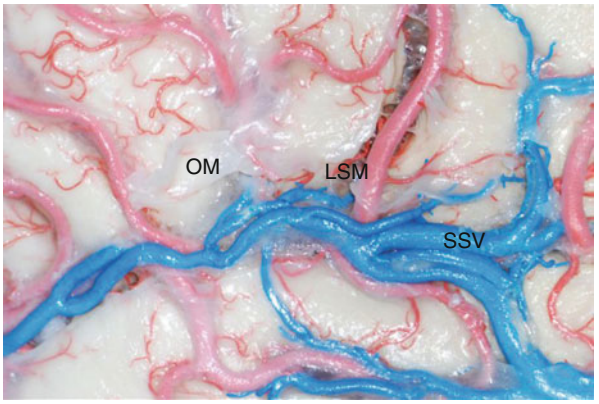

Fig. 38 Left lateral view after magnification and outer membrane removal: the superficial sylvian vein is situated between the superficial sylvian membrane and the outer arachnoid membrane. *OM* outer arachnoid membrane, *LSM* lateral sylvian membrane. For abbreviations, see Fig. 37.

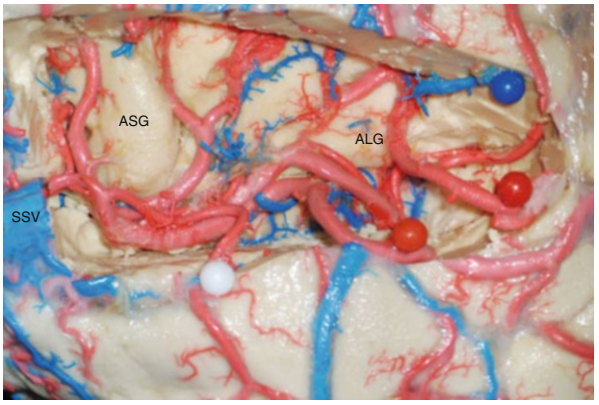

Fig. 39 Left lateral view of the insular cortex after frontal, parietal, and temporal opercula removal; the insular venous drainage is draining upward and downward to the superficial sylvian vein. *SSV* superficial sylvian vein, *ASG* anterior insular short gyrus, *ALG* anterior insular long gyrus

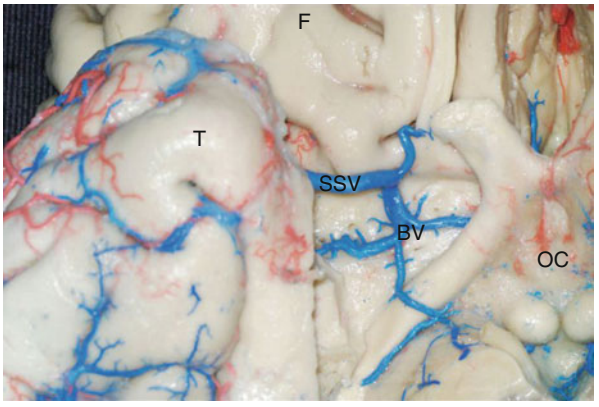

Fig. 40 Right inferior view of the brain: the second part of the basal vein is missing. For abbreviations, see Fig. 37

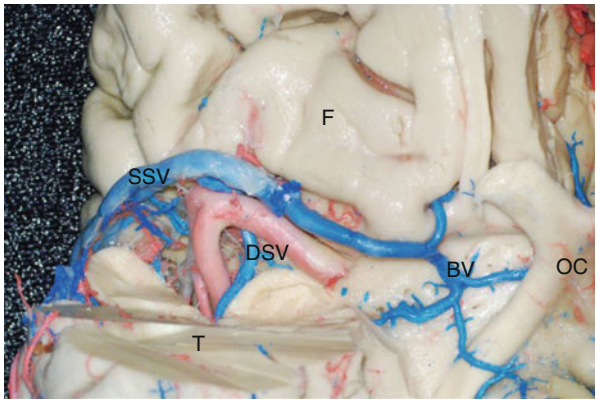

Fig. 41 Right inferior view of the brain (same as 40) after temporal pole removal: the deep sylvian vein is draining into the superficial sylvian vein (For abbreviations, see Fig. 37)

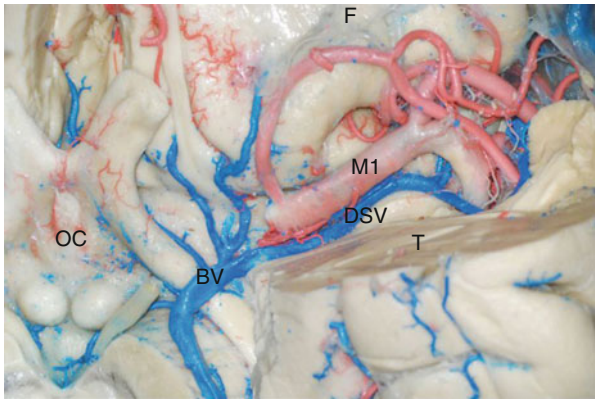

Fig. 42 Left inferior view after temporal pole removal: the deep sylvian vein is draining into the basal vein (For abbreviations, see Fig. 37)

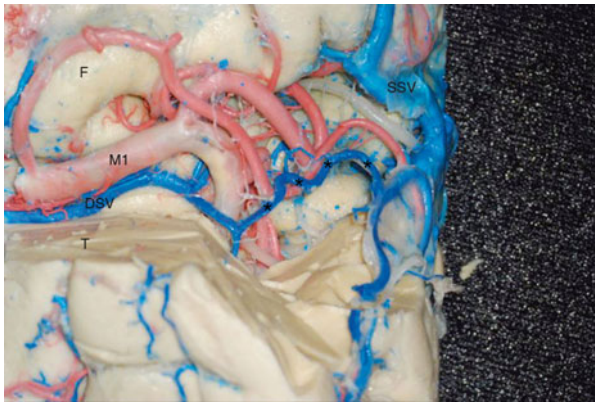

Fig. 43 Left inferior view after temporal pole removal (same than 42). The front is on the top of the figure, and the left is on the right of the figure: there is an anastomosis between the superficial and deep sylvian veins: **** (For abbreviations, see Fig. 37)

Cisterns [10] (Figs. 44, 45, 46, 47, 48, and 49)

Classically, there are two types of arachnoid membranes: outer and inner; the outer arachnoid membrane surrounds the brain and forms a barrier that normally prevents the cerebrospinal fluid from escaping into the subdural space. The subarachnoid space, situated between the pia mater and the outer arachnoid membrane, is divided by trabeculae, septa, and inner membranes into compartments named cisterns that contain cerebrospinal fluid, arteries, veins, and nerves.

The sylvian cistern can be divided into anterior and posterior compartments:

- The anterior compartment (sphenoidal compartment) extends laterally from the origin of the middle cerebral artery to the limen insulae; it is separated medially from the carotid cistern by the thin proximal sylvian membrane extended from the posterior part of the orbital gyri to the anterior part of the medial surface of the uncus. The superior wall is formed by the posterior part of the orbital gyri and the lateral part of the anterior perforated substance, while the inferior wall is made up of the superior and anterior aspect of the temporal lobe (planum temporale). The anterior compartment contains the M1 segment, the beginning of M2, the lenticulostriate arteries, and some branches arising from Heubner and the deep sylvian vein.
- The posterior compartment, behind the limen insulae, opens onto the lateral cerebral surface and is divided into medial and lateral parts by the intermediate sylvian membrane extending between the frontoparietal operculum and the medial edge of the superior and transverse temporal gyri; the medial part located between the medial part of the opposing surfaces of the frontoparietal and temporal operculae and extending into the insular cleft contains M2 trunks and M3 branches; the lateral part located in the lateral part of the cleft between the operculae is limited medially by the intermediate sylvian membrane and laterally by the lateral sylvian membrane; the superficial sylvian veins pass between this membrane and the outer arachnoid membrane.

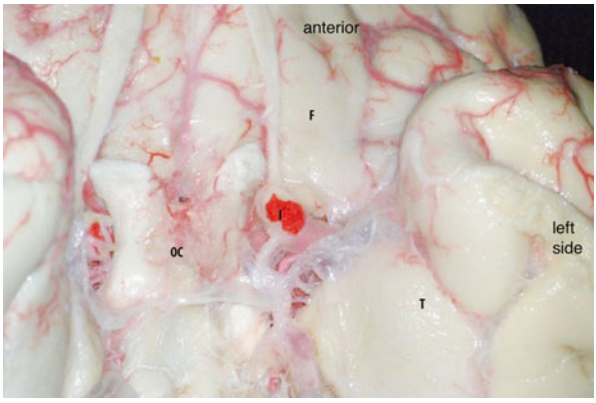

Fig. 44 Inferior view of the brain covered with arachnoid. *OC* optic chiasm, *F* frontal lobe, *T* temporal lobe, *I* internal carotid artery, *M* middle cerebral artery, *A* anterior choroidal artery, *LS* lenticulostriate arteries, *P* proximal sylvian membrane, *IS* intermediate sylvian membrane

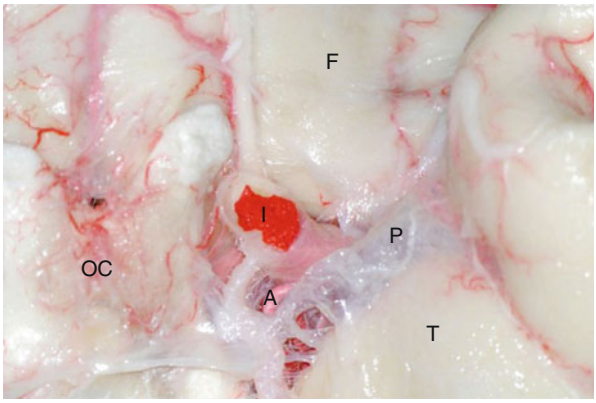

Fig. 45 Same view with magnification (For figure caption, see Fig. 44)

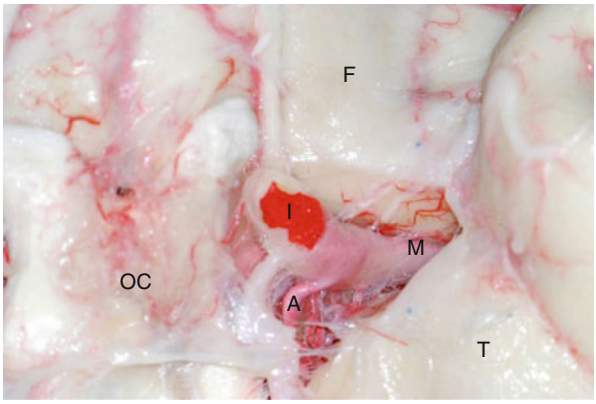

Fig. 46 Opening of the proximal sylvian membrane (For figure caption, see Fig. 44)

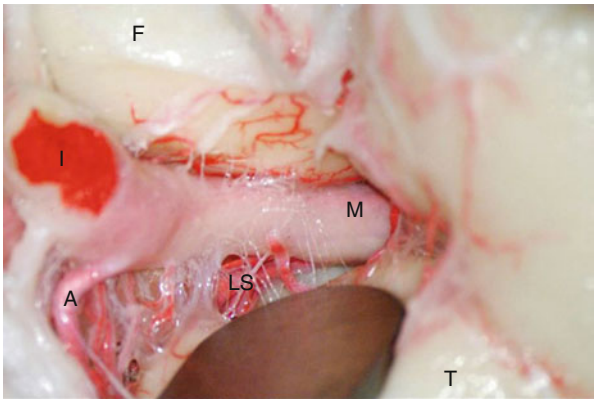

Fig. 47 Left inferior view of the anterior compartment of the sylvian cistern (For figure caption, see Fig. 44)

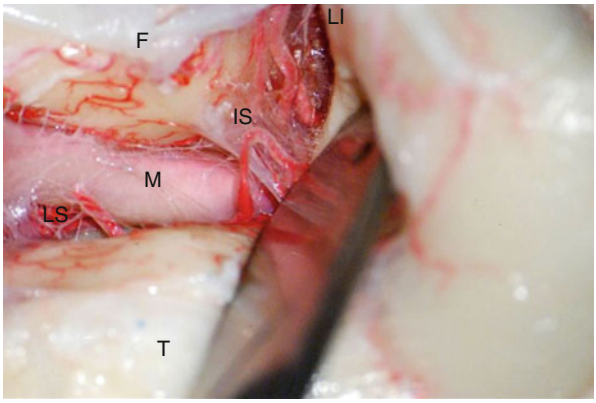

Fig. 48 Opening of the limen insulae (For figure caption, see Fig. 44)

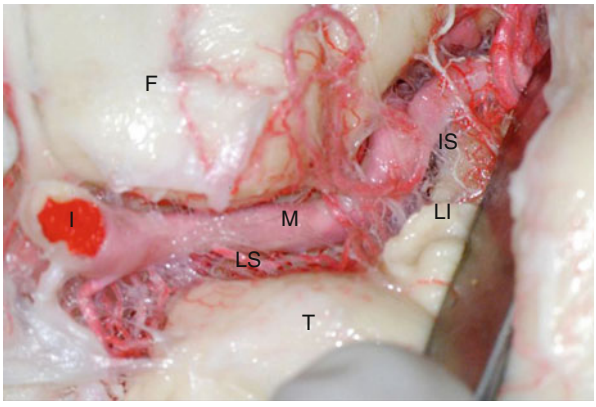

Fig. 49 Left inferior view of the anterior and posterior compartments of the sylvian cistern. *LI* limen insulae (For figure caption, see Fig. 44)

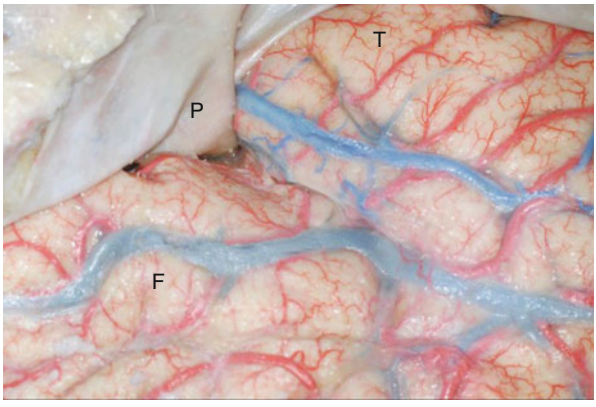

Fig. 50 Stepwise cadaveric right pterional approach. Right superficial view after dura mater opening. *F* frontal lobe, *T* temporal lobe, *OM* outer sylvian membrane, *P* pterion covered with dura mater, *LI* limen insulae, *DSV* deep sylvian vein

Pterional approach is the most popular neurosurgical approach to expose the insular area through the sylvian fissure. We present a step-by-step right cadaveric pterional approach (Figs. 50, 51, 52, 53, 54, and 55), and we conclude with the visualization of an MCA bifurcation aneurysm on a left cadaveric pterional approach (Fig. 56).

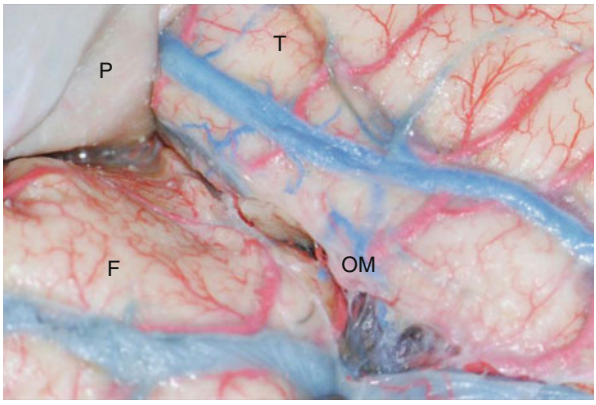

Fig. 51 Opening of the outer arachnoid sylvian membrane. *T* temporal lobe, *F* frontal lobe, *P* pterion covered by the dura mater, *OM* outer arachnoid membrane

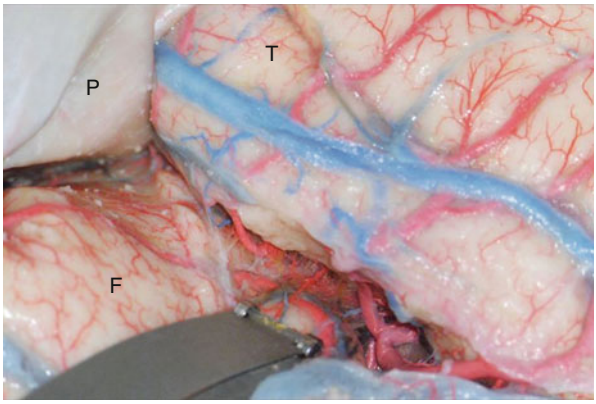

Fig. 52 Visualization of M2 and M3 MCA segments

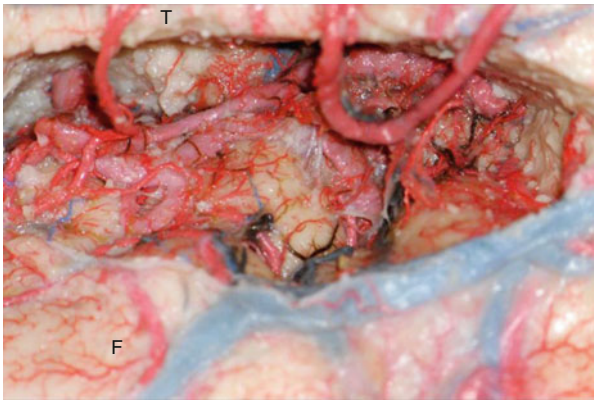

Fig. 53 After removal of the temporal operculae and with magnification, visualization of M2 and M3 MCA segments. *T* temporal lobe, *F* frontal lobe

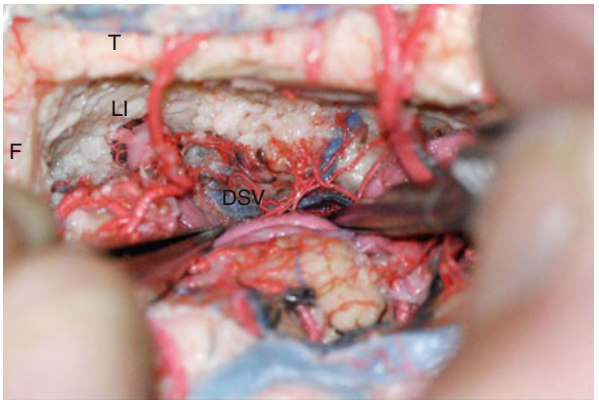

Fig. 54 Visualization of the deep sylvian vein draining here the temporal operculae. *T* temporal lobe, F frontal lobe, *LI* limen insulae, *DSV* deep sylvian vein

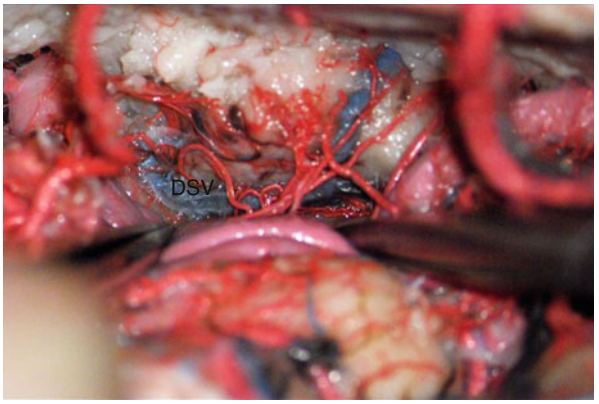

Fig. 55 id with magnification. *DSV* deep sylvian vein

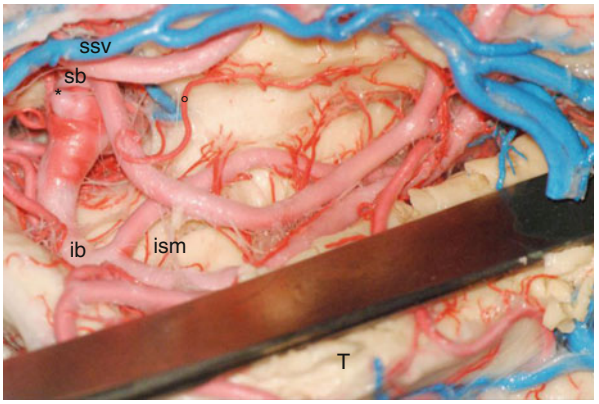

Fig. 56 Cadaveric left pterional approach. *T* temporal lobe, *mca bifurcation aneurysm, *sb* mca superior branch, *ib* mca inferior branch, *SSV* superficial sylvian vein, ° perforator, *ism* intermediate sylvian membrane

Discussion

In our study, in accordance with Varnavas [31], Ture [26], and Afif [1], we have rediscovered the three anatomical constants regarding the vascularization of the insula:

The superior periinsular sulcus is the only sulcus on the lateral surface of the brain without an artery along its axis; the insular arteries cross perpendicular to this sulcus toward the suprasylvian structures without entering the sulcal space itself.
The superior branch of the MCA supplies the anterior insular pole and both the anterior and middle short gyri in 100 % of cases.
In at least 90 % of cases, the artery that supplied the central insular sulcus continued on to become the central artery.

We have found long perforating insular arteries (4.55 per hemisphere whose diameter was equal to or larger than 0.3 mm) vascularizing the corona radiata. In the literature, Varnavas [31] described in 24.5 % of specimens a larger perforating artery (0.4 mm) at the junction of the superior and inferior limiting sulci, arising from the angular artery in 76 % of instances. The destination and purpose of this perforator were unknown. Ture [26] found an average of 9.9 insular arteries in each hemisphere, mostly in the posterior insular region, similar to perforating arteries and, for some of them, supplying the corona radiata. For Yasargil [35], when performing a surgery in the insular area, there is occasionally a larger diameter perforator (0.2–0.5 mm) at the posterosuperior corner of the insula which has been intentionally preserved.

According to Wen [33] and to our study [2], we think that a perforator lesion at the level of the superior part of the posterior short gyrus and at the level of the superior periinsular sulcus adjacent to the posterior short gyrus can produce an ischemia of the corticonuclear fasciculus, while a perforator lesion at the level of the superior part of the long gyri and in the superior periinsular sulcus adjacent to the long gyri can produce an ischemia of the corticospinal fasciculus. The postoperative permanent deficit in some patients can easily be explained by a lesion of a long insular perforator and not by a lenticulostriate lesion, when the ischemic stroke on MR images is located in the corona radiata above the internal capsule (Fig. 57). In insular tumors, Yasargil [34, 36] recommended decompressing the tumors and avoiding coagulating of M2 and M3 branches at the posterior part of the insula which may sometimes supply a single branch vascularizing the lentiform nucleus or the internal capsule.

We recommend for insular approach that care is taken of every perforating artery arising from the M2 segment, from the M3 segment, and from the junction of the M2 and M3 segments, especially if they penetrate into the superior part of the posterior short gyrus and into the superior limiting sulcus adjacent and if they penetrate into the superior part of the long gyri and the superior limiting sulcus adjacent.

Considering the lenticulostriate arteries (LSAs) and the possibility of damage during surgery, Moshel [17] has defined two groups:

1. Insular gliomas with an MR imaging-defined tumor volume located lateral to the LSAs on stereotactic angiography displace the LSAs medially by expanding the insula, have well-demarcated tumor boundaries on MR images, and can be completely resected with minimal neurological morbidity.

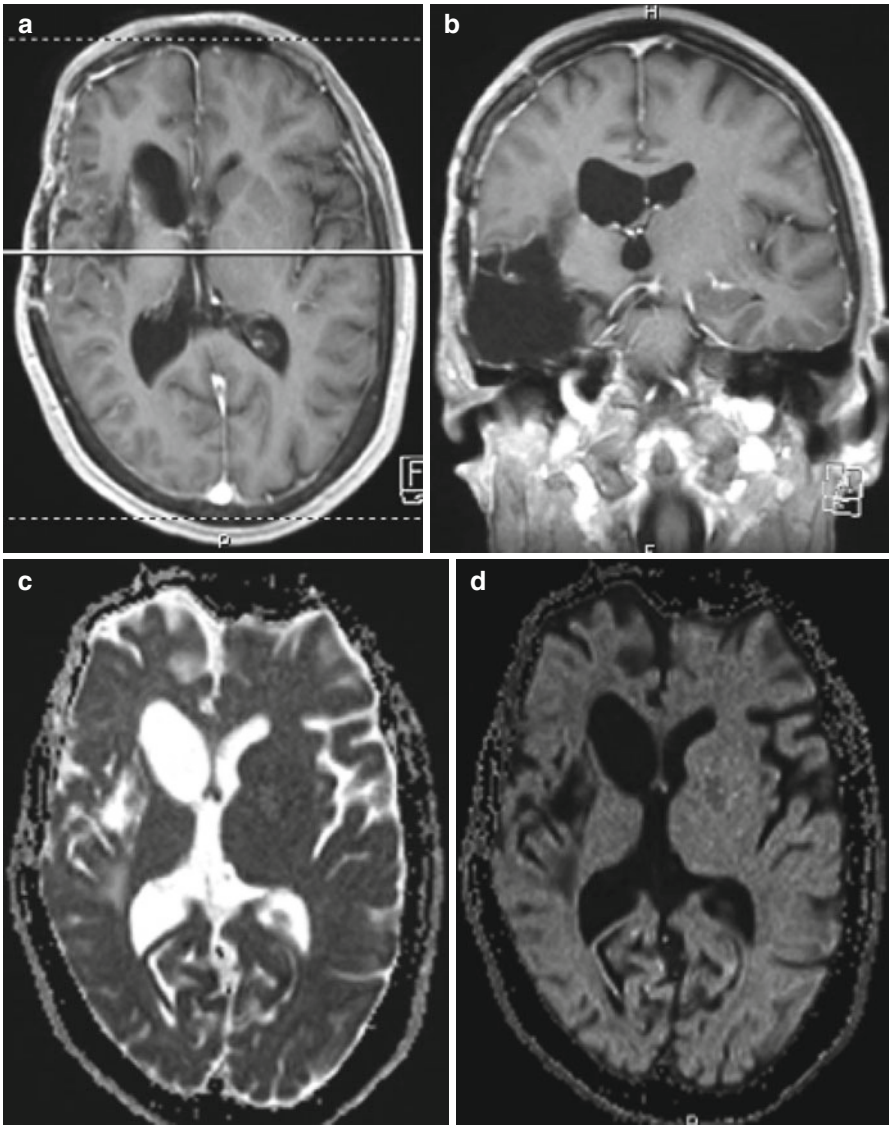

Fig. 57 Photography of an MR scan after temporo insular surgery, showing an ischemic stroke in the region of the corona radiata above the internal capsule. (**a**) Axial T1 MRI scan with contrast injection, (**b**) coronal T1 MRI scan with contrast injection, (**c**) axial ADC (apparent diffusion coefficient) MRI scan, and (**d**) axial diffusion MRI scan

2. Insular tumors that appear to surround the LSAs and do not displace these vessels medially are poorly demarcated from normal brain parenchyma on MR images and are associated with higher rates of neurological morbidity if aggressive resection is pursued. Saito [21] has suggested performing a preoperative three-dimensional 3 T time of flight (TOF) to clearly visualize the LSAs and their relationships with the tumor margins.

Concerning insular surgery, other authors have suggested using the MEPs (motor evoked potentials) [18, 23] or the ESM (subcortical electrical stimulation mapping) when the tumor invades the posterior lobule (long gyri) [6, 22]. Duffau [4, 5] uses an intraoperative electrical stimulation under local anesthesia, associated with neuronavigation and/or ultrasonography and sometimes a 3D angio-CT in the stereotactic image guide system to follow the perforators during surgery. Lang, Hentschel, and Vanaclocha [8, 11, 30], in addition to the stimulation, use a subpial dissection of the tumor with preservation of all large perforating arteries arising from posterior M2. We think that direct cortical and subcortical electrical stimulation must be used in insular surgery as said by the abovementioned authors, but it only allows us to avoid direct injury to the subcortical white matter tract such as corticospinal fasciculus.

Conclusion

A good knowledge of the landmarks in the insular area, associated with the preservation of the LSAs and of the long insular perforators during operative dissection, must be considered before performing surgery in the sylvian fissure and insula to avoid permanents weakness.

Conflict of Interest: None

References

1. Afif A, Mertens P (2010) Description of sulcal organization of the insular cortex. Surg Radiol Anat 32(5):491–498
2. Delion M, Mercier P (2014) Microanatomical study of the insular perforating arteries. Acta Neurochir (Wien). doi:10.1007/s00701-014-2167-9
3. Donzelli R, Marinkovic S, Brigante L, de Divitiis O, Nikodijevic I, Schonauer C, Maiuri F (1998) Territories of the perforating (lenticulostriate) branches of the middle cerebral artery. Surg Radiol Anat 20(6):393–398
4. Duffau H, Capelle L, Lopes M, Faillot T, Sichez JP, Fohanno D (2000) The insular lobe: physiopathological and surgical considerations. Neurosurgery 47(4):801–810, Discussion 810–811
5. Duffau H, Taillandier L, Gatignol P, Capelle L (2006) The insular lobe and brain plasticity: lessons from tumor surgery. Clin Neurol Neurosurg 108(6):543–548
6. Duffau H, Peggy Gatignol ST, Mandonnet E, Capelle L, Taillandier L (2008) Intraoperative subcortical stimulation mapping of language pathways in a consecutive series of 115 patients with Grade II glioma in the left dominant hemisphere. J Neurosurg 109(3):461–471
7. Gibo H, Carver CC, Rhoton AL Jr, Lenkey C, Mitchell RJ (1981) Microsurgical anatomy of the middle cerebral artery. J Neurosurg 54(2):151–169
8. Hentschel SJ, Lang FF (2005) Surgical resection of intrinsic insular tumors. Neurosurgery 57(1 Suppl):176–183, discussion -83

9. Herman LH, Ostrowski AZ, Gurdjian ES (1963) Perforating branches of the middle cerebral artery. An anatomical study. Arch Neurol 8:32–34
10. Inoue K, Seker A, Osawa S, Alencastro LP, Matsushima T, Rhoton AL Jr (2009) Microsurgical and endoscopic anatomy of the supratentorial arachnoidal membranes and cisterns. Neurosurgery 65(4):644–665
11. Lang FF, Olansen NE, DeMonte F, Gokaslan ZL, Holland EC, Kalhorn C, Sawaya R (2001) Surgical resection of intrinsic insular tumors: complication avoidance. J Neurosurg 95(4): 638–650
12. Lasjaunias P, Berenstein A, Ter Brugge KG (2001) Surgical neuroangiography, vol 1: clinical vascular anatomy and variations, 2nd edn. Springer, New York
13. Lazorthes G, Gouaze A, Salomon G Vascularisation et ciruculation de l'encéphale.tome 1: anatomie descriptive et fonctionnelle (L'artère cérébrale moyenne) 113–25
14. Marinkovic SV, Kovacevic MS, Marinkovic JM (1985) Perforating branches of the middle cerebral artery. Microsurgical anatomy of their extracerebral segments. J Neurosurg 63(2): 266–271
15. Marinkovic SV, Milisavljevic MM, Kovacevic MS, Stevic ZD (1985) Perforating branches of the middle cerebral artery. Microanatomy and clinical significance of their intracerebral segments. Stroke 16(6):1022–1029
16. Mercier P, Fournier HD, Brassier G, Papon X, Cronier P, Velut S, Pillet J (1994) The perforating arteries of the anterior part of the circle of Willis; Micro-anatomical study. Rivista di Neuroradiologica 7(Suppl 4):79–83
17. Moshel YA, Marcus JD, Parker EC, Kelly PJ (2008) Resection of insular gliomas: the importance of lenticulostriate artery position. J Neurosurg 109(5):825–834
18. Neuloh G, Pechstein U, Schramm J (2007) Motor tract monitoring during insular glioma surgery. J Neurosurg 106(4):582–592
19. Rhoton AL Jr (2002) The supratentorial cranial space: microsurgical anatomy and surgical approaches. Neurosurgery 51(4):S1–S410
20. Rosner SS, Rhoton AL Jr, Ono M, Barry M (1984) Microsurgical anatomy of the anterior perforating arteries. J Neurosurg 61(3):468–485
21. Saito R, Kumabe T, Inoue T, Takada S, Yamashita Y, Kanamori M, Sonoda Y, Tominaga T (2009) Magnetic resonance imaging for preoperative identification of the lenticulostriate arteries in insular glioma surgery. Technical note. J Neurosurg 111(2):278–281
22. Signorelli F, Guyotat J, Elisevich K, Barbagallo GM (2009) Review of current microsurgical management of insular gliomas. Acta Neurochir (Wien) 152(1):19–26
23. Simon M, Neuloh G, von Lehe M, Meyer B, Schramm J (2009) Insular gliomas: the case for surgical management. J Neurosurg 110(4):685–695
24. Tanriover N, Kawashima M, Rhoton AL Jr, Ulm AJ, Mericle RA (2003) Microsurgical anatomy of the early branches of the middle cerebral artery: morphometric analysis and classification with angiographic correlation. J Neurosurg 98(6):1277–1290
25. Tanriover N, Rhoton AL Jr, Kawashima M, Ulm AJ, Yasuda A (2004) Microsurgical anatomy of the insula and the sylvian fissure. J Neurosurg 100(5):891–922
26. Ture U, Yasargil MG, Al-Mefty O, Yasargil DC (2000) Arteries of the insula. J Neurosurg 92(4):676–687
27. Ture U, Yasargil DC, Al-Mefty O, Yasargil MG (1999) Topographic anatomy of the insular region. J Neurosurg 90(4):720–733
28. Umansky F, Gomes FB, Dujovny M, Diaz FG, Ausman JI, Mirchandani HG, Berman SK (1985) The perforating branches of the middle cerebral artery. A microanatomical study. J Neurosurg 62(2):261–268
29. Umansky F, Juarez SM, Dujovny M, Ausman JI, Diaz FG, Gomes F, Mirchandani HG, Ray WJ (1984) Microsurgical anatomy of the proximal segments of the middle cerebral artery. J Neurosurg 61(3):458–467
30. Vanaclocha V, Saiz-Sapena N, Garcia-Casasola C (1997) Surgical treatment of insular gliomas. Acta Neurochir (Wien) 139(12):1126–1134, discussion 34–5

31. Varnavas GG, Grand W (1999) The insular cortex: morphological and vascular anatomic characteristics. Neurosurgery 44(1):127–136, discussion 36–8
32. Vincentelli F, Caruso G, Andriamamonjy C, Rabehanta P, Graziani N, Grisoli F, Gouaze A, Vigouroux RP (1990) Micro-anatomy of collateral perforating branches of the middle cerebral artery. Neurochirurgie 36(1):3–14, discussion -5
33. Wen HT, Rhoton AL Jr, de Oliveira E, Castro LH, Figueiredo EG, Teixeira MJ (2009) Microsurgical anatomy of the temporal lobe: part 2–sylvian fissure region and its clinical application. Neurosurgery 65(6 Suppl):1–35, discussion 6
34. Yasargil MG (1996) Microneurosurgery, IV Bth edn. G Thieme, New York, pp 263–267
35. Yasargil MG, Caglar YS (1999) The insular cortex: morphological and vascular anatomic characteristics, Comments. Neurosurgery 44(1):136–138
36. Yasargil MG, Reeves JD (1992) Tumours of the limbic and paralimbic system. Acta Neurochir (Wien) 116(2–4):147–149

Author Index Volume 1–43

J. Schramm (ed.), *Advances and Technical Standards in Neurosurgery,*
Advances and Technical Standards in Neurosurgery, Vol. 43,
DOI 10.1007/978-3-319-21359-0

C

F

G

H

I

M

Subject Index Volume 1–43

J. Schramm (ed.), *Advances and Technical Standards in Neurosurgery,*
Advances and Technical Standards in Neurosurgery, Vol. 43,
DOI 10.1007/978-3-319-21359-0

D

E

T